GAS ABSORPTION EXPERIMENTS IN A PILOT PLANT COLUMN WITH THE SULZER STRUCTURED PACKING MELLAPAK

THESE No 984 (1991)

PRESENTEE AU DEPARTEMENT DE CHIMIE

ECOLE POLYTECHNIQUE FEDERALE DE LAUSANNE

POUR L'OBTENTION DU GRADE DE DOCTEUR ES SCIENCES TECHNIQUES

PAR

MARCELO HENRIQUES DE BRITO

Ingénieur mécanicien diplômé Universidade Federal do Rio de Janeiro
de nationalité brésilienne

acceptée sur proposition du jury :

Prof. U. von Stockar, rapporteur
Prof. E. Plattner, corapporteur
Dr M. Laso, corapporteur

Lausanne, EPFL
1992

To my parents and my family,
with love.

This work was carried out at the Institute of Chemical Engineering (Institut de Génie Chimique) of the Swiss Federal Institute of Technology from November 1987 to October 1991. I recognize the important support and advice of many people in specific aspects of this work in the acknowledgements at the end of each chapter. For their contribution to this work as a whole, I express my gratitude as follows:

First, I would like to thank very much Prof. Dr. U. von Stockar for having accepted me as his PhD student, for providing support, advice and stimulating discussions and for giving me freedom to carry out this work.

Many thanks to Prof. Dr. E. Plattner for agreeing to examine this thesis. His interest in this thesis was important. Many thanks to Dr. M. Laso not only for his expertise, but also for the friendly and open discussions and contribution from the very beginning of this work.

This work would not have been possible without the technical and financial support of SULZER BROTHERS LIMITED. For entrusting me to carry out this research, I thank very much Dr. W. Meier and Dr. P. Bomio. I am indebted to Dr. P. Collins, who helped to review the manuscript and provided valuable suggestions. My thanks to Dr. L. Spiegel for discussions. For providing the means and for sending me to Switzerland, I am particularly grateful to Mr. E. Casanova, Dr. Ch. Etter, Mr. G. Bally, Mr. H. Bieri, Mr. A. Kounitzky and Mr. M. Hintermüller.

The technical and personal contributions received from different members of the Institute of Chemical Engineering was most useful in the progress of this work. Many thanks ! The relationship with the class of chemical engineering students 1991, with whom I had most contact (and a lot of fun!), was very important to me.

Last but not least, I cannot forget many friends who made my life in Switzerland very pleasant, interesting and exciting. I remember also my friends in Brazil who visited me, wrote to me and did not forget me. All of them are important to me and a constant source of encouragement.

October, 1991

ABSTRACT

Data for the volumetric mass transfer coefficient, k_La, and the effective area, of structured packings have rarely been reported in the literature. This is despite the ever-increasing importance of structured packings in industrial separation columns for absorption and distillation processes.

This work verified that the CO_2-NaOH reaction is suitable for the determination of effective mass transfer area. The kinetic parameter of this reaction which governs the absorption flux, was evaluated with a wetted wall column, which provides a known mass transfer area. Normally, this kinetic parameter is calculated with data obtained from other literature sources. Since there is a large disagreement, the value obtained with the wetted wall column was used in absorption columns packed with MELLAPAK for the determination of effective areas. The desorption of O_2 from demineralized water into air is suitable for the determination of k_La values. The measured desorption rates are actually related to the overall volumetric liquid side mass transfer coefficient, which in turn is very close to k_La, since O_2 is sparingly soluble in water, even by comparison with CO_2. Therefore the gas side resistance is negligible.

The effective area for mass transfer and the k_La of the SULZER packings MELLAPAK 125.Y, 250.Y and 500.Y were measured under industrial-scale operating conditions, with a broad range of gas and liquid flows, in a pilot plant with a column having an internal diameter of 295 mm and a packing height of 420 mm. The experimental procedure and apparatus employed in this work were checked by making additional measurements of effective area for 25 mm ceramic ring packing; these values were compared with literature data. The influence of the drip point density of the liquid distributor and of a higher packing height of MELLAPAK 125.Y were also studied.

This contribution shows that the effective mass transfer area for MELLAPAK 125.Y, 250.Y and 500.Y can be higher than the defined geometric area of the packing. The ratio of the effective area to the geometric area is a function of a Reynolds number defined with the liquid characteristic velocity and packing hydraulic diameter. For MELLAPAK with relatively low specific geometric area in particular, the space between the sheets is sufficient to permit droplet formation and turbulence enhancement, both of which magnify effective area.

Empirical correlations for the k_La of MELLAPAK 250.Y and 500.Y are proposed. The k_La values for MELLAPAK 250.Y and 500.Y are higher than for irregular packings with the same geometric area. The k_La for MELLAPAK 125.Y varies with the liquid and gas flowrates in a different way than that for MELLAPAK 250.Y, 500.Y and irregular packings.

A model for predicting the liquid phase mass transfer coefficient, k_L, for MELLAPAK 250.Y and 500.Y is proposed. In the development of this model, the experimental data from this work were considered together with the penetration theory. The value of k_L increases with the liquid and gas flow and decreases with the geometric area of the packing. Higher k_L values are associated with irregular packings with equal geometric area.

Recommendations for improvements in the surface structure of MELLAPAK, enhancing liquid film renewal rate, as well as suggestions for future research projects end this thesis.

RESUME

Des mesures du coefficient volumétrique de transfert de masse, k_La, et de l'aire effective pour le transfert de matière des garnissages réguliers ne sont guère décrites dans la littérature, malgré le fait que les garnissages réguliers font l'objet d'une utilisation croissante dans des colonnes industrielles de séparation pour l'absorption de gaz et la distillation.

Cette recherche a vérifié que la réaction de CO_2 avec NaOH convient pour la détermination des aires effectives. Le paramètre cinétique de cette réaction qui définit le flux d'absorption a été évalué avec une colonne à film tombant, où l'aire de transfert de matière est connue. Généralement, ce paramètre cinétique est calculé avec des données tirées d'autres sources bibliographiques. Comme il n'y a pas accord dans la littérature pour ces données, les résultats obtenus avec la colonne à film tombant ont été utilisés pour déterminer l'aire effective des colonnes d'absorption garnies avec MELLAPAK. La désorption, dans l'air, de l'O_2 dissous dans l'eau déminéralisée est adéquate pour la détermination du k_La. Les taux de désorption mesurés sont en effet liés au coefficient global de transfert de matière en phase liquide, qui est très proche du k_La, parce que l'O_2, même comparé au CO_2, est un gaz très peu soluble dans l'eau. Ansi, la résistance en phase gazeuse est négligeable.

L'aire effective de transfert de masse et le k_La des garnissages SULZER MELLAPAK 125.Y, 250.Y et 500.Y ont été mesurés dans des conditions industrielles, sur des grands domaines de débits gazeux et liquide, dans une installation pilote comprenant une colonne avec un diamètre interne de 295 mm et une hauteur de garnissage de 420 mm. Des expériences d'aire effective avec des anneaux en céramique de 25 mm ont été réalisées pour vérifier la procédure expérimentale et l'appareillage employés dans ce travail. Ces résultats ont été comparés à ceux de la littérature. L'influence de la densités de points de distribution du liquide et d'une hauteur plus grande de MELLAPAK 125.Y ont été aussi examinées.

Cette recherche montre que l'aire effective peut être plus grande que celle définie par la géométrie du MELLAPAK. Le rapport entre l'aire effective et géométrique du garnissage est fonction d'un nombre de Reynolds basé sur le débit liquide et la taille du garnissage. Plus l'aire géométrique du MELLAPAK est grande, plus réduit devient l'espace entre les lamelles du garnissage et, par conséquent, plus faible est la possiblité de formation de gouttes de liquide et de turbulence dans l'interface gaz-liquide, qui pourraient augmenter l'aire effective.

Pour les k_La des garnissages MELLAPAK 250.Y et 500.Y, des corrélations empiriques sont proposées. Les valeurs du k_La des MELLAPAK 250.Y et 500.Y sont plus grandes que celles des garnissages irréguliers de même aire géométrique. La variation du k_La du MELLAPAK 125.Y avec les débits liquide et gazeux est différente de celle présentée par MELLAPAK 250.Y, 500.Y et les garnissages irréguliers.

Un modèle pour le coefficient de transfert de masse en phase liquide, k_L, du MELLAPAK 250.Y et 500.Y est proposé. Ce modèle combine les résultats expérimentaux de ce travail avec la théorie de la pénétration. Le k_L croît avec les débits liquide et gazeux et décroît avec l'aire géométrique du garnissage. Les garnissages irréguliers de même aire géométrique que MELLAPAK présentent un k_L plus grand.

Un changement de la surface du MELLAPAK, favorisant le renouvellement du film liquide, ansi que des projets futurs de recherche sont proposés.

ZUSAMMENFASSUNG

Trotz zunehmendem Gebrauch von geordneten Packungen in industriellen Absorptions- und Destillationskolonnen findet man in der Literatur kaum Angaben über Messungen und Korrelationen der spezifischen Austauschfläche und des k_La-Wertes.

Diese Arbeit zeigt, dass die chemische Reaktion von CO_2 mit wässriger NaOH zur Messung der spezifischen Austauschfläche geeignet ist. Die konstanten Reaktionsparameter dieser Reaktion, welche die Absorptionsrate kontrollieren, wurden zu einem Term zusammengefasst. Normalerweise werden diese Parameter mit Hilfe von Daten aus der Literatur berechnet. Wegen abweichender Angaben in verschiedenen Quellen wurde dieser Term mittels einer Dünnschichtkolonne mit bekannter Stoffaustauschfläche ermittelt. Diese Resultate wurden auf die mit MELLAPAK gerüstete Absorptionskolonne übertragen, um deren spezifische Austauschfläche zu bestimmen. Die Desorption von Sauerstoff aus demineralisiertem Wasser in Luft ist ein geeignetes System zur Bestimmung der k_La-Werte. Die gemessene Desorptionsrate liefert den flüssigkeitsseitigen Stoffdurchgangskoeffizienten. Dieser Wert ist demjenigen des k_La praktisch gleich, da Sauerstoff in Wasser im Gegensatz zu CO_2 sehr schwerlöslich ist. Somit ist der gasseitige Widerstand für den Stoffübergang vernachlässigbar.

Die spezifischen Austauschflächen und die k_La-Werte der SULZER-Packungen MELLAPAK 125.Y, 250.Y und 500.Y wurden unter industriellen Betriebsbedingungen gemessen, u.a. mit grosser Bandbreite der Gas- und Flüssigkeitsdurchsätze. Zu diesem Zweck wurde eine Pilotanlage eingesetzt, die eine Kolonne von 295mm Innendurchmesser und eine Packungshöhe von 420mm aufweist. In dieser Arbeit wurden Messungen der Austauschfläche durchgeführt, um den experimentellen Ablauf und die Anlage zu prüfen. Bei diesen Versuchen wurden keramische 25 mm Ringe verwendet. Die Ergebnisse dieser Messungen wurden mit denjenigen der Literatur verglichen. Zusätzlich wurde der Einfluss der Flüssigkeitsverteilung und der Packungshöhe der M125.Y untersucht.

Es zeigte sich, dass die effektive Austauschfläche für MELLAPAK 125.Y, 250.Y und 500.Y grösser sein kann als die totale geometrische Fläche. Das Verhältnis der effektiven Austauschfläche zu der geometrischen Austauschfläche ist eine Funktion der Reynolds-Zahl, die den Flüssigkeitsdurchsatz und den hydraulischen Durchmesser beinhaltet. Je grösser die geometrische Fläche der MELLAPAK ist, desto kleiner wird der Abstand zwischen den Lamellen der Packung und damit die Wahrscheinlichkeit, dass sich Tropfen und Turbulenzen an der Phasengrenze bilden, welche die effektive Austauschfläche vergrössern würden.

Empirische Korrelationen für die Berechnung des k_La-Wertes für MELLAPAK 250.Y und 500.Y werden vorgeschlagen. Die k_La-Werte von MELLAPAK 250.Y und 500.Y sind grösser als diejenigen der ungeordneten Packungen mit der gleichen geometrischen Oberfläche. Die Abhängigkeit des k_La-Wertes von MELLAPAK 125.Y von der spezifischen Flüssigkeitsbelastung ist anders als diejenige von MELLAPAK 250.Y und 500.Y und der ungeordneten Packungen.

Modelle zur Berechnung des flüssigseitigen Stoffübergangskoeffizienten k_L von MELLAPAK 250.Y und 500.Y werden vorgeschlagen. Die experimentellen Daten dieser Arbeit wurden hierfür mit der "Penetrations-Theorie" verknüpft. Der k_L-Wert wird mit zunehmendem Flüssigkeits- und Gasdurchsatz grösser, mit zunehmender spezifischer geometrischer Fläche aber kleiner. Ungeordnete Packungen mit gleichen geometrischen Flächen wie MELLAPAK haben höhere k_L-Werte als diese.

Vorschläge für eine Änderung der MELLAPAK-Oberfläche, die mehr Flüssigkeitsfilmerneuerung erzeugen würde, und Anregungen für zukünftige Projekte schliessen diese Doktorarbeit ab.

RESUMO

O emprego de enchimentos estruturados em colunas industriais de processos de separação (absorção de gases e destilação) vem continuamente crescendo. Apesar disto, a literatura apresenta poucos dados experimentais do coeficiente volumétrico de transferência de massa, k_La, e da área efetiva de enchimentos estruturados.

No presente trabalho foi verificado que a reação de CO_2 com NaOH é adequada para determinar áreas efetivas. O parâmetro cinético desta reação que fixa o fluxo de absorção foi obtido com uma coluna de filme vertical, cuja área de transferência de massa é conhecida. Geralmente, este parâmetro cinético é calculado com dados obtidos de referências bibliográficas. Como esses dados são conflitantes, os resultados obtidos com a coluna de filme vertical foram utilisados para medir áreas efetivas dos enchimentos MELLAPAK. A desorção de O_2 de água demineralisada para o ar é adequada para medir o k_La. O fluxo medido de desorção é na realidade relacionado ao coeficiente global de transferência de matéria da fase líquida, cujo valor é muito próximo do k_La, pois O_2 é um gás muito pouco solúvel na água, menos ainda que o CO_2. Desta forma, a resistência em fase gasosa é desprezível.

A área efetiva de transferência de massa e o k_La dos enchimentos SULZER MELLAPAK 125.Y, 250.Y e 500.Y foram medidos em condições industriais, em uma larga faixa de variação das vazões de líquido e de gás. A coluna na instalação piloto tinha um diâmetro interno de 295 mm e uma altura de 420 mm. A metodologia experimental foi testada através de experiências com anéis cerâmicos de 25 mm. Os resultados obtidos foram comparados aos da literatura. A influência de números de pontos de molhamento/m^2 do distribuidor e de uma altura maior de MELLAPAK 125.Y foram adicionalmente examinadas.

Esta contribuição mostra que a área efetiva de transferência de massa para MELLAPAK 125.Y, 250.Y e 500.Y pode assumir valores maiores do que a área geométrica definida pelo enchimento. A razão entre a área efetiva e a área geométrica é uma função do número de Reynolds englobando a vazão de líquido e o diâmetro hidráulico do enchimento. Um aumento da área geométrica do MELLAPAK diminui o espaço disponível entre as placas do enchimento e, assim, reduz a possibilidade de formação de gotas de líquido e de turbulências na interface gás-líquido, ambos responsáveis pelo aumento efetivo de área.

Correlações empíricas para o k_La de MELLAPAK 250.Y e 500.Y são sugeridas. Os valores de k_La do MELLAPAK 250.Y e 500.Y são mais elevados do que de enchimentos não estruturados com mesma area geométrica. A variação do k_La do MELLAPAK 125.Y com as vazões de líquido e de gás não é semelhante à observada nos MELLAPAK 250.Y e 500.Y e nem em outros enchimentos estruturados.

Um modelo para prever o coeficiente de transferência de matéria em fase líquida, k_L, dos MELLAPAK 250.Y e 500.Y é proposto. Para sua elaboração, os dados experimentais deste trabalho foram utilizados conjuntamente com a teoria da penetração. O k_L aumenta com o fluxo de líquido e gás e diminui com a área geométrica do enchimento. Enchimentos não estruturados apresentam valores de k_L mais altos.

Encerrando esta tese, é proposta uma modificação da surperfície do enchimento MELLAPAK, que ativa a renovação do filme de líquido, assim como são sugeridos trabalhos futuros.

CHAPTER V - MEASURING THE VOLUMETRIC MASS TRANSFER COEFFICIENT k_La

CHAPTER VI - EVALUATING THE LIQUID PHASE MASS TRANSFER COEFFICIENT k_L

SCOPE OF THIS WORK

This work presents comprehensive and experimental data for describing the mass transfer process in three different types of the SULZER structured packing MELLAPAK used in industrial and laboratory separation columns for distillation and absorption processes. The data is useful for the design of the necessary packing height in the column. For structured packings, similar measurements and data analysis were not found in the literature, which justifies this work.

This investigation consists of four major tasks:

1) Experimental confirmation of the adequacy of reaction CO_2-NaOH as a method for obtaining the specific mass transfer area. The experiments were carried out in a wetted wall column, whose interfacial area is equal to the mass transfer area and could be changed. The parameters which influence the absorption rate were determined. (Chapter III)
2) Measurement in a pilot plant column of the specific mass transfer area of the SULZER structured packings MELLAPAK 125.Y, 250.Y and 500.Y. (Chapter IV)
3) Measurement in a pilot plant column of the volumetric mass transfer coefficient - k_La - for the SULZER structured packings MELLAPAK 125.Y, 250.Y and 500.Y. The physical desorption of oxygen dissolved in demineralized water into air was used. (Chapter V)
4) Evaluation of the liquid phase mass transfer coefficient independent of the specific mass transfer area, with a proposed model. (Chapter VI)

The k_La is used for the design of the height of packed columns with the HTU-NTU method. Measurements of the effective area for mass transfer further the comprehension of mass transfer in a packing and as a result help in the design of new packing geometries. In addition, an estimation of the mass transfer area is also required for the determination of k_L, as well as k_G, from k_La and k_Ga measurements respectively. The liquid phase mass transfer coefficient, k_L, expresses the resistance to mass transfer in the liquid boundary layer at the phase interface.

Measured k_La and mass transfer area values must still be valid after scale-up or scale-down. Although the SULZER structured packing MELLAPAK with homogeneous packing porosity offers a low Peclet number for radial mixing (Meier (1979)) and almost no backmixing, there will be a generally higher confidence in the measurements if the column used approaches industrial scale. Norman (1961) in his book has already stated that laboratory scale plants may not be adequate for obtaining data for irregular packings, as still frequently reported in the literature.

The measurements were carried out under industrial-scale operating conditions, within a broad range of F-Factors and specific liquid loads, which were similar for the mass transfer area and k_La experiments. The working temperature and pressure were the same for all experiments, thus eliminating their influence, which was not studied. The determination of the influence of physical properties was also beyond the scope of this work.

The experimental results are given in the form of tables and graphics. Special attention was accorded to the evaluation of the error associated with the measured values. Error propagation and statistical analyses were carried out in all cases to determine the level of confidence associated with the determination of the different experimental variables. The open literature rarely analyses the errors inevitably associated with these types of measurements.

This work demanded organization skills for the planning and systematic execution of the experiments in a pilot plant and in a laboratory scale apparatus. The careful selection and calibration of different measuring instruments may have been an asset for obtaining reproducible and coherent results.

The thesis is composed of 7 chapters. Each chapter can be read independently and at the end of each conclusions are drawn. Each chapter has its own nomenclature and reference list.

The thesis begins with this introduction. Basic concepts from the research field are briefly reviewed. Nevertheless, for a complete understanding of this work, knowledge of mass transfer processes is required. A literature research of published work concerned with mass transfer area and k_La in packed columns was carried out to define the method to use for the measurements and to have an overview of the works concerned with irregular packings. A conclusion of the literature review closes this introduction.

Chapter II describes the pilot plant and the analytical equipment, as well as the background for the planing and conduct of the experiments. The experiments with the wetted wall column are reported in chapter III, and their results are used for the evaluation of the mass transfer area of MELLAPAK in chapter IV. The k_La measurements with MELLAPAK are described in chapter V.

The k_La experiments were actually carried out before the mass transfer area experiments. This sequence was justified by the fact that k_La experiments were easier and safer to execute, thus being an introduction to the work in the complex pilot plant. Actually, the k_La measurements used the know-how of planning and conducting experiments, obtained beforehand with the laboratory scale apparatus with the wetted wall column.

Chapter VI gives data for the actual liquid side mass transfer coefficient k_L independent from the mass transfer area. A simple model with theoretical basis for predicting k_L for MELLAPAK 250.Y and 500.Y is proposed.

Chapter VII summarizes the work. Discussions of limitations and recommendations for future projects, as well as a new structure for MELLAPAK end this last chapter and the thesis.

All detailed information concerning the experiments and results are given in the various appendices, so that a specialist may in a short period of time understand and reproduce the experiments. In this way, the main text should be more fluent to read.

1 Presentation of the research field

The goal of this section is to introduce basic concepts and equations which will be used in this thesis. After an introduction to gas absorption, topics in mass transfer fundamentals to this work are presented. There follows brief discussion of the design of packed columns. This section ends with a description of the SULZER structured packing MELLAPAK.

1.1 Introduction to gas absorption and absorption columns

Gas absorption is an industrial unit operation in which a gas mixture has its composition changed as a liquid solvent absorbs one or more of the components of the gas mixture. Desorption or stripping is the reverse of absorption in that one or more components dissolved in the liquid solution are removed by the gas flow. The gas flows countercurrently or concurrently with respect to the solvent flowing downwards due to gravity in the absorption column. The absorption column is a vertical cylindrical item of equipment in which this mass transfer process takes place. Absorption columns have been equiped with trays. However, packings assure best gas-liquid area for the mass transfer, with minimum gas-side pressure drop. There are two types of packing: irregular (random, dumped, not structured) and structured (ordered, regular). The latter type offers lower pressure drop with higher mass transfer efficiency and capacity (section 1.3, chapter I), in addition to permitting a higher degree of confidence in predicting performance. The packings are made of different materials in order to achieve better wettability or to withstand corrosion. Figure 1.1 shows, schematically, an absorption column with its internals.

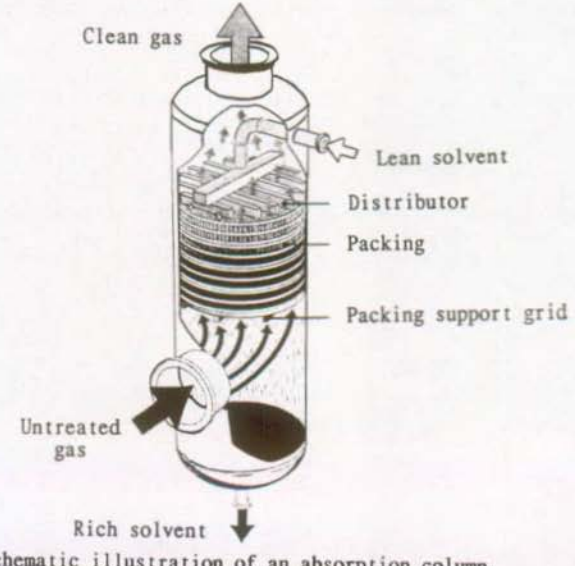

Figure 1.1 Schematic illustration of an absorption column. (courtesy of SULZER BROTHERS LIMITED).

The separation efficiency of a column depends strongly on how the liquid is spread radially as it progresses down the column. The liquid distribution is related to the packing, but also to the initial liquid distribution. An efficient initial liquid distribution is more important for irregular packings than for structured packings, since the former have more difficulty in spreading the liquid, as pointed out by Perry et al. (1990).

The liquid distributor must therefore ensure an even liquid distribution over the column section. The drip point density of the distributor determines how well this initial distribution is achieved; it depends also on the pattern of the distribution points and on the uniformity of the liquid flow from the distribution points. A drip point density of 100 points/m^2 for industrial distributors and more than 300 points/m^2 for distributors for research projects is suggested in Perry et al. (1990). The packing type, operational conditions (flow rate, range of operation) and the solvent used (physical properties and danger of plugging) determine the type of distributor to be employed.

The goal of the gas absorption can be to purify a gas before discharge to the environment (eg. removal of NH_3, CO_2, H_2S), or product recovery (eg. recovery of organic vapor mixtures -Duss and Bomio (1991), alcohols and NH_3), or the production of mixture of gases for further use in an industrial plant (eg. sweeting of a sour gas stream, ie. removal from H_2S).

Absorption of gases in a liquid solvent may occur with or without chemical reaction. Since the liquid solvent is generally water, which is the cheapest liquid solvent, physical absorption is most commonly used. Chemical reaction of the solute (absorbed gas) with the solvent, or a component thereof, increases the absorption rate. As an example, when it is desired to reduce the partial pressure of CO_2 to low levels (ppm), the absorption of CO_2 by potassium carbonate (potash) solutions is more economical than physical absorption of CO_2 in water, because the solubility of CO_2 in K_2CO_3 solutions, as well as the reaction rate, is higher, especially when this reaction is catalyzed with potassium arsenite or arsenic trioxide. Other possible "chemical" solutions are amines (MEA and DEA). However, in the case of the amines, there is a substantial temperature difference between absorber and desorber, which is likely to increase the cost of the plant (Danckwerts and Sharma (1966)).

When characterizing the flow in the column, instead of using absolute gas and liquid flowrates, the concepts F-Factor and specific liquid load are frequently employed. The F-Factor is defined with the gas velocity by:

$$\text{F-Factor} = w_G \cdot \sqrt{\rho_G} \tag{1.1}$$

where the gas velocity is given by:

$$w_G = \frac{G}{\rho_G \cdot A_c \cdot 3600} \tag{1.2}$$

The specific liquid load is defined as the liquid flowrate per column cross section:

$$B = \frac{L}{\rho_L \cdot A_c} \tag{1.3}$$

The experimental results throughout this work will be given in terms of the specific liquid load and F-Factor.

1.2 Topics in fundamentals of physical and chemical absorption

A concentration profile for binary absorption is presented in figure 1.2. In the bulk of each phase, turbulence causes a thorough mixing, and thus a uniform concentration within each phase. At the gas-liquid interface, there is a concentration equilibrium, since the interface offers in principle a negligible resisfance.

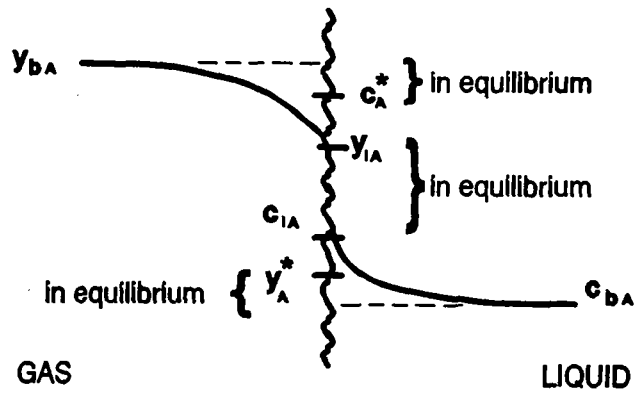

Figure 1.2 Concentration profile for binary absorption.

The absorption rate is related to the concentration driving force, as expressed by the concentration profile. The gas-liquid interface reduces the flow motion of the fluid and the slow process of molecular diffusion is the limiting process of mass transfer. The resistance to the mass transfer process is due to the transfer process from the bulk to the phase interface in the gas and from the interface to the bulk of the liquid. An absorption followed by chemical reaction changes the concentration driving force and as a consequence the concentration profile.

This section discuss the topics in mass transfer fundamentals of physical and chemical absorption which will be used further in this work.

1.2.1 Physical absorption

The mass transfer rate per unit of gas-liquid effective area is given by the following empirical correlation:

$$n = k_L \cdot (c_{iA} - c_{bA}) = k_G \cdot p \cdot (y_{bA} - y_{iA}) \qquad (1.4)$$

The absolute rate of mass transfer is therefore the product of the concentration driving force, the coefficient of mass transfer (k_L or k_G) and the effective mass transfer area. The inverse of the product of the coefficient of mass transfer and the effective area is the resistance to the mass transfer. This resistance to mass transfer depends principally on the hydrodynamics of the flow over the packing. This resistance is thus related to the packing itself (geometry and material), to the liquid and gas velocities over the packing and physical properties of the liquid and of the gas.

It is common practice to work with overall mass transfer coefficients, thus eliminating the interfacial concentrations of equation (1.4), which are difficult to determine. Hence:

$$n = k_{oL} \cdot (c_A^* - c_{bA}) = k_{oG} \cdot p \cdot (y_{bA} - y_A^*) \qquad (1.5)$$

The relationship between the overall mass transfer coefficient and the local mass transfer coefficient in the liquid-phase is given by:

$$\frac{1}{k_{oL}} = \frac{1}{k_L} + \frac{1}{k_G \cdot H} \qquad (1.6)$$

or

$$\frac{1}{k_{oG}} = \frac{1}{k_G} + \frac{H}{k_L} \qquad (1.7)$$

The Henry constant - H - is an equilibrium constant, defined as:

$$H = \frac{p_A}{c_A} \qquad (1.8)$$

where p_A is the partial pressure of component A in the gas.

The lower the solubility of the gas in the liquid, the higher is the value of the Henry constant. The concentration profile becomes steeper on the liquid side (c_{iA} further from c_{bA}) and flatter on the gas side (y_{bA} closer to y_{iA}). For high gas-in-liquid solubilities the reverse holds.

As will be explained in section 5.1, chapter V, gases which are sparingly soluble in liquid are used for the determination of k_La, to overcome the difficulty of measuring interfacial concentrations.

Since the liquid film mass transfer coefficient k_L quantifies the concentration difference in the liquid side, there have been a number of attempts to calculate its value.

The film theory of Lewis and Whiteman (1924) is the first to predict k_L theoretically. This theory proposed that the resistance to molecular diffusional mass transfer is due to laminar layers in the gas and liquid phase at the interface. The thickness of these layers would depend on the relative velocity of each phase, as obtained from fluid dynamics calculations. The interface is supposed to offer no resistance or to change with the time. The velocity of the phases at the interface is zero. The liquid phase mass transfer coefficient, k_L, for equimolecular counterdiffusion is given by:

$$k_L = \frac{D_L}{\delta_L} \qquad (1.9)$$

The above equation is also valid for unidirectional diffusion for very dilute systems. Otherwise a correction factor - the film factor - must be included, as explained in von Stockar and Wilke (1991).

Actually, in a gas-liquid contacting apparatus the gas-liquid interface is in constant movement with an elastic form. A liquid element is only for a certain time in contact with the gas, when transient mass transfer takes place. These short contact times are not sufficient to create a linear concentration profile in the boundary layer. Actually, the concentration profile becomes a function of the time. Higbie (1935), considering that all fluid elements should have the same contact period, proposed:

$$k_L = 2 \cdot \sqrt{\frac{D}{\pi \cdot t}} \qquad (1.10)$$

Instead of supposing a constant contact time, Danckwerts (1951) introduced a mathematical function describing the renewal process, in which the factor for the random surface renewal rate - s - is constant. Mathematical manipulations yield:

$$k_L = \sqrt{D \cdot s} \qquad (1.11)$$

Both equations (1.10) and (1.11) predict a dependence of the liquid phase coefficient on the square root of the diffusivity, which has been frequently confirmed by the literature (section 2.2.2, chapter I).

Chapter VI uses the penetration theory for building a semi-empirical model for predicting k_L for MELLAPAK 250.Y and 500.Y.

1.2.2 Chemical absorption

The chemical absorption reaction changes the driving forces, and raises the absorption rate by comparison with physical absorption. The absorption rate is dependent on the reaction rate and on the diffusion rate of the reaction species to the reaction zone. Levenspiel (1972) discussed the different concentration profiles resulting from different reaction velocities. The reactants, the products of the reaction, as well as the dissolved ions influence the diffusional mass transfer, the solubility and the reaction rate.

Consider the reaction: $A + z\,B \longrightarrow$ products
where:
the reactant A comes from the gas phase; the reactant B is in the liquid phase and z is the ratio of the stochiometric coefficients

The chemical reaction takes place in the liquid phase, after component A from gas is absorbed and has diffused to the reaction plane.

The reaction velocity for a reaction of m-th order in respect to A and n-th order in respect to B with a reaction rate constant of K_{mn} is:

$$r_A = K_{mn} \cdot c_A^m \cdot c_B^n \qquad (1.12)$$

The differential equations which resulted from a differential mass balance, assuming unidimensional and steady state mass transfer are:

$$D_A \cdot \frac{\partial^2 c_A}{\partial z^2} - r_A = 0 \qquad (1.13.a)$$

$$D_B \cdot \frac{\partial^2 c_B}{\partial z^2} - z \cdot r_A = 0 \qquad (1.13.b)$$

where z is the distance to the phase interface.

Different concentration profiles due to different boundary conditions and the influence of the chemical reaction on diffusion processes are possible. A mathematical solution of the differential equation systems (1.13.a) and (1.13.b), to obtain concentration profiles for all such possibilities, is difficult and sometimes impossible. A modified form of equation (1.4), incorporating an enhancement factor E representing the effects of chemical reaction, is, however, more readily soluble:

$$n = E \cdot k_L \cdot (c_{iA} - c_{bA}) \qquad (1.14)$$

The Hatta modulus is defined by:

$$Ha = \frac{1}{k_L} \cdot \sqrt{\frac{2}{m+1} \cdot K_{mn} \cdot D_A \cdot c_{A_i}^{(m-1)} \cdot c_{B_b}^{n}} \qquad (1.15)$$

and expresses the ratio of the maximum chemical reaction rate to the maximum diffusional mass transfer process. The enhancement factor for an instantaneous reaction, using the film theory, is given by:

$$E_i = 1 + \frac{D_B}{D_A} \cdot \frac{c_{B_b}}{z \cdot c_{A_i}} \qquad (1.16)$$

The enhancement factor of a second order irreversible reaction may be determined graphically, as a function of the Hatta modulus and of the enhancement factor for an instantaneous reaction, using an approximate solution proposed by van Krevelen and Hoftijzer (1947.a).

Effective areas for mass transfer in gas-liquid systems can be experimentally determined by absorption followed by chemical reaction. Such a chemical method demands that the absorption rate be independent of k_L. The absorption rate is in this case directly proportional to the effective area. The method is explained mathematically in section 1.2, chapter III.

Effective areas and $k_L a$ may be simultaneously obtained with the "Danckwerts plot method". This method uses chemical reactions which have absorption rate dependent on the k_L. The absorption rate is measured for different reaction rate constants by adding small amount of catalyst. The square of the absorption rate is plotted versus the product of the rate constant with the concentration of the reactant in the liquid phase. From the slope of the line and its ordinate, the values of the effective area and of $k_L a$ are respectively determined (Sharma and Danckwerts (1970)). Very slow chemical reactions may be used for determining $k_L a$, if the concentration of the absorbed substance in the bulk of the liquid is null.

1.3 The design of absorption columns

There are three different types of problem specification with absorption columns. In the design calculation, it is desired to determine the dimensions and configuration of the packed column which would effect the required reduction of the mole fraction of a gaseous compound in a gas mixture. The performance calculation of an existing column is carried out to evaluate the composition of the gas flow at the outlet after a change of any parameter which influences the mass transfer process. It is actually a simulation problem. The third problem situation is the evaluation from experimental data, of parameters for the first two types of problems mentioned above. This section discusses aspects of design calculations which will be referenced later in this thesis. Sections 1.2 in chapter IV and V address the third type of problem specification.

The column diameter for countercurrent operation is determined by the liquid-gas ratio L/G and the gas flowrate, as there is a minimum column diameter below which countercurrent operation is not possible, ie. the column is flooded. Closer to flooding conditions, the pressure drop and liquid holdup increase rapidly and the efficiency decreases rapidly, until there is a lack of stability of column operation.

The prediction of how far the operating conditions are from flooding is a source of controversy in the literature, as explained by Fair and Bravo (1990) and Kunesh (1987). The distance from flooding is usually defined, for a given liquid flowrate, in terms of the ratio of the actual vapor superficial velocity to the maximal possible vapor superficial velocity, when countercurrent operation is no longer possible. This approach is usually found in standard texts in chemical engineering, such as McCabe and Smith (1976) and Grassmann and Widmer (1974). However, it is difficult to determine the maximum possible vapor superficial velocity.

The capacity limit for the SULZER structured packing MELLAPAK is defined by Spiegel and Meier (1987) as "the vapor load where a pressure drop of 10 mbar/m occurs". The "% capacity" is the ratio of the vapor velocity at operating conditions to the maximum vapor superficial velocity for the same L/G ratio. Fair and Bravo (1990) do point out that it is possible that for high liquid loads, the maximum capacity could occur at a lower pressure drop. The range of variation of L/G in this work is within the range of variation of the ratio L/G implemented by the software SULPAK (SULZER BROTHERS LIMITED (1989)) to perform capacity calculations for MELLAPAK. The empirical correlations on which these calculations are based uses data given by Spiegel and Meier (1987). Therefore, the "capacity approach" will be used throughout this work.

Columns tend to be designed with 70 to 75 % of flooding, but with F-Factors not higher than 3.5 (Meier et al. (1979)). The capacity limit is about 5 to 10 % lower than the flooding point (Spiegel and Meier (1987)). Therefore, columns tend to be designed at 80 % of capacity.

The HETP method has been frequently used for determining the column height. The HETP method considers that the column is composed of a series of stages with a HETP (height equivalent to a theoretical plate - or stage) constant over the column. The method of determination of the NTP (number of theoretical plates - or stages) is presented in books such as McCabe and Smith (1976) and Grassmann and Widmer (1974). The column height is then:

$$h = HETP \cdot NTP \tag{1.17}$$

The HTU-NTU method developed by Chilton and Colburn (1935), for the determination of the packing height, is more fundamental. This method results from a differential mass balance in the column, with the assumptions of plug flow for the gas and liquid phase and of even gas and liquid distributions over the column cross section. The method is simplified when mass transfer coefficients, especially overall mass transfer coefficients, are independent of the concentration.

The column height for liquid side controlled systems, using the volumetric mass transfer coefficient as in equation (1.4), is:

$$h = HTU_L \cdot NTU_L \tag{1.18}$$

where:

$$HTU_L = \frac{B}{k_L \cdot a} \cdot \frac{1}{3600} \tag{1.19}$$

and

$$NTU_L = \int_{x_\alpha}^{x_\omega} \frac{(1-x)_{i,m}}{(1-x).(x_i-x)} \cdot dx \tag{1.20}$$

with the term:

$$(1-x)_{i,m} = \frac{(1-x_i) - (1-x)}{\ln \frac{1-x_i}{1-x}} \tag{1.21}$$

The equations to calculate the column height with the overall volumetric mass transfer coefficient, as in equation (1.5), not requiring thus the knowledge of concentrations at the gas-liquid interface, are given by:

$$h = HTU_{oL} \cdot NTU_{oL} \tag{1.22}$$

where:

$$HTU_{oL} = \frac{B}{k_{oL} \cdot a} \cdot \frac{1}{3600} \tag{1.23}$$

and

$$NTU_{oL} = \int_{x_\alpha}^{x_\omega} \frac{(1-x)^*_m}{(1-x).(x^*-x)} \cdot dx \tag{1.24}$$

with the term:

$$(1-x)^*_m = \frac{(1-x^*) - (1-x)}{\ln \frac{1-x^*}{1-x}} \tag{1.25}$$

The integral of equation (1.24) can be evaluated graphically or numerically. Both are troublesome. Therefore, the equation (1.25) and the

term (1-x) are, when possible, assumed to be equal to unity, which is true for dilute systems (small liquid mole fraction). A direct integration of equation (1.24) is also straightforward, when the equilibrium and operating lines are assumed to be straight. Simple approximate procedures for determination of NTU where the operating and equilibrium lines are curved, are given by von Stockar and Wilke (1991).

The packing height can also be evaluated with the gas-phase height of a transfer unit and gas phase number of transfer units if the mass-transfer is gas-side controlled. These expressions are also given by von Stockar and Wilke (1991).

1.4 The SULZER structured packing MELLAPAK

The structured sheet metal packing MELLAPAK was developed by the company SULZER BROTHERS LIMITED (in Winterthur, Switzerland) and was introduced to the market in the second half of the 1970's (Meier et al. (1977)). MELLAPAK 250.Y offers higher separation efficiency, with higher capacity and less pressure drop, than Pall rings, as measured by Meier et al. (1977). Irregular packings also offer declining efficiency as the column diameter and height are increased. This is due to channeling and wall flow. As a result, repacking existing columns with MELLAPAK improves separation efficiency. The catalog of SULZER BROTHERS LIMITED (1991) presents industrial application of MELLAPAK in separation columns for distillation and absorption processes.

The MELLAPAK packing is made of corrugated metal sheets with perforations, arranged such that the gas and the liquid flowing between adjacent sheets undergo periodic redistribution within the packed bed. MELLAPAK has similar geometry to the SULZER metal gauze packing, which was studied by Zogg (1972) and Bereiter (1975). The adjustable geometric parameters are the slope angle of the corrugation and the corrugation height (Figure 1.3). As a result, different packing geometric areas are obtained.

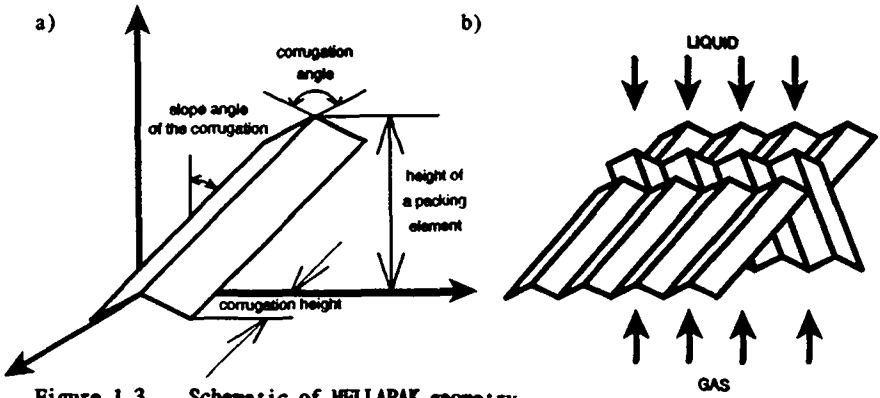

Figure 1.3 Schematic of MELLAPAK geometry.
(a) important geometric parameters.
(b) sheets forming flow channels.

The MELLAPAK type is identified by a number and a letter. The number corresponds to the packing specific geometric surface area, and the letter Y and X after the number corresponds to the slope angle of the corrugation, which can be 45° and 30° respectively. The higher the specific geometric area, the higher the separation efficiency, but the lower the capacity. MELLAPAK 250.Y is the most used type, because it offers the most usually suitable compromise between high separation efficiency and high capacity values.

Different materials are used to manufacture MELLAPAK. This work employed only metal packings, the most widely used. Figure 1.4 shows the three types of MELLAPAK used in this work.

Figure 1.4 Three different types of the SULZER structured packing MELLAPAK - 125.Y, 250.Y and 500.Y.

The performance characteristics of the packing MELLAPAK are described by Spiegel and Meier (1987). This publication presents efficiency, pressure drop and capacity curves for various types of MELLAPAK. A correlation for the gas side mass transfer coefficient $k_G a$ is proposed. Data from this publication was used by SULZER BROTHERS LIMITED (1989) in the development of the software SULPAK to perform capacity calculations with MELLAPAK. This software was used in this work.

This work decided to carry out $k_L a$ and effective area measurements with MELLAPAK, due to the broad utilization of this packing. As it will be pointed out in section 2, published measurements with structured packings seems to be scarcely available.

2 State of art of the research field related to this work.

This section presents a literature review of the specific mass transfer area (section 2.1) and of the volumetric mass transfer coefficient - $k_L a$ - (section 2.2) of packed columns with structured and irregular packings. In each section, this review breaks down into two parts: first, experimental methodologies already used for obtaining mass transfer area (section 2.1.1) and $k_L a$ (section 2.2.1) data are presented; In a second part, correlations derived from experimental and theoretical work for mass transfer area (section 2.1.2) and $k_L a$ (sections 2.2.2) are listed. The accuracy of the correlations is discussed.

Based on the literature survey, in section 2.3, the relevance of this thesis is defined, the validity of employed experimental methodologies for measuring mass transfer areas and $k_L a$ are discussed and information which is used in subsequent chapters is introduced.

2.1 Literature review of mass transfer area of packed columns

2.1.1 Measurements of mass transfer area of packed columns

A specific area is defined as the available area per packing volume. In a packed column, apart from the specific area effective for mass transfer, other specific areas are recognized:

a)	the specific geometric area of the packing	a_p
b)	the specific wetted area of the packing	a_w
c)	the specific gas-liquid interfacial area	a_i
d)	the specific effective area	a_e
	for physical mass transfer	
	for chemical mass transfer	

Methods for measuring these areas and relationships between them are presented below. This analysis is justified by the fact that the data available in the literature are not always necessarily related to the effective mass transfer area of interest. Nevertheless, these data have been used for design and analysis of effective area of different mass transfer processes in separation columns equipped with packings.

The measurement of the specific geometric area of a packing is straightforward. A method for measuring this area, which was used in this work, is given in appendix B (topic 2.b, step 8). The specific geometric area is not only dependent on the nominal size of the packing, but also on its shape. As an example, 25 mm Intalox saddles offer a specific geometric area of 206 m^2/m^3, whereas 25 mm Berl saddles have a specific geometric area of 250 $m^2/^3$ (Perry (1984)). However, the geometric area of the packing is not a design parameter.

Values of the specific geometric area, and consequently of the specific effective area, may be influenced by the packing density of irregular packings, which depends on the method of packing the column. With this argument, Sahay and Sharma (1973) justify why their values for effective

areas of 25 mm ceramic intalox saddles are about 25 % lower than those from Doble (cited in Danckwerts and Sharma (1966)). The authors attribute this to a 10 % lower packing density of their column.

The wetted area of the packing is defined by the part of the geometric area over which there is a liquid film. It may be measured using the dye technique. This method was employed by Mayo et al. (1935), who analyzed the liquid flow and wetting in 13 and 25 mm ring packings made of paper. However, paper packings exhibit a capillary effect not necessarily present in packings made of other materials. This limits the use of the dye technique. Another method for measuring wetted area is suggested by Andrieu and Lespinasse (1973). The method consists in deposing a silver layer of constant thickness over a glass packing. The layer will be dissolved by dilute nitric acid as it flows over the packing. The experimental procedure is troublesome and as for the measurements with the dye technique may only be valid for the same packing material of the original investigation.

The wetted area depends on the surface tension interaction between the liquid and the packing. Organic solvents, having lower surface tension, present excellent wettability, and the wetted area and the geometric area tend to be equal. However, aqueous solutions, which are widely used, have a wettability strongly dependent on the characteristics of the packing surface. According to the values of critical surface tension published by Onda et al. (1967), aqueous solutions present decreasing wettability over glass, ceramic and plastic packing surfaces in that order. Furthermore, the state of the surface has a decisive influence on wettability. The wetted area can increase significantly with an appropriate packing material and shape, surfactants and a physical or chemical surface treatment. Hüttinger and Brauer (1982) give examples of the influence of these variables on the HETP of packed columns. Thus, the difference between wetted and geometric area is frequently non-negligible.

Dharwadkar and Sawant (1985) show that for aqueous solutions, 38 mm Intalox saddle ceramic packings offer an effective area 40% higher than polypropylene Intalox saddles of the same size. This increase is expected as ceramic packings are better wetted by aqueous solutions than are polypropylene packings. Linek et al. (1984) rendered plastic packing surfaces chemically hydrophilic and obtained effective areas 40 to 130 % higher than those of untreated packing. The effective areas obtained with such hydrophilic packings are similar to those of well wetted metallic or ceramic packings of the same size.

A change of the packing size changes the wetted area differently than the effective area for mass transfer, as explained by Shulman et al. (1955.b). They point out that "wetted areas increase as packing size decreases. The effective area, however, is the smallest for the smallest packings in spite of the fact that they possess the largest total surface and wetted area". The authors explain that "the small packings were found to have very large static holdups which exist in the packing as pockets of almost stagnant water. This water can account for the large wetted area, but is practically useless for absorption, because it comes to equilibrium with the gas very rapidly. In the larger packings there are fewer points of contact and resulting crevices, and so the water must spread out over the surface and the effective area is more closely related to the wetted area."

The specific gas-liquid interfacial area is defined by the area of the

gas-liquid interface per packing volume. It may not be obtained by measurements. This area results of the packing wettability and of the gas-liquid interaction, strongly influenced by the form of the packing geometry. The interface can consist of a liquid film over the packing or of droplets, bubbles and extra areas. Hüttinger and Brauer (1982) point out that by the use of packings which force the formation of droplets (eg. Telleretes and NSW-packing) instead of packings which tend to form liquid film (eg. Raschig rings and Pall rings), the poor wettability becomes an asset, improving mass transfer in the columns by up to 15%. Droplets increase the interfacial area significantly.

Bravo and Fair (1982) point out that "the effective interfacial area may differ from the actual interfacial area". The possible presence of stagnation pockets (or zones) during physical absorption, basically present with irregular packings, reduce the effective interfacial area for mass transfer. Stagnation pockets are regions saturated with the dissolved gas and the concentration driving force tends to zero as a result of little or no turbulence, as pointed out by Bergbauer et al. (1979) and Murthy and Rao (1979). The stagnation pockets result from the liquid held between packing elements and from slow thin liquid films. Therefore, the importance of stagnation pockets may be related to both size and shape of the packing. Puranik and Vogelpohl (1974) think that for irregular packings with nominal size greater than 19 mm, the percentage of inactive effective area due to stagnation pockets, for physical absorption, is negligible.

Values of the specific effective area for physical and for chemical mass transfer, and of the difference between these values, are requested since gas absorption may occur with or without chemical reaction. Unfortunately, a reliable method for directly measuring effective areas for mass transfer during physical absorption in packed columns was not found, as shown below.

Shulman et al. (1955.b) claim to obtain effective area values by dividing $k_G a$ data from NH_3 absorption experiments by k_G values measured with the vaporization of packings (raschig rings (13mm, 25mm and 38mm) and Berl Saddles (13mm and 25mm)) made of naphthalene into air. This method - sublimation method - causes a change of the packing's surface and structure. The packing in an ordinary absorption process acts to bring the phases into contact, but should not be subject to changes. Moreover, Yoshida and Koyanagi (1958), using the results of Shulman et al. (1955.b), explain that "the effective areas in packed columns used for vaporization are larger than those for absorption columns, because semi stagnant liquid pockets may be effective for vaporization but relatively ineffective for absorption". Therefore, the use of the sublimation method may not be suitable for obtaining actual values of effective areas for physical absorption.

Yoshida and Koyanagi (1958) publish values for mass transfer area. The absorption of pure CO_2 into water and methanol is used. Table 1.6 in section 2.2.1 lists characteristics of the packing and column employed in their work. The authors define a liquid Reynolds number for packed columns which they consider to be equal to a Reynolds number in bead columns, provided that "a packed and a bead column of an equal height show equal values of the number of liquid phase transfer units for the same system at a given temperature" and that "the spheres in the bead column are of the same size as the packings in the packed column". The values of effective area are obtained by comparing the Reynolds numbers at given values of the number of transfer units in the packed and bead column.

The method of determining HTUG data for comparing to that produced by a column packed with a thoroughly wetted porous packing was used by Echarte et al. (1984) for evaluating mass transfer area. The authors used data from water cooling experiments, rather than ammonia or methanol absorption in water since the former is "a source of gas-side mass transfer coefficient", without the inconvenience that the system "may induce a change in the wettability of the packing". The precision and validity of the methods above for estimating effective areas is doubtful.

An indirect estimative of effective area of structured packings is suggested by Fair and Bravo (1987). The authors expect that "mass transfer coefficients for corrugated gauze packings should be directly applicable to corrugated sheet metal or plastic packings of the same geometry and for the same flow and system parameters". However, for obtaining effective area values, a very strong assumption is made in that the effective area of metal gauze packings is considered to equal the wetted and geometric area. The authors are not self-consistent, since Bravo and Fair (1982) recognize that "*the value of the effective area is composed not* only by the wetted area over the packing but also by the area provided by suspended and falling droplets, gas bubbles within liquid puddles, ripples on the liquid film surface, and any contribution from film falling on the walls of the column". All these facts do contribute decisively to create more effective mass transfer area than the wetted area. Therefore, it is not reasonable to assume that metal gauze packings may not present more effective area than the fully-wetted surface. It is regrettable though that their values may not be valid, especially since no other published values for the effective area of structured packings was found.

Specific effective areas for chemical absorption is determined with the use of absorption followed by a chemical reaction, in which the absorption rate is independent of the mass transfer resistance in the liquid phase. There are also works in which effective areas were determined simultaneously with the $k_L a$ using the "Danckwert's plot method" (section 1.2.2). Landau et al. (1977) state that chemical methods are the only ones which "do not require verification by another kind of measurement and which can yield from a single measurement an overall value of the interfacial area". The review paper of Guillen et al. (1982) expresses the same opinion. Landau et al. (1977) draw attention, however, to the necessity of a careful choice of a "suitable reaction" and to the extensive experimental time required.

The difference between the effective areas for chemical absorption and physical absorption is hard to predict. The influence of stagnation pockets with chemical absorption may be less than for physical absorption. Thus, the effective area may be smaller for physical absorption. During chemical absorption, concentrations profiles are generally steeper, with greater driving forces. However, reactions with evolution of heat or with products that inhibit the reaction may change the concentration profile and the effective area. Yoshida and Miura (1963) believe that effective areas for chemical and physical absorption are equal for a rapid second order irreversible reaction, when "the absorption rate is controlled by diffusion of the solute gas and the reactant through the liquid film to the thin reaction zone. This means that the absorption rate at the moving part of the interface is so high that absorption at the semi stagnant part becomes insignificant with that of the moving part". For absorption with a moderately fast first order reaction, the whole interfacial area is effective and is different from the effective area for physical absorption.

Several chemical systems have been used for evaluating the mass transfer area for different gas-liquid systems in aqueous solutions (Laurent et al. (1975), Sharma et Danckwerts (1970) and Sridharan and Sharma (1976)) and also in organic solvents (Allenbach et al. (1977)). Laurent and Charpentier (1974) are of the opinion that chemical methods produce values independent of the chemical system (organic or aqueous solvents). Since many gases have higher solubility and diffusivity in organic solvents than with water and, in addition, may be associated with high heats of reaction, which would make it difficult to maintain isothermal conditions, many reactions for the measurement of effective areas in organic solvents may not be suitable from the point of view of kinetics (Sridharan and Sharma (1976)).

Table 1.1 overleaf lists those chemical systems which have been used for determining the mass transfer area in packed columns. The packings tested with the respective column are listed in the table 1.2. Explanations of symbols used in the tables follow. The experiments were basically carried out at ambient pressure and at temperatures of between 20 to 30 °C. All experiments employ irregular packings.

In principle, with chemical systems, it is very difficult to change physical properties without loosing control over the reaction rate and over the other physical properties. Some works try to vary the viscosity of the solution with carboxymethyl cellulose (Lee and Kim (1982) and Sedlies et al. (1987)) and sugar (Rizzuti and Brucato (1989)). Surfactants such as Triton X-100 (Lee and Kim (1982)) and Tween 20 from Serra Co. (Seddlies et al. (1987)) seem to change the surface tension without acting on other physical parameters. However, Seddelies et al. (1987) did have technical problems with reduced surface tension due to serious foam formation.

The sulfite method, employing the oxidation of Na_2SO_3, has been frequently proposed for giving estimates of various mass transfer parameters, such as effective areas and $k_L a$, according to the range of reaction rate. Different cobalt or copper concentrations define these ranges. There is controversy regarding the reaction orders with respect to sulfite, catalyst (copper or cobalt) and especially oxygen (Linek and Vacek (1981)). Linek et al. (1981) recommend that "it is not justifiable to adopt kinetic constants of the reaction reported in the literature; the constants must be determined experimentally separately for each production charge of sulfite". Delaloye (1986) carries out such experiments with a wetted wall column to verify the kinetics of the reaction and no reproducible results are obtained. In view of the results, further use of the method is not recommended. The reaction kinetics may be very sensitive to trace impurities, so that reproducibility is almost impossible. Nevertheless, effective area values of Danckwerts and Rizvi (1971) seem to be consistent with those of Danckwerts and Guillham (1966), although different methods are used.

The absorption of CO_2 diluted with air into NaOH solutions is frequently used. Sharma and Danckwerts (1970) consider that the reaction is a "very convenient system to use". The authors do point out that "this system cannot be easily used when effective areas are higher than 10 cm^2/cm^3 because of the evolution of heat". However, packed columns present lower values of specific effective areas. The applicability of this reaction for obtaining effective area values is subject of chapter III.

Table 1.1 **Measurements of mass transfer area using chemical methods. (Chemical methods employed)**

Reference	Chemical system used
Bennett - Goodridge (1970)	Absorption of trace quantities of radioactive $C^{14}O_2$ in NaOH solutions.
Bornhütter - Mersmann (1991)	Absorption of CO_2 into a solution of NaOH.
Danckwerts - Guillham (1966)	Absorption of pure CO_2 into different solutions (Na_2SO_4; buffer solutions of K_2CO_3 with $KHCO_3$ and KClO; NaOH solutions with Na_2SO_4).
Danckwerts and Rizvi (1971)	Absorption of O_2 from air into Na_2SO_3 with $CoSO_4$ as catalyst.
Dharwadkar - Sawant (1985)	Absorption of CO_2 in air into solutions of NaOH with Na_2CO_3.
Gianetto and Sicardi (1972)	Absortion of CO_2 in air into NaOH solutions.
Jhaveri and Sharma (1968)	Absorption of O_2 into different solutions (cuprous chloride and sodium dithionite). Absorption of iso-butylene in aqueous H_2SO_4.
Joosten - Danckwerts (1973)	Absorption of pure CO_2 into carbonate buffer solutions.
Kolev (1973)	Absorption of CO_2 in air into solutions of NaOH.
Krötzsch and Kürten (1979)	Absorption of O_2 from air into Na_2SO_3 solutions with $CoSO_4$ as catalyst.
Lee and Kim (1982)	Absorption of CO_2 in air into buffer solutions (K_2CO_3, $KHCO_3$, KCl and NaOCl).
Linek et al. (1984)	Absorption of CO_2 in air into solutions of NaOH.
Linek et al (1974)	Absorption of pure O_2 into Na_2SO_3 solutions with $CoSO_4$ as catalyst.
Merchuk (1980)	Absorption of CO_2 in air into NaOH solutions.
Mohunta et al. (1969.a)	Absorption of CO_2 in air into a solution of NaOH.
Neelakantan et al. (1982)	Absorption of pure O_2 in aqueous solutions of ammonium sulfite.
Richards et al. (1964)	Absorption of pure CO_2 into carbonate buffer solutions with arsenious oxide ions.
Rizzuti and Brucato (1989)	Absorption of pure CO_2 into a buffer solution (K_2CO_3 and $KHCO_3$) with arsenious oxide ions.
Sahay and Sharma (1973)	Absorption from O_2 from air in diothionite solutions and absorption of lean CO_2 in NaOH and diethanolamine solutions.
Sedelies et al. (1987)	Absorption of O_2 into Na_2SO_3 solutions.
Vidwans and Sharma (1967)	Absorption of pure CO_2 into aqueous solutions of NaOH and MEA.
Yoshida and Miura (1963)	Absorption of CO_2 in air into solutions of NaOH and KOH.

Table 1.2 **Measurements of mass transfer area using chemical methods. (Packing type and equipment used for investigation)**

Reference	Packing			Column	
	type	sizes [mm]	material	diameter [mm]	height [mm]
Bennett - Goodridge (1970)	RR	9.5	ceramic	76	610
		6		50	
Bornhütter - Mersmann (1991)	PR	50	plastic	1000	***
	HF	50,90	plastic		
		50	steel		
	EP	number 3	plastic		
	SF				
Danckwerts - Guillham (1966)	RR	38	ceramic	460	3650
Danckwerts and Rizvi (1971)	RR	38	ceramic	500	4000
	PR		plastic		
	IS	50			
	IS	38	ceramic		
Dharwadkar - Sawant (1985)	PR	38	inox	385	1155
			plastic		
		50	steel		
			plastic		
	IS	38			
Gianetto and Sicardi (1972)	RR	6	ceramic	60	300
	BS				
	SP		glass		
Jhaveri and Sharma (1968)	RR	9.5	ceramic	44	250 to 600
Joosten - Danckwerts (1973)	RR	13	ceramic	110	***
	IS				
Kolev (1973)	RR	25x25x3	ceramic	190	1900
		25x16x3			
		25x11x3			
		25	plastic		
	IS	35	ceramic		
		50		500	
		70			
	PR	50	plastic		
	RR	25		190	
Krötzsch and Kürten (1979)	RR	15	metal	300 and	800 and
	PR	15,25,35,50		500	1500
		25, 35, 50	ceramic		
		25, 50	plastic		
	TR	25	plastic		
Lee and Kim (1982)	#	9.5,13	ceramic	120	500
			plastic		
Linek et al. (1984)	PR	15,25,35,50	plastic	290	1000
Linek et al. (1974)	RR	15	plastic	143	680
			ceramic		
Merchuk (1980)	RR	6	plastic	100	600
	FR	8	ceramic		
	mixture of spirals and flat rings				

Table 1.2 (continued).

Reference	Packing			Column	
	type	size [mm]	material	diameter [mm]	height [mm]
Mohunta et al. (1969.a)	RR	9.5,13,19	***	102	***
Neelakantan et al. (1982)	RR	9	glass	50	***
Richards et al. (1964)	RR	13	ceramic	102	254
Rizzuti and Brucato (1989)	RR	10	glass	80	580
Sahay and Sharma (1973)	RR	25	ceramic plastic	200	870
	IS		ceramic plastic		
	PR		inox plastic		
Sedelies et al. (1987)	PR	25	plastic	***	3000
Vidwans and Sharma (1967)	RR	9.5	ceramic	43.7	460 to 1310
	RR IS	9.5 13	ceramic	100	610
	RR	9.5	ceramic	200	920
Yoshida and Miura (1963)	RR	25 13	porcelain	120	762

List of packing types

code	description
BS	Berl saddles
EP	Envipak
FR	Flat rings
HF	Hiflowring
IS	Intalox saddles
PR	Pall rings
RR	Raschig rings
SF	Snowflake
SP	Spheres
TR	Tellrettes

Notes

*** information not given

not clearly explained

2.1.2 Predictions of mass transfer area of packed columns

In this section, correlations from experimental and theoretical work for predicting specific mass transfer area of packings are listed chronologically. This sequence is adopted since it is interesting to follow an evolution of the proposals of the influence of physical properties and of different packing types and materials. Details of the experimental works cited in this section, which used the chemical method, are listed in tables 1.1 and 1.2. However, it was not intended to explain how the correlations were developed. In most cases, the models are functions of dimensionless numbers. These numbers are defined in the table 1.3 with a physical interpretation. All physical properties are related to the liquid. In the end of this section, the predictive power of the correlations is discussed.

Table 1.3 Dimensionless numbers.
(all physical properties are related to the liquid).

Name	Definition	Physical interpretation
Capillary	$Ca = \frac{\mu . w_L}{\sigma}$	ratio of viscous forces and surface tension forces.
Froude	$Fr = \frac{w_L^2 . a_p}{g}$	ratio of inertia and gravity forces.
Galileo	$Ga = \frac{d_p^3 . g_p}{\nu^2}$	ratio of bouyancy and viscous forces.
k_σ	$k_\sigma = \frac{\rho . g}{a_p^2 . \sigma}$	ratio of gravity and surface tension forces.
Reynolds	$Re = \frac{w_L}{a_p . \nu_L}$	ratio of inertia and viscous forces.
Schmidt	$Sc = \frac{\mu}{\rho . D}$	ratio of molecular momentum and mass transfer diffusivity.
Weber	$We = \frac{w_L^2 . \rho}{\sigma . a_p}$	ratio of inertia and surface forces.

Note: The Reynolds number may be defined with the packing size in the numerator instead of the packing specific area.

The first correlations for the ratio of wetted area to the geometric area use data from the dye technique experiments: those of Fujita and Sukuma in 1956, and Hikita in 1960. Both correlations are cited by Mohunta et al. (1969.a). Shulman et al. (1955.b) with the Raschig rings naphthalene packings - sublimation method - (section 2.1.1, chapter I) also suggest an equation for the ratio of the wetted to the geometric area. Mada and

coworkers in 1964 (cited in Echarte et al. (1984)) also propose a correlation based on the experimental data of Shulman (1955.b) and Yoshida and Koyanagi (1962) for aqueous and organic liquid systems flowing over beds of Raschig rings and Berl saddles. For Echarte et al. (1984), the equation "is applicable only to wetting systems".

The frequently-cited work of Onda et al. (1967) gives a dimensionless expression for the wetted area.

$$\frac{a_w}{a_p} = 1 - \exp\left[-1.45 \cdot \left[\frac{\sigma_{cr}}{\sigma}\right]^{0.75} \cdot Re^{0.1} \cdot Fr^{-0.05} \cdot We^{0.2}\right] \qquad (1.26)$$

The authors have tried to consider the wettabilty of the packing. Hüttinger and Brauer (1982) consider that the Onda correlation does not correctly predict the influence of the surface tension. The above equation is frequently used for predicting effective areas. The review of Laurent and Charpentier (1974) state that the above correlation is the most general one to use with a maximum error of about 20%, except for Pall rings, where it is conservative with underestimation of 50%, because a part of the liquid is obliged to disperse in the gas phase as droplets, thereby increasing the effective area.

Semmelbauer (1967), in a theoretical work, propose the following correlation for the effective area:

$$\frac{a_e}{a_p} = C_1 \cdot \left[\frac{w_L \cdot d_p}{\nu}\right]^{C_2} \cdot \left[\frac{\rho \cdot d_p^2}{\sigma}\right]^{0.5} \qquad (1.27)$$

where the coefficients C_1 and C_2 have values of 0.00608 and 0.455 respectively for Raschig rings and 0.00755 and 0.455 for Berl saddles. Deviations were estimated as up to 40 %. Dividing the above equation of Semmelbauer (1967) by the equation of Onda et al (1967), Jackson and Marchello (1970) obtained the ratio of the effective area to the wetted area in terms of dimensionless numbers. However, the equation of Semmelbauer uses data from experimental works of wetted area and indirect determination of effective areas to evaluate the coefficient and the exponent.

The equation (1.28) of Mohunta et al. (1969.a) seems to be the first to correlate actual effective area measurements with the use of the chemical method (see tables 1.1 and 1.2). However, no physical property was varied. There is agreement with the measurements cited in the review of Danckwerts and Sharma (1966). The equation is given below with the Reynold's number defined in table 1.3. The values predicted are about 20 % smaller than those given by the Hikita and Onda correlations.

$$\frac{a_e}{a_p} = 0.175 \cdot Re^{1/3} \qquad (1.28)$$

The data from Gianetto and Sicardi (1972) (see tables 1.1 and 1.2) of the ratio of the effective area to the geometric were plotted against the ratio of the pressure drop with liquid flow to the pressure drop in the absence of liquid flow. The idea is that this ratio of pressure drops is influenced by interaction between the gas and liquid flows, and by the changes in the void fraction of the column. The ratio of the effective area to the geometric area increased asymptotically to about 0.19. The authors did not derive any analytical relationship.

Kolev (1973), using data from him (see tables 1.1 and 1.2) and from others, proposes a model, in which the liquid surface tension accounts for wettability. The author claims that the equation correlates the data with a deviation of ± 20 %.

$$\frac{a_e}{a_p} = 0.583 \cdot k_\sigma^{0.49} \cdot Fr^{0.196} \cdot (a_p \cdot d_p)^{0.42} \qquad (1.29)$$

A review article collecting data obtained by different methods was published by Puranik and Vogelpohl (1974) suggesting the generalized correlation:

$$\frac{a_e}{a_p} = 1.045 \cdot Re^{0.041} \cdot We^{0.133} \cdot \left[\frac{\sigma_{cr}}{\sigma}\right]^{-0.182} \qquad (1.30)$$

The authors assume a relationship between effective area and hold up, which is composed of a static and a dynamic hold up, as already suggested by Shulman et al. (1955.a). The experimental findings from Bornhütter and Mersmann (1991) do not confirm this assumption. Puranik and Vogelpohl (1974) also propose a term to be added to equation (1.30) evaluating the effective area in chemical absorption. The term is for the prediction of the effectiveness of stagnation pockets during chemical absorption. This term results from theoretical reasoning regarding the Hatta modulus (equation (1.15)) and k_L with and without chemical reaction. This term is considered unsuitable by Baldi and Sicardi (1975), "since it does not take into consideration the absorption capacity of the liquid phase. In fact the semi stagnant liquid pockets can be effective to mass transfer or not, depending on the ratio between the absorption capacity and the rate of absorption".

Murthy and Rao (1979) use the two hold-up models (vertical surface and random angle models) suggested by Davidson (1959) to develop their two correlations. The model is for practical usage difficult, since the independent parameter is not a physical property or an operating condition (liquid or gas flows), but a volume of a sphere of equivalent volume to the liquid hold up, calculated either for the vertical surface or for the random angle model from Davidson (1959). A constant term given by $(0.5/d_p)$ should be added when the effects of absorption followed by chemical reaction are to be accounted for.

Zech and Mersmann (1979) modeled the liquid flow over the packing as composed of rivulets. With data of mass transfer coefficients for liquid phase controlled systems and with theoretical reasoning, however, without the use of effective area data, the authors proposed:

$$\frac{a_e}{a_p} = C_1 \cdot Re^{0.5} \cdot \left[\frac{\rho \cdot g \cdot d_p^2}{\sigma}\right]^{0.45} \cdot (a_p \cdot d_p)^{-0.5} \qquad (1.31)$$

with the constant C_1 equal to 0.0222, 0.0155, 0.0085 for Berl saddles, Raschig rings and spheres respectively.

Lee and Kim (1982) (tables 1.1 and 1.2) correlated their experimental results, which were obtained for a range of surface tension and viscosity values.

$$\frac{a_e}{a_p} = 1.140.10^{-4} . w_L^{0.25} . (1-\varepsilon)^{-0.43} . d_p^{-1.03} . \sigma_{cr}^{1.04} . \mu^{0.38} . \sigma^{-0.28} \qquad (1.32.a)$$

With dimensionless groups, the authors propose:

$$\frac{a_e}{a_p} = 1.69.10^2.\left[w_L.\frac{\mu}{\sigma}\right]^{0.35}.\left[\frac{\sigma_c}{\sigma_{ref}}\right]^{1.03}.\left[a_p\ .\ d_p.(1-\epsilon)^{1/3}\right]^{-1.88} \quad (1.32.b)$$

where σ_{ref} is the critical surface tension of glass.

It should be noted that the exponents of the different parameters are different in equations (1.32.a) to (1.32.b), as it is the case for the exponent of the liquid velocity, which changes from 0.25 to 0.35.

Bravo and Fair (1982), correlated data from a data bank consisting mainly of results with test systems from distillation, but also from absorption. No description of these test systems and the assumptions made is given. The model is based on randomly arranged packing elements and applies to others as long as the packings have similar shapes and identifiable nominal diameters. A safety factor of 1.6 is recommended for 95 % confidence in design. This model is the first and the only one to admit the influence of the gas flow rate and of the packing height.

$$\frac{a_e}{a_p} = 0.02533\ .\ (Ca_L\ .\ Re_G)^{0.392}.\sigma^{0.5}.h^{-0.4} \quad (1.33)$$

with $Re_G = \dfrac{6.G.\rho_G}{a_p.\mu_G.A_c}$

The product $(Ca_L.Re_G)$ is defined as the loading parameter.

The fluid dynamics in irrigated packings modeled by Shi and Mersmann (1985) is that "the liquid flows in the form of uniformly distributed rivulets, which partly wet the surface of the packing. A rivulet is a narrow film whose width is not determined by the equipment but it spreads freely". With theoretical considerations and experimental measurements of rivulet width for water and organic solvents, a correlation for the wetted area is developed.

The authors do remark that the effective area depends not only on the wetted area, but also on the formation of drops, static liquid hold-up within the packing and on the renewal of liquid surface, which depends in turn on the kinetic energy of the liquid flowing downwards, Marangoni effects and on the non-wettability of the solid surface. Therefore, a correction factor C_1, which depends on the packing size, is introduced. This factor, which results from correlations of data in the literature, can be bigger than 1, and increases with increasing packing size.

$$\frac{a_e}{a_p} = \frac{0.76.C_1.w_L^{0.4}.v^{0.2}}{(1\ -\ 0.93\cos\theta)}.\left[\frac{\rho}{\sigma.g}\right]^{0.15}.\left[\frac{a_p^2}{\epsilon}\right]^{0.6}.\frac{1}{a_p} \quad (1.34)$$

with $C_1 = C_2.d_p^{1.1}$

where C_2 is 52 and 138 for ceramics and plastic packings respectively.

Linek et al. (1984) (see tables 1.1 and 1.2) suggest an empirical equation for fitting their results which considers wettability:

$$\frac{a_e}{a_p} = 0.0277 \cdot W^{3.477} \cdot Re^{(0.641-0.047.W)} \cdot (a_p \cdot d_p)^{1.585} \qquad (1.35)$$

where $W = \frac{(1 + \cos\theta)}{2}$

Sedelies et al. (1987) (see tables 1.1 and 1.2) propose a correlation for effective areas of aqueous solutions without additives. The correlation reproduces their results with an accuracy of ± 30%.

$$a_e = (25.1 \pm 5) \cdot B^{(0.52 \pm 0.06)} \qquad (1.36.a)$$

The work of Sedelies et al. (1987) did however vary the viscosity and two different correlations fit their results, ie. effective area was found to be a function of viscosity only for viscosities of 5 cP and above.

$$a_e = (23.5 \pm 3.9) \cdot B^{(0.56 \pm 0.04)} \qquad (1.36.b)$$

for $\mu \leq 0.005$ kg/m.s

and

$$a_e = (7.2 \pm 3) \cdot \mu^{(-0.31 \pm 0.06)} \cdot B^{(0.42 \pm 0.12)} \qquad (1.36.c)$$

for $\mu > 0.005$ kg/m.s

The work from Rizzuti and Brucato (1989) (see tables 1.1 and 1.2) has also studied the effect of viscosity, varied by adding sugar. The correlation of their data (table 1.1) is:

$$a_e = 2.944 \cdot 10^4 \cdot \nu^{0.28} \cdot w_L^{0.313} \qquad (1.37.a)$$

for $1.24\ 10^{-6} \leq \nu \leq 1.54\ 10^{-6}$

and

$$a_e = 0.1651 \cdot 10^{-0.625} \cdot (\nu)^{-0.625} \cdot w_L^{0.313} \qquad (1.37.b)$$

for $1.54\ 10^{-6} \leq \nu \leq 2.3\ 10^{-6}$

Recently, Schultes (1990) developed, with the aid of dimensionless analysis, a model for the ratio of the effective area to the packing area. Using k_La and k_Ga data from the literature and their correlation for k_La and k_Ga, the author determined exponents and coefficients of the model, as follows:

$$\frac{a_e}{a_p} = 1.5.(a_p.d_h)^{-0.5}.\left[\frac{w_L.d_h}{\nu}\right]^{-0.2}.\left[\frac{w_L^2.\rho.d_h}{\sigma}\right]^{0.75}.\left[\frac{w_L^2}{g.d_h}\right]^{-0.45} \qquad (1.38)$$

with $d_h = 4.\frac{\varepsilon}{d_p}$

With this model, effective areas bigger than the geometric are possible. This equation was compared to the works from Hikita in 1956, Shulman et al. (1955.b), Onda et al. (1967), Semmelbauer (1967), Mohunta et al. (1969.a), Zech and Mersmann (1979) and with 35 mm metal Pall rings with a CO_2-water system at 1 bar and 293 K. The author considers that his equation predicts values in the middle of the range of those predicted by the aforementioned correlations, which do not always result from data from actual effective area measurements.

Table 1.4 uses the above information to compare the influence of the liquid flow velocity, liquid physical properties and packing dimensions on the ratio of the effective area to the geometric area, according to the different references. The last two lines give the average of each exponent and its standard deviation.

Table 1.4 Influence of different parameters on the ratio of the effective area to the geometric area.

$$\frac{a_e}{a_p} \text{ proportional to } w_L^{C_1} \cdot \mu^{C_2} \cdot \rho^{C_3} \cdot \sigma^{C_4} \cdot a_p^{C_5} \cdot d_p^{C_6}$$

CORRELATION NUMBER	C_1	C_2	C_3	C_4	C_5	C_6
1.27	0.455	-0.455	0.955	-0.5	-2.167	1.455
1.28	0.333	-0.333	0.333	***	-0.333	***
1.29	0.392	***	0.49	-0.49	-0.364	0.42
1.30	0.307	-0.041	0.174	0.049	-0.174	***
1.31	0.5	-0.5	0.95	-0.45	-1.0	0.4
1.32.b	0.35	0.35	***	-0.35	-1.88	-1.88
1.33	0.392	0.392	***	0.108	***	***
1.34	0.4	0.2	-0.05	-0.15	0.2	1.1
1.36.a	0.52	***	***	***	***	***
1.36.b	0.56	***	***	***	***	***
1.36.c	0.42	-0.31	***	***	***	***
1.37.a	0.313	0.28	-0.28	***	-1.0	***
1.37.b	0.313	-0.625	0.625	***	-1.0	***
1.38	0.4	0.2	0.55	-0.75	-0.1	***
average	0.392	-0.023	0.486	-0.317	-0.758	0.299
standard deviation	0.060	0.36	0.38	0.30	0.78	1.3

Notes: *** values not given
For the computation of the average and standard deviation, the series of equations (1.36) and (1.37) were not considered. The correlation (1.35) of Linek et al. (1984) is not listed, since the exponent on the Reynolds number depends on the wettability.

The dependence of the ratio of the effective to geometric area on the various parameters are not consistent from source to source. For the various models which have been proposed, the assumed dependence on some variables has not been verified experimentally. In regard to the absolute value of the ratio of the effective area to geometric area, the works from Schultes (1990) and Kolev (1973) dismiss equations, which do not accept effective areas higher than the geometric. Increasing the liquid load would be expected to cause an increase of effective areas to values even higher than the geometric area of the packing, as found experimentally by Bornhütter and Mersmann (1991), Linek et al. (1984), Krötsch and Kürten (1979) and Sahay and Sharma (1973). Furthermore, Schultes (1990) points out that packings with small specific geometric area and big packed columns present, in practice, values of the ratio of the effective to the geometric area higher than unity.

The literature indicates a dependence of the ratio of the effective to the geometric area on the liquid flow to the power of 0.392. The small standard deviation reflects good agreement. Experimental work from Jhaveri and Sharma (1968) and Sahay and Sharma (1973) and the review publication from Danckwerts and Sharma (1966) just plot the effective area as a function of the liquid load. However, the curvature of the plots tend to indicate that the ratio of effective to geometric area is also a function of the packing's material, size and type. Dharwadkar and Sawant (1985) suggest different exponents for different packing types, varying between 0.315 to 0.695. The lowest values are for steel packings, the highest values for polypropylene packings. The type of packing and its size also have an influence.

There is much disagreement in the literature concerning the influence of viscosity. The correlations of Lee and Kim (1982), Sedelies et al. (1987) and Rizzuti and Brucato (1989) seem to be the only ones resulting from experimental work in which the viscosity was varied. The most recent correlations given in table 1.4 predict an increase of the effective area with increasing viscosity, except for the experimental work of Rizzuti and Brucato (1989) (equation (1.37.b)) and Sedelies et al. (1987) (equation (1.36.c)) with high viscosities. Kolev (1973) does not agree with works which predicted that the effective area strongly decreases with increasing viscosity. Shi and Mersmann (1985) explain the increase of effective areas with the viscosity on the basis of an increase in the liquid hold up, which usually increases the wetted area.

There is also no agreement regarding the values of the exponents on the liquid density and surface tension. Liquid density does not seem to have been varied by any investigator. The surface tension was varied by Sedelies et al. (1987). Systems with lower surface tension should provide increased wettability. However, at high gas flows, the liquid may separate more easily from the packing. If droplets are formed, then the effective area can even be enhanced.

Many of the correlations consider the packing size and geometric area. Since the shape and material of the packing has an influence not only on the geometric area, but also on the gas liquid interaction, the type and material of packing should also be a parameter in the correlations. For Kolev (1973), however, the influence of the packing material on the effective area reduces when the packing's size increases as well as the specific liquid load.

The influence of the gas flow is considered only by Bravo and Fair (1982) (correlation (1.33)) as an important in determining effective areas. The works may have accorded little importance to the influence of the gas flow, since in the experimental studies, it was generally kept constant and also at low values, which are sometimes not given.

The correlations implicit assume countercurrent operation of the column. Krötsch and Kürten (1979) found experimentally that with the same gas flow, effective areas for countercurrent operation are higher than cocurrent. Nevertheless, the experimental work of Danckwerts and Guillham (1966) and Joosten and Danckwerts (1973) uses concurrent absorption, supposing that the transport phenomena are equivalent for countercurrent absorption. However, gas-liquid turbulence are enhanced with countercurrent operation, which would be expected to lead to higher values of effective areas.

2.2 Literature review of k_La of packed columns

2.2.1 Measurements of k_La of packed columns

The literature has frequently defined k_La as "the liquid phase mass transfer coefficient", which is not accurate. The actual "liquid phase mass transfer coefficient" is k_L, not the product k_La, which can be experimentally measured. This product is termed "the volumetric mass transfer coefficient k_La" in this work.

Table 1.5 overleaf lists the methods mentioned in the literature, which have been used for determining k_La in packed columns. The packings tested, with the respective column, are listed in the table 1.6. Explanations of symbols used in the tables follow. The experiments in the literature were basically carried out at ambient pressure and at temperatures of between 20 to 30°C. Except for the work of Bereiter (1975) with the SULZER metal gauze structured packing BX, all other experiments are with irregular packings.

The majority of the experiments are carried out using physical methods with water as a solvent. Chemical methods use either the Danckwert's plot method or slow chemical reactions (section 1.2.2). Perhaps the only significant experimental work with regard to viscosity is that of Delaloye et al. (1991). They used liquids of widely varying viscosity: sodium alginate, glycerol and polyethylene glycol. The experiments confirm that the viscosity has an influence on the diffusion coefficient of the absorbed gas. Therefore, the authors recommend that future research should associate k_La determination with precise determination of diffusivity coefficients in the solutions employed. No investigator seems to have studied the effect of varying density. The surface tension and the wettability are difficult to change while maintaining all other parameters constant (Coughlin (1969)), particularly the viscosity. Onda et al. (1968) used a non-foaming surfactant and the surface tension of the solution was 47 10^{-3} N/m. The k_La data are smaller than those obtained with water, which has a surface tension about 50 % higher.

Linek et al. (1984) found k_La values for absorption and desorption experiments "identical within the margin of experimental error". Deed et al. (1947) believe that "there is no clear experimental evidence that there is any difference between HTUL or HTUG values for packed columns as found from absorption and rectification experiments. Rectification tests are, however, peculiar unsuitable for the reliable determination of these quantities." However, the authors draw attention to the fact that with measured values of HTUL from desorption or absorption experiments, "it is not safe to extrapolate the data to low liquid rates" which may be met in rectification, in contrast to absorption processes.

The literature seems to neglect the influence of axial dispersion in the evaluation of the k_La data from experiments. Recently, von Stockar and Lu (1991) state that "neglecting deviations from plug flow in countercurrent contactors results in overestimated HTU values when evaluating pilot plant experiments and in underestimation of the required number of transfer units when designing a new separator". The authors suggest a procedure for correcting NTU values in design problems and HTU values obtained from experiments. Furthermore, a uniform liquid distribution over a cross section can also affect the measured k_La values. Thus, Arwikar and Sandall (1980) have mentioned that entrance effects may distort experimental data.

Table 1.5 Measurements of the volumetric mass transfer coefficient $k_L a$. (methods employed)

Reference	Method and system used
Arwikar and Scandall (1980)	physical absorption of pure CO_2 saturated with water vapor into water.
Bereiter (1975)	physical absorption of CO_2 in ethanol.
Billet and Mackowiak (1980)	physical absorption of CO_2 into water.
Billet and Mackowiak (1977)	physical desorption of CO_2 from water into air.
Bornhütter - Mersmann (1991)	physical desorption of CO_2 from water into air.
Cooper et al. (1941)	physical desorption of CO_2 from water into air.
Coughlin (1969)	chemical absorption of O_2 into Na_2SO_3 solutions.
Delaloye et al. (1991)	physical desorption of O_2 from water, glycerol, sodium alginate and polyethylene glycol into air.
Dharwadkar - Sawant (1985)	chemical absorption of pure CO_2 into sodium carbonate and bicarbonate solutions.
Echarte et al. (1984)	physical desorption of CO_2 from water and glycerol solutions.
Knoedler and Bonilla (1954)	vacuum desorption of O_2 from water.
Koch et al. (1949)	physical absorption of CO_2 from air into tap and distilled water.
Krötsch (1982)	chemical absorption of diluted CO_2 in air into sodium carbonate and bicarbonate solutions.
Linek et al. (1984)	physical absorption of atmospheric O_2 into O_2-free water and physical desorption of O_2 from water into pure N_2.
Mangers and Ponter (1980)	physical absorption of CO_2 into water and aqueous glycerol solutions.
Merchuk (1980)	physical absorption of CO_2 into water.
Mohunta et al. (1969.b)	physical desorption of O_2 from water and of CO_2 from aqueous glycerol solutions into air.
Onda et al. (1968)	physical absorption of pure CO_2 into water, CCl_4 and methanol.
Onda et al. (1959)	physical absorption of pure CO_2 and H_2 into water.
Rixon (1948)	physical desorption of CO_2 from water. physical absorption of CO_2 into water.
Sahay and Sharma (1973)	physical absorption of pure CO_2 into tap water.
Schultes (1991)	physical desorption of CO_2 from water into air.
Sherwood and Holloway (1940)	physical desorption of O_2, H_2 and CO_2 from water into air.
Vivian et al. (1967)	physical desorption of CO_2 from water.
Vivian and King (1964)	physical desorption of C_3H_6, CO_2, O_2, H_2 and He from water into air.
Yoshida and Koyanagi (1958)	physical absorption of CO_2 into tap water and methanol.

Table 1.6 Measurements of the volumetric mass transfer coefficient $k_L a$. (Packing and equipment used for investigation)

Reference	Packing			Column	
	type	size [mm]	material	diameter [mm]	height [mm]
Arwikar and Scandall (1980)	RR	6	ceramic	79	60 to 550
Bereiter (1975)	RP	BX	metal gauze	185	171
Billet and Mackowiak (1980)	NSW	a,b,c 25	plastic	150	1400
	TR	25			
	PR	25			
Billet and Makowiak (1977)	RR	50	ceramic	300	700 and
	IR	25	metal		1200
	BR	25,35,50	inox		
Bornhütter - Mersmann (1991)	PR	50	plastic	1000	***
	VSP	25			
	EP	number 3			
	HF	50,90-0,90-6			
		50	metal		
	TP	number 2			
	SF				
Cooper et al. (1941)	RR	50	metal	762 (square tower)	2184
Coughlin (1969)	RR	9.5	plastic ceramic	76	1524
Delaloye et al. (1991)	RR	25	glass	300	1000
Dharwadkar - Sawant (1985)	PR	38	inox plastic	385	1155
	PR	50	steel plastic		
	IS	38	plastic		
Echarte et al. (1984)	RR	25	ceramic	400	330 and
		58			900
Knoedler and Bonilla (1954)	ST		***	152	610
Koch et al. (1949)	RR	9.5	ceramic	152	1323
		13		254	1030
		19			1052
		32			1137
					1024
Krötzsch (1982)	TR	25	plastic	300	700 and 1400
Linek et al. (1984)	PR	15,25,35,50	plastic	290	1000
Mangers and Ponter (1980)	RR	25	glass	100	500
Merchuk (1980)	RR	4,6,9.5	plastic	100	600
		9.5	ceramic		
	BS	6	plastic		
	spirals and flat rings of plastic				
Mohunta et al. (1969.b)	RR	9.5,13,19	***	76 and 102	***
Onda et al. (1968)	RR	10	***	60 and	200 to
	BS	13		120	300
	SP	13,25			
	rods	14			

Table 1.6 (continued).

Reference	Packing			Column	
	type	size [mm]	material	diameter [mm]	height [mm]
Onda et al. (1959)	RR	6,8,10	ceramic	60	300
Rixon (1948)	RR	25	stoneware	380	4572
				248	7760
	RR	38		685	5486
Sahay and Sharma (1973)	RR	25	ceramic	200	870
	IS				
	PR		steel		
	IS		plastic		
	RR				
	PR				
Schultes (1990)	EP	32,60,80	plastic	***	***
	HF	50			
		25	metal		
		38	ceramic		
	BR	12,50	metal		
	TP	50	metal		
Sherwood and Holloway (1940)	RR	38	ceramic	508	203
		13,25,38,50			152 to 1245
	BS	13,25,38			
Vivian et al. (1967)	RR	13,19	ceramic	152	305
Vivian and King (1964)	RR	25	ceramic	305	305 and 610
		38			
Yoshida and Koyanagi (1958)	SP	13,25	glass	120	203 and 406
	RR	15,25	ceramic		
	BS	13,25			

List of packing types

code	description
BS	Berl saddles
BR	Bialecki rings
EP	Envipak
HF	Hiflowring
IR	I-13 Ring
IS	Intalox saddles
PR	Pall rings
RP	SULZER structured packing
RR	Raschig rings
SF	Snowflake
SP	spheres
ST	Stedman triangular packing
TP	Top Pack
TR	Tellrettes

Notes

*** information not given

2.2.2 Predictions of k_La and of k_L of packed columns

In this section, correlations from experimental and theoretical work for predicting k_La or HTUL (section 2.2.2.1) and k_L (section 2.2.2.2) of packings are listed chronologically. This sequence is adopted since it is interesting to follow the evolution of the proposals for the influence of physical properties and of different packing types and materials. Details of the experimental works cited in this section are listed in tables 1.5 and 1.6. However, it was not intended to explain how the equations were developed. In most cases, the models are functions of dimensionless numbers. These numbers are defined in table 1.3, section 2.1.2, with a physical interpretation. All physical properties referred to are those of the liquid. In the end of this section, the predictive power of the correlations and of information from experimental works are discussed.

2.2.2.1 Predictions of k_La of packed columns

The pioneering experimental work by Sherwood and Holloway (1940) (see tables 1.5 and 1.6) suggests the following correlation with a coefficient - C_1 - and exponent - C_2 - which are adjustable parameters, packing dependent.

$$\frac{k_La}{D} = C_1 \cdot \left[\frac{w_L}{\nu}\right]^{C_2} \cdot Sc_L^{0.5} \qquad (1.39)$$

where the coefficient C_1 is, however, not dimensionless. A correction for the temperature is:

k_La proportional to $e^{(\text{coefficient} \cdot T)}$

For Sherwood and Holloway (1940), this coefficient is 0.023, where the temperature is in °C. Vivian and King (1964) suggest latter that the coefficient should be 0.020.

Knoedler and Bonilla (1954) (see tables 1.5 and 1.6) propose, for the stedman triangular packing, operated below the loading point:

$$\frac{k_La}{D} = 3.5 \cdot 10^5 \cdot (\rho.w_L)^{0.77} \cdot Sc^{0.53} \qquad (1.40)$$

The first theoretical model for HTUL for packings is proposed by Davidson (1959). Three different situations are modeled. In all three cases, the packings are assumed to be made of a large number of vertical surfaces. In the first and second situation, the height is equal to the packing's size - d - and is completely wetted. However in the second situation, there is an equal probability that the packing is inclined in all angles, from 0 to $\pi/2$, with respect to the horizontal. In the third situation, the packing may present different lengths and inclination angles with equal probability. Each situation changes the value of the coefficient C_1. The third situation (C_1 = 0.1833) gives the smallest HTUL values, and the best agreement with experimental data.

$$\frac{HTU_L}{d} = C_1 \cdot (2\pi.Re)^{2/3} \cdot Sc^{0.5} \cdot Ga^{-1/6} \qquad (1.41)$$

The statistical approach of Davidson is also used by Bridgewater and Scott (1974), who reasoned with for a three dimensional distribution of surfaces. The resulting equation (C_1 = 0.247) is almost identical to the second situation modeled by Davidson (C_1 = 0.244).

Using available data from a large data bank for a variety of columns and packings, Cornell et al. (1960) suggest an equation for HTUL which considers the packing height:

$$HTU_L = C_1 \cdot Sc^{0.5} \cdot C_2 \cdot \left[\frac{h}{3.048}\right]^{0.15} \qquad (1.42)$$

This equation is part of the Monsanto model, which also includes an expression for HTUG. The packing parameter C_1 is a function of the packing size and type and of the superficial liquid mean velocity. The flooding correction factor C_2 is a function of the percentage flood. The parameters C_1 and C_2 are described graphically by Cornell et al. (1960).

Norman (1961) proposes a generalized equation for different sizes of Raschig rings and Berl saddles measured by different sources. The predictive accuracy is claimed to be ± 20 %.

$$\frac{k_L a}{D} = 530 \cdot \left[\frac{\rho . w_L}{\mu}\right]^{0.75} \cdot Sc^{0.5} \qquad (1.43)$$

The equation of Mohunta et al. (1969.b) was developed using theoretical reasoning and experimental data (see tables 1.5 and 1.6). The review paper of Au Yeung and Ponter (1983) states that this correlation "fits the bulk of the available data in the literature and those of the authors to within ± 20 %". Krötsch (1982) states that this correlation fits his data well.

$$k_L a \cdot \left[\frac{a_p . \nu}{g}\right]^{2/3} \cdot \left[\frac{\nu}{g^2}\right]^{1/9} = 0.0025 \cdot \left[\frac{\mu . w_L^3 . a_p^3}{\rho . g^2}\right]^{1/4} \cdot Sc^{-1/2} \qquad (1.44)$$

The only equation for HTUL of structured packings seems to be the one of Bomio (1977) for the SULZER gauze packing BX. Data of Bereiter (1975) (see tables 1.5 and 1.6) was used. The angle α is related to the geometry of the packing and is defined by Bereiter.

$$HTU_L = 2.45 \cdot 10^{-3} \cdot \left[\frac{Re}{\sin \alpha}\right]^{0.22} \cdot Sc^{0.5} \qquad (1.45)$$

The first attempt to investigate the effect of viscosity on $k_L a$ is that of Mangers and Ponter (1980). Their experimental data (see tables 1.5 and 1.6) seems to be correlated to within ± 6 % with:

$$\frac{k_L a}{D} = 3.22 \cdot 10^{-3} \cdot \left[\frac{w_L}{\nu}\right]^{C_1} \cdot Sc^{0.5} \cdot Ga^{0.27} \cdot \frac{1}{(1-\cos\theta)} \qquad (1.46.a)$$

where:
$$C_1 = 0.49 \cdot \left[(1-\cos\theta)^{0.6} \cdot \left[\frac{\rho . \sigma^3}{\mu^4 . g}\right]^{0.2}\right]^{0.108} \qquad (1.46.b)$$

The difficulty with the above equation is to have precise data for the contact angle θ. When the packing is completely wetted, the authors suggest that there is a change of the dependency on the liquid flow. It is suggested therefore that "for very viscous liquids, the liquid becomes the continuous phase and dispersed bubble flow results". The exponent of the viscosity is no longer a function of the wetting angle, and becomes -0.574. The correlation to be used is:

$$\frac{k_L a}{D} = 2.03 \cdot \left[\frac{w_L}{\nu}\right]^{1.44} \cdot Sc^{0.5} \cdot Ga^{-0.183} \qquad (1.46.c)$$

The Monsanto mass transfer model (equation (1.42) from Cornell et al. (1960)) is improved by Bolles and Fair (1982) with new functions for the parameters C_1 and C_2. These parameters are described graphically by Bolles

and Fair (1960). An extensive data bank is used. Their data bank is mainly from distillation experiments with physical properties similar to water. The authors however admit that "most of the systems studied had relatively low liquid phase resistance to mass transfer". The authors claim that "for the improved model, the safety factor required for reasonable confidence (95%) is 1.70. This compares to 1.87 for the Monsanto model" (correlation (1.42)). These safety factors indicate the overdesign or waste in commercial design of the packing height as a result of poor model reliability.

A semi-theoretical correlation based on the random length and random angle statistical model of Davidson (1959) is developed by Ponter and Au-Yeung (1982). The stagnant liquid or dry patch, which may occur, is taken into account with a mixing factor - C_1 - and the ratio of the maximum effective length to the size of the packing.

$$\frac{HTU_L}{d} = 0.1833 \cdot C_1 \cdot \left[\frac{l_e}{d}\right]^{1/2} \cdot Sc^{0.5} \cdot \left[(2\pi.Re).\frac{a_p}{a_e}\right]^{-0.61} \cdot Ga^{-1/6} \qquad (1.47)$$

The maximum effective length and the mixing length are functions of the Reynolds number, contact angle, surface tension, liquid viscosity and density. The maximum effective length is also a function of the contact angle - θ - and increases with the Reynolds number and with μ. The authors have claimed that the correlation is also valid for organic systems.

Billet (1983) has developed, from theoretical considerations, the equation:

$$k_L a = \frac{1}{C_1} \cdot \left[\frac{\rho.g}{\mu}\right]^{1/6} \cdot D^{0.5} \cdot a_p^{2/3} \cdot w_L^{1/3} \qquad (1.48)$$

where the coefficient C_1 is specific to each packing and is related to the contact length, i.e. the length over which a liquid renewal occurs.

The experimental data of Echarte et al. (1984) (see tables 1.5 and 1.6) is correlated by an equation with a correlation coefficient of 98%. The equation is very similar to the model of Davidson (1959) (equation 1.41).

$$HTU_L = 1.552 \cdot (4.Re.\frac{a_p}{a_e})^{0.375} \cdot Sc^{0.5} \cdot Ga^{-1/6} \cdot d \qquad (1.49)$$

For broader use, the authors suggest the employment, for the coefficient and for the exponent on the Reynolds number, the values of 1.580 and of 0.367, instead of 1.552 and 0.375, respectively.

In the theoretical work of Shi and Mersmann (1985), with a hydraulic model of a rivulet irrigating the packing, a correlation for $k_L a$ is developed:

$$k_L a = 0.91 \cdot C_1 \cdot \left[\frac{D}{d_p}\right]^{1/2} \cdot \left[\frac{w_L^{3.6} \cdot \rho^{0.6} \cdot g^{0.4} \cdot a_p^{4.8}}{(1-0.93\cos\theta)^4 . \sigma^{0.6} . \nu^{0.2} . \epsilon^{2.4}}\right]^{1/6} \qquad (1.50)$$

where C_1 is packing dependent (equation (1.34), section 2.1.2, chapter I).

The most recently correlation for $k_L a$ identified in the course of this work is due to Schultes (1990) (see tables 1.5 and 1.6). The coefficient C_1 results from comparing the model with data from him and from different authors and is a function of the packing type, material and size.

$$k_L a = C_1 \cdot \left[\frac{g}{\mu}\right]^{1/6} \cdot \left[\frac{D}{d_h}\right]^{0.5} \cdot a_p^{2/3} \cdot w_L^{1/3} \cdot \left[\frac{a_e}{a_p}\right] \qquad (1.51)$$

The ratio of the effective area to the geometric area of the packing was also modeled, and may be found in equation (1.38), section 2.1.2, chapter I. The author estimates the deviation to be ± 20 %.

Tables exist in the literature comparing the influence of different exponents on $k_L a$ values (Mangers and Ponter (1980), Echarte et al. (1984), Shi and Mersmann (1985) and Delaloye et al. (1991)). Table 1.7 analyses the information in terms of minimum, maximum and average values and standard deviation. Table 1.7 also distinguishes between works which propose semi-theoretical correlations, works which correlate experimental data and the only work with a correlation for structured packings (Bonio (1977)). The latter is originally a correlation for HTUL (correlation (1.45)) and is transformed into a $k_L a$ for comparison.

Table 1.7 Dependence of $k_L a$ on the parameters B, μ and ρ.

Parameter		exponent affecting the parameter minimum	maximum	average	standard deviation
B	a)	1/3	0.77	0.61	0.18
	b)	0.452	1.0	0.76	0.17
	c)	----	----	0.78	----
μ	a)	-0.458	0.53	-0.19	0.44
	b)	----	----	-0.5 (*)	----
	c)	----	----	-0.28	----
ρ	a)	0.1667	1.0278	0.40	0.32
	b)	----	----	----	----
	c)	----	----	0.28	----

List of references used to compute the values:
a) correlations from theoretical works: (1.40), (1.41), (1.43), (1.44), (1.48), (1.49), (1.50) and (1.51).
b) predictions from experimental works: Arwikar and Scandall (1980), Billet and Mackowiak (1977), Coughlin (1969), Delaloye et al. (1991), Koch et al. (1949), Onda et al. (1959), Rixon (1948), Sahay and Sharma (1973) and Vivian and King (1964).
c) Correlation (1.45) for the SULZER gauze packing (Bonio (1977)).

Note (*): The authors actually propose that the ratio $k_L a/\sqrt{D}$ decreases in approximately inverse proportion to the square root of μ.

The most important influence on $k_L a$ is the specific liquid load, a dependence, which is experimentally easily varied. The packing material may have an influence on the exponent of the liquid load. Sahay and Sharma (1973) suggest different exponents for plastic packings than for other packings tested (table 1.6.b, section 2.2.1) in contrast to Coughlin (1969), who suggest the same value for ceramic and polymeric packing.

Vivian et al. (1967) showed that "at higher liquid rates and depending on the gas rate, HTUL is found to increase less rapidly and even to decrease with increasing liquid rate". These results confirmed the data of Sherwood and Holloway (1940). The influence of flooding conditions on k_La was also pointed out by Cooper et al. (1941) and by Cornell et al. (1960). Billet and Mackowiak (1977) gave two correlations for the packings they measured (table 1.4.a, section 2.2.1, chapter I) according to the proximity to flooding conditions. The exponent which influences the liquid load is always the same. The difference is with the coefficient, which is higher for k_La values above 80 % of flooding.

The estimates of the k_La at higher viscosities in the literature vary widely. The standard deviation in table 1.7 is high. If, with increasing viscosity, the mixing between packing elements is less, the renewal rate will decrease and so will the liquid phase mass transfer coefficient k_L. This reasoning would support the works which predict a decrease of k_La with increasing viscosity.

The prediction of the influence of the viscosity and density in the literature is not only based on theoretical reasoning, but results also from the use of dimensionless numbers. This may explain why the exponent of the viscosity has the same absolute value as the exponent of the density, however the sign is different, as in the equations from Sherwood and Holloway (1940), Davidson (1959), Norman (1961), Mohunta et al. (1969.b), Billet (1983), Echarte (1984) and Bomio (1977).

From the experimental work of Delaloye et al. (1991), the ratio of k_La with the square root of the diffusivity is found to change with about the inverse of the square root of the viscosity. The exponent of the liquid load remains fairly constant with a change of the viscosity and is on average equal to 0.76, being equal to the average value of experimental works as shown in table 1.7. Mangers and Ponter (1980) also measure the effect of increasing viscosity, proposing an exponent in the correct range. However, since the column of Mangers et al. (1980) was small and they do not seem to consider the effect of the viscosity on the diffusivity of the absorbed gas, as Delaloye et al. (1991) do, only the latter work is compiled in table 1.7.

The diffusivity influences k_La according to the penetration and surface renewal theory (section 1.2.1, chapter I). The k_La is accepted by all to be a function of the square root of the diffusivity, with the exception of Knoedler and Bonilla (1954) (equation (1.40)).

The predictive performance of the listed correlations is doubtful, particularly where changes of physical properties are concerned. For irregular packings, with aqueous solutions similar to water, perhaps the equation most convenient to use is that of Mohunta et al. (1969.b), as recommended by Laurent and Charpentier (1974) for different packings and materials and whose validity was checked by Au Yeung and Ponter (1983). The review of Au-Yeung and Ponter (1983) thinks additionally that although the classical equation of Sherwood and Holloway is "the most useful for estimating liquid film mass transfer coefficients for columns packed with a large variety of Raschig rings and Berl saddles and for gas and liquid rates up to the loading point", the simple correlation of Norman (1961) "is more convenient to use".

2.2.2.2 Predictions of k_L of packed columns

The correlations for predicting the liquid phase mass transfer coefficient k_L of irregular packings listed below do not originate directly from experiments. They result from dimensionless analysis and theoretical reasoning.

A correlation is proposed by van Krevelen and Hoftijzer (1947.b), since Sherwood and Holloway (1940) "did not succeed in deriving a generally valid dimensionless k_L equation". The last term on the right hand side of the equation accounts for absorption followed by chemical reaction.

$$k_L \cdot \frac{\delta_L^{1/3}}{D} = 0.015 \cdot \left[\frac{w_L}{a_w \cdot \nu}\right]^{2/3} \cdot Sc^{1/3} \cdot \frac{\delta_L \cdot \sqrt{\frac{K}{D}}}{\tanh(\delta_L \cdot \sqrt{\frac{K}{D}})} \qquad (1.52)$$

where: $a_w = a_p \cdot (1 - \exp(5000 \cdot w_L))$ and $\delta_L = \sqrt[3]{\frac{\mu^2}{\rho^2 \cdot g}}$

The review paper from Au-Yeung and Ponter (1983) points out that the equation "does not express the correct relationship between the coefficient and the physical properties of the liquid". The same review paper states that "Sherwood and Pigford in 1952 reported that the equation does not correlate the absorption data of Sherwood and Holloway (1940) accurately with deviations as large as 50 percent".

Onda et al. (1959) propose an equation similar to the one from van Krevelen and Hotijzer above. However, the exponent of the Schmidt number is 0.5, in agreement with the penetration theory.

Shulman et al. (1955.b) obtain k_L by dividing $k_L a$ values from different sources by their mass transfer area data. Since the mass transfer area data come from indirect measurements (section 2.1.1, chapter I), it may be that the predictive power of the correlation is doubtful:

$$\frac{k_L d_s}{D} = 25.1 \cdot \left[\frac{d_s \cdot w_L}{\nu}\right]^{0.45} \cdot Sc^{0.5} \qquad (1.53)$$

where d_s is the diameter of a sphere with the same packing surface area.

With dimensionless analysis and using data from other research, Semmelbauer (1967) proposes:

$$\frac{k_L d_p}{D} = C_1 \cdot Re^{0.59} \cdot Sc^{0.5} \cdot Ga^{0.17} \qquad (1.54)$$

In the Reynolds number, the packing size is used in the numerator instead of the specific geometric area of the packing, as given in table 1.3, section 2.1.2. The coefficient C_1 is 0.32 for Raschig rings and 0.25 for Berl saddles, independent of the packing material. The equation is valid for $3 < Re < 3000$ for $10 <$ packing size < 50 mm and for flows independent of the gas flow below the loading point. The author admit large deviations, which are not quantified.

Onda et al. (1968) propose a correlation which results from reported $k_L a$ values from the literature divided by wetted area values given by their equation (equation (1.26), section 2.1.2, chapter I).

$$k_L \cdot \left[\frac{\rho}{g.\mu}\right]^{1/3} = 0.0051 \cdot \left[\frac{L}{a_w.\mu}\right]^{2/3} \cdot Sc^{-1/2} \cdot (a_p.d_p)^{0.4} \qquad (1.55)$$

The publication of Echarte et al. (1984) points out that "the failure of the Onda correlation for dealing with large differences in viscosity can also be seen from their own data on CO_2 absorption in ethanol (ν = 1.5 cSt) and carbon tetrachloride (ν = 0.6 cSt)".

Kolev (1976), using data from different authors for various types of packings, with various liquid loads, suggest the correlation below, which is claimed to have a predictive accuracy of ± 20 %. This equation demands knowledge of the effective area.

$$\frac{k_L.d_p}{D} = 0.030 \cdot (4.Re)^{0.5} \cdot \left[\frac{a_e}{a_p}\right]^{-0.5} \cdot Ga^{0.28} \cdot Sc^{0.5} \qquad (1.56)$$

Zech and Mersmann (1979) consider that the liquid flows in rivulets through the packing, which is a system of parallel cylindrical channels with the same specific area and voidage as the packing. Perfect mixing takes place at the end of packing elements. Using the penetration model, and assuming laminar flow, the authors derive theoretically:

$$k_L = C_1^{-1/3} \cdot \left[\frac{6.D}{\pi.d_p}\right]^{1/2} \cdot \left[\frac{\rho.g.d_p}{\sigma}\right]^{-0.15} \cdot \left[\frac{w_L.d_p.g}{3}\right]^{1/6} \qquad (1.57)$$

The coefficient C_1 is the same as in correlation (1.31). The model for k_L above allows for no dependence on the viscosity, which contradicts all models above. The Zech and Mersmann theoretical model was dismissed by Ponter et al. (1980) as "being no more accurate than the purely empirical correlation of Sherwood and Holloway".

Shi and Mersmann (1985) develop a model for k_L also using rivulet flow as hydraulic model. Their model for k_L give together with their model for effective area (equation (1.34)) their $k_L a$ correlation - equation (1.50).

Concluding, the predictive accuracy of the above correlations of k_L has frequently been dismissed by other authors. The use of the k_L correlations is generally not straightforward, as it is the case of correlations (1.55) and (1.56). Estimates of k_L may vary widely. For example, the exponent on the liquid flow, an important parameter, varies from 0.16 (Zech and Mersmann (1979)) up to 0.59 (Semmelbauer (1967)). Consequently, k_L may be more rapidly and accurately determined by simply dividing $k_L a$ values with values for the effective area. These values should be carefully selected from the literature.

2.3 Discussion

Structured packings have scarcely been employed for measurements of effective areas and k_La values. There is an attempt from Fair and Bravo (1987) to evaluated effective area of structured packings. However, such values have not been directly measured, but calculated using somewhat doubtful procedure. Bereiter (1975) measures k_La values of the SULZER structured packing BX using a column packed with only one packing element, which was artificially cut into two, thus not being representative of a typical BX packing. Results from Bereiter are discussed in section 3.5, chapter V. In view of the facts above, this research is justified, since industrial separation columns are increasing equipped with structured packings.

Laboratory scale columns, with probable associated maldistribution and wall effects, are used by most of the published work for obtaining effective areas and k_La values of irregular packings. Such measurements are, however, carried out with a limited range of flowrates, with the gas flow being particularly kept to small values. A broad range of operational conditions in industrial-scale should be employed, if the data is to be of practical use for design of industrial columns.

With present technology, effective areas are only measured with chemical systems, even though the reaction kinetics are not easily defined. The sulfite method has been shown to be unsuitable for determination of effective areas of packed columns. Another widely used reaction is that of CO_2 with NaOH. In this case, little importance seems to have been accorded to verifying whether the kinetics of this reaction really enables effective area measurements.

A chemical system is suitable for determining effective areas if the absorption rate is proportional to the available effective area of the gas-liquid interface. The proportionality factor must remain constant within the range of flows and concentrations used in the experiments. In order to control the adequacy of the chemical system and for accessing the value of the proportionality factor, it is important to carry out experiments in an apparatus in which the effective area may be varied.

Effective areas obtained with chemical method may differ from effective areas for physical absorption. This is not the case for structured packings, which force the flow in defined channels, avoiding the formation of stagnations zones. Consequently, the whole gas-liquid interfacial area of structured packings would be expected to be identical to effective areas for chemical and physical absorption.

Effective areas for distillation may be higher than that for absorption, as suggested by Bravo and Fair (1982), Yoshida and Koyanagi (1962) and Onda et al. (1968). In contrast to absorption, the simultaneous and significant boiling in the liquid phase with condensation in the vapor phase for distillation may provide a continuous formation of interfacial area within each phase. In addition, the Marangoni effect is present particularly during distillation. The Marangoni effect would explain why with a surface tension distribution on the film, especially for very soluble gases, the film becomes unstable and breaks up into rivulets and droplets. Both facts above tend to increase effective areas.

It has been occasionally accepted that effective areas of irregular packings may be higher than the geometric areas. If structured packings are more efficient than irregular packings, is this difference due to an even higher effective area? The answer to this question may contribute for the development of new packing geometries.

The k_La values of packed columns are determined by either absorption or desorption experiments of sparingly soluble gases in aqueous solutions. A preference for the system CO_2-water-air has been accorded by the literature. However, when compared to other gases such as O_2, N_2 and H_2, CO_2 still exhibits a high solubility in water, which may slightly influence the k_La values measured. This point is discussed in section 1.1, chapter V.

The liquid side mass transfer coefficient, k_L, cannot be determined directly by experimentation. However, the k_L may be obtained by simply dividing carefully chosen literature experimental data or correlations for k_La by values for the effective area.

Empirical correlations for predicting k_La and effective area values are not necessarily more inaccurate than correlations resulting from theoretical reasoning. Modeling the liquid flow over a packing with only one correlation for describing different flow regimes may be an oversimplification. In the experimental and theoretical work of Schmuki and Laso (1990), five different hydrodynamics regimes of a liquid flow over an inclined flat surface (flow of wetting liquid, droplet flow, linear rivulet, meandering rivulet, oscillating rivulet) are described. The flow regimes depend on the liquid flow rate, physical properties of the liquid-solid system and on the inclination of the surface. The transitions between the flow regimes were measured experimentally as a function of the surface inclination, viscosity and surface tension. A model for the transition from linear rivulet to meandering rivulet is proposed by Schmuki and Laso (1990).

The authors explain that different flow regimes cause dramatic changes in mass transfer rates between the liquid and the surrounding gaseous phase. Consequently, the use of only one correlation for describing effective area for different flow regimes and transitions may be inaccurate. For a rough estimate, simple empirical correlations may be more convenient to use.

Physical properties of systems employed by the majority of effective area and k_La experiments reported in the literature are similar to water and air. Thus, it is not astonishing that suggested correlations involve contradictory dependencies on different parameters, since these dependencies have not always been confirmed experimentally. Such experiments may require the development of new experimental methodologies, since a change of a single physical property should not cause an unpredictable change of other physical properties. In this work, the influence of physical properties on measured effective area and k_La values of structured packings has not been treated. However, this subject demands closer attention and is left as a recommendation for future work.

Based on the literature survey, the goals of this thesis were set, as given in the beginning of this chapter in the section "scope of this work".

NOMENCLATURE FOR CHAPTER I

a	[m^2/m^3]	specific mass transfer or geometric area
A	[m^2]	mass transfer or cross-sectional area
B	[m^3/m^2h]	specific liquid load (equation (1.3))
c	[mol/m^3]	concentration
C	[-]	factors for empirical model
d	[m]	diameter or size of the packing
D	[m^2/s]	diffusivity
F-Factor	[$m/s.\sqrt{kg/m^3}$]	equation (1.1)
g	[m/s^2]	gravity
G	[kg/h] [mol/h]	gas flowrate
h	[m]	packing height
H	[$Pa.m^3/mol$]	Henry constant
HTU	[m]	height of a transfer unit
HETP	[m]	height of a theoretical plate
k_G	[$mol/m^2.s.Pa$]	gas phase mass transfer coefficient
k_L	[m/s]	liquid phase mass transfer coefficient
K		reaction constant rate
l	[m]	characteristic packing length
L	[kg/h] [mol/h]	liquid flowrate
n	[mol/m^2s]	specific mass transfer absorption rate
NTS	[-]	number of theoretical stages
NTU	[-]	number of transfer units
p	[mmHg] [atm] [Pa]	pressure
r	[mol/m^2s]	reaction rate
t	[s]	time
T	[K]	temperature
w	[m/s]	superficial velocity
x	[mol/mol]	liquid-phase mol fraction
y	[mol/mol]	gas-phase mol fraction
z	[m]	coordinate
ε	[-]	void fraction of the packing
μ	[kg/ms]	dynamic viscosity
ν	[m^2/s]	kinematic viscosity
ρ	[kg/m^3]	density
θ	[deg]	wettabilty contact angle
σ	[N/m]	surface tension
δ	[m]	film thickness

Dimensionless Numbers
(see table 1.3, section 2.1.2)

Fr	[-]	Froude number
Ga	[-]	Galileo number
Pe	[-]	Peclet number
Sc	[-]	Schmidt
Sh	[-]	Sherwood
Re	[-]	Reynolds
We	[-]	Weber number

Subscripts

A	refers to component A
b	bulk
c	column
cr	critical
e	effective
G	gas
h	hydraulic
i	interface
L	liquid
m	logarithmic average
o	overall
p	packing
s	sphere
w	wetted
α	begin - in
ω	end - out
1, 2 ...	indexes

Superscript

*	equilibrium
-	mean

REFERENCES FOR CHAPTER I

ALLLENBACH, U.; WIRGES, H.-P. and W.-D. DECKWER (1977). "Ermittlung von Stoffaustauschparametern in Gas-Flüssig-Reaktoren mit Hilfe der säurekatalysierten Isobutenhydratation". Verfahrenstechnik 11(12), 751-754.

ARWIKAR, K.J. and O.C. SANDALL (1980). "Liquid phase mass transfer resistance in a small scale packed distillation column". Chem.Eng.Sci. 35(11), 2337-2343.

ANDRIEU, J. and B. LESPINASSE (1973). "Mesure directe de l'aire mouillée d'un garnissage d'anneaux de raschig en verre pyrex dans une colonne arrosée à contre-courant". Chimie et Industrie - Génie chimique 106 (11), 825-833.

AU-YEUNG, P. and A.B. PONTER (1983). "Estimation of liquid film mass transfer coefficients for randomly packed absorption columns". The Can.J.of Chem.Eng. 61(4), 481-493.

BALDI, G. and S. SICARDI (1975). "Effective mass transfer areas in packed columns during chemical absorption". Chem.Eng.Sci. 30(7), 769-770.

BENNET, A. and F. GOODRIDGE (1970). "Hydrodynamic and mass transfer studies in packed absorption columns. Part II: The measurement of total interfacial area". Trans.Instn.Chem.Engrs. 48, T241-T244.

BEREITER, R. (1975). "Druckverlust und Flüssigkeitsseitiger Stoffaustausch in Sulzer Gewebepackungen". Zürich: PhD Thesis ETH-Zürich 5618.

BERGBAUER, W.; HÖRNER, B. and K. DIALER (1979). "Zur Interpretation effektiver Austauschflächen in Systemen Gas/Flüssigkeit". Chem.Ing.Tech. 51(1), 38-39.

BILLET, R. (1983). "Fluiddynamisches Verhalten und Wirksamkeit von Gegenstromapparaten für Gas-Flüssig-Systeme bei flüssigkeitsseitigem Stoffübergangswiderstand". Festschrift der Fakultät für Maschinenbau, Ruhr-Universität Bochum, pages 24-31.

BILLET, R. and J. MACKOWIAK (1980). "Neuartige Füllkörper aus Kunststoffen für thermische Stofftrennverfahren". Chemie Technik 9(5), 219-226.

BILLET, R. and J. MACKOWIAK (1977). "Flüssigkeitsseitiger Stoffübergang bei der Absorption in Füllkörperkolonnen und ihr verfahrenstechnischer Vergleich.". Chemie-Technik 6(11), 1977, 455-461.

BOLLES, W.L. and J.R. FAIR (1982). "Improved mass-transfer model enhances packed-column design". Chemical Engineering 89(July 12), 109-116.

BOMIO, P. (1977). "Stoffaustauschmessungen an der Sulzer-Packungen aus Kunststoff". Chem.Ing.Tech. 49(11), 895-897.

BORNHÜTTER, K. and A. MERSMANN (1991). "Stoffübergang mit modernen Füllkörpern grosser Abmessungen". Chem.Ing.Tech. 63(2), 132-133.

BRAVO, J.L. and J.R. FAIR (1982). "Generalized correlation for mass transfer in packed distillation columns". Ind.Eng.Chem.Process Des.Dev. 21, 162-170.

BRIDGEWATER, J. and A.M. SCOTT (1974). "Statistical models of packing: application to gas absorption and solids mixing". Trans.Inst.Chem.Engrs. 52, 317-324.

CHILTON, T.H. and A.P. COLBURN (1935). "Distillation and absorption in packed columns - A convenient design and correlation method". Ind.Eng. Chemistry 27(3), 255-260.

COOPER, C.M.; CHRISTL, R.J. and L.C. PEERY (1941). "Packed tower performance at high liquor rates". Trans.Am.Inst.Chem.Eng. 37, 979-996.

CORNELL, D.; KNAPP, W.G. and J.R. FAIR (1960). "Mass transfer efficiency - packed columns - part I". Chem.Eng. Progress 56(7), 68-74.

COUGHLIN, R.W. (1969). "Effect of liquid-packing surface interaction on gas absorption and flooding in a packed column". AIChE J. 15(5), 1969, 654-659.

DANCKWERTS, P.V, and A.J. GUILLHAM (1966). "The design of gas absorbers I - Methods for predicting rates of absorption with chemical reaction in packed columns, and tests with 1 1/2 in raschig rings". Trans.Instn.Chem.Engrs. 44, 1966, T42-T54.

DANCKWERTS, P.V. and S.F. RIZVI (1971). "The design of gas absorbers. Part II: Effective interfacial areas for several types of packing". Trans.Instn.Chem.Engrs. 49, 124-127.

DANCKWERTS, P.V and M.M. SHARMA (1966). "The absorption of carbon dioxide into solutions of alkalis and amines (with some notes on hydrogen sulphide and carbonyl sulphide)". The Chemical Engineer 44, CE244-CE280.

DAVIDSON, J.F. (1959). "The hold-up and liquid film coefficient of packed towers. Part II: Statistical models of the random packing". Trans.Instn.Chem.Eng. 37, 131-136.

DEED, D.W.; SCHUTZ, P.W. and T.B. DREW (1947). "Comparison of rectification and desorption in packed columns". Ind.Eng.Chem. 39(6), 766-774.

DELALOYE, M.M.; VON STOCKAR, U. and X.-P. LU (1991). "The influence of the viscosity on the liquid-phase mass transfer resistance in packed columns". The Chemical Engineering J. 47, 51-61.

DELALOYE, M.M. (1986). "Influence de la viscosité du liquide sur le transfer de matière dans une colonne a garnissage à l'échelle pilote". Lausanne: PhD thesis EPFL 657.

DHARWADKAR, S.W. and S.B. SAWANT (1985). "Mass transfer and hydrodynamics characteristics of tower packings larger than 0.025 m nominal size". The Chemical Engineering J. 31, 15-21.

DUSS, M. and P.BOMIO (1991). "Rückgewinnung organischer Dämpfe aus Abgasströmen mit Absorptionsverfahren". Chem.Ing.Tech. 63(4), 388-389.

ECHARTE, R.; CAMPANA, H. and E.A. BRIGNOLE (1984). "Effective areas and liquid film mass transfer coefficients in packed columns". Ind.Eng.Chem.Process Des.Dev. 23(2), 349-354.

FAIR, J.R. and J.L. BRAVO (1990). "Distillation columns containing structured packing". Chem.Eng.Progress january, 19-29.

FAIR, J.R. and J.L. BRAVO (1987). "Prediction of mass transfer efficiencies and pressure drop for structured tower packings in vapor/liquid service". I.Chem.E.Symp.Ser. 104, A183-A201.

GIANETTO, A. and S. SICARDI (1972). "Interfacial areas in countercurrent absorption columns". Ing.Chim.Ital. 8(6), 181-182.

GRASSMANN, P. and F. WIDMER (1974). "Einführung in die thermische Verfahrenstechnik". Berlin: Walter de Gruyter 2. Edition, chapter 6 and 7.

GUILLEN, J.M.P.; PITARCH, M.A.O. and F.L. MATEOS (1982). "Determinacion del area interfacial y de los coeficientes de materia en sistemas de contacto gas-liquido por metodos quimicos". Ingenieria Quimica 14, 179-186.

HIGBIE, R. (1935). "The rate of absorption of a pure gas into a still liquid during short periods of exposure". Trans.Am.Instn.Chem.Eng. 31, 365-389.

HUTCHINGS, L.E.; STUTZMAN, L.F. and H.A. KOCH (1949). "Gas absorption: mass transfer coefficients as function of liquid, gas rates, tower packing characteristics". Chem.Eng.Progress 45(4), 253-268.

HÜTTINGER, K.J. and F. BAUER (1982). "Benetzung und Stoffaustausch in Filmkolonnen". Chem.Ing.Tech. 54(5), 449-460.

JACKSON, G.S. and J.M. MARCHELLO (1970). "Effective and wetted areas for absorption in packed columns". J.Chem.Eng.Japan 3(2), 263-264.

JHAVERI, A.S. and M.M. SHARMA (1968). "Effective interfacial area in a packed column". Chem.Eng.Sci. 23, 669-676.

JOOSTEN, G.E.H. and P.V. DANCKWERTS (1973). "Chemical reaction and effective interfacial areas in gas absorption". Chem.Eng.Sci. 28, 453-461.

KNOEDLER, E.L. and C.F. BONILLA (1954). "Vacuum degasification in a packed column". Chem.Eng.Progress 50(3), 125-133.

KOCH, H.A.; STUTZMAN, L.F.; BLUM, H.A. and L.E. HUTCHINGS (1949). "Gas absorption: Liquid transfer coefficients for the carbon dioxide-air-water system". Chem.Eng.Progress 45(11), 677-682.

KOLEV, N. (1976). "Wirkungsweise von Füllkörperschüttungen". Chem.Ing.Tech. 48(12), 1105-1112.

KOLEV, N. (1973). "Wirksame Austauschfläche von Füllkörperschüttungen". Verfahrenstechnik 7(3), 71-75.

KRÖTZSCH, P. (1982). "Measurements of liquid-phase mass transfer in packed columns". Ger.Chem.Eng. 5, 131-139.

KRÖTZSCH, P. and H. KÜRTEN (1979). "Druckverlust und Stoffaustauschfläche in Füllkörperschüttungen". Verfahrenstechnik 13(12), 939-944.

KUNESH, J.G. (1987). "Recent developments in packed columns". The Can.J.of Chem.Eng. 65, 907-913.

LANDAU, J.; BOYLE, J.; GOMAA, H.G. and A.M. AL TAWEEL (1977). "Comparison of methods for measuring interfacial areas in gas-liquid dispersions". The Can.J.of Chem.Eng. 55, 13-18.

LAURENT, A. and J.-C. CHARPENTIER (1974). "Aires interfaciales et coefficients de transfer de matière dans les divers types d'absorbeurs et de réacteurs gaz-liquide". The Chemical Engineering J. 8, 85-101.

LAURENT, A.; PROST, Ch. and J.-C. CHARPENTIER (1975). "Détermination par méthode chimique des aires interfaciales et des coefficients de transfer de matière dans les divers types d'absorbeurs et de réacteurs gaz-liquide". Journal de chimie physique 72(2), 236-244.

LEE, W.K. and Y.-H. KIM (1982). "Effective mass transfer area and mass transfer coefficient in a packed gas-absorber". Hwahak Konghak (J.of the Korean Inst.of Chem.Eng) 20(2), 123-132.

LEVENSPIEL, O. (1972). "Chemical reaction engineering". John Wiley & Sons, second edition, chapter 13.

LEWIS, W.K. and W.G. WHITMAN (1924). "Principles of gas absorption". Ind.Eng. Chemistry 16(12), 1215- 1220.

LINEK, V.; PETRICEK, P.; BENES, P. and R. BRAUN (1984). "Effective interfacial area and liquid side mass transfer coefficients in absorption columns packed with hydrophilised and untreated plastic packings". Chem.Eng.Res.Des. 62(1), 13-21.

LINEK, V.; STOY, V.; MACHON, V. and Z. KRIVSKY (1974). "Increasing the effective interfacial area in plastic packed absorption columns". Chem.Eng.Sci. 29, 1955-1960.

LINEK, V. and V. VACEK (1981). "Chemical engineering use of catalyzed sulfite oxidation kinetics for the determination of mass transfer characteristics of gas-liquid contactors". Chem.Eng.Sci. 36(11), 1747-1768.

McCABE, W.L. and J.C. SMITH (1976). "Unit operations of chemical engineering". McGraw-Hill Book Co., 3rd Edition, pages 711-714.

MANGERS, R.J. and A.B. PONTER (1980). "Effect of viscosity on liquid film resistance to mass transfer in a packed column". Ind.Eng.Chem.Process Des.Dev. 19(4), 530-537.

MAYO, F.; HUNTER, T.G. and A.W. NASH (1935). "Wetted surface in ring-packed towers". J.of the Society of Chemical Industry 54, 375-385.

MEIER, W. (1979). "Sulzer-Kolonnen für Rektifikation und Absorption". Technische Rundschau Sulzer 2/1979, 49-61.

MEIER, W.; HUNKELER, R. and W.D. STOCKER (1979). "Sulzer Mellapak - Eine neue, geordnete Packung für Stoffaustausch-Apparate". Chem.Ing.Tech. 51(2), 119-122.

MEIER, W.; STOECKER, W.D. and B. WEINSTEIN (1977). "Performance of a new, high efficiency packing". Chem.Eng.Progress 73(11), 71-77.

MERCHUK, J.C. (1980). "Mass transfer characteristics of a column with small plastic packings". Chem.Eng.Sci. 35, 743-745.

MOHUNTA, D.M.; VAIDYANATHAN, A.S. and G.S. LADDHA (1969.a). "Effective interfacial areas in packed columns". Indian Chemical Engineer April, 39-42.

MOHUNTA, D.M.; VAIDYANATHAN, A.S. and G.S. LADDHA (1969.b). "Prediction of liquid-phase mass transfer coefficients in columns packed with raschig rings". Indian Chemical Engineer July, 73-79.

MURTHY, M.S. and A.V. RAO (1979). "Interfacial area for packed towers". J.Indian Inst.Sci. 61(1), 1-19.

NEELAKANTAN, K. and J.K. GEHLAWAT (1982). "New chemical systems for the determination of liquid-side mass transfer coefficient and effective interfacial area in gas-liquid contactors". The Chemical Engineering J. 24, 1-6.

NORMAN, W.S. (1961). "Absorption, Distillation and Cooling Towers". New York: John Wiley & Sons, chapter 6.

ONDA, K.; SADA, E. and Y. MURASE (1959). "Liquid-side mass transfer coefficients in packed towers". AIChE J. 5(2), 235-239.

ONDA, K.; TAKEUCHI, H. and Y. KOYAMA (1967). "Effect of packing materials on the wetted surface area" (in japanese). Chem.Eng.Japan 31, 126-134.

ONDA, K.; TAKEUCHI, H. and Y. OKUMOTO (1968). "Mass transfer coefficients between gas and liquid phases in packed columns". J.of Chem.Eng.Japan 1, 56-62.

PERRY, R.H. (1984). "Perry's chemical engineer's handbook". 6th Edition. McGraw-Hill Book Co., page 18.23.

PERRY, D.; NUTTER, D.E. and A. HALE (1990). "Liquid distribution for optimum packing performance". Chem.Eng.Progress january, 30-35.

PONTER, A.B. and P.H. AU-YEUNG (1982). "Estimation of liquid film mass transfer coefficients for columns randomly packed with partially wetted rings". The Can.J.of Chem.Eng. 60, 94-99.

PONTER, A.B.; PFENNIGWERTH, G.L. and R.J. MANGERS (1980). "Liquid film mass transfer coefficients for packed columns using organic and aqueous systems". Chem.Ing.Tech. 52(8), 656-657.

PURANIK, S.S. and A. VOGELPOHL (1974). "Effective interfacial area in irrigated packed columns". Chem.Eng.Sci. 29, 501-507.

RICHARDS, G.M.; RATCLIFF, G.A. and P.V. DANCKWERTS (1964). "Kinetics of CO_2 absorption-III First-order reaction in a packed column". Chem.Eng.Sci. 19, 325-328.

RIXON, F.F. (1948). "The absorption of carbon dioxide in and desorption from water using packed towers". Trans.Instn.Chem.Eng. 26, 119-130.

RIZZUTI, L. and A. BRUCATO (1989). "Liquid viscosity and flow rate effects on interfacial area in packed columns". The Chemical Engineering J. 41, 49-52.

SAHAY, B.N. and M.M. SHARMA (1973). "Effective interfacial area and liquid and gas side mass transfer coefficients in a packed column". Chem.Eng.Sci. 28, 41-47.

SCHMUKI, P. and M. LASO (1990). "On the stability of rivulet flow". J.Fluid Mech. 215, 125-143.

SCHULTES, M. (1990). "Einfluss der Phasengrenzfläche auf die Stoffübertragung in Füllkörperkolonnen". Düsseldorf: VDI-Verlag.

SEDELIES, R.; STEIFF, A. and P.-M. WEINSPACH (1987). "Mass transfer area in different gas-liquid reactors as a function of liquid properties". Chem.Eng.Technol. 10, 1-15.

SEMMELBAUER, R. (1967). "Die Berechnung der Schütthöhe bei Absorptionsvorgängen in Füllkörperkolonnen". Chem.Eng.Sci. 22, 1237-1255.

SHARMA, M.M. and P.V. DANCKWERTS (1970). "Chemical methods of measuring interfacial area and mass transfer coefficients in two-fluid systems". British Chemical Engineering 15(4), 522-528.

SHERWOOD, T.K. and F.A.L. HOLLOWAY (1940). "Performance of packed towers - Liquid film data for several packings". Trans.Am.Instn.Chem.Eng. 36, 39-70 and 181-182.

SHI, M.G. and A. MERSMANN (1985). "Effective interfacial area in packed columns". Ger.Chem.Eng. 8, 87-96.

SHULMAN, H.L.; ULLRICH, C.F. and N. WELLS (1955.a). "Performance of packing columns - I. Total, static and operating holdups". AIChE J. 1(2), 247-253.

SHULMAN, H.L.; ULLRICH, C.F.; PROULX, A.Z. and J.O. ZIMMERMAN (1955.b). "Performance of packing columns - II. Wetted and effective interfacial areas, gas- and liquid-phase mass transfer rates". AIChE J. 1(2), 253-258.

SPIEGEL, L. and W. MEIER (1987). "Correlations of the performance characteristics of the various Mellapak Types". I.Chem.E.Symposium Series 104, A203-A215.

SRIDHARAN, K. and M.M SHARMA (1976). "New systems and methods for the measurement of effective interfacial area and mass transfer coefficients in gas-liquid contactors". Chem.Eng.Sci. 31, 767-774.

SULZER BROTHERS LIMITED (1991). "Separation columns for distillation and absorption". Winterthur: Publication number 221306.

SULZER BROTHERS LIMITED (1989). "SULPAK - Sulzer design and sizing program for packed columns".

VAN KREVELEN, D.W. and P.J. HOFTIJZER (1947.a). "Kinetics of gas-liquid reactions - Part I: general theory". Rec.Trav.Chim. 67, 563-586.

VAN KREVELEN, D.W. and P.J. HOFTIJZER (1947.b). "Studies of gas absorption - I. Liquid film resistance to gas absorption in scrubbers". Rec.Trav.Chim. 67, 49-66.

VIDWANS, A.D. and M.M. SHARMA (1967). "Gas-side mass transfer coefficient in packed columns". Chem.Eng.Sci. 22, 673-684.

VIVIAN, J.E.; BRIAN, P.L.T. and V.J. KRUKONIS (1967). "Gas absorption in packed columns: liquid phase resistance in the loading region". AIChE J. 13(1), 174-175.

VIVIAN, J.E. and C.J. KING (1964). "The mechanism of liquid-phase resistance to gas absorption in a packed column." AIChE J. 10(2), 221-227.

VON STOCKAR, U. and X.-P. LU (1991). "Simple and accurate short-cut procedure to account for axial dispersion in countercurrent separation columns". Ind.Eng.Chem.Res. 30, 1248-1257.

VON STOCKAR, U. and C.R. WILKE (1991). "Absorption". Kirk-Othmer; Encyclopedia of Chemical Technology vol 1. John Wiley & Sons, forth edition, 38-93.

YOSHIDA, F. and T. KOYANAGI (1958). "Liquid phase mass transfer rates and effective interfacial area in packed absorption columns". Ind.Eng.Chemistry 50(3), 365-374.

YOSHIDA, F. and T. KOYANAGI (1962). "Mass transfer and effective interfacial areas in packed columns". AIChE J. 8(3), 309-316.

YOSHIDA, F. and Y. MIURA (1963). "Effective interfacial area in packed columns for absorption with chemical reaction". AIChE J. 9(3), 331-337.

ZECH, J.B. and A. MERSMANN (1979). "Liquid flow and liquid phase mass transfer in irrigated packed columns". I.Chem.E.Symposium Series 56, 2.5/39-47.

ZOGG, M. (1972). "Strömungs- und Stoffaustauschuntersuchungen an der Sulzer-Gewebepackung". Zürich: PhD thesis ETH-Zürich 4886.

1 Description of the pilot plant

For this work, since industrial operating conditions were required, a large and operatively complex pilot plant occupying 5 floors at the Institute of Chemical Engineering was used. This plant is that used by Delaloye (1986) for experiments with glass rings of 25 mm, with important modifications made for this work. As with MELLAPAK 125.Y, 250.Y and 500.Y broader ranges of F-Factors are attainable than with irregular packings, and as the column had to be frequently repacked to test different types of packing, the gas circuit, the column structure and its frame were changed. Numerous other changes were executed in accordance with the specific needs of the experiments in this work, ensuring reliable and safe plant operation.

A detailed and simplified flow-sheet of the pilot plant is given in figure 2.1. The gas and liquid sampling circuits is shown in figure 2.4, section 4.3. A listing of all instrumentation and equipment, as well as the function of each may be found in the table in the appendix A. The code used to identify each element is explained at the end of this table. The function of each circuit is given below.

The pilot plant had basically four main circuits:
- The gas circuit
- The large circuit of solution
- The small circuit of solution
- The gas temperature-and-humidity-regulating circuit

The gas circuit assured a gas flow with its temperature regulated at 22 ± 3 °C. The gas humidity was maintained at saturaton level, which prevented heat effects due to evaporation of the solvent in column COL1. For the experiments to measure the mass transfer area, a known and constant CO_2 concentration in the air was required.

The large circuit supplied a constant liquid flow at 22 ± 3 °C. Actually, the pilot plant worked in a pseudo-steady state, but since the ratio between the volume of the main reactor and the liquid flow was so big (high residence time in reactor R11), and because of the fact that R11 was thoroughly agitated, the pseudo-steady state did not introduce error during the data treatment. Thus no correction to the data in subsequent processing was considered necessary. The concentration at the column inlet varied less between any two samples than the experimental error in the determination of its absolute value. The large circuit also included equipment to perform measurements of the liquid flowrate and neutralization of the solution before discharging it to the drain. As a concentrated NaOH solution can cause health hazards, a system to fill the main reactor with solid grains of NaOH using basin R13 was conceived, so that there was no contact with the NaOH solution during its preparation.

The small circuit of the solution established equilibrium conditions between air and water at the column COL1 inlet and outlet during k_La experiments (see section 2, chapter V). This circuit was also used for other manipulations, such as filling R11 without having to open it and cleaning COL1 (during the experiments for measuring the mass transfer area).

The gas temperature-and-humidity-regulating circuit circulates demineralized water in the column COL2 at a given temperature, so that the gas flowing to COL1 had its temperature and humidity regulated.

(a)

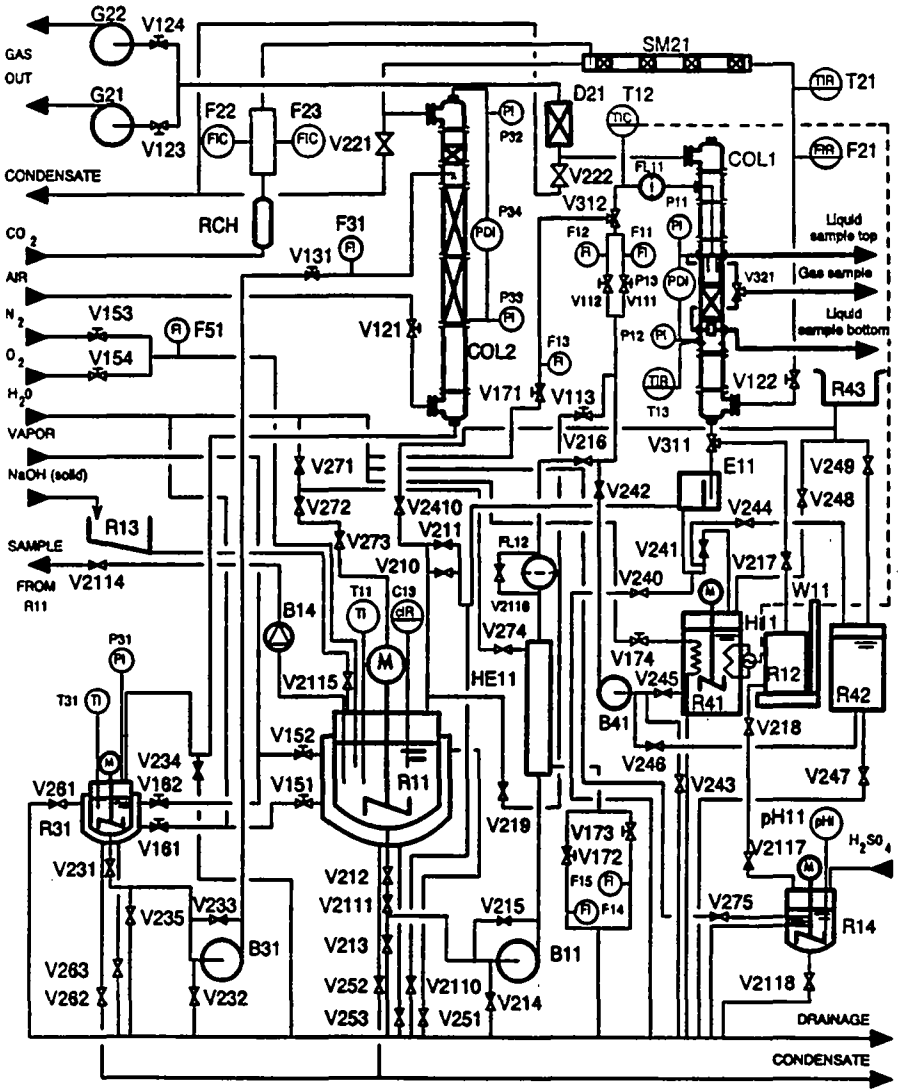

Figure 2.1 The pilot plant.
(a) Schematic showing all plant elements.

(b)

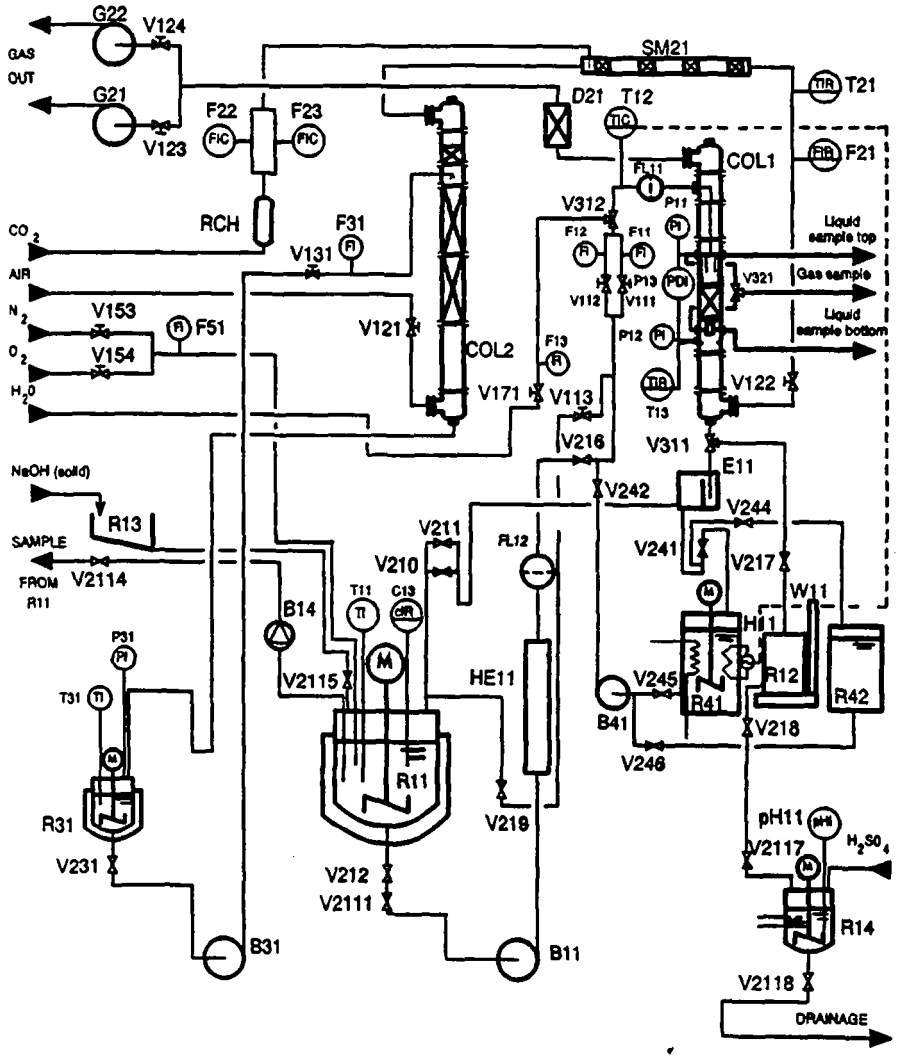

(b) Schematic showing principal plant elements only.

2 Description of the flows and of the equipment in the gas circuit

The section 2.1 describes the flow in the gas circuit. The sections 2.2 through 2.4 describe features of the gas circuit important for the experiments to measure the mass transfer area. The CO_2 system was not employed during, and did not affect the results of, the k_La experiments.

2.1 Flow in the gas circuit

In the gas circuit, air from the laboratory was aspirated through V121, flowed up through the COL2, was mixed in SM21 with CO_2, which came from the CO_2 manifold, and whose flow rate was regulated by the evaporator RCH and by the mass flow controllers F22 and F23. Measurements of the total flow conditions were made with T21 and F21, and the flowrate was regulated manually with V122. The gas entered at the bottom of COL1, flowed up through the packing, flowed out through mist eliminator D21, and was aspirated by G21 (or G22) before being discharged to the laboratory.

2.2 The CO_2 manifold

Liquified carbon dioxide, under high pressure, was stored in steel gas cylinders. An ordinary valve outlet regulator installed at the bottle would provide flows with the order of magnitude of 0.9 m^3/h, which is less than the required constant gas flows of 1 to 8 m^3/h, because with the large expansion (throttling), the gas cools down greatly.

Therefore, a gas manifold (from CARBAGAS AG, in Lausanne, Switzerland) of 4 bottles was built. During an experiment, three bottles supply CO_2 and the extra one was kept as a reserve. Although it was not possible to know precisely how much liquified CO_2 was available, the bottles were not employed once they were nearly empty. The liquid drawn from the bottles was gasified in the evaporator RCH. The evaporator had a potentiometer, which allowed adjustment of the temperature of the demineralized water in the evaporator. The temperature range of the water in the RCH was between 5 and 85°C and was set to 60°C. There was always water around the coil inside the evaporator before electrical power was switched on.

The pressure of the gas was reduced, in two stages to 5 bars, before it reached the mass flow controllers.

2.3 Mass flow controllers

To measure and guarantee a stable flow of CO_2, two BROOKS model 5851E (from ROSEMOUNT AG, in Baar, Switzerland) mass flow controllers were installed in the pilot plant. The CO_2 flow could be adjusted up to about 9.2 m^3/h.

The mass flow controllers were connected to a BROOKS model 5876 Dual Channel Power Supply, Read-Out, and Control Unit (from ROSEMOUNT AG, in Baar, Switzerland). This could be operated either with independent mass flow control channels, where the flowrate was set through the command potentiometers, or with one channel slaved to the master, the option chosen for this work. In this case, the output signal from Channel 1 was used as the command signal for Channel 2. When operating the mass flow controllers for the CO_2 system, it was necessary to have a pressure at the inlet of at least four bars higher than at the outlet.

Calibration was carried out by the manufacturer using a volumetric gas flow measuring instrument. A calibration certificate was furnished. However, it was not necessary for this work to know the absolute value of the CO_2 flow, but to have a constant value of the CO_2 concentration in the air, which had to be measured accurately by a gas analyzer (section 5.2.1 in chapter II).

2.4 The SULZER SMV static mixer

The four SMV mixing elements in stainless steel (from SULZER Brothers Limited, in Winterthur, Switzerland) provide a homogeneous mixture of CO_2 with the air coming from the column COL2. They were installed in the gas circuit of the pilot plant as shown in figure 2.2. The SULZER SMV static mixer was chosen because it gives a better homogeneous mixture than empty pipe, without a significant increase in the pressure drop.

The SMV mixing element (figure 2.2) used in this work consisted of five corrugated plates stacked in parallel to form a regular structure of open, intersecting channels. The mixing of the gases occured between neighboring plates, where opposing channel directions bring the individual streams into contact. Inhomogeneities were reduced by transversal displacement in the channels, avoiding backflowmixing. The gas was mixed further as it left the mixing element due to the momentum of the intersecting channel streams.

This effect was maximized with no additional pressure drop, by leaving a space of twice the internal diameter between each element of the mixer. To achieve a homogeneous mixture across the cross-section of the duct, the plates of the mixing elements were placed at 90° angles to one another. Each SMV element employed in this work had an external diameter of 161.9 mm, a length of 90 mm, a hydraulic diameter of mixing elements of 38.5 mm, a void fraction of 0.97 and a Newton number of 1.9.

The CO_2 inlet tube had four holes. The tube was perpendicular to the plates of the first element. Each hole of the tube had a diameter of 8 mm, such that the exit velocity of the CO_2 from each hole was about the same as the velocity of the resulting mixture of air with 1% CO_2.

The value of the Reynold's number indicated that the flow was turbulent. The number of mixing elements was determined by the required homogenity of the gas mixture, defined as the ratio of the standard deviation of the gas mole fraction to its mean value. With the standard deviation at the mixer outlet (= 0.001) and with the mean mole concentration (= 0.01), using Figure 12 on page 7 of the SULZER catalog "Mixing Process Equipment" (1987), it was determined that four SMV mixer elements would be needed.

The relationship between the homogenity of the gas mixture and the number of mixing elements, however, is valid only if the velocity is high enough to have no influenced of density differences between the gases. If CO_2 is mixed into air in a horizontal empty pipe, the concentration profile reveals a high concentration of denser CO_2 forming a stable layer in the lower part of the tube. According to Tauscher and Streiff (1979), the SMV mixer assures a homogeneous concentration pattern even at low gas flow velocity, provided that the Froude number, Fr, defined as equation 2.1, is greater than 20.

$$Fr = \frac{w_G^2}{(\Delta\rho/\rho).\varepsilon^2.d_h.g} \qquad (2.1)$$

This indicates that the gas flow had to be higher than 140 m^3/h. In the plant, after the static mixers and before the packing in the column, there was a horizontal pipe length of about 3 m and a vertical pipe length of about 8 m, plus the fittings and valves in the pipeline, which was considered to assure a homogeneity of the CO_2 throughout in the gas flow.

The pressure drop across the static mixer is given by:

$$\Delta p = Ne.\rho.v^2.\frac{L}{d} \qquad (2.2)$$

The pressure drop across the static mixers was below 60 mm H_2O, what caused no problems to the ventilators.

a)

b)

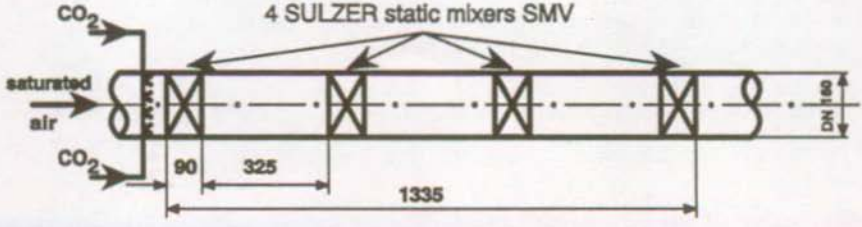

Figure 2.2 The SULZER SMV static mixer.
(a) consecutive elements placed at 90° angles to one another (illustration courtesy of SULZER BROTHERS LIMITED).
(b) installation in the pilot plant.

3 Description of the flows in the liquid circuits

3.1 Flow in the large circuit of the solution

In the large circuit, the solution stored in the reactor R11 flowed through the valves V212 and V2111, was pumped by B11, had its temperature regulated by the heat exchanger HE11, and flowed through the filter FL12 and valve V216. Then there was a choice between valve V111 with the rotameter F11 or valve V112 with the rotameter F12 (V113 was a by-pass valve, which together with valve V219 lead the solution back to R11). Then the solution flowed through the three way valve V312, and the temperature was measured by T12. The solution was filtered by FL11, and flowed into COL1. After COL1, the solution passed through V311, was degassed in E11, and flowed back into R11 through the siphon, whose height could be changed (valves V211 or V210).

From the control board (in office H4 595), V311 was opened for hold-up or liquid flow rate measurements. The solution passed through V217 and flowed into R12. The weight of the solution accumulated inside R12 during a measured time was given by the balance W11. During the $k_L a$ experiments, the reactor R14 was not connected to the outlet of valve V218. The water accumulated in R12 was directly discharged in the drain by opening V218. During the experiments for measuring the specific mass transfer area, the reactor R14 was necessary to neutralize the NaOH solution. Thus, the NaOH solution flowed by gravity into R14 by opening V218 and V2117. Concentrated sulfuric acid was slowly added into R14, which was thoroughly stirred and cooled by industrial water. When a pH of approximate 9 was attained, the valve V2118 was opened and the liquid was discharged into the drain. This neutralization demands attention, because after pH 10, the turning zone is narrow and the generation of heat is considerably high.

3.2 Flow in the small circuit of the solution

In this circuit, the solution stored in R41 could have its temperature regulated. From R41, the solution flowed through valve V245, was pumped by B41, and up through valve V242. The instrumentation measured flows properties, as described for the large circuit. The solution flowed into COL1, down by gravity into R41, passing through valve V311, the degasser E11 and the valve V241. The reactor R42, in parallel with R41, had fiberglass walls, supporting corrosive media. For reactor R42, the circuit was the same, but the valves V245 and V241 were closed and the valves V246 and V244 were opened.

3.3 Flow in the gas temperature-and-humidity-regulating circuit

In this circuit, the demineralized water stored in the reactor R31 flowed through the valve V231, was pumped by B31, flowed through the valve V131, down through column COL2, and back to R31, passing through a siphon. The column COL2 was packed with 12 stainless steel packing elements of 125.Y plus an element acting as a mist eliminator. The packing 125.Y was chosen because of its small pressure drop and high capacity (COL2 could not flood before COL1). A SULZER VKG distributor with drip point density of 234 points/m^2 was installed. A hoist for disassembling COL2 could be installed on the hook on the top of the frame in which COL2 was built.

4 The main column

4.1 Description

The main glass column (from QVF GLASSTECHNIK GmbH, in Reinach, Switzerland) had an average internal diameter of 295 mm. (Glass columns present a wavy internal surface). It had 6 parts, as shown in figure 2.3. The numeration of each part is from the top to the bottom of the column.

The column was built in a frame and there was a platform around the column and a hoist above it in order to make the procedure to pack the column easier. This procedure for structured and dumped packings is given in the appendix B.

The structured packings MELLAPAK 250.Y, 500.Y and 125.Y in stainless steel used in this work were supplied by SULZER Brothers Limited (in Winterthur, Switzerland). The section 1.4 in chapter I has introduced them. The ceramic rings of 25 mm were bought from KUHNI AG (in Allschwil, Switzerland), which represents VFF-FüLLKöRPER GMBH (in Ransbach-Baumbach, Germany).

Part 4 of the column originally had an internal flange for a glass support grid. This inside flange, being very thick, caused premature flooding. A support to suspend the SULZER support grid with MELLAPAK had to be built. Due to this support and the distributor, the maximum packing height was two packing elements (420 mm) for all k_La experiments and mass transfer area experiments until run 38. Part 3 of the column was introduced when it was necessary to conduct experiments with 25 mm ceramic rings and to study the effect of the packing height. A flexible tube was installed in the gas circuit at the gas column outlet, so that the column height could be changed.

4.2 The liquid distributor

The SULZER multiple stage distributor type VKRM (from SULZER Brothers Limited, in Winterthur, Switzerland) in stainless steel, was designed to cover a broad range of specific liquid load with only one liquid distributor. This avoided dismounting the column just to swap the distributor. However, the distributor did not work for specific liquid loads between 25 and 38 m^3/m^2h and between 80 and 90 m^3/m^2h. This distributor is designed such that for a given specific liquid load, there was a constant liquid level inside. This made the liquid flow uniformly from the distribution points.

The distributor had 36 tubes (diameter of 20 mm) over a cross-section with a diameter of 295 mm, which gives 527 points/m^2, an excellent drip point density, eliminating all possible entrance effects. Its height was 400 mm plus a locating grid of 30 mm. This liquid distributor was tested at the SULZER liquid distributor test rig. For the last experiments in chapter IV, the drip point density was reduced to 117 points/m^2. Figure 4.12 in section 3.7 in chapter IV shows the distribution points in the cross section of the tower.

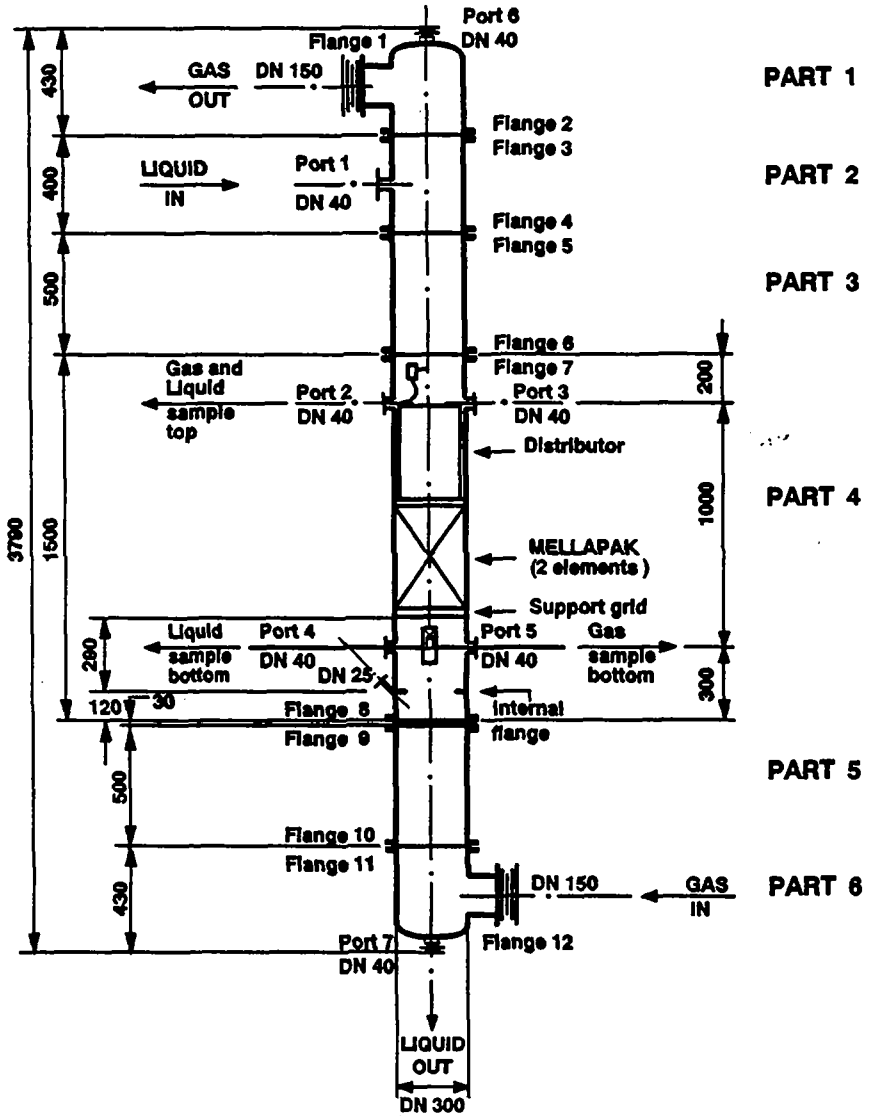

Figure 2.3 The main column COL1.

4.3 Gas and liquid sampling

Gas sampling during the experiments to measure the mass transfer area (Chapter IV) was necessary. Before each experiment, the calibration of the BINOS 1 gas analyzer (section 5.2.1, chapter II) had to be carried out.

The flow in the gas sampling circuit (figure 2.4) is determined by the 3-way valve V321, depending whether the sample to be pumped out by the peristaltic pump B21 came from the top or from the bottom of the packing. Compressed air flowed in the tubes by V322 in order to clean or eventually dry the tubes. Calibration gases for the gas analyzer could be introduced by V323. The rotameter after the gas analyzer indicated the flow rate in the gas analyzer, which had to be less than 150 Nl/h.

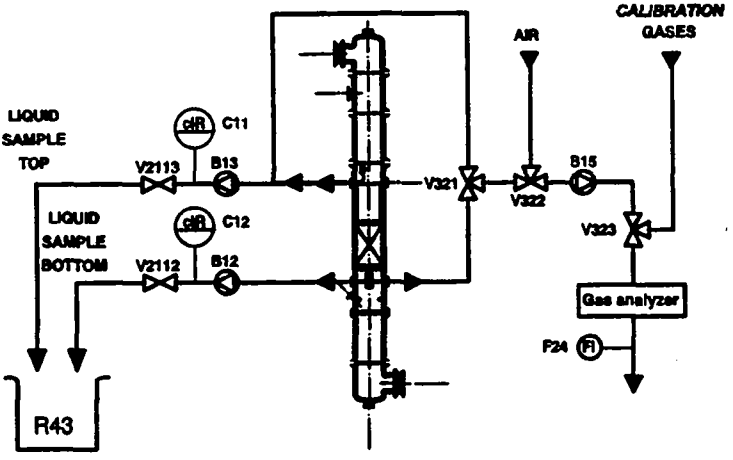

Figure 2.4 The gas and liquid sampling circuits.

A special collector to take liquid samples at the bottom of the column was designed (figure 2.5), so that no air bubbles could be entrained. Its efficiency was confirmed during tests before definitive mounting of the column. With this device, gas sampling could also be done. Its position at the bottom of the column could have been changed, but during this work, it was always installed at the column axis 10 mm beneath the packing's supporting grid. The collector did not interfere with the gas flow, ie. its presence caused no local flooding. The peristaltic pump B12 pumped continually liquid sample through a small chamber in front of the pO_2 probes during the k_La experiments. For the measurements of the specific mass transfer area, the liquid samples were pumped into the R43, where flasks would collect liquid samples for titration (section 5.2.2, chapter II).

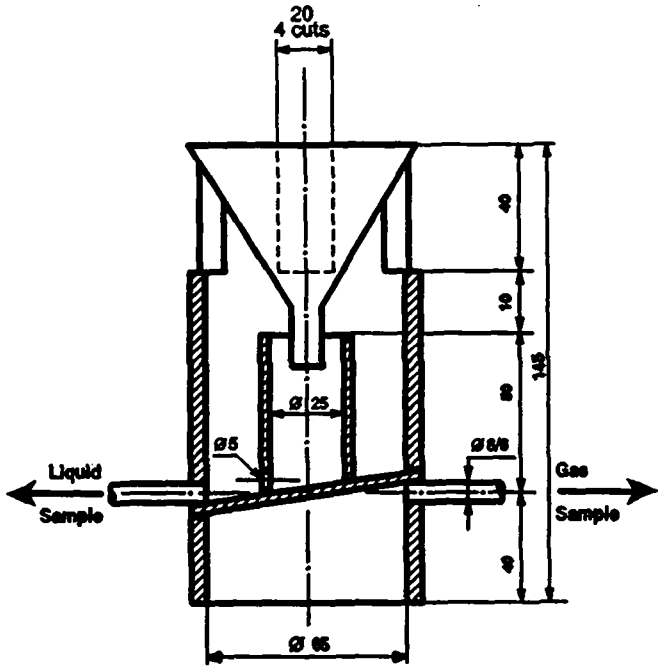

Figure 2.5 Scheme of the collector for sampling at the bottom of the column.

For liquid sampling at the top of the column, a small cup was installed next to the column wall at the outlet of one of the 36 tubes of the distributor. This small cup was fixed to the distributor's locating grid. There was a continuous overflow from the top of the cup. A flowrate of 3 to 4 l/h was pumped out from the cup by a peristaltic pump. For the small specific liquid load of 12 m^3/m^2h, there was a liquid outlet flow of about 23 l/h per tube of distributor. The sampling could have been taken directly from the inside of the distributor, but the liquid height in the distributor would then have had an influence on the value measured by the pO_2 probes (section 5.3.2, chapter II).

Great attention was given to the presence of air bubbles in the liquid drawn off from the top of the column. For specific liquid loads below 55 m^3/m^2h, irrespective of the velocity of the peristaltic pump, no bubbles were observed. However, for higher specific liquid loads, bubbles with diameter of about 2 mm were entrained from time to time. These bubbles come from the inside of the distributor, as the inlet liquid splashes. The column was opened to verify such an assumption, which was confirmed. The overflow of the cup under the distributor was carefully controlled. The liquid with these bubbles were indeed a precise sample of the liquid inside the distributor. It is thus assumed that these bubbles bring no contribution to the mass transfer process (see section 3.7, chapter IV, for a discusion of the impossibility of having measured extra mass transfer).

5 Instrumentation

In the section 5.1, the instrumentation used for all experiments is described. The sections 5.2 and 5.3 gives detailed information of the equipment used for the experiments to measure the mass transfer area and the $k_L a$ respectively.

The figure 2.6 shows a picture of the main column with the instrumentation.

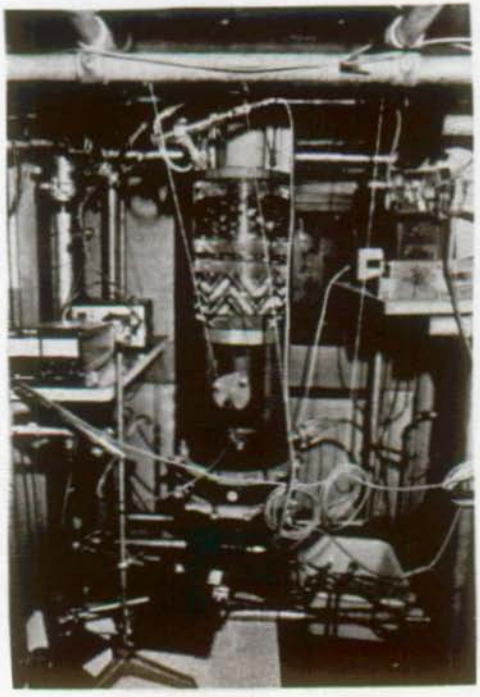

Figure 2.6 The main column COL1 with the instrumentation.

5.1 Instrumentation for all experiments

5.1.1 Liquid flowrate

The rotameter G51.14 (code F11) or G41.12 (code F12) (from KROHNE AG, in Basel, Switzerland) was used for the measurements of the specific liquid load, depending on this value. The determination of several liquid flowrates corresponding to the chosen positions of the rotameters' metering float were performed immediately after a series of runs (as defined in section 6.1, chapter II). Such practice had the convenience of not wasting the solution in reactor R11, thus emptying the reactor only when it was necessary.

The liquid flowrate was determined by measuring the weight of solution accumulated in R12 during a lapse of time when the 3-way valve V311 was opened to the exterior position. The density was determined by measuring the weight of the solution in a known volume, such as a measuring cylinder. If the level in reactor R11 was low, it was difficult to measure large liquid flowrates. Therefore, large liquid flowrates were measured first. Small specific liquid loads (below 20 m^3/m^2h) were difficult to keep constant with the valve V112, while the pump B11 was working. The by-pass circuit with V113 and V219 had to be used, reducing pressure on valves V111 and V112.

5.1.2 Gas flowrate

The principle of the volumetric instrument to measure the gas flow (from BARCOL-AIR AG, in Stäfa, Switzerland) is based on the external flow over a cylinder, when the pressure difference between the stagnation point and the point at a position of 180° is related to the actual flowrate. This instrument has the advantage of averaging the flow throughout the section. Using a table furnished by BARCOL-AIR AG, it was possible to derive the following equations:

with the 160 mm diameter tube: $G = \exp(4.066) * \sqrt{\Delta p}$ (2.3.a)

with the 100 mm diameter tube: $G = \exp(3.093) * \sqrt{\Delta p}$ (2.3.b)

where Δp is the pressure difference in [Pa] read by a pressure sensor (from ROLF MURI AG, in Rüschlikon, Switzerland), which transformed a pneumatic signal in a voltage. This voltage, corresponding to a pressure drop, was treated by a computer program, which calculated the gas flow taking into account a different pressure and temperature inside the column. The F-Factor was then evaluated as:

$$\text{F-Factor} = \frac{G}{A_c} \cdot \frac{1}{3600} \cdot \sqrt{\rho_G} \qquad (2.4)$$

where the ideal gas equation was used to calculate the gas density.

The absolute value of the gas flow and F-Factor had no influence on the computation of either the mass transfer area or $k_L a$. Inaccurate F-Factors could indeed potentially render the conclusions of this work invalid. Although it is very difficult to verify the calibration of gas flow instruments, a simple experiment indicated that the values given by the instrument used in this work were reasonable.

Data from measurements of pressure drop as a function of the F-Factor for 4 elements of the packing MELLAPAK M500.Y with no liquid throughput were compared to those given by SULZER BROTHERS LIMITED (in an internal communication). They were within a deviation of ± 10 %. The agreement was particularly good for F-Factors between 1 and 2. Differences of up to 5 % in equal gas flowrates in different runs (definition in section 6.1, chapter II) were expected.

An error of 10 % in the evaluation of the F-Factor is assumed in this work.

5.1.3 Pressure and temperature instrumentation

The manometric pressures inside the column were measured with U-tubes filled with water. The pressure in the laboratory was determined with a barometer.

For measuring gas and liquid temperatures in the pilot plant different types of temperature sensors were used. The most important temperature measurements were those of the gas and liquid inlet. For these measurements, Pt100 temperature sensors (from TRANSMETRA AG, in Schaffhausen, Switzerland) connected to digital thermometers with output voltage (from WALDSEE ELECTRONIC GmbH, in Bad Waldsee, Germany) were employed. The thermometers were calibrated with melting ice to set the zero and boiling water to set the range.

5.2 Instrumentation for specific mass transfer area experiments

5.2.1 The BINOS 1 gas analyzer

The infra-red gas analyzer BINOS 1 (from LEYBOLD-HERAEUS, in Hanau, Germany) was used to measure the mole fraction of CO_2 in the CO_2 - air gas mixture. The catalog from LEYBOLD-HERAEUS gives detailed information.

The performance of the BINOS available at the institute was first checked using a mixture of CO_2 and N_2 supplied by two mass flow controllers. These preliminary experiments indicated that linearity was maintained. At the beginning of each experiment, a calibration with N_2 (from CARBAGAS AG, in Lausanne, Switzerland) to establish the zero level and with a calibrated gas mixture with certificate of 1% CO_2 in synthetic air (from CARBAGAS AG, in Lausanne, Switzerland) to set the range was carried out. The zero level and the range were set at the front plate of the equipment. The error of the determination of the concentration of CO_2 was estimated at 3%.

5.2.2 The titration of carbonate solutions

The titration curve results from the neutralization of the hydroxide and carbonate ions. The carbonate anion is titrated to the stepwise addition of protons to form bicarbonate and CO_2. The equations governing the titration of carbonate solutions result from a charge balance combined with ionization equilibrium expressions. The titration curve equation is deduced in Butler (1982). The reactions underlying the process are explained in section 1.1, chapter III. There are three inflection points as shown in figure 2.7 for the titration with 1 mol/l HCl. The first equivalence point corresponds to a pH given by the carbonate, the second to ions bicarbonate and the third equivalence point to dissolved CO_2.

A personal computer compatible with IBM-PC/AT was employed with a precise feeding instrument - DOSIMAT 665 - and a pH-meter - pH METER 632 (both equipments from METROHM AG, in Herisau, Switzerland) for the automatic titration of the carbonate content of samples. The two instruments are shown in figure 2.8.

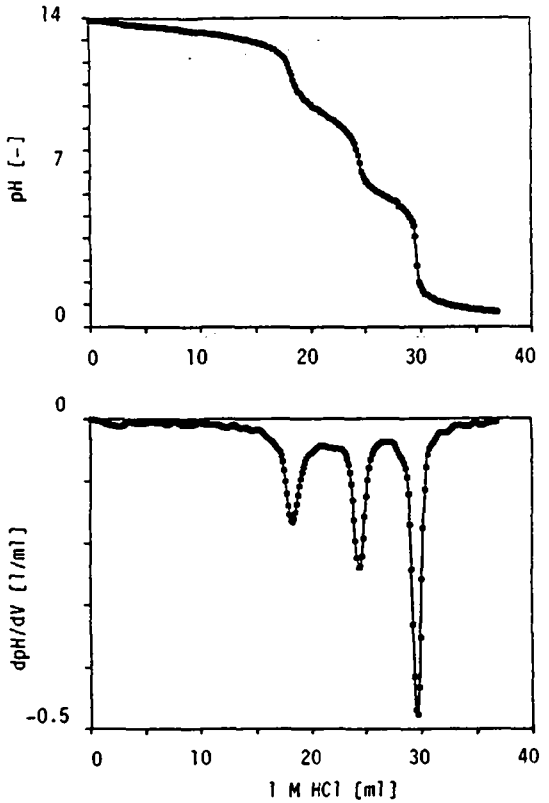

Figure 2.7 **Titration curve of carbonate solutions with 1 M HCl.**

The program DOSPH8.PGM was responsible for analog data acquisition from the DOSIMAT and from the pH-METER using a RTI-815 multifunction input/output board from *ANALOG DEVICES*. The program DOSPH8.PGM was written with the computer language ASYST version 2.01. The titration curve in figure 2.7 was made with an earlier version of the program DOSPH8.PGM.

The program DOSPH8.PGM was developed for the experiments with the wetted wall column (Chapter III) and was the same for the experiments to measure the mass transfer area (Chapter IV). The accuracy of the results was confirmed with a potentiograph E536 (from METROHM AG, in Herisau, Switzerland). Reproducibility of the results with different operators was obtained as long as the sample to be titrated was well stirred. The titration procedure with the program is given as a step of the procedure mass transfer area experiments in appendix C.

Figure 2.8 Experimental set for the titration of carbonate.

A sample of 15 ml was mixed with the same volume of 1 mol/l HCl and was brought to the DOSIMAT. The pH electrode was plunged into the solution. In a first stage, HCl 1 mol/l was added to reduce the pH to a selected value between 9.0 and 12.0, depending on the carbonate concentration. In a second stage, with the exchange unit having 0.1 mol/l HCl, the titration continued, and the program started to store data from the DOSIMAT and from the pH-METER. Each pair of data was a point of the titration curve. A stored data point resulted from an average of 20 points. A new point was obtained every 200 ms. The acquisition stopped at a pH of 2.7.

From the derivative of the titration curve without the first equivalence point, two peaks were clearly identified. The acid added between them is proportional to the carbonate concentration:

$$[CO_3^{=}] = (V_{eq3} - V_{eq2}) \cdot \frac{1}{V_s} \cdot c_a \qquad (2.5)$$

The initial concentration of hydroxide ions is proportional to the acid added to the first equivalence point. This value was evaluated with:

$$[OH^-] = (V_s + V_{HCl\ 1M} + V_{eq2} \cdot c_a) \cdot \frac{1}{V_s} - [CO_3^{=}] \qquad (2.6)$$

where: $V_{HCl\ 1M}$ is the volume of HCl 1M added in the first part of the program.

The results were stored in a file when the program was over. In the appendix P, the listing of the program DOSPH8.PGM is given.

5.3 Instrumentation for k_La experiments

5.3.1 Description of pO_2 probes

Dissolved oxygen electrodes, also known as pO_2 probes or pO_2 sensors, measure the partial pressure of oxygen, present either dissolved in liquids or in a gas mixture. The pO_2 probes do not measure directly the oxygen concentration, but a value which is proportional to this concentration. The proportionality factor depends on the state and conditions of the sample, thus requiring calibration before use.

The oxygen diffuses through a gas permeable teflon membrane, non-conductive, which separates the single electrode body from the fluid where the oxygen's partial pressure has to be measured. The electrode body contains a platinum cathode and a reference anode (Ag-AgCl) immersed in an electrolyte solution of gel-KCl.

In contrast to pH electrodes, which give as an output a voltage proportional to the activity of the ions, the pO_2 probes are a polarographic amperometric cell. When a constant voltage from an external power supply (amplifier) is applied to the electrodes, there occurs a selective reduction of the oxygen ions at the cathode. The value of the applied voltage to the anode is chosen in a way that only the oxygen and no other gas can react. The chemical reaction generates a current linearly proportional to the oxygen's partial pressure.

In principle, pO_2 electrodes may be immersed in all media, provided they last. The generated current does not change when the electrode passes from the atmosphere into a liquid in which the dissolved O_2 is in equilibrium with the air. The liquid must not in this case contain chemical or biological agents which could partly consume the dissolved O_2. In the absence of oxygen, the current of the electrode is not completely zero, due to impurities and other factors. The electrode's signal amplifier overcomes this problem by offsetting this dark current.

A concentration gradient is established between the bulk of the sample and the cathode, as there is a slight consumption of oxygen. The concentration gradient between the bulk of the sample and the membrane must be negligible, through adjustment of a minimal sample flow, above which probe response is not sensitive to the sample flow.

Dissolved oxygen electrodes are discussed in detail by the operating manual from INGOLD AG; further information is available in Mossier (1988).

5.3.2 Use of pO_2 probes

Two pO_2 probes (from INGOLD AG, in Urdorf, Switzerland) with a diameter of 19 mm, a length of 150 mm, and incorporating a temperature compensation were used to measure the dissolved oxygen concentration at the column inlet and outlet. For the reactor R11, there was a 420 mm long INGOLD pO_2 probe having a diameter of 25 mm.

The probes had to be polarized for at least 6 hours before use. They were actually kept constantly polarized by three independent amplifiers type IL533 (from INGOLD AG, in Urdorf, Switzerland) The program KLA4.PGM (section 5.3.3, chapter II) guided probe calibration.

The longer probe in reactor R11 gives only an indicative value. A precise calibration was not necessary. Nevertheless, a good indicative value indicated to sufficient accuracy if the water in reactor R11 was saturated enough with O_2 before the runs. An easy calibration may be performed with an O_2 simulator from INGOLD. This device simulates two different situations: water in equilibrium with nitrogen or water in equilibrium with air. The need for the O_2 simulator is to check the connecting cable and amplifier.

Figure 2.9 shows the rig which was built to perform calibration of the two smaller probes. The cylinders were actually bubble columns filled with demineralized water. It was verified that at the gas inlet, the air bubbles were uniformly distributed over the cross-section.

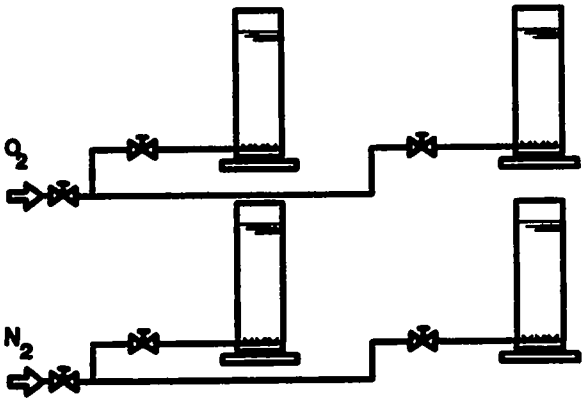

Figure 2.9 Rig for probe calibration.

Calibration begins with setting the zero level (absence of O_2) and continues with setting the balance (100 % of O_2). Afterwards, the zero of probes were tested again in a different cylinder from the one previously used to set the zero level. A linearity control was sometimes carried out by bubbling air through the cylinders and verifying the response. A final calibration control was done with the column under operating equilibrium conditions, when steady state conditions were achieved.

The broader the difference between the chosen conditions to fix the zero level and the balance, the more precise will be the calibration. This reasoning justifies the use of nitrogen (in the absence of oxygen) to set the zero level and 100 % oxygen to set the balance.

Notation:
- a - read value for the balance
- b - read value for the zero level
- c - concentration equivalent to absence of oxygen
- d - concentration equivalent to 100 % oxygen
- x - given condition
- y - read value

As there is linear relationship between y and x:

$$y = \frac{a - b}{d - c} \cdot x - \frac{a - b}{d - c} \cdot c + b \qquad (2.7)$$

The error associated with determination of y is given by an error propagation study:

$$\Delta y = \frac{x}{d} \cdot \Delta a + (1 - \frac{x}{d}) \cdot \Delta b + (\frac{a.x}{d^2} - \frac{a}{d}) \cdot \Delta c + \frac{x}{d^2} \cdot \Delta d \qquad (2.8)$$

With b = 0 and c = 0, equation (2.7) becomes:

$$y = \frac{a}{d} \cdot x \qquad (2.9)$$

or, dividing (2.8) by (2.9):

$$\frac{\Delta y}{y} = \frac{\Delta a}{a} + \frac{(d - x) \cdot \Delta b}{a \cdot x} + \left|\frac{1}{d} - \frac{1}{x}\right| . \Delta c + \left[\frac{1}{a.d}\right] . \Delta d \qquad (2.10)$$

The equation (2.10) confirms that a broader difference between the zero level and the balance reduces the error associated with probe calibration. However, these were not greater than 1%. Nevertheless, data acquisition distortions could have increased these values.

Both pO_2 probes were placed outside the column at the same level where the liquid sampling was performed. The tubing had an inside diameter of 4 mm and the shortest possible length. The pO_2 probes were put into a pyrex cylinder. A space of 12 mm was left in front of the probes for the sample flow. The volume of this chamber was about 4 ml. The liquid entered at the bottom and flowed to the top, so that any bubbles present were immediately evacuated.

5.3.3 The data acquisition program KLA4.PGM

The program KLA4.PGM was written with ASYST version 2.01. This program did not perform data processing, which was done after each experiment with LOTUS 123. The program KLA4.PGM was responsible for data acquisition and offered guidance for the measurements. An important goal of the program was to be efficient, simple, user friendly and easily understood by others. The structure of the program is given in figure 2.10.

From the main routine 7 procedures may be called. With procedure P02.CAL.KLA, probes were calibrated. INPUT.KLA asks for general information concerning the experiment, such as date, atmospheric pressure, packing type and number, so that the run was identified. Data acquisition of measurements of equilibria concentrations were performed with EQ.KLA. For the actual desorption experiments with the possibility of changing the liquid flowrate, the procedure DES.KLA was employed. The results were stored in a file with the procedure STORE.KLA. A listing of the file was printed out with the subroutine PRTFILE.KLA. A data transfer to two Lotus 123 files in a diskette

was executed by procedure DISK.KLA after each run. Also with the main menu, data from the plant could be displayed on the screen.

The procedure PO2.CAL.KLA for probe calibration had a menu with seven possibilities: (1) calibration of probe C13; (2) calibration of probe C11; (3) calibration of probe C12; (4) simultaneous calibration of C11 and C12 (the option frequently used); (5) control of the probe response read by the computer; (6) display of calibration values; and (7) exit of this part of the program. The support subroutines PO2.CAL.ZERO and PO2.CAL.BALANCE were to set the zero level and the balance of the probes respectively. PO2.CAL.VALUE evaluates the correlation for data acquisition.

The support subroutine CONC.MEAS.IN performs acquisition of the analog values from the probes. A first average was done between 120 values. The final value was an average from the 16 averages taken before. The support subroutine CONC.MEAS transforms these values into the corresponding concentrations.

The support subroutine INST.DATA.IN performs acquisition of the analog values from the pressure sensor related to the gas flow rate measurement F21 (section 5.1.2, chapter II). As before, a first average was done between 120 values. The final value was an average from 16 averages taken before. The support subroutine INST.DATA transform these values into meaningful values, as explained in section 5.1.2, chapter II.

A listing of the program is available in appendix 0.

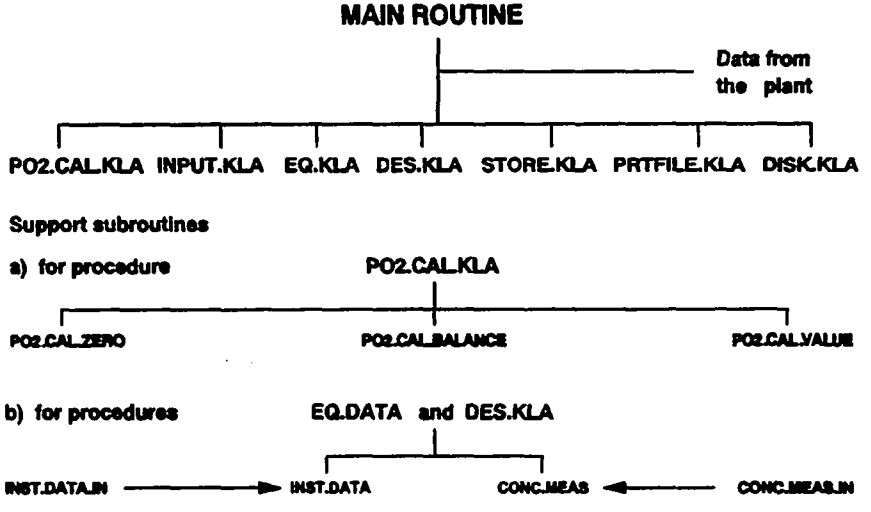

Figure 2.10 Structure of the program KLA4.PGM.

6 Background for conducting the experiments

6.1 Chosen operating conditions

The experiments had to show the evolution of the mass transfer area and of $k_L a$ in respect to the liquid load, the F-Factor and to the MELLAPAK type (change in the available geometric area). Similar conditions for both experimental series were required in order to obtain the liquid phase mass transfer coefficient - k_L - separated from the mass transfer area.

A matrix of capacities was used to determine the range of operation. Table 2.1 is for MELLAPAK 250.Y. The area which is not shaded is the range of experimental operation, in terms of % capacity.

Table 2.1 Experimental matrix with "% capacity" for MELLAPAK 250.Y.

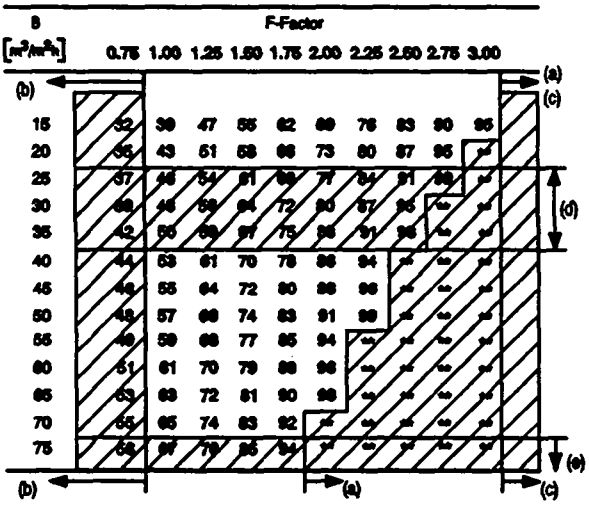

Remarks for table 2.1:

The values in the matrix stand for "% capacity", calculated with the program SULPAK supplied by SULZER BROTHERS LIMITED (section 1.3, chapter I). Values for the densities: ρ_L=1000 kg/m³ and ρ_G=1.0 kg/m³.

** stands for more than 100 % capacity.

Explanation of the fields:

a) above capacity conditions.
b) F-Factor lower than 0.8. During the experiments to determine the mass transfer area of 250.Y, these conditions should be avoided (section 1, chapter IV).
c) F-Factor greater than 3, which would demand a great consumption in CO_2 with the mass transfer area experiments.
d) The liquid distributor did not work with specific liquid loads between 25 to 38 m³/m²h.
e) The pump can furnish a maximum specific liquid load of about 75 m³/m²h.

During the experiments, it was, however, very difficult - and unnecessary - to have round values for the flowrates. To be sure of reproducibility of experimental conditions, chosen positions of the metering floats of the rotameters F11 and F12 and chosen values given by the gas flow sensor F21 were kept constant. These values correspond respectively to specific liquid loads and F-Factors close to the values selected with the experimental matrix for 250.Y. For the other packings (125.Y, 500.Y and rings), the same F-Factors and rotameter metering float positions were employed whenever required. Some experiments were carried out when the capacity values were greater than 100 %, but the column was not flooded. Flow conditions of low capacity were not of interest.

The specific liquid load values for the mass transfer area experiments were 4 to 8 % smaller than those for the $k_L a$ experiments for a given position of the metering float of the rotameters. This was due to the fact that the density of NaOH solutions was about 8% higher than water.

The liquid and gas temperature were set at 22°C, as with the wetted wall column experiments (chapter III). This temperature corresponded to the average laboratory temperature, making temperature control easier due to small heat losses. Temperature fluctuations were less than 3°C. With the heat exchanger HE11, the inlet liquid temperature was rapidly regulated. The temperature of the water which flows in the column COL2 was controlled by cooling or heating R31. Thus, the control of the air's inlet temperature was possible, but not easy.

The pressure in the column was close to the laboratory pressure, which fluctuated, but in the range of 715 to 735 mmHg. Such fluctuations have no important influence on the measured values and they have not been taken into account during the calculations.

During the experiments, it was easier to change the liquid flowrate than the gas flowrate. This fact led to planning the experiments in such way that the gas flow was set and the liquid load was varied. Only one parameter at a time was changed.

The following definitions have been applied for all experiments in the pilot plant:

DATA POINT	acquisition of an experimental value either by reading directly from the equipment or given by the computer.
POINT	group of "data points" with the same liquid load.
RUN	group of "points" with the same gas flow.
TWIN POINTS	"points" with the same liquid and gas flowrate, not necessarily from the same run.
SET	group of all "twin points" with the same liquid and gas flowrate.

A point is identified by two figures. The first figure denotes the run and the second figure defines the order inside the run, when the point was measured. In this sense, the point 3.2 corresponds to the 2nd liquid load measured in run 3. A set is also identified by two figures. The first figure denotes the packing (1- 250.Y; 2- 500.Y; 3- 125.Y; 4- ceramic rings; 5- 125.Y with 3 elements) and the second is for sorting the set according the liquid load as primary key and F-Factor as secondary key.

The standard deviation for the mean value $\bar{x}$ of a set is given by:

$$\sigma = \sqrt{\frac{1}{N-1} \cdot \Sigma(x_i - \bar{x})^2} \qquad (2.11)$$

where: N is the number of twin points
x_i is the result of one of the twin points.

These definitions will be used throughout chapters IV and V. As an exception, runs 49 and 50 each had a constant liquid load with three different F-Factors.

The importance of planning the experiments in order to always have for a point at least one correspondent twin point in a different run was to confirm the reproducibility and to evaluate the uncertainty associated with the value.

6.2 Procedures for the experiments in the pilot plant

The procedures were developed to increase the efficiency of the work, to make all runs uniform so that no step was forgotten and finally to make it possible for co-workers to be immediately operational. The procedures for the experiments had a flowchart for a global view of the succession of steps to be followed. Each step was composed of a series of tasks. The sequence of tasks took into account security and facility of displacement.

The flowcharts for the experiments to measure the mass transfer area and the volumetric mass transfer coefficient (k_La) are given in figure 4.1 (section 2, chapter IV) and figure 5.1 (section 2, chapter V) respectively. The procedure together with the steps is also explained in chapters IV and V. All the steps with its tasks are available in the appendix C and D for the experiments to measure the mass transfer area and the k_La respectively. At the end of the procedure an estimation of required material is given together with a table explaining how to obtain the gas and liquid flowrates. A risk analysis for the experiments is enclosed in appendix E. The book "Hazards in the chemical laboratory" edited by L. Bretheric is given as a reference.

A version of the procedure in French, together with the flow sheet (see section 1, chapter II) and with the table instrumentation and equipment (appendix A) were available inside plastic envelopes on all floors of the laboratory and on the control board in office H4 595. While the experiments were carried out, the position of all valves and the situation of all equipments were noted on the check-list, -"Etat de l'installation"-, hanging on the wall on the fourth floor, for a global view of the state of the pilot plant.

ACKNOWLEDGEMENTS FOR CHAPTER II

I would like to express my recognition for the following people, who have contributed to the necessary modification work in the pilot plant.

Atelier IGC (Lucien Vallotton, Pierre-André Perroud; Mr. G. Magnin; Gérard Ferini and Jean-Claude Rapit), Mr. Decosterd (*Office des constructions fédérales*), Mr. B. Immer and Mr. Gut (Service des Batiments), Mr. Colomb and Mr. Mebdouhi and Mr. Mittaine (Service électrique), Mr. Prince (Service Technique), Mr. Brelaz and Mr. Cotier (Service d'explotation), Mr. Polonghini, workers from AEROVENT, workers from GREMLICH Installation Sanitaires.

The SULZER structured packings MELLAPAK were provided courtesy of Dr. P. Bomio. For technical suggestions from SULZER, many thanks to Mr. Heinz Meierhofer. I appreciated the design and tests of the two liquid distributors by Mr. Philipp Süess. The SULZER SMV static mixers were provided courtesy of Mr. F. Streiff and Dr. J.-E. Juvet.

NOMENCLATURE FOR CHAPTER II

a	$[m^2/m^3]$	specific mass transfer area
A	$[m^2]$	cross-sectional area
B	$[m^3/m^2.h]$	specific liquid load (equation (1.3))
c	[mol/l]	concentration
d	[m]	pipe diameter
d_h	[m]	hydraulic diameter of mixing element channels
F-Factor	$[m/s.\sqrt{kg/m^3}]$	equation (1.1)
g	$[m/s^2]$	acceleration due to gravity
G	$[m^3/h]$	gas flowrate
k_L	[m/s]	liquid phase mass transfer coefficient
L	[m]	length
V	[ml]	volume of acid added
w	[m/s]	velocity
Δp	[Pa]	pressure drop
$(\Delta\rho/\rho)$	[-]	relative density difference
ρ	$[kg/m^3]$	density
ϵ	[-]	void fraction of mixing elements
σ		standard deviation (equation (2.11))

Dimensionless Number

Fr	[-]	Froude number (equation (2.1))
Ne	[-]	Newton number (equation (2.2))

Subscripts

c	column
G	gas
L	liquid
s	sample
eq2	second equivalence point
eq3	third equivalence point
a	HCl 0.1 M

REFERENCES FOR CHAPTER II

BRETHERICK, L. (1981). "Hazards in the chemical laboratory". 3rd. Edition. London: The Royal Society of Chemistry, page 481.

BROOKS INSTRUMENT DIVISION, EMERSON ELECTRIC CO.
"Installation and operating instructions Brooks Mass Flow Controller Model 5851E". Catalog X-5851E, February, 1989.
and
"Brooks control and read out equipment for thermal mass flowmeter model 5876". Catalog X-5870-E-NL, January, 1990.

BUTLER, J.N. (1982). "Carbon dioxide equilibria and their applications". Addison-Wesley Publishing Company, Chapter III.

DELALOYE, M. (1986). "Influence de la viscosité du liquide sur le transfert de matière dans une colonne à garnissage à l'échelle pilote". Lausanne: PhD Thesis EPFL 657.

INGOLD AG.
"Manuel d'utilisation de l'électrode à PO2". (en français)
"Anleitung zur PO2-Elektrode". (auf Deutsch)

LEYBOLD HERAEUS GMBH.
"Betriebsanleitung Infrarot - Gasanalysator BINOS 1".

MOSSIER, J.-L. (1988). "Calorimétrie de systèmes à forte demmande d'oxygène". Lausanne: PhD Thesis EPFL 751, pages 179-184.

TAUSCHER, W.A. and F.A. STREIFF (1979). "Static mixing of gases". Chem. Eng. Progress April, 61-65.

SULZER BROTHERS LIMITED (1987). "Mixing Process Equipment". Catalog e/23.27.06.40-V.87-100.

1 Problem analysis

In section 2.1.1, chapter I, some chemical systems, which were employed for the evaluation of effective mass transfer area were presented and discussed. One of the problems with the application of chemical methods are the incertainties with respect to the evaluation of kinetic parameters and whether the values actually do correspond to the effective area. The kinetics of chemical reactions may be influenced by numerous parameters, which in some cases are difficult to maintain constant and to evaluate. There is a real danger that the results might tend to be not reproducible and meaningless.

Therefore, It was first tested whether the already used reaction of carbon dioxide with sodium hydroxide was convenient for obtaining mass transfer area values. A wetted wall column was chosen because the effective area for mass transfer is identical to the interfacial area, which is precisely defined and is easily changed. In a second stage, effective mass transfer areas of different types of MELLAPAK were measured (Chapter IV). This chapter presents a brief study of the reaction and experimental results with the evaluation of the parameter ϕ which determines the absorption rates.

1.1 The reaction CO_2 with NaOH

The section 1.1.1 describes how the concentrations of dissolved CO_2, bicarbonate and carbonate ions change with the pH of the solution. In section 1.1.2, the reaction kinetics of CO_2 with OH ions is discussed.

1.1.1 Equilibria in solution

Carbon dioxide dissolved in water hydrates to form H_2CO_3, whose mol concentration is about 10^{-3} smaller than simple dissolved CO_2. Both have no charge and do not influence the acid base equilibrium. Therefore, in this section, the concentration of H_2CO_3 will be considered together with the concentration of CO_2. The relationship between the concentration of CO_2 in acid solutions and the concentration in the gas phase (partial pressure) is:

$$c^*_{CO_2} = [CO_2] = \psi \cdot p \cdot y_{iCO_2} \qquad (3.1)$$

The empirical coefficient ψ is dependent on the temperature and on the composition of other ions in solution (ionic strength).

With increasing pH, hydrated CO_2 ionizes to give bicarbonate and carbonate ions. Two equilibrium equations are possible:

$$[H^+].[HCO_3^-] = K_{a1}.[CO_2] \qquad (3.2.a)$$

$$[H^+].[CO_3^{=}] = K_{a2}.[HCO_3^-] \qquad (3.2.b)$$

In dilute solutions at 25 °C, $K_{a1} \simeq 10^{-6.3}$ and $K_{a2} \simeq 10^{-10.3}$ (Buttler (1982)). These coefficients have a complicated dependence on the presence of other salts and on temperature.

When there is no CO_2 gas phase in equilibrium with the solution, an increase of the pH by addition of a base does not change the carbonate content of the solution. The carbonate content of a solution is:

$$c_T = [CO_3^{=}] + [HCO_3^{-}] + [CO_2] \quad (3.3)$$

Using the equations (3.2.a), (3.2.b) and (3.3), it is possible to obtain the concentrations of each carbonate species.

$$\frac{[CO_3^{=}]}{c_T} = \frac{K_{a1}.K_{a2}}{K_{a1}.K_{a2} + K_{a1}.[H^+] + [H^+]^2} \quad (3.4.a)$$

$$\frac{[HCO_3^{-}]}{c_T} = \frac{K_{a1}.[H^+]}{K_{a1}.K_{a2} + K_{a1}.[H^+] + [H^+]^2} \quad (3.4.b)$$

$$\frac{[CO_2]}{c_T} = \frac{[H^+]^2}{K_{a1}.K_{a2} + K_{a1}.[H^+] + [H^+]^2} \quad (3.4.c)$$

The ion product of water is:

$$[H^+] \; . \; [OH^-] = K_w \quad (3.4.d)$$

where K_w is 10^{-14}.

The figure 3.1 plots the series of equations (3.4) as a function of the pH. Note how different pH values changes the composition of each species. In a graphic where the concentration is plotted versus the pH, different carbonate content - c_T - dislocate the curves vertically, but the shape remains the same. The concentrations of ions H^+ and OH^- are straight lines.

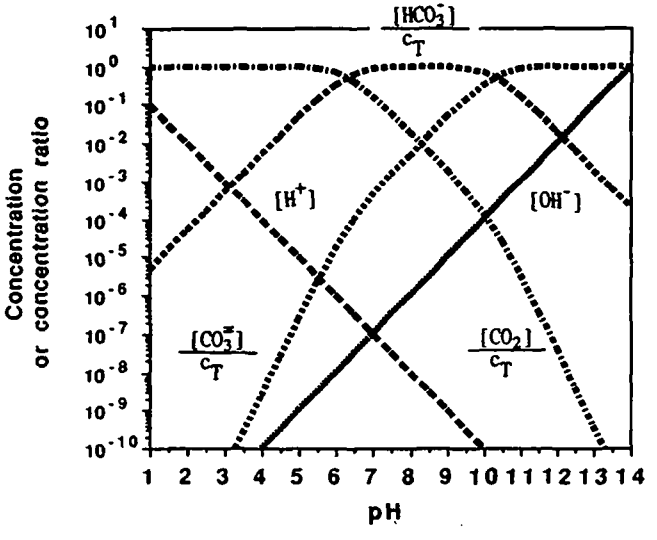

Figure 3.1 Concentration of carbonates species as a function of the pH. (adapted from Buttler (1982), figure 2.2).

The alkalinity, A, is quantified as the equivalent amount of strong base necessary to be neutralized so that the solution has a pH corresponding to a solution of pure CO_2 and water.

$$A = 2.[CO_3^{=}] + [HCO_3^{-}] + [OH^{-}] - [H^{+}] \qquad (3.5)$$

The concentration of bicarbonate ions falls sharply with higher pH and the alkalinity is composed of the carbonate ion and of the ion hydroxide terms. During the titration of such solutions, at first the ion hydroxide is neutralized. Then, the ion carbonate and bicarbonate are neutralized. The distance between two equivalence points of the titration curve of carbonate solutions (figure 2.7, section 5.2.2, chapter II) is proportional to the carbonate content. The distance until the equivalence point of smaller pH is proportional to the alkalinity. The pH values of the three equivalence points of the titration curve are given by the equations (3.6) below.

For a solution of CO_2 dissolved in H_2O at low pH, the alkalinity is zero. The carbonate and hydroxide ion concentrations are negligible. From equation (3.5), $[H^+]$ is equal to the concentration of bicarbonate ion. The pH may be calculated from equations (3.1) and (3.2.a).

$$pH = -\frac{1}{2} \cdot \log(K_{a1}.w.p.y_{CO_2}) \qquad (3.6.a)$$

When the pH value is given by a solution of sodium bicarbonate, the alkalinity equals the carbon content of the solution (equation (3.3)). The concentration of hydrogen and hydroxide ions are negligible at this pH. The concentration of dissolved CO_2 equals the concentration of carbonate ions. Equations (3.4.a) and (3.4.c) give the pH value:

$$pH = \frac{1}{2} \cdot (pK_{a1} + pK_{a2}) \qquad (3.6.b)$$

When the pH value is given by a solution of sodium carbonate, the alkalinity is equal to twice the carbon content of the solution (equation (3.3)). The CO_2 and $[H^+]$ concentrations are negligible compared to the concentration of bicarbonate and hydroxide ions. Thus, the concentration of hydroxide ions equals the concentration of bicarbonate ions. Equations (3.4.b) and (3.4.d) thus give a quatratic equation.

$$\left[C_T \cdot \frac{K_{a1}}{K_w} - 1\right].[H^+]^2 = K_{a1}.K_{a2} + K_{a1}.[H^+] \qquad (3.6.c)$$

For a carbonate concentration of 0.01 mol/l, the pH would be 11.1.

In order to obtain the titration curve mathematically, a charge balance together with the equations (3.4.a), (3.4.b) and (3.4.d) is used. The concentration of the cation sodium and of the anion chlore are expressed in terms of the alkalinity and of the acid concentration respectively, taking the dilution into account. This calculation is found in Buttler (1982).

1.1.2 Reaction kinetics

The reaction of CO_2 with OH ions occurs first as a fast reaction forming bicarbonate. If there is even more hydroxide ion available, bicarbonate will react instantaneously with the ions hydroxide forming carbonate ion. The higher the pH, the more the equilibria of the latter reaction is shiffted towards the formation of carbonate.

When the concentration of hydroxide ions is very high and constant, the reaction of CO_2 with NaOH solutions is said to be pseudo-first order, and sodium carbonate will be formed, as given by the reaction:

$$CO_2 + 2\ NaOH \longrightarrow Na_2CO_3 + H_2O$$

This reaction was recommended by Sharma and Danckwerts (1970) for measuring the effective area of gas-liquid contact apparatus, provided the effective areas are not greater than 1000 m^2/m^3 (due to the generation of heat). The reaction rate is given by :

$$r = K_{OH} \cdot c_{CO_2} \qquad (3.7.a)$$

The pseudo first order reaction rate constant is given by:

$$K_{OH} = K.c_{OH} \qquad (3.7.b)$$

Lack of hydroxide ions at the surface, ie. depletion, alters the first-order character of the reaction. The depletion effect was studied by Danckwerts and Kennedy (1958). This work drew attention to the fact that the OH ions may diffuse to the reaction zone more rapidly than the carbonate ions can diffuse away from it.

In this work, it was decided to work with NaOH solutions of concentrations between 1.6 and 2 M to prevent depletion effects. In figure 3.1, it may be seen that the bicarbonate concentration becomes negligible. This same concentration range was chosen by Mohunta et al. (1969) for research work with irregular packings.

1.2 Calculation methodology

The mass transfer rate for absorption with chemical reaction is different than for physical absorption. The enhancement factor, E, as introduced in section 1.2.2, chapter I, quantifies this difference.

$$n = \frac{N}{A_e} = E \cdot k_L \cdot (c_{iA} - c_{bA}) \qquad (1.14)$$

The Hatta modulus expresses the ratio of the maximum chemical reaction rate to the maximum diffusional mass transfer process. For the pseudo first order reaction of CO_2 with NaOH, the equation (1.15) for the Hatta modulus defined in section 1.2.2, chapter I, becomes:

$$Ha = \frac{1}{k_L} \cdot \sqrt{K_{OH} \cdot D_{CO_2}} \qquad (3.8)$$

When the Hatta modulus is greater than 3 and much smaller than the enhancement factor for an instantaneous reaction (Sharma and Danckwerts (1970)), the enhancement factor for a fast pseudo first order reaction is equal to the Hatta modulus. In addition, there is no dissolved CO_2 at the bulk of the solution. Considering the two facts above and substituting equation (3.8) into (1.14) yields:

$$n = \frac{N}{A_e} = \frac{1}{k_L} \cdot \sqrt{K_{OH} \cdot D_{CO_2}} \cdot k_L \cdot c_{iCO_2} \qquad (3.9.a)$$

or

$$n = \frac{N}{A_e} = \sqrt{K_{OH} \cdot D_{CO_2} \cdot (c_{iCO_2})^2} \qquad (3.9.b)$$

The concentration of dissolved CO_2 at the interface is in equilibrium with the concentration of the gas phase at the interface, as given by equation (3.1). Like the pseudo-first order rate constant, the diffusivity of CO_2 in the solution and the factor ψ should be constant within the range used. Thus, equations (3.9.b) and (3.1) give:

$$n = \frac{N}{A_e} = \phi \cdot y_{iCO_2} \qquad (3.10)$$

where: $$\phi = \sqrt{K_{OH} \cdot D_{CO_2}} \cdot \psi \cdot p \qquad (3.11)$$

The parameter ϕ is the mass transfer absorption rate per unit of effective area, when there is a pure CO_2 gas phase at a certain pressure. As shall be pointed out in section 3, there is literature which has suggested different correlations for estimating separately the values of the pseudo first order reaction rate constant, of the diffusion coefficient and of the CO_2 solubility. These values multiplied give the parameter ϕ (section 3, chapter III). This work, however, proposes to determine the parameter ϕ directly, without measuring each parameter separately.

The accuracy of equation (3.10) was verified by data obtained in a wetted wall column, where the effective area was known. This area could be changed by varying the height of the falling liquid film and is:

$$A_e = \pi \cdot d \cdot h \qquad (3.12)$$

The error in the determination of the effective area is:

$$\Delta(A_e) = \pi.d.\Delta(h) + \pi.h.\Delta(d) \qquad (3.13)$$

The absorption rate is determined by an increase in the carbonate concentration in the solution:

$$N = \frac{L}{\rho} \cdot (c_{CO_3\ \omega} - c_{CO_3\ \alpha}) \cdot \frac{1}{60} \qquad (3.14)$$

The error in the determination of the absorption rate is:

$$\Delta N = \frac{\partial(N)}{\partial(\Delta c_{CO_3})} \cdot \Delta(\Delta c_{CO_3}) + \frac{\partial(N)}{\partial L} \cdot \Delta(L) \qquad (3.15.a)$$

where: $$\Delta c_{CO_3} = (c_{CO_3\ \omega} - c_{CO_3\ \alpha}) \qquad (3.15.b)$$

Hence:

$$\Delta(N) = \left[\frac{\Delta(\Delta CO_3)}{\Delta CO_3} + \frac{\Delta(L)}{L} \right] .N \qquad (3.15.c)$$

Equation (3.10) demands the measurement of the concentration of CO_2 at the gas-liquid interface. Such measurement is difficult in practice with current technology. Only bulk concentrations can be measured. For the wetted-wall column experiments, because of the short column height and large gas flows, the concentration at the interface was constant and equal to the concentration in the bulk of the gas flow, since the gas-phase mass transfer resistance may be considered negligible.

The CO_2 concentration in the gas was reduced progressively until a value, below which a change in the carbonate concentration could no longer be detected. If the gas-phase resistance was important, the absorption rate would not change linearly with the CO_2 concentration in the gas phase.

The parameter ϕ is defined by:

$$\phi = \frac{1}{A_e} \cdot \frac{N}{y_{CO_2}} \qquad (3.16)$$

Therefore, the parameter ϕ is equal to the slope of the plot of the absorption rate versus the CO_2 concentration in the gas divided by the interfacial area. The experiments were carried out with two different heights for the wetted wall column in order to determine the parameter ϕ and to be sure that different effective areas do not influence its value.

The error in the evaluation of the parameter ϕ is:

$$\Delta\phi = \phi \cdot \left[\frac{\Delta(\text{slope})}{\text{slope}} + \frac{\Delta(A_e)}{A_e} \right] \qquad (3.17.a)$$

where:

$$\text{slope} = \frac{N}{y_{CO_2}} \qquad (3.17.b)$$

For calculating the concentration of CO_2, the gas flowrates had to be known. There was no gas analyser available for measuring a broad range of concentration with high values of CO_2 concentration. The mass flow controllers, such as the ones used in the pilot plant (section 3.2, chapter II), were used to adjust a constant mass flowrate. After each experiment, the absolute values of the mass flowrates of the CO_2 and air were measured with a soap column. A soap column is an instrument for volumetric gas flow measurement (end of section 2, chapter III).

The mass fractions of CO_2, air and water vapor were calculated once the mass flows were known. The moisture content was taken into account, knowing the partial pressure of water vapor, which was correlated with data from Wärmeatlas (1974). The following equation was obtained:

$$P_w := 10. ** ((1./(T_w+273.15)) * (-2283.6125) + 6.15746330) \qquad (3.18)$$

The mole fraction was determined from the mass fraction using the molecular weight of the gases. An accurate evaluation of the error of the CO_2 mole fraction is difficult. Due to the small vapor content, a conservative calculation not considering water was made:

$$\Delta(\%CO_2) = \frac{G_{CO_2}}{G_G} \cdot \left[\frac{\Delta(G_{CO_2})}{G_{CO_2}} + \frac{\Delta(G_G)}{G_G} \right] \qquad (3.19)$$

2 Materials and methods

The experiments were carried out in a laboratory scale apparatus with the wetted wall column (figure 3.2). The wetted wall column had a diameter of 27 mm, and the film height could be regulated up to 80 mm. The column was kept perfectly horizontal. The wetted wall column was enclosed during the experiments by a glass dome, and the gas mixture surrounded the column.

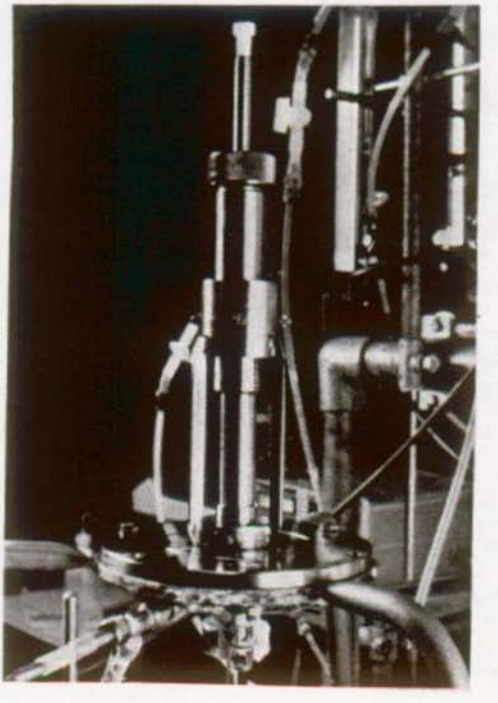

Figure 3.2 The wetted wall column.

Figure 3.3 shows a simplified flow-sheet of the apparatus. The code, the description and function of the most important instrumentation and equipment are given in the table 3.1.

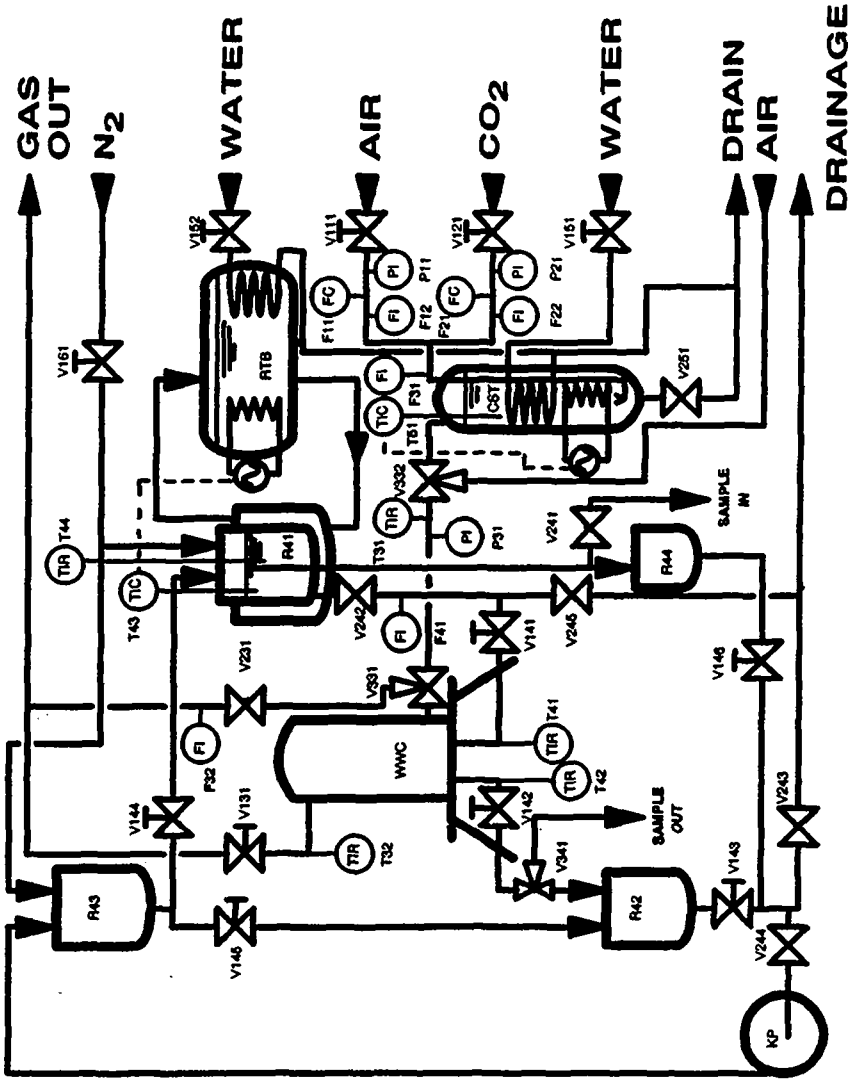

Figure 3.3 The laboratory-scale apparatus with the wetted wall column.

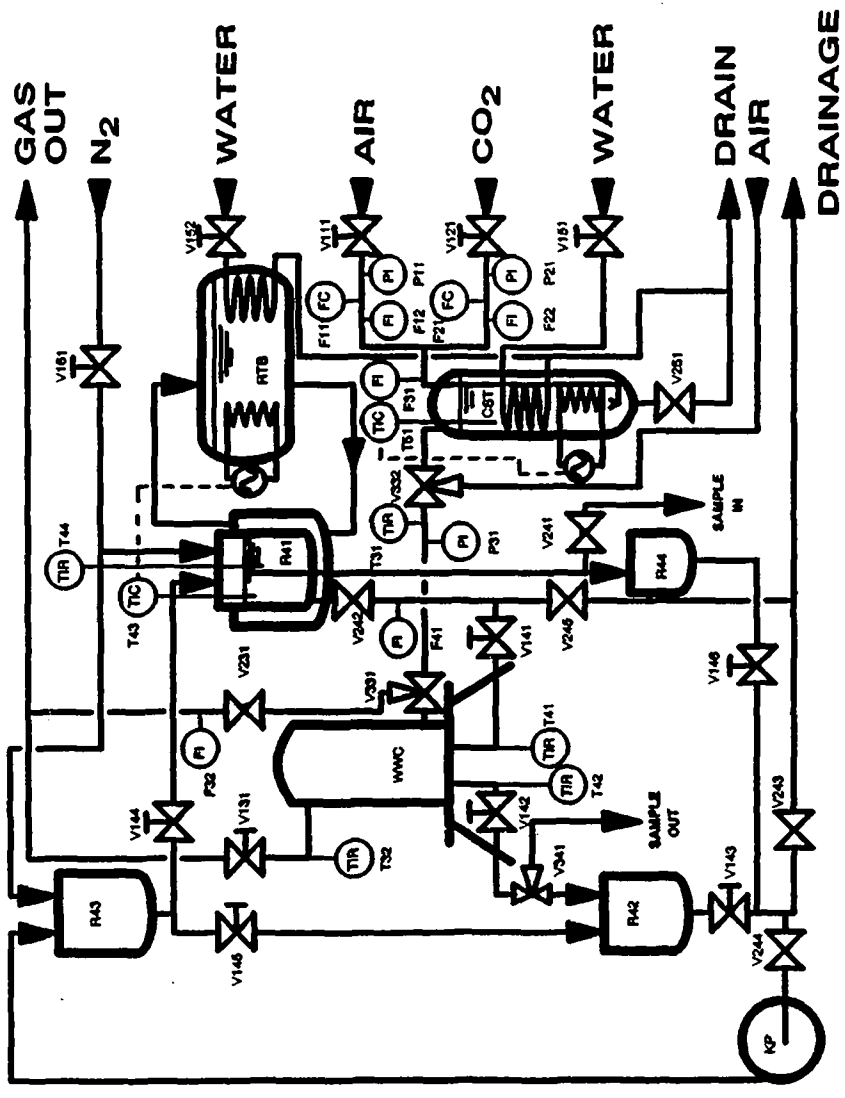

Figure 3.3 The laboratory-scale apparatus with the wetted wall column.

Table 3.1 Most important elements of the laboratory scale apparatus.

CODE	DESCRIPTION	FUNCTION
WWC	Wetted wall column	known effective area is changed by varying the height of the film.
CST	Bubble column	Saturation and thermostatisation of the inlet gas.
F11	Mass flow controller	BROOKS 0-5000 ml Maintains a constant air flow.
F12	Rotameter BROOKS	For air flow entering BC up to 200 Nl/h.
F21	Mass flow controller	BROOKS 0-10000 ml. Maintains a constant CO_2 flow.
F22	Rotameter BROOKS	For CO_2 flow entering BC up to 160 Nl/h.
F31	Rotameter BROOKS	For the total gas flow entering BC.
F32	Soap column	Volumetric determination of the gas flowrate.
F41	Rotameter KROHNE	G18.12 DN 13 stainless steel float. Flow of the NaOH solution in the WWC.
KP	Centrifugal pump	LEROY-SOMER 90 W, type LSMM63EY 70 Pumps solution to reactor R3.
P11	Manometer	Pressure of the inlet gas flow (max 2.5 bar).
P21	Manometer	Pressure of the inlet CO_2 flow (max. 2.5 bar).
P31	U-tube (WATER)	Pressure at the inlet of WWC.
R41	Main reactor	Stocking of solution with constant level before WWC.
R42	Low reactor	Stocking of solution after WWC.
R43	High reactor	Stocking of solution before R1.
R44	Overflow reactor	Stocking of the solution from the overflow of R1.
RTB	Thermostatic bath	Temperature control of R1.
T31	Pt-100 sensor	Temperature of the inlet gas mixture in the WWC.
T32	Pt-100 sensor	Temperature of the outlet gas mixture from the WWC.
T41	Pt-100 sensor	Temperature of the inlet solution in the WWC.
T42	Pt-100 sensor	Temperature of the outlet solution from the WWC.
T43	Thermostat	For regulation of RTB for thermostating R1.
T44	Pt-100 sensor	Temperature in R1.
T51	Pt-100 sensor	Water temperature in CST. For heater regulation.

Explanation of the code for the instrumentation and equipment in table 3.1.

X a b

X: installation component

a: 1- air; 2- CO_2; 3- gas mixture; 4- solution; 5- Water; 6- N_2

b: component number

The valves were not listed because their function may be understood with the flow-sheet. However, a code was given, and it is referenced in the main text. A valve has three numbers after the letter V. The first number states if the valve acted as a globe valve (1), as a gate valve (2) or as a 3-way valve (3). The plant can be completely drained when all valves are opened.

With a NaOH solution the stability of the film was tested after a change of the column's height. The device to keep the column perfectly horizontal was adjusted. The film inside the column was without waves, however, this was a rather difficult task.

Emmert and Pigford (1954) have suggested wetting agents for eliminating rippling when the column is high. They have also stated that "when a liquid film falls along a vertical surface, wave formation begins at the free surface after several inches of travel". Their data for long wetted wall columns (3.73 ft = 1136.9 mm) with wetting agents "compare favorably with those of Peaceman in wetted-wall columns so short (40 mm) that rippling had not begun". Vivian and Peacemen (1956) have actually recommended the use of short wetted wall column because it "avoids rippling and provides short contact time between the gas and liquid".

The wetted wall column in this work was short (80 and 52 mm) and the film was laminar. Emmert and Pigford (1954) states that the flow is laminar, if the Reynolds number is less than 1200. For wetted wall columns, the Reynolds number is defined as:

$$Re = \frac{4 \cdot \Gamma}{\mu} \qquad (3.20.a)$$

$$\text{where:} \quad \Gamma = \frac{m_L}{P} \cdot \frac{1}{60} \qquad (3.20.b)$$

In this work, wetting agents could have an effect on the reaction rate. However, such substances were not necessary. The experiments could begin when the column wall was completely wetted, the film was well formed and the solution was well collected at the bottom, so that end effects due to stagnation would not occur. A film without waves could not actually be seen. With a pencil, its presence could be detected. The column glass dome was then mounted.

About 20 l of a NaOH solution with a concentration between 1.6 and 2.0 mol/l was put in the reactor R42 at the beginning of each experiment. The pump KP pumped all the solution up to R43. The valve V144 was then opened, and the solution would flow by gravity into the reactor R41. In this reactor the liquid level was always kept constant, since there was a overflow tube which would conduct the excess of solution into R44. It was important for the stability of the film that the liquid level in R41 did not change during the experiments.

The reactor R41 had a jacket which kept the solution inside at 22 ± 3 °C. The water flowing in the jacket came from the thermostatic bath RTB, and its temperature was set by the thermostat T43. An atmosphere of nitrogen was continuously present on the liquid surface so that the solution did not react with the CO_2 in the laboratory air.

When the valve V242 was opened, the solution flowed from reactor R41 into the wetted wall column. This flow was regulated with the valve V141. The outlet solution flowed through the valve V142 into the reactor R42. The liquid should not entrain gas at the outlet of the column. A transparent tube permitted visual control to check if bubbles were present.

The experiments with concentrated NaOH presented health hazards. Since the flows and the size of the equipments were small, the possibility of a leakage hazard was easy to minimize. Gloves and glasses were used as precautions during the experiments.

Sample taking was possible with the valves V241 and V341 for the liquid inlet and outlet respectively. Small flasks collected the samples of the liquid for the titration of its carbonate content. This titration was carried out with the experimental set shown in figure 2.8, section 5.2.2 in chapter II. The titration procedure is explained in this section. The analytical procedure was developed for these experiments and it was also used for the experiments to determine mass transfer area of MELLAPAK in the pilot plant.

The liquid flowrate was measured during the experiments between two samplings. The solution flowed through the valve V341 during a measured time into flasks (from 500 to 1000 ml) which were weighed with and without the liquid solution. The density of the solution was determined by measuring the weight of a known volume given by a measuring cylinder.

The air and the CO_2 flows were set and maintained constant by two independent mass flow controllers, F11 and F21 respectively. After the mass flow controllers, there were rotameters (F12 and F22) for giving a rough idea of the value of the absolute flows. Then, the gas mixture bubbled through demineralized water in the bubble column CST for thermostating and saturation, thus eliminating heat effects due to evaporation during the absorption in the wetted wall column. As it is more rapid to saturate an air stream than to regulate its temperature, the bottom of the bubble column was heated and the top was cooled by a cooling coil. The temperature T51 was chosen so that the temperature of the inlet gas read by T31 would be about 22°C. The gas then flowed through the valve V331 into the column. After the wetted wall column, the outlet gas was discharged into the ventilation of the laboratory.

With the experiment over, the gas flows were diverted to the soap column, by using the 3-way valve V331, just before the inlet of the wetted wall column. The volumetric gas flow was measured using a soap column.

A soap column is a volumetric gas flow instrument. The time for a soap bubble to rise was measured. The column had to be in a perfectly vertical position and its wall could not be dry. Only one bubble may raise up at a time. The soap column had a capacity of 2600 ml and was built specially for these experiments.

The volumetric flow was easily calculated with the cross sectional area, the height of the soap column and the time travelled by the soap bubble:

$$G = \frac{A_s \cdot h_s}{t} \cdot \frac{3600}{1000} \qquad (3.21)$$

The CO_2 mole fraction was calculated with a small computer program, as explained in section 1.2, chapter III.

3 Results and Discussions

The appendix F gives the results for the experiments with the wetted wall column for the heights of 80 mm and 52 mm. Figure 3.4 presents the results for the dependence of absorption rates on the mole fraction of CO_2 in the gas mixture with the error bars reflecting the fluctuations of the measurements.

The values used in all equations for determining the absorption rate and gas concentration, as well as the associated error were all average values from experimental data, which are taken under stationary conditions. The different error bars are result of ineviatble fluctuations associated with such experiments.

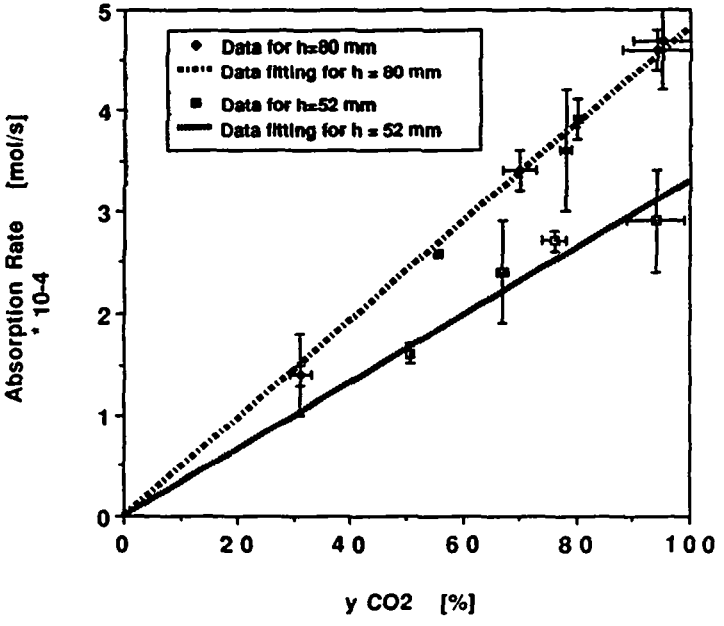

Figure 3.4 Absorption rate versus mol fraction of CO_2.

Table 3.2 presents the range of flow rates measured and molarity of the solutions.

Table 3.2 **Range of experimental variables.**

Variable	Range	
	h = 80 mm	h = 52 mm
m_L [kg/min]	0.42 - 0.58	0.66-0.68
G [l/h]	176 - 397	214 - 401
c_{OH} [mole/l]	1.1 - 2.0	1.8 - 1.9

The results were not influenced by fluctuations of these variables, which were different during the experiments. The film thickness in the laminar case actually depends on the liquid flow rate. If the liquid flow had no influence on ϕ, neither could the film thickness. According to equation (3.11) (section 1.2, chapter III), the parameter ϕ does not depend on hydrodynamics; this was confirmed experimentally.

The evaluation of ϕ from the slope of the curves is given in the table 3.3. The slope was evaluated with the least square method. If the mole fraction of CO_2 is zero, then the absorption rate must be zero too. This physical condition was imposed.

Table 3.3 **Evaluation of the parameter ϕ.**

h [mm]	A_e [m^2]	Slope [mol/s]	ϕ [$mol/m^2.s$]
52 ± 1	$(44 \pm 2).10^{-4}$	$(3.3 \pm 0.1) .10^{-4}$	$(7.5 \pm 0.6).10^{-2}$
80 ± 1	$(68 \pm 3).10^{-4}$	$(4.82 \pm 0.05).10^{-4}$	$(7.1 \pm 0.4).10^{-2}$

The average value for the parameter ϕ which shall be used throughout chapter IV is:

$$\phi = (7.3 \pm 0.5)\ 10^{-2}\ mol/m^2s$$

This means that the parameter ϕ was measured with an error of less than 7 %.

This parameter could be obtained with data or correlations from the literature. The work from Nijsing et al. (1959) measured, with the laminar jet technique, kinetic parameters governing the absorption of CO_2 into NaOH solutions at 20 °C and with a CO_2 pressure atmosphere of 150 mmHg. Their results are listed in table 3.4.

Table 3.4 Values published by Nijsing et al. (1959).

[OH] [mol/l]	K_{OH} [1/s]	D [m^2/s]	$c^*_{CO_2}$ [kg/m^3]
2.07	17700	$1.14 \cdot 10^{-9}$	$1.68 \cdot 10^{-1}$
1.05	6060	$1.41 \cdot 10^{-9}$	$2.38 \cdot 10^{-1}$

The parameter ϕ is proportional to the parameter ψ and to the total pressure of the system (equation (3.11)). For the evaluation of the parameter ϕ at the pressure of 725 mmHg with data from Nijsing et al. (1959), the values of their absorption rates were multiplied by the factor 4.833 (=725/150). The results are in table 3.5.

Table 3.5 Results using data from Nijsing et al. (1959).

[OH] [mol/l]	absorption rate (p = 150 mmHg)	ϕ at 725 mmHg
2.07 M	= $1.72\ 10^{-2}$ mol/m^2s	= $8.3\ 10^{-2}$ mol/m^2s
1.05 M	= $1.58\ 10^{-2}$ mol/m^2s	= $7.6\ 10^{-2}$ mol/m^2s

The value found with this work is between 4 and 12 % smaller. The difference is within the range of experimental uncertainty.

Pohorecki and Moniuk (1988) published correlations for the kinetic parameters of the reaction of CO_2 in different aqueous electrolyte solutions. For their measurements, they also used a laminar jet. Their work points out that "the discrepancies between the results obtained by various authors are very big". Further, "there is also no agreement as to the effect of the kind of cations present in the solutions". With this argument, the authors dismissed a correlation because "it leads to the paradoxical conclusion that the influence of the presence of one kind of ion in the solution can be different and depends on the compound by which the ions are introduced". However, the authors were not self consistant, since they used for the solubility just such a correlation. The correlation for the diffusivity was also quoted from others.

For a 2 M NaOH solution at 22°C and using the value of 1.177 kg/m.s for the viscosity (Vazques et al. (1889), the values below were obtained following the procedure suggested by Pohorecki and Moniuk (1988):

H_w = 0.03694 kmol/m^3.bar H = 0.01956 kmol/m^3.bar

D_w = $1.8262\ 10^{-9}$ m^2/s D = $1.5516\ 10^{-9}$ m^2/s

K^{∞} = 6613.4 m^3/kmol.s K = 14468.5 m^3/kmol.s

Thus, for a pressure of 725 mmHg,

$\phi = 1.2\ 10^{-1}$ mol/m².s

This value is 64 % higher than the value obtained in this work and 44 % higher than the value calculated with data from Nijsing et al (1959). Table 3.6 shows the value of the reaction rate constant for a 2 M NaOH solution suggested by different authors, illustrating wide disagreement. So this is where the main difference is to be found. This work proposes no individual value for the reaction rate, since it was measured simultaneously with other parameters giving the parameter ϕ, as defined in section 1.2, equation (3.11).

Table 3.6 Rate constant for a 2 M NaOH solution at 295 K.

Reference	Rate constant [m³/kmol.s]
Pinsent et al. (1956)	6629
Nijsing et al. (1959)	9000
Astarita cited in Tseng et al. (1988)	9582
Pohorecki and Moniuk (1988)	14469

There are equations for determining when the reaction is pseudo first order (Sharma and Danckwerts (1970)), using the conditions pointed out in section 1.2. For this calculation, however, the values of certain parameters must be known, and these values are contradictory in the different literature sources, as shown above.

However, even if there is a disagreement in the literature with respect to the values of the necessary parameters, there is an agreement that the reaction is pseudo first order, suitable for measuring mass transfer area of gas-liquid contacting systems (Sharma and Danckwerts (1970) and Guillen et al. (1982)). This reaction has been used for obtaining mass transfer areas of packed columns recently by Bornhütter and Mersmann (1991) and some time ago by Mohunta et al. (1969).

Knowing beforehand that the reaction might be pseudo first order, this work did check the kinetics. These are independent of the hydrodynamics of the column, and this was verified when the height and flowrates were changed, but the absorption rate remained proportional to the concentration of CO_2 in the gas. No depletion could have been detected, since a reduction of the CO_2 partial pressure and the height of the film, reduced the absorption rate proportionally.

The use of other devices, such as a laminar jet, is possible, but the contact time is so short that a difference of the carbonate concentration may be so small that a precise evaluation of the absorption rate may be more difficult. If the wetted wall column were not useful for the determination of the kinetics due to depletion, the whole method would not be valid for the packed column. The flow of NaOH solution over the packing can actually be seen as a series of wetted wall columns, since the film is renewed from time to time.

4 Conclusions

This chapter has presented the reaction of CO_2 with NaOH solutions. There is disagreement in the literature for the values of the reaction rate constant, which confirms the necessity of these experiments. There is, however, agreement that the reaction can be used for the measurement of the mass transfer area in packed columns. However, an experimental verification of the suitability of the reaction for measuring effective areas was required.

Another goal of the work presented in this chapter was to calculate the parameter ϕ, wich governs the absorption rate. With two different heights of a wetted wall column, the parameter ϕ, as defined by equation (3.11), was found to be:

$\phi = (7.3 \pm 0.5).10^{-2}$ mol/m^2.s

at 22°C, 725 mmHg and $1.6 < [OH^-] < 2.0$ mol/l.

Thus, the error in its determination is less than 7 %.

This parameter is independent of the effective area, of the CO_2 concentration in the gas flow and of hydrodynamic conditions.

ACKNOWLEDGEMENTS FOR CHAPTER III

I would like to thank Dr. Ted Randolph for very interesting suggestions at the beginning of this work. I would also like to thank Dr. Comninellis for supplying me with some equipment. Last but not least, my thanks to Miss Réjanne Fredez for helping with the initial titrations of this work.

NOMENCLATURE FOR CHAPTER III

A	[m^2]	area
c	[mol/m^3]	concentration
d	[m]	diameter
D	[m^2/s]	diffusivity
E	[-]	enhancement factor
G	[l/h]	gas flowrate
h	[mm]	height
H	[kmol/m^3.bar]	solubility constant
k_L	[m/s]	liquid phase mass transfer coefficient
K	[m^3/kmol.s]	second order reaction rate constant
KOH	[1/s]	pseudo-first order reaction constant rate
K_{a1}	[-]	ionization constant (equation (3.2.a))
K_{a2}	[-]	ionization constant (equation (3.2.b))
K_w	[-]	ion product of water (equation (3.4.d))
L	[kg/min]	liquid flowrate
m	[kg/min]	mass flow rate
n	[mol/m^2.s]	specific absorption rate
N	[mol/s]	absorption rate

p	[mmHg]	pressure
P	[m]	perimeter
r	[mol/m^3.s]	reaction rate
t	[s]	time
T	[K]	temperature
y	[mol/mol]	gas-phase mole fraction
μ	[kg/m.s]	viscosity
ρ	[kg/m^3]	density
ϕ	[mol/m^2.s]	as defined by equation (3.11)
Ψ	[mol/m^3.mmHg]	as defined by equation (3.1)

Subscripts

A	refers to component A
b	bulk
CO_2	carbon dioxide
e	effective
i	interface
L	liquid
OH	hydroxide ion
s	soap column
w	water
α	begin - in
ω	end - out

Superscript

*	equilibrium
∞	infinite dilution

REFERENCES FOR CHAPTER III

BORNHUTTER, K. and A. MERSMANN (1991). "Stoffübertragung mit modernen Füllkörpern grosser Abmessungen". Chem.-Ing.Tech. 63(2), 132-133.

BUTTLER, J.N. (1982). "Carbon dioxide equilibria and their applications". Addison-Wesley Publishing Company, chapters II and III.

DANCKWERTS, P.V. and A.M. KENNEDY (1958). "The kinetics of absorption of carbon dioxide into neutral and alkaline solutions". Chem.Eng.Sci. 8, 201-215.

EMMERT, R.E. and R.L. PIGFORD (1954). "A study of gas absorption in falling liquid films". Chem.Eng.Progress 50(2), 87-93.

GUILLEN, J.M.P.; PITARCH, M.A.O. and F.L. MATEOS (1982). "Determinacion del area interfacial y de los coefficientes de materia en sistemas de contacto gas-liquido por metodos quimicos". Ingenieria Quimica 14, 179-186.

MOHUNTA, D.M.; VAIDYANATHAN, A.S. and G.S. LADDHA (1969). "Effective interfacial areas in packed columns". Indian Chemical Engineer April, 39-42.

NIJSING, R.A.T.O.; HENDRIKSZ, R.H. and H. KRAMERS (1959). "Absorption of CO_2 in jets and falling films of electrolyte solutions, with and without chemical reaction". Chem.Eng.Sci. 10, 88-104.

PINSENT, B.R.W.; PEARSON, L. and F.J.W. ROUGHTON (1956). "The kinetics of combination of carbon dioxide with hydroxide ions". Trans.Faraday Society 52, 1512-1520.

POHORECKI, R. and W. MONIUK (1988). " Kinetics of reaction between carbon dioxide and hydroxyl ions in aqueous electrolyte solutions". Chem.Eng.Sci. 43(7), 1677-1684.

SHARMA, M.M. and P.V. DANCKWERTS (1970). "Chemical methods of measuring interfacial area and mass transfer coefficients in two-fluid systems". British Chemical Engineering 15(4), 522-528.

TSENG, P.C.; HO, W.S. and D.W. SAVAGE (1988). "Carbon dioxide absorption into promoted carbonate solutions". AIChE J. 34(6), 922-931.

VAZQUEZ, G.; ANTORRENA, G.; CHENLO, F. and F. PALEO (1989). "Effect of viscosity on interfacial area in the absorption of CO_2 by carbonate/bicarbonate systems". Chem.Biochem.Eng.Q. 3(1-2), 7-12.

VIVIAN, J.E. and D.W. PEACEMAN (1956). "Liquid-side resistance in gas absorption". AIChE J. 2(4), 437-443.

WARMEATLAS (1974). Düsseldorf: VDI, page Db4.

1 Problem analysis

The specific effective area for mass transfer is defined as the absolute effective area divided by the packing volume. The effective mass transfer area is not the sole design parameter for gas-liquid contactors. However, knowledge of the values of this parameter and of the factors affecting these values could be valuable for design of packings for separation columns.

Knowledge of the value of the mass transfer area also serves to extract value of the liquid phase mass transfer coefficient - k_L - as well as that of the gas-phase mass transfer coefficient - k_G - from the volumetric mass transfer coefficients $k_L a$ and $k_G a$ respectively. The coefficients k_L and k_G cannot be directly obtained experimentally.

A literature review is available in section 2.2, chapter I. For structured packings, no measurements seem to be reported (see tables 1.1 and 1.2, chapter I). In this work, the specific mass transfer area of three different types of the SULZER structured packing MELLAPAK was measured (250.Y, 500.Y and 125.Y), so that the influence of the geometric surface area could be investigated.

1.1 The system CO_2-NaOH for measuring mass transfer area

In this section, a brief summary of chapter III is given. The review from Sharma and Danckwerts (1970) has considered this system as a "very convenient system to use" for determining effective areas.

The absorption of CO_2 into NaOH solutions occurs with the following chemical reaction:

$$CO_2 + 2\,NaOH \longrightarrow Na_2CO_3 + H_2O$$

This pseudo-first order reaction is adequate for obtaining values of effective mass transfer areas. The local chemical absorption rate is:

$$N = n.A_e = A_e \cdot \sqrt{K_{OH} \cdot D_{CO_2} \cdot (c_{iCO_2})^2} \qquad (3.9.b)$$

The concentration of dissolved CO_2 at the interface is in equilibrium with the concentration of the gas phase at the interface, as given by:

$$c^*_{CO_2} = \Psi \cdot p \cdot y_{iCO_2} \qquad (3.1)$$

Like the pseudo-first order rate constant, the diffusivity of CO_2 in the solution and the factor Ψ are constant within the range used, equation (3.1) and (3.9.b) give:

$$N = n.A_e = A_e \cdot \phi \cdot y_{iCO_2} \qquad (3.10)$$

where: $$\phi = \sqrt{K_{OH} \cdot D_{CO_2}} \cdot \Psi \cdot p \qquad (3.11)$$

The physical interpretation of equation (3.11) is that the absorption rate is independent of the mass transfer coefficients and of hydrodynamic conditions, ie. the whole interfacial area is uniformly effective.

There is disagreement in the literature for the values of the reaction rate constant. Therefore, instead of using different correlations to determine separately the values of each parameter in equation (3.11) and then multiplying these values to obtain ϕ, this parameter was determined directly with a wetted wall column (section 2, chapter III).

In a wetted wall column, the effective area was known and was equal to the interfacial area. Two different areas were selected for the experiments and the CO_2 mole fraction in the gas phase was reduced to the smallest possible value, below which a precise measurement of the absorption rates would not be possible. It was confirmed that the parameter ϕ is independent of the effective area and of the CO_2 mole fraction.

$\phi = (7.3 \pm 0.5).10^{-2}$ mol/m^{2}s

at 22°C, 725 mmHg and $1.6 < [OH^-] < 2.0$ M.

The experiments in the pilot plant were conducted under the same experimental conditions as with the wetted wall column, ie. same temperature, pressure and ionic strength range. All effects related to these variables were in this way eliminated. Since the parameter ϕ is independent of the CO_2 mole fraction, this work decided to use 1 % CO_2 in the gas phase, what reduces the absorption rates (equation (3.10)) and costs.

1.2 Calculation methodology

Equation (3.10) demands the measurement of the concentration of CO_2 at the gas-liquid interface, which with current technology is very difficult to carry out. Only bulk concentrations can be measured. If in the pilot column, the gas-phase mass transfer resistance is negligible, then the gas concentration at the interface is approximately the same as the concentration in the bulk. Spiegel and Meier (1987) propose a model for predicting the gas side Sherwood number. However, the empirical coefficient contained therein was not published. Fair and Bravo (1990) suggested that with their publication "from a data plot one can infer values in the range of 0.018 to 0.040". Using the value of 0.0338 proposed by Fair and Bravo (1990):

$$Sh_G = \frac{k_G \cdot d_h}{D_{CO_2}} = 0.0338 \cdot Re_G^{0.8} \cdot Sc_G^{1/3} \qquad (4.1)$$

where:

$$Re_G = \frac{\rho_G \cdot w_G \cdot d_h}{\mu_G \cdot \cos 45^\circ} \qquad (4.2.a)$$

$$d_h = \frac{4}{a_p} \qquad (4.2.b)$$

$$Sc = \frac{\mu_G}{\rho_G \cdot D_G} \qquad (4.2.c)$$

Actually, the original model suggests the interfacial area and not the geometric area in the equation (4.2.b). For a rough estimation a_p was used.

The specific absorption rate is:

$$n = \phi \cdot (y - \Delta y) = k_G \cdot \frac{\rho_G}{M_G} \cdot \Delta y \qquad (4.3)$$

where Δy accounts for the concentration gradient in the gas phase.

Thus:

$$\frac{\Delta y}{y} = \frac{\phi}{k_G \cdot \frac{\rho_G}{M_G} + \phi} \qquad (4.4)$$

The above ratio is almost independent of the CO_2 concentration in the gas flow. For MELLAPAK 250.Y, with F-Factors of 0.85, 1.1 and 2.1, the ratio given by equation (4.4) are respectively 16.4 %, 14.1 % and 8.6 %. Some dependence on packing density would be expected through the factor k_G in equation (4.4). The packing density governs the hydraulic diameter and thereby the k_G (equation (4.1)). Using equations (4.1) and (4.2), it is seen that k_G is proportional to the geometric area of MELLAPAK at the power of 0.2. This means that the MELLAPAK type should not change significantly the above values. For MELLAPAK 500.Y, for a F-Factor of 0.85, the ratio of equation (4.4) is 14.6 %. For MELLAPAK 125.Y, for a F-Factor of 2.1, the lowest that will be used, the ratio of equation (4.4) is 9.8 %.

The above values are very conservative. Dharwadkar and Sawant (1985) estimated 10 to 15 % resistance to be on the gas side with the CO_2-NaOH system for their measurements of effective areas in columns packed with irregular packings. The gas superficial velocity was between 0.09 and 0.17 m/s. Yoshida and Miura (1963) suggested that the gas phase resistance accounted for less than 5 % of the overall resistance in their experiments with CO_2 and NaOH. The gas flows were not published. Both sets of authors did not consider the gas side resistance in their calculations.

The packing height has actually two effects. First, the danger of depletion, i.e. lack of [OH] ion at the interface (section 1.2, chapter III), increases especially for low liquid loads. Second, the equation (3.10) cannot be used directly for obtaining values for effective mass transfer area, because the CO_2 mole fraction changes with the packing height.

With two packing elements and 1 % CO_2 in the gas flow at the column inlet, the absorption rates are small, according to equation (3.10). As a consequence, the consumption of NaOH is reduced, the increase of the liquid temperature is kept to negligible values of less than 1°C and depletion effects are prevented. The ratio of consumed [OH] ion to available [OH] ion was estimated to be about 1 % with MELLAPAK 250.Y.

A differential mass balance for the CO_2 must be established for integrating (3.10) through the packing height. Thus:

$$L \cdot dc = \phi \cdot y_{iCO_2} \cdot dA_e \qquad (4.5)$$

where: $$dA_e = a \cdot A_c \cdot dz \qquad (4.6)$$

The boundary conditions are: $x\ (z=0) = c_\alpha$ and $x\ (z=h) = c_\omega$.

The notation has the following meaning: at the top of the column ($z = 0$) are c_α and y_ω and at the bottom ($z = h$) are c_ω and y_α.

The small "a" denotes the specific mass transfer area, which is the effective mass transfer area per unit of packing volume. The absolute effective mass transfer area is "A_e". The column cross-section is "A_c".

The operating line assuming constant gas and liquid flow rate is:

$$y = \frac{L}{G} \cdot (c - c_\omega) + y_\alpha \qquad (4.7)$$

For integrating (4.5), the gas side resistance will not be considered. As mentioned before, this practice is common:

$$y \cong y_{CO_2 b} \cong y_{CO_2 i} \qquad (4.8)$$

With equations (4.5) to (4.8), yields:

$$\frac{G}{L} \cdot \ln \frac{y_\alpha}{\frac{L}{G}\cdot(c_\alpha - c_\omega) + y_\alpha} = \frac{a \cdot \phi \cdot A_c \cdot h}{L} \qquad (4.9)$$

The logarithmic mean for the gas concentration is defined as:

$$y_m = \frac{y_\alpha - y_\omega}{\ln \frac{y_\alpha}{y_\omega}} \qquad (4.10)$$

From (4.9), (4.10) and (4.7), with the condition that $y(c=c_\alpha) = y_\omega$:

$$a_L = \frac{L \cdot (c_\omega - c_\alpha)}{\phi \cdot A_c \cdot h \cdot y_m} = \frac{B \cdot \Delta CO_3^{=}}{\phi \cdot h \cdot y_m} \qquad (4.11)$$

$$a_G = \frac{G \cdot (y_\alpha - y_\omega)}{\phi \cdot A_c \cdot h \cdot y_m} = \frac{G \cdot \Delta y_{CO_2}}{\phi \cdot A_c \cdot h \cdot y_m} \qquad (4.12)$$

There are then two possibilities for evaluating the effective specific mass transfer area, either by measuring the concentrations in the liquid phase (equation (4.11)) or by measuring the concentrations in the gas phase (equation (4.12)). The indexes L and G were used to distinguish the two equations. The ratio between equations (4.11) and (4.12) express the error in the mass balance.

Both quantities have been measured in this work, although more confidence is placed in values obtained for a_L (4.11) as the specific liquid load and carbonate concentrations are measured more accurately than the molar gas flow and the concentrations in the gas phase (sections 5.1 and 5.2, chapter II). This shall be discussed in the next section.

The error in the determination of the specific mass transfer area is given by:

$$\frac{\Delta a_L}{a_L} = \left|\frac{\Delta(\Delta CO_3^{=})}{\Delta CO_3^{=}}\right| + \left|\frac{\Delta\phi}{\phi}\right| + \left|\frac{\Delta y_m}{y_m}\right| + \left|\frac{\Delta B}{B}\right| + \left|\frac{\Delta h}{h}\right| \qquad (4.13)$$

$$\frac{\Delta a_G}{a_G} = \left|\frac{\partial(\Delta y_{CO_2})}{\Delta y_{CO_2}}\right| + \left|\frac{\Delta G}{G}\right| + \left|\frac{\Delta\phi}{\phi}\right| + \left|\frac{\Delta y_m}{y_m}\right| + \left|\frac{\Delta h}{h}\right| \qquad (4.14)$$

2 Materials and methods

Experiments were carried out in the pilot plant presented in chapter II, and whose main column had an internal diameter of 295 mm. The packing height was of two elements (420 mm) for all MELLAPAK types. The packing height for the experiments with 25 mm ceramic rings was 800 mm. There were additional experiments with 125.Y with a packing height of 630 mm. The broad range of F-Factors (equation (1.1)) and specific liquid loads (equation (1.3)) for the experiments and also the need for a column close to industrial size justified the need of such a complex apparatus (as discussed in chapter I). The procedure to pack the column with the structured and irregular packings is given in the appendix B. Chapter II gives the background for conducting the experiments. Capacity is defined in section 1.3, chapter I. The definitions of "run", "point", "set" and "data point" are to be found at the end of section 6.1, chapter II.

In order to evaluate the mass transfer area, the following values had to be measured: the liquid flow rate, the carbonate concentration of the solution and the CO_2 concentration of the gas flow at the inlet and outlet of the column. To determine the F-Factor, the gas flow rate, atmospheric pressure, gas pressure and temperature at column inlet were measured. The computer program GINTA.PGM was made with the part of the program KLA4.PGM for gas flow measurement (section 5.3.3, chapter II). In appendices G to K, the gas and liquid flowrates for each point are given together with the results. The inlet gas and liquid temperature were maintained at 22°C, as for the experiments with the wetted wall column (chapter III).

The procedure for the experiments is outlined in figure 4.1, and the steps are described in detail in the appendix C. Required material and manpower is given at the end of the appendix C. Risk analysis is in appendix E. After the experiments in the pilot plant, titrations for the determination of carbonate content of the samples were carried out with the experimental set shown in figure 2.8, section 5.2.2, chapter II. The titration procedure was explained in this section and it was also used for the experiments with the wetted wall column.

A run begins with the calibration of the BINOS gas analyzer and by setting the gas and liquid flows for the absorption experiments. For the measurement of one point, after a minimum period of 5 minutes to assure steady state conditions of the flow in the column, 6 liquid samples (three flasks for liquid inlet and three flasks for liquid outlet), 12 data points for the CO_2 concentration (six for the gas inlet and six for the gas outlet) and 6 data points for the gas flow, pressure and temperature were taken. A data point for the gas flow, pressure and temperature was obtained at each two minutes. A pair of liquid samples (inlet-outlet) was taken at steady state conditions of the flow every 4 minutes. At least 6 titrations were executed, giving three values for the difference in the carbonate concentration between the column inlet and outlet for the average to use in equation (4.11). If there was an uncertainly of the carbonate content of a flask, the titration was repeated for confirmation.

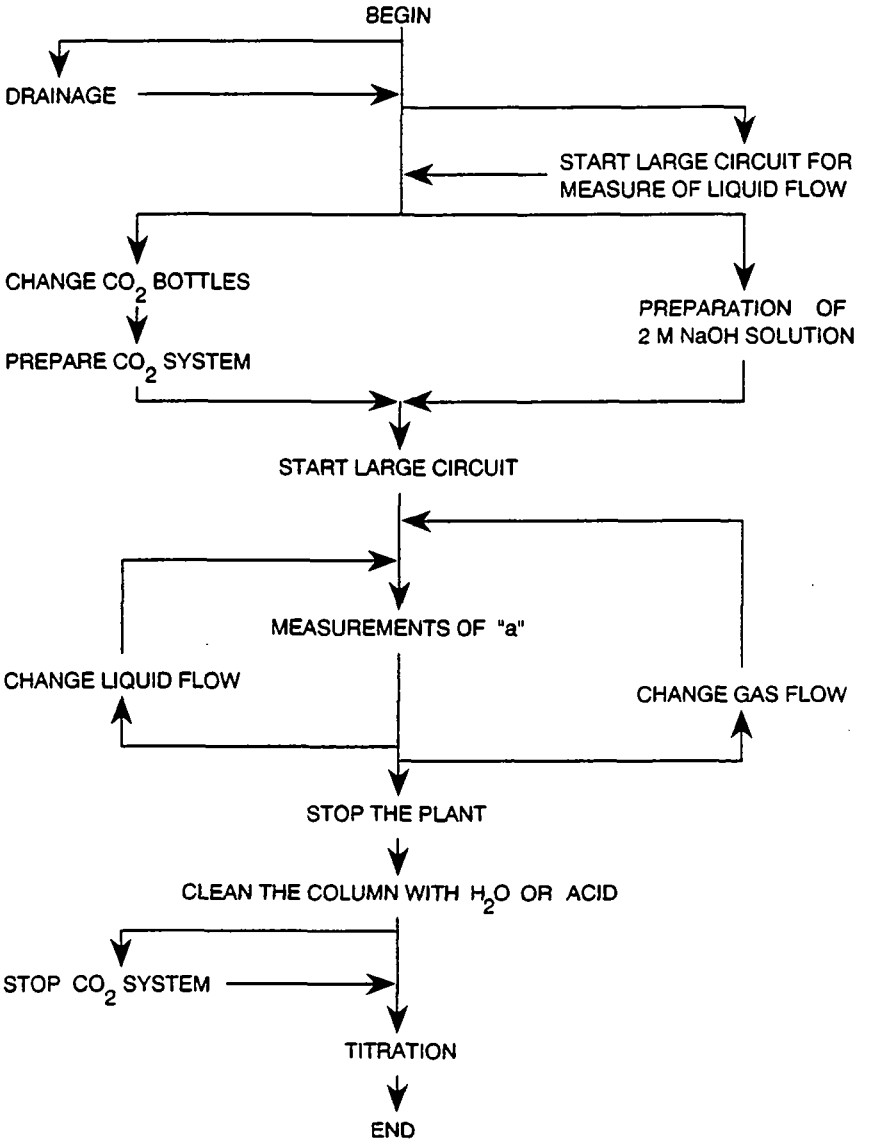

Figure 4.1 Flowchart of the procedure for the specific mass transfer area experiments.

The measurements of the liquid flow were executed as given in section 5.1.1, chapter II. These measurements were carried out when it was decided to change the solution in the reactor R11. The neutralization after the measurement of the liquid flow is explained in section 3.1, chapter II and in the procedure given in the appendix C. The solution was neutralized when the carbonate content was so high, that it left the concentration range used in the experiments with the wetted wall column.

The column was cleaned from time to time to avoid deposition of carbonate on the packing surface, which could influence the wettability. At the beginning of section 2.1, chapter I, it was pointed out that the wettability is an important parameter for the formation of effective areas.

The procedure for running the experiments, together with risk analysis (appendix E) and control of possible leakages in the system, was determined using water and air. The actual experiments were carried out with MELLAPAK 250.Y (runs 1 to 14 and 35 to 38), with 500.Y (runs 15 to 21, 33 and 34) and with 125.Y (runs 22 to 31). The runs with 25 mm ceramic rings (runs 39 to 46) were important in order to confirm the absolute values from the other measurements (section 3.6). The last experiments were with three packing elements of MELLAPAK 125.Y (runs 47 to 50) for studying the influence of the packing height and of the drip point density.

Section 5, chapter II, describes all necessary instrumentation used during these experiments. Equations (4.13) and (4.14) were developed for estimating the error in the mass transfer area values. The terms on the right hand side of these equations are in decreasing order of error. The order of magnitude of these terms is given in table 4.1.

Table 4.1 Estimation of experimental precision.

Variable	Precision	Remarks
B	< ± 1 %	see section 5.1.1, chapter II
G	< ± 10 %	see section 5.1.2, chapter II
ϕ	± 7 %	see section 4, chapter III
ΔCO_3	± 14 %	for two elements of MELLAPAK 125.Y
	± 8 %	for two elements of MELLAPAK 250.Y
	± 5 %	for two elements of MELLAPAK 500.Y
	± 7 %	for 25mm ceramic rings with h=800 mm
	± 8 %	for three elements of MELLAPAK 125.Y
Δy_{CO_2}	± 44 %	for two elements of MELLAPAK 125.Y
	± 27 %	for two elements of MELLAPAK 250.Y
	± 16 %	for two elements of MELLAPAK 500.Y
	± 8 %	for 25mm ceramic rings with h=800 mm
	± 44 %	for three elements of MELLAPAK 125.Y
y_m	± 3 %	
h	< ± 1 %	

These values are conservative. Table 4.2 presents the estimation of the error in evaluating the mass transfer area with equations (4.13) and (4.14) using the values from table 4.1. The table 4.2 also gives the average ratio of the standard deviation of a set divided by its mean, as defined by the equation (2.11) in section 6.1, chapter II. The latter values are smaller and more realistic.

Table 4.2 **Estimate in evaluating the mass transfer area.**

	Error (a)	Error (b)	Remarks
a_L	26 %	15 %	for two elements of MELLAPAK 125.Y
	20 %	9 %	for two elements of MELLAPAK 250.Y
	17 %	8 %	for two elements of MELLAPAK 500.Y
	20 %	4 %	for three elements of MELLAPAK 125.Y
	19 %	4 %	for 25mm ceramic rings with h=800 mm
a_G	65 %	25 %	for two elements of MELLAPAK 125.Y
	48 %	21 %	for two elements of MELLAPAK 250.Y
	37 %	13 %	for two elements of MELLAPAK 500.Y
	65 %	27 %	for three elements of MELLAPAK 125.Y
	29 %	4 %	for 25mm ceramic rings with h=800 mm

Code: column (a): with equations (4.13) and (4.14) and table 4.1.
column (b): average for all sets of the ratio $\frac{\sigma}{\bar{x}}$.

The precision of a_L is principally influenced by the the evaluation of the parameter ϕ and the carbonate content. The error of parameter ϕ was obtained with the wetted wall column experiments. The titration of carbonate was considered to be as accurate as possible with the equipment available. The higher the packing and the greater its efficiency of absorption, the less important are the errors. This explains why the scatter was big with two elements of MELLAPAK 125.Y, the packing with less separation efficiency. The low density of MELLAPAK 125.Y also plays a role as discussed in more detail in section 3.4, chapter IV.

The mass transfer area evaluated using equation (4.12) is less reliable, because it was not possible to measure the molar gas flow and the CO_2 concentration difference in the gas phase precisely. For large gas flows and high packing efficiency, the measured difference of the CO_2 mole fraction in the gas was sometimes not detected by the gas analyzer, rendering impossible the determination of a_G.

With large F-Factors, during the experiments with MELLAPAK 125.Y, there was liquid in the outlet gas samples. Droplet formation is impeded less by MELLAPAK 125.Y than by denser packings, and some droplet carryover in the gas stream at the top of the column was observed with this packing. The sampling position had to be changed after run 23. The point 22.4 was not considered for computing the average of the set 3.12, since the gas outlet sample may have been erroneous (liquid in the circuit). The position of the gas outlet sampling was changed and was installed over the distributor until

run 38, reducing the likelihood of contact with the liquid drops. After this change, there was a slight decrease of the concentration measured at the gas outlet by the gas analyzer.

The concentration measured by the gas analyzer might have been influenced by the gas inside the distributor, which could react with the liquid pool in the distributor. There could have been therefore an increase of the mass transfer area values calculated with equation (4.12). Nevertheless, the logarithmic mean for the gas concentration (equation (4.10)) did not seem to be significantly influenced, as points with same liquid and gas flowrates for MELLAPAK 250.Y and 500.Y presented the same values, within experimental uncertainty, before and after the change of the position of the gas sampling.

The measurements of mass transfer rates has always a considerably degree of uncertainty, particularly in complex and big apparatus with large flows. This has been pointed out by Fair and Bravo (1987). The authors compare data from two different sources and they explain that "sets of data by Billet were obtained in a small diameter column where, in the experience of the authors, there tends to be less data scatter than found in larger columns". In spite of the apparently large scatter, which are not surprising, the measurements can be considered to be reproducible and correct.

Some experiments with MELLAPAK 250.Y (sets 1.5, 1.9, 1.10 and 1.14) and with MELLAPAK 125.Y (sets 3.6, 3.8, 3.11, 3.13 and 3.14) are cases where column operation was at over 100 % capacity according to the program SULPAK. Only for the sets 1.10 and 1.14 flooding on the collar was observed. The pressure drop would stay constant, although a puddle was formed on the packing collar. The data from the experiments did not seem to fluctuate more than usual with the high values of capacity. For MELLAPAK 500.Y, all experiments were carried out under 100 % capacity.

The error in the mass balance is given by the ratio between equations (4.11) and (4.12). The values for each point are available together with the results in appendix G to K. The average of all points for each packing type is given in the table 4.3. The mass balance indicates that the error may be of the order of 20 %. Nevertheless, it should be borne in mind that the uncertainties associated with a_G are higher than those associated with a_L (table 4.2). Thus, the mass balance check on the accuracy of effective area may be misleading pessimistic.

Table 4.3 Average of the ratio $\frac{a_G}{a_L}$ (mass balance ratio).

	Average of the ratio aG/aL
for two elements of MELLAPAK 125.Y	1.00
for two elements of MELLAPAK 250.Y	0.83
for two elements of MELLAPAK 500.Y	0.70
for three elements of MELLAPAK 125.Y	0.88
for 25mm ceramic rings with h=800 mm	1.19

3 Results and discussions

In this section, measurements of specific mass transfer area are presented and their significance discussed. Capacity is defined in section 1.3, chapter I. Definitions of run, point, and set are to be found at the end of section 6.1, chapter II. Error bars are plotted in the figures in sections 3.1 to 3.3 for showing the uncertainty of the data, although this makes difficult the identification of some points.

3.1 The specific mass transfer area for MELLAPAK 250.Y

The table in the appendix G presents the results for runs 1 to 14 and 35 to 38. Figure 4.2 plots the specific mass transfer area - a_L - evaluated from measured data according to the equation (4.11) as a function of the F-Factor. The error bars show an error of ± 20 % (table 4.2, section 2, chapter IV) in the evaluation of the mass transfer area and ± 10 % in the evaluation of the F-Factor (section 5.1.2, chapter II). These errors are considered conservative estimates.

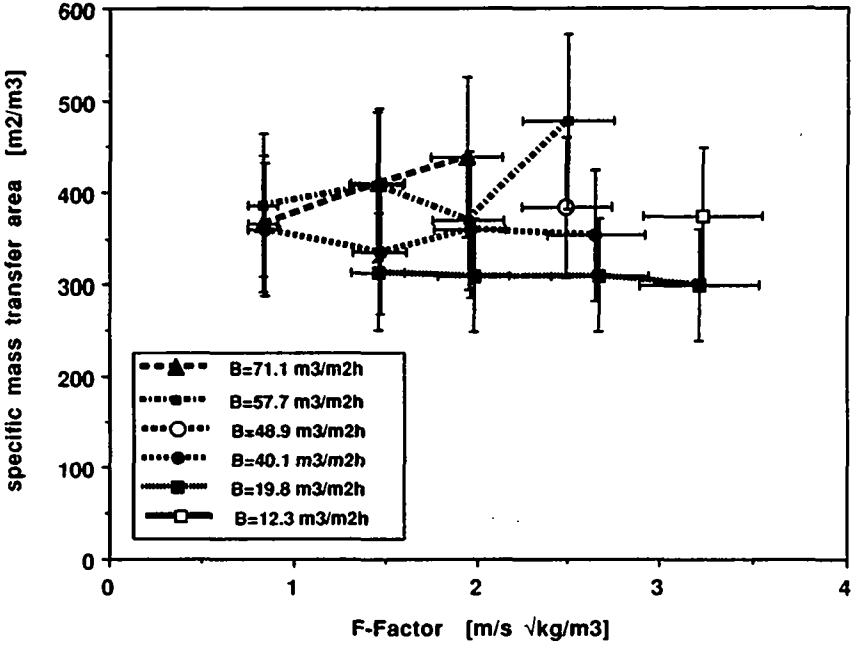

Figure 4.2 Mass transfer area versus F-Factor for MELLAPAK 250.Y.

The mass transfer area is constant at low F-Factors at far from full capacity conditions. With low specific liquid loads, for F-Factors of about

0.85 to 1.5 and even 2.0, the values of the mass transfer area were similar. This shows that a possible influence of the volumetric gas phase mass transfer coefficient - $k_G a$ - was not detected.

The influence of the specific liquid load is very clear. The higher the specific liquid load, the higher the effective area. An increase of the specific liquid load reduces, however, the value of the F-Factor at which F-Factor plays a role. The fluctuation of the mass transfer area values is also greater.

The most striking fact is that not only are the values for the specific mass transfer areas higher than the geometric area of the packing (250 m^2/m^3), but the values can actually be almost twice as high. The values are between 300 to 450 m^2/m^3, which corresponds to a ratio of the effective area to the geometric area of 1.2 to 1.8. This fact will be discussed later.

3.2 The specific mass transfer area for MELLAPAK 500.Y

The table in the appendix H presents the results for runs 15 to 21 and 33 to 34. Figure 4.3 plots the specific mass transfer area - a_L - evaluated from measured data according to the equation (4.11) as a function of the F-Factor. The error bars show an error of ± 17 % (table 4.2, section 2, chapter IV) in the evaluation of the mass transfer area and ± 10 % in the evaluation of the F-Factor (section 5.1.2, chapter II). These errors are considered conservative estimates.

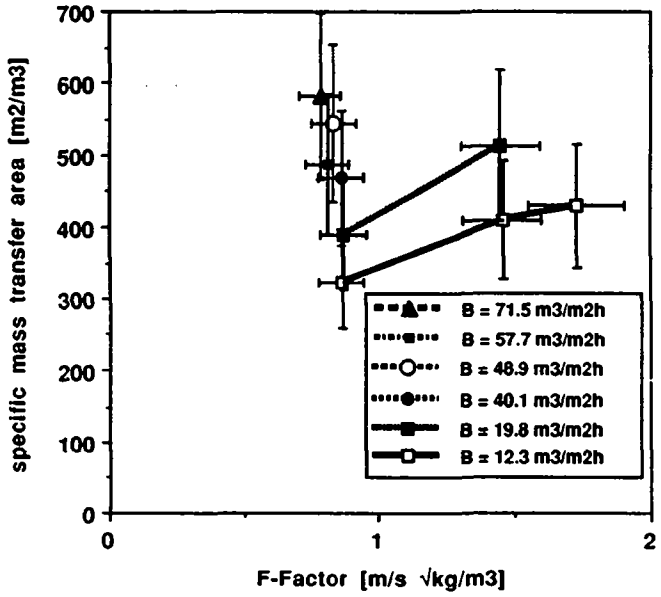

Figure 4.3 Mass transfer area versus F-Factor for MELLAPAK 500.Y.

Both the specific liquid load and the F-Factor have a clear influence on the values of the mass transfer area. A small specific liquid load of 12.3 m^2/m^3 presents effective areas lower than the geometric independent of the F-Factor. With an increase of the specific liquid load and of the F-Factor, the mass transfer area increases greatly, reaching values which may or may not be higher than the geometric (500 m^2/m^3).

For specific liquid loads greater than 40.1 m^3/m^2h, it was not possible to measure with F-Factors of 1.4, due to flooding. The distributor does not work with specific liquid loads between 25 and 38 m^3/m^2h (section 4.3, chapter II). Therefore, more experiments with smaller specific liquid loads and changing F-Factors were carried out.

For a constant F-Factor of the order of magnitude of 0.85, the ratio of the effective mass transfer area to the geometric area varies from 0.65 to 1.17. Effective areas are lower than the geometric for specific liquid loads less than 48.9 m^2/m^3. An empirical correlation obtained by least square regression using the sets with F-Factor of the order of magnitude of 0.85 is given by:

$$a_e = 150 \cdot B^{0.312} \qquad (4.15)$$

The figure 4.4 shows the good correspondence between measured values and the correlation (4.15).

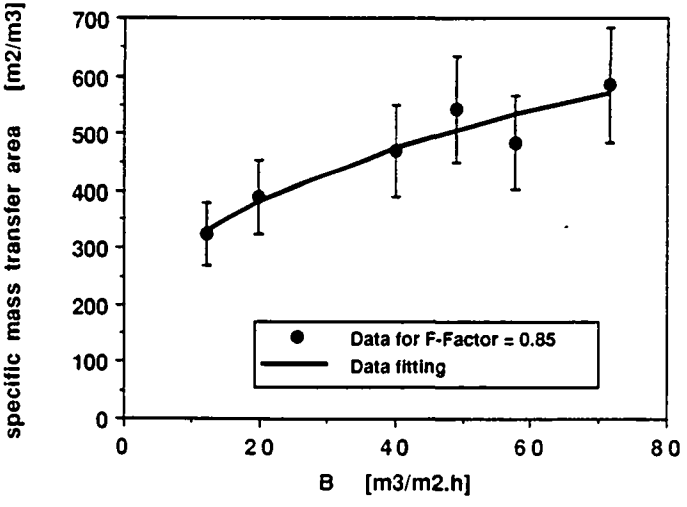

Figure 4.4 Mass transfer area for MELLAPAK 500.Y with F-Factor of 0.85.

3.3 The specific mass transfer area for MELLAPAK 125.Y

The table in appendix I presents the results for runs 22 to 31. Figure 4.5 plots the specific mass transfer area - a_L - evaluated from measured data according to the equation (4.11) as a function of the F-Factor. The error bars show an error of ± 26 % (table 4.2, section 2, chapter IV) in the evaluation of the mass transfer area and ± 10 % in the evaluation of the F-Factor (section 5.1.2, chapter II). These errors are considered conservative estimates.

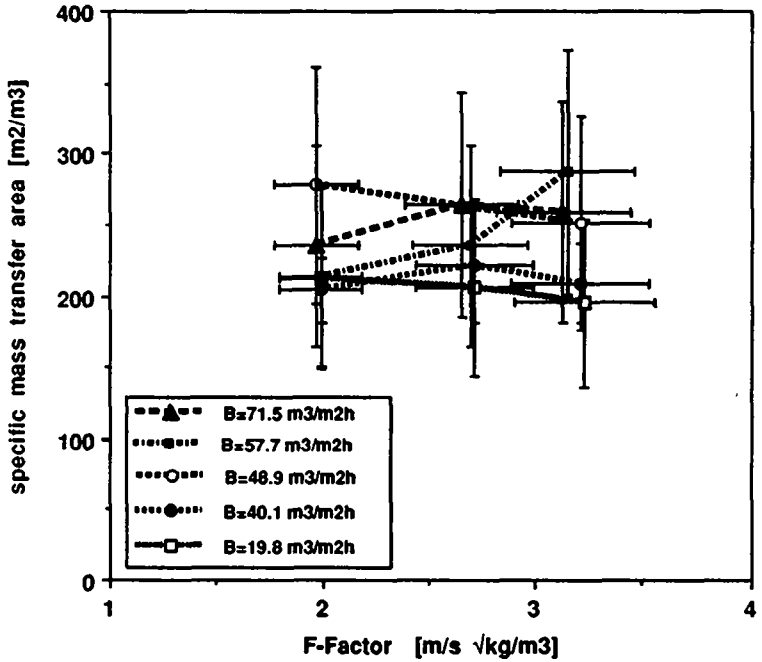

Figure 4.5 Mass transfer area versus F-Factor for MELLAPAK 125.Y.

Considering the experimental errors, the influence of the specific liquid load cannot be confirmed. The effective mass transfer area is apparently independent of the F-Factor. However, for the specific liquid load of 57.7 m^3/m^2h, there was an unexpected increase with a F-Factor of 3.2. This seems misleading since for the higher specific liquid load of 71.5 m^3/m^2h, such an increase of the effective area with the F-Factor was not observed. Actually, one has straight horizontal bands. These bands displace vertically with the specific liquid load.

All measured mass transfer area values were higher than the geometric area of 125 m^2/m^3. The values vary between 200 to 275 m^2/m^3, which corresponds to a range of ratio of effective to geometric area of 1.6 to 2.2.

3.4 Comparison and discussion of mass transfer areas of MELLAPAK

Figure 4.6 overleaf presents all specific mass transfer area measurements as a function of the F-Factor. The error bars are omitted for clarity. The ordinate on the left is for the specific mass transfer area and the ordinate on the right is for the specific geometric area.

The values for the specific mass transfer area for MELLAPAK 500.Y for given a specific liquid load and F-Factor are higher than for 250.Y, which in turn are higher than for 125.Y. This is in accordance with the expectation that the effective area increases with the geometric area.

As an example, for the specific liquid load of 19.8 m^3/m^2h (black squares) or 40.1 m^3/m^2h (white squares), there is an increase in the value of the specific mass transfer area with the geometric area.

The effective mass transfer area depends primarily on the packing and on the specific liquid load. The influence of the F-Factor is apparently linked to the packing.

For MELLAPAK 500.Y, an increase of the F-Factor causes an increase of the mass transfer area. However, for 125.Y, the F-Factor has little influence on the effective area values. With the packing 250.Y, the influence of the F-Factor becomes important only for high F-Factors near the full capacity. This fact leads to the conclusion that increasing the specific geometric area of a packing, which reduces the porosity, increases the possibility of a earlier influence of the F-Factor.

The horizontal lines of the mass transfer area with the F-Factor for a given specific liquid load supports the contention that the gas-side resistance is unimportant. If the k_G were important, it would change with the gas flow. The tendency would be that the gas concentration in the equations (4.11) and (4.12) would change too. Thus, the values of the specific mass transfer area would not be constant as above.

For irregular packing, the geometric area is not a linear function of the packing's size. In the case of rings, for example, the geometric area varies with the inverse of the square of the packing size, since the length and the diameter follow the same scaling law. However for MELLAPAK the geometric surface changes with only one characteristic length of the packing, the corrugation height, since the height of an element is aproximately constant.

Equation (4.2.b) predicts a dependence of the specific geometric area with the hydraulic diameter, which determines the flow. The specific geometric area changes inversely with the corrugation height (section 1.4, chapter I). Thus, the hydraulic diameter of MELLAPAK increases aproximately linearly with the corrugation height.

Therefore, it is possible to build a general correlation in which the ratio of the effective mass transfer area to the geometric area would depend almost exclusively on the dimensionless Reynolds number, which considers the specific liquid velocity and the hydraulic diameter, which is related to the packing size and geometric area.

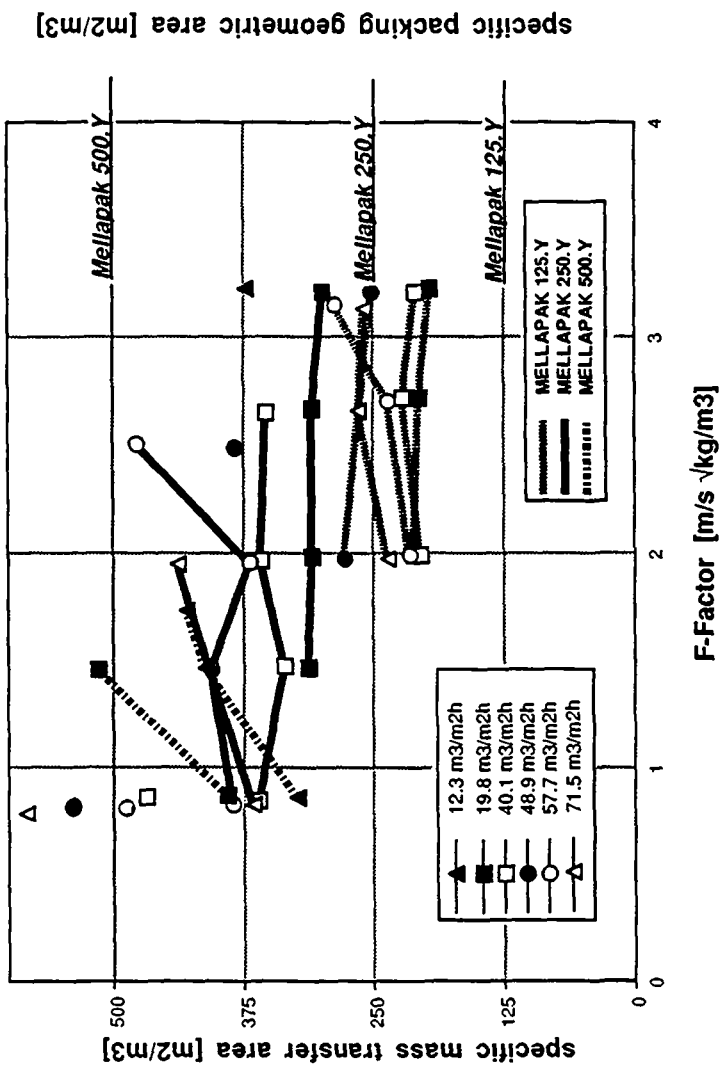

Figure 4.6 Mass transfer area versus F-Factor for all MELLAPAK types.

The Reynolds number is defined by analogy to equation (4.1) as:

$$Re = \frac{\rho_L \cdot w_L \cdot d_h}{\mu_L \cdot \cos 45^\circ} \qquad (4.16)$$

Since the hydraulic diameter of the packing is defined by equation (4.2.b), the definition of the Reynolds number (equation (4.16) is actually a multiple of the definition given in table 1.3 by a factor of (4/cos 45°). For the density and viscosity of NaOH solutions, the values of 1077 kg/m^3 and 1.177 .10^{-3} kg/m.s (Vazquez et al. (1989)) were respectively used. The correlation in figure 4.7 is given by:

$$\frac{a_e}{a_p} = 0.22 \cdot Re^{0.34} \qquad (4.17)$$

The applicability of this correlation with systems having different viscosities and densities has not been experimentally determined. An important consequence of equation (4.17) is that the ratio of the effective area to the geometric increases with decreasing packing surface at constant specific liquid load. The specific effective area is dependent on the specific geometric area to the power of 0.66.

The correlation is plotted in the figure 4.7 with all sets. More to the right are principally data from 125.Y and to the left data from 500.Y.

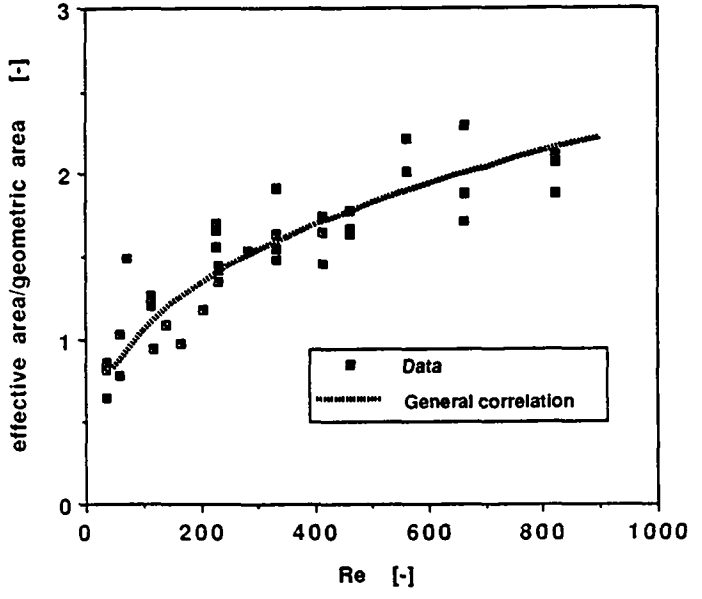

Figure 4.7 The ratio $\frac{a_e}{a_p}$ as a function of Reynolds number.

Figure 4.8 plots all the experimental data with the correlations which result from the general correlation (4.17). The correlation (4.15) for MELLAPAK 500.Y at low F-Factors is also plotted.

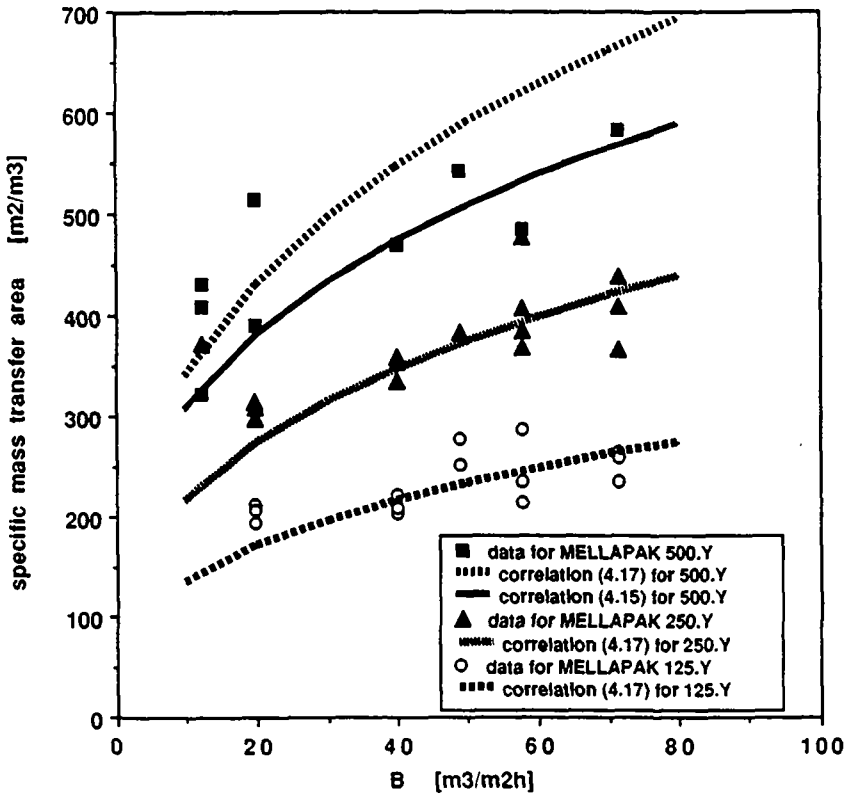

Figure 4.8 Correlations from the general correlation (4.17):

$a_e = 157 \cdot B^{0.34}$ for MELLAPAK 500.Y

$a_e = 99 \cdot B^{0.34}$ for MELLAPAK 250.Y

$a_e = 63 \cdot B^{0.34}$ for MELLAPAK 125.Y

The agreement is particularly good for MELLAPAK 250.Y and 125.Y, especially if the error associated with each point is considered. For MELLAPAK 500.Y at low F-Factors, the correlation (4.15) gives more realistic values. However, mass transfer areas of MELLAPAK 500.Y near full capacity might be better evaluated with the general correlation (4.17). Nevertheless, both correlations have similar exponents on the specific liquid load.

A very important consequence of the general correlation (4.17) is that the ratio of the effective area to the geometric area can exceed as much as a factor 2. The question arises as to why.

At first thought this fact may be surprising, because the geometric form of MELLAPAK might lead to suppose that the liquid flows smoothly over the packing sheets without detachment. The maximal possible value for the effective area would correspond to a total wetted packing. Unfortunately, it is not possible to visualize the flow inside the packing, since it is opaque. Through the glass column walls, the liquid was observed to flow as a film attached to the sheets near the column wall. The liquid does not seem to fall into the holes and the gas does not seem to bubble through the liquid. The holes might provide additional interfacial area. These visual observations at the column wall do not entitle us to show the presence of additional mass transfer surface to the wetted packing.

There is formation of liquid drops inside MELLAPAK 125.Y, since small drops carried over by large gas flows were observed at the top of the column, which actually once disturbed the gas sampling circuit at the gas outlet (section 2, chapter IV). This packing is less effective in suppressing droplet formation and the drag associated with it than denser packings.

This observation is in line with the fact that MELLAPAK 125.Y has the highest ratio of effective to geometric area. Such a phenomenon is due to the formation of liquid drops and the influence of turbulence at the gas-liquid film interface. The sheets are further apart, offering more possibilities of formation of droplets and waves. This fact may also cause great fluctuations of the mass transfer area values. This is perhaps why the scatter in the measured effective area of MELLAPAK 125.Y was more important. Additionally, the relatively small packing height for MELLAPAK 125.Y, which is the less efficient, also tends to increase the scatter of the results.

Concluding, the larger the specific geometric area, the smaller the ratio of the effective area to the the geometric area. A reduction of the specific geometric area increases the space between sheets. The porosity of the packing is bigger. There are more chances for the formation of drops and waves which can contribute to an increase of the effective area, which can be higher than the available geometric area.

Further research could study if chemical systems, which have ions in the solution, may influence the size of liquid drops. The smaller the liquids drops are, the higher is the specific area offered by a drop. It may be that for physical systems, fewer drops are formed or the drops have another size. The results obtained in this work may be compared to those already published, since the chemical system used in this work was frequently employed in experimental works, the literature use chemical methods and other methods for measuring effective mass transfer areas do not seem to be reliable (section 2.1.1, chapter I).

3.5 Comparison with information from the literature

In section 2.1.1, it was shown that the only work which tries to estimate effective area of structured packings is that from Fair and Bravo (1987). These authors propose, without experimental verification, that "for the structured gauze packings it is reasonable for one to assume that the packing is completely wet and that the interfacial area is the same as the packing surface".

However, in an earlier work by Bravo and Fair (1982), with irregular packings, they accept that "the value of the effective area is composed not only by the wetted area over the packing but also by the area provided by suspended and falling droplets, gas bubbles within liquid puddles, ripples on the liquid film surface, and any contribution from film falling on the walls of the column". Thus, there is no plausible reason why structured metal gauze packings should not present such additional effective areas.

Consequently, the work of Fair and Bravo (1987) has serious deficiencies in determinating "values of interfacial areas that were back-calculated from mass transfer efficiency data" from the literature. Furthermore, in this work they actually calculate ratios of effective area to geometric area for MELLAPAK 250.Y as high as 1.2. Therefore, there is no reason why in the present work values at least as high as 1.2 should not be obtained.

The physics of the flow in structured packings is different from that of irregular packings. Thus a direct comparison of the results of this thesis with works using irregular packings is difficult. However, since no other information is available within the literature concerning structured packings, it is nonetheless necessary to consider what is known about irregular packings and attempt to relate this to the present work.

In principle, for irregular packings, the effective areas are smaller than the specific geometric area defined by the packing. However, Bornhütter and Mersmann (1991) have measured effective areas for modern irregular packings with large size. Their results show that the ratio of the effective area to the geometric can be greater than 1 (of the order of 1.5). According to Linek et al. (1984), hydrophilised plastic Pall rings of 25, 35 and 50 mm do present a ratio of the effective area to the geometric area, which can at high liquid flowrates increase up to about 1.2. Sahay and Sharma (1973) have measured effective areas of 25 mm stainless steel Pall rings 1.16 times higher than the specific geometric area of the packing.

Schultes (1990) and Kolev (1973) dismiss the models in the literature which assume that the effective area must always be smaller than the geometric area for irregular packings (section 2.1.2, chapter I). The model from Onda et al. (1967) (correlation (1.26)) used to predict effective areas, falls in this category according to Schultes and Kolev. Moreover, Schultes states that big columns with high specific liquid loads can present effective areas greater than the geometric. Shi and Mersmann (1985) predict also that effective areas can be higher than the geometric.

The reason why effective area can be higher than the geometric area has not been frequently discussed in the literature. Bornhütter and Mersmann (1991) seem to have observed in modern irregular packings a strong formation of droplets for high specific liquid loads. The authors claim that this explains why the measured effective area is higher than the geometric.

As mentioned in section 2.1.1, chapter I, Hüttinger and Bauer (1982) indicate that irregular packings which force the formation of droplets present higher interfacial area and enhanced mass transfer. The presence of droplets may explain why Pall rings 25 mm are more efficient than 25 mm raschig rings (Eckert et al. (1958)), although they have about the same specific geometric area. The enhanced mass transfer of Pall rings should be due to a greater effective area. As seen above, the effective area of Pall rings can be bigger than the geometric.

For a given packing volume, structured packings offer an increased efficiency for mass transfer (Meier et al. (1977)). There are irregular packings which offer a bigger geometric area than MELLAPAK 250.Y, as 13 mm rings, without being more efficient for mass transfer. This is due to MELLAPAK 250.Y providing more effective area, which is in part the result of droplet formation and high turbulence.

The value of the exponent of the general correlation (4.17) and of correlation (4.15) is similar to the average of the models proposed in the literature predicting the influence of the specific liquid load on the effective mass transfer areas for irregular packings (table 1.4, section 1.2.2, chapter I). The works from Mohunta et al. (1969), Kolev (1973) and Puranik and Vogelpohl (1974) suggest exponents of 1/3, 0.392 and 0.307 respectively. These models might have considered a laminar flow over a surface when the exact exponent of the specific liquid load is then 1/3. Structured packings offer a defined surface over which a liquid may flow, in contrast to irregular packings. It is therefore reasonable to admit that if the power of 1/3 of the specific liquid load is justified for the irregular packings, which have no defined channels, then this power should be applicable for structured packings. The trends of the present results are thus in accordance with the literature.

There are very clear hints not only that the observed trends are correct, but also that the ratio of effective to geometric area can exceed unity. However, it must be verified if the absolute values can really be high. Therefore, experiments in the next section were carried out.

3.6 The specific mass transfer area for 25 mm ceramic rings

With the same experimental procedure, evaluation method and apparatus as used for MELLAPAK (section 1 and 2, chapter IV), measurements were carried out with an irregular packing, whose specific mass transfer area was published by different sources. A literature search chose the works of Sahay and Sharma (1973), Kolev (1973), Yoshida and Miura (1963) and Yoshida and Koyanagi (1958). All furnished measured data for the effective area of 25 mm ceramic rings. The data of Yoshida and Koyanagi (1958) result from an indirect measurement of mass transfer area (section 2.1.1, chapter I). The other works used chemical systems and equipments listed respectively in tables 1.1 and 1.2, chapter I.

The 25 mm ceramic rings have a geometric area of 195-210 m^2/m^3. The exact figure depends on the packing procedure used and the evaluation carried out by the source in the literature. With the packing procedure given in appendix B, the value of 200 m^2/m^3 was found.

The data in table 4.4 was calculated from published equations and it was used in planning the experiments with ceramic rings. The design gas velocity is lower than the maximum gas velocity, above which countercurrent operation is not possible anymore. This packing does not allow so large gas flows for a given specific liquid load, as MELLAPAK.

Table 4.4 Design gas velocity with correspondent pressure drop for maximum number of theoretical stages for 25 mm ceramic Rings. (VFF-Füllkörper (1986)).

	B [m^3/m^2h]			
	12.3	19.8	40.1	57.7
w_G [m/s]	0.96	0.79	0.46	0.25
Δp [mmH_2O/m]	130	122	97	74

The table in the appendix J presents the results for runs 39 to 47. The figure 4.9 plots the specific mass transfer - a_L - evaluated from measured data according to the equation (4.11) as a function of the F-Factor. The error bars shows an error of ± 19 % (table 4.2, section 2, chapter IV) in the evaluation of the mass transfer area and ± 10 % in the evaluation of the F-Factor (section 5.1.2, chapter II). These errors are considered conservative estimates.

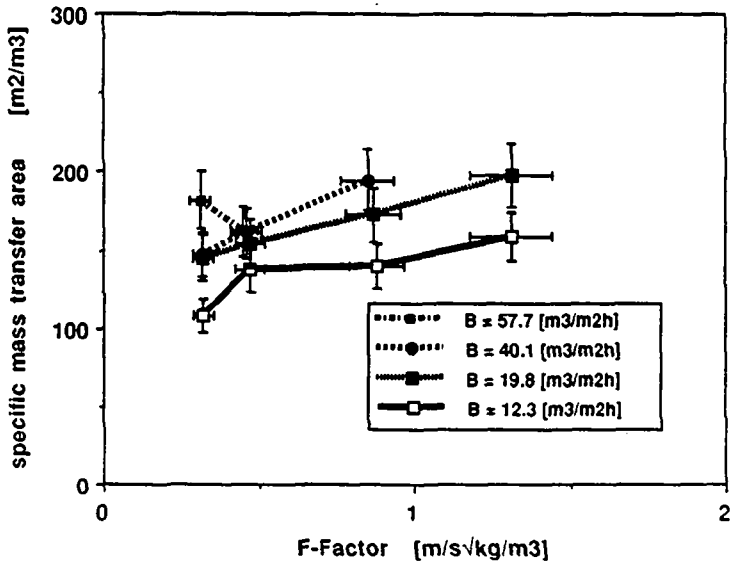

Figure 4.9 Mass transfer area versus F-Factor for 25 mm ceramic rings.

A first important conclusion is that all values for effective areas were below the packing's geometric area of 200 m^2/m^3.

There is a clear dependence of the specific mass transfer area on the F-Factor even for F-Factors far from full capacity conditions as shown in the figure 4.9. Such a dependence is not mentioned in the literature, in which the gas flows used are rarely cited. The F-Factor has more influence on increasing the effective area, when the specific liquid loads are high.

A possible influence of the gas phase mass transfer coefficient $k_G a$ is difficult to evaluate. The literature does not consider this mass transfer resistance (section 1.2, chapter IV). The influence of this resistance should be within experimental uncertainty. It is important to note that for the lowest specific liquid load of 12.3 m^3/m^2h, the values of mass transfer area for F-Factors between 0.46 to 0.88 were constant. If the gas phase resistance were important, it would be more pronounced with this liquid load, as turbulence are less present.

Figure 4.10 compares the data from the literature with this work. Experimental conditions from the literature is summarized in table 4.5. The error bars shows an error of ± 19 % in the evaluation of the mass transfer area for the data of this thesis (table 4.2, section 2, chapter IV). This error is considered conservative estimate.

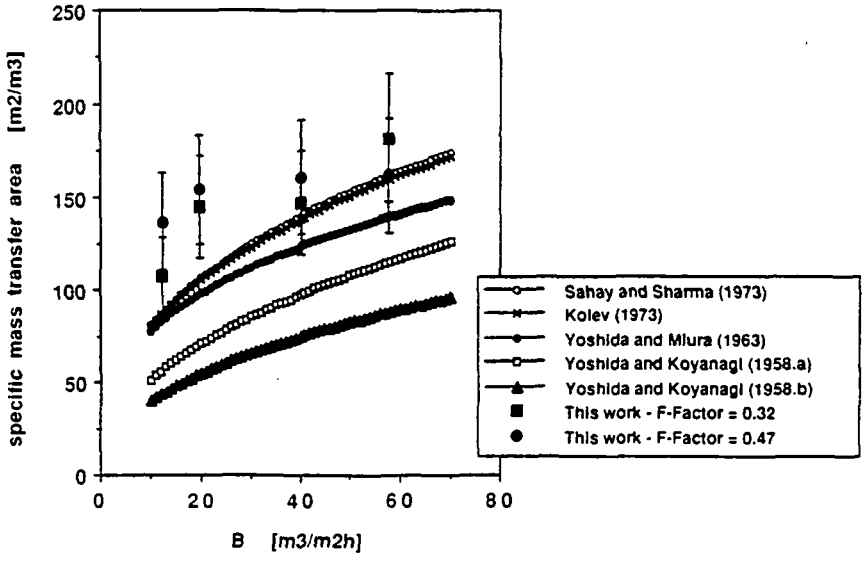

Figure 4.10 Mass transfer area versus liquid load for 25 mm rings.

The curve from Sahay and Sharma's experiments comes from reproducing their plot and extrapolating to liquid loads higher than 30 m^3/m^2h. The curves from Kolev (1973) come from their correlation (equation (1.29)) fitted to their results (using ρ = 1077 kg/m^3 and σ = 72.0 10^{-3} N/m from Vasquez et al. (1989)). The correlation from Kolev fits also Sahay and Sharma's data. The curve from Yoshida and Miura (1963) is actually an equation for wetted areas (proposed by Hikita in 1956), which they consider to fit their data very well. Yoshida and Miura (1963) concluded that the effective area is equal to the wetted area. The two curves from Yoshida and Koyanagi (1958) for different packing heights come from reproducing their plot and extrapolating to liquid loads higher than 30 m^3/m^2h. These data do not result from a chemical method, but from an indirect measurement (section 2.1.1, chapter I).

It must be admitted that the tendency is that the measurements of this work are higher than the literature. Nevertheless, the difference is within the range of experimental error. For a gas velocity of about 0.3 m/s, the values from the first three references are about 5 to 20 % lower. For a gas velocity of about 0.4 m/s, the values from the first three references are about 10 to 37 % lower. There is also a tendency that the values of this work approach those of the literature with increasing specific liquid loads. The trend of the effective area with the specific liquid load is about the same in all works.

It is important to examine the experimental conditions from the literature. Table 4.5 presents the column characteristics and the range of flowrates used by the four works with data plotted in figure 4.10. Gas flows will be now discussed in terms of the gas velocity and not F-Factors.

Table 4.5 **Experimental conditions from the literature.**

REFERENCE NUMBER	COLUMN CHARACTERISTICS height [mm]	diameter [mm]	RATIO $\frac{h}{d}$	RANGE B $[m^3/m^2h]$	w_G [m/s]
1	870	200	4.4	< 40	0.3
2	1900	190	10.0	not given	not given
3	762	121	6.3	< 30	not given
4.a	203	120	1.7	< 30	not given
.b	406	121	3.4		
this work	800	295	2.7	12 - 71	0.3 - 1.1

Reference number:
1- Sahay and Sharma (1973); 2- Kolev (1973); 3- Yoshida and Miura (1963)
4- Yoshida and Koyanagi (1958)
Note:
The data of reference 4 result from an indirect measurement of mass transfer area (section 2.1.1, chapter I). The other works used chemical systems and equipments listed respectively in tables 1.1 and 1.2, chapter I.

It is striking that the diameters are small for high packed columns. For irregular packed columns in particular, channelling (i.e. the tendency of the liquid to flow through the wall) becomes more significant when the ratio of packing height to diameter increases. Yoshida and Koyanagi (1958) (reference 4) detect that increasing the packing height decreases the effective area. For them "it is conceivable that the liquid distribution becomes worse as the packed height increases". Yoshida and Miura (1963) (reference 3) with a higher packed column, however with the same diameter, find higher values for the effective area.

The considerable large packing height and low NaOH solution normality may also falsify the data of Kolev (1973). The measurements actually employed the same reaction as in this work with NaOH solutions of 0.2 to 0.4 mol/l. The possibility of depletion effects cannot be eliminated. Depletion is the lack of hydroxide ions at the interface, which, disturbing the pseudo-first-order character of the reaction of CO_2 with NaOH, causes the method not to be adequate for measuring effective areas (section 1.1, chapter III).

Vidwans and Sharma (1967) have measured interfacial areas for 3/8" ceramic raschig rings in columns with different diameters. Their findings are that the effective areas "in the 4.37 cm i.d. column, at a given liquid superficial velocity, are about 15-20 per cent lower than the corresponding value in the 10 and 20 cm i.d. perspex columns. This difference can be attributed to the wall-effect present in the 4.37 cm i.d. column, where the ratio of tower diameter to packing size was only 4.6 which is less than the recommended value of 8". This would also imply that with 25 mm rings, the column diameter must be at least 200 mm (8 times 25 mm). The column of this work with an internal diameter of 295 mm packed with 25 mm rings respects the above rule. With this argument, the only work the results of which may be considered reliable is reference 1 in table 4.5.

Even this work has been dissmissed by Norman (1974), who points out that "small-scale experiments may be useful for comparative purposes, but to extend the range of the work we need much more information about the effects of the 'apparatus variables' such as tower diameter, packed height, packing orientation and liquid distribution, together with a more critical appraisal of the reliability and reproducibility of the experimental results".

Low specific liquid loads reinforce channelling. Templeman and Porter (1965) prove this with 13 mm rings. In addition, low specific liquid loads reinforce the tendency of the liquid to flow independently of the gas, and exacerbate maldistribution (Stikkelman et al. (1989)), thus reducing the specific effective areas.

The tendency for F-Factors to be maintained at low levels (much lower than typically employed in industrial columns) is probably explicable in terms of the necessity to maintain CO_2 concentration in the gas at easily measurable levels. If the CO_2 flows are low, the total gas flow rates must also be low. Higher F-Factors demand a greater CO_2 supply, which was made possible by the multi-bottle manifold complex which was built for this work (section 2.1, chapter II).

If the gas flows are not published, they can be estimated when the gas composition is known. Kolev (1973) used CO_2 from an ordinary bottle. The CO_2 concentration was 2 to 3 % in a column with a diameter of 190 mm. The flows from the bottle could not have been greater than 0.9 m^3/h, due to the Joule-Thomson effect, if the maximum gas outlet velocity was 20 m/s and the outlet tube had 4 mm. The maximum possible gas velocity in the column would be of the order of 0.4 m/s. However, commercial packed columns may be operated at higher gas loads when small liquid loads are used (table 4.4).

In summary, the data in the literature could have been influenced by high ratios of the packing height to column diameter, low range and small specific liquid loads and very low F-Factors. All three factors have the tendency to reduce the values of effective mass transfer areas.

The column in this work has a larger cross sectional area with a small ratio of the packing height to the column diameter. Specific liquid loads and F-Factors comparable to those used in industrial columns were used. In addition to all facts described so far, it may be that the tendency of discrepance stems from entrance effects. In this work, the liquid distributor had a high drip point density, which may have been highly above the values used by other authors.

3.7 The influence of drip point density and of packing height

The liquid distributor in the present work originally had a drip point density of 527 points/m^2 (section 4.2, chapter II). This was in an effort to minimize entrance effects. The value corresponds to the upper limit of density used for research liquid distributors, which should be higher than 300 points/m^2 according to Perry et al. (1990).

Some experiments with 3 packing elements of MELLAPAK M125.Y were carried out with 28 of the 36 available drip points blocked. The resulting drip point density was 117 points/m^2, which is in the upper limit of commercial distributors. Nutter Engineering, quoted in Perry et al. (1990), "has found that 100 points/m^2 works well for most sizes of random and structured packings". Fair and Bravo (1990) state that "observations show that at least 12 pour points/ft^2 (about 130 pour points/m^2) of cross sectional tower are needed".

Figure 4.11 overleaf shows the new pattern of the distributor, which tried to assure a geometric uniformity of the distribution points across the column's cross section. A smaller drip point density would be impossible to attain with the available distributor, since the measurements were already only possible with a specific liquid load of 19.8 m^3/m^2h. At higher rates, the distributor would have overflowed.

The results for the runs 49 and 50, which kept the specific liquid load constant and varied the gas flows, are given in the table in the appendix K. With the new drip point density of 117 points/m^2 and using 3 elements of M125.Y, the value of the specific effective area - a_L - for a specific liquid load of 19.8 m^3/m^2h and F-Factor of 2.7 was 156 ± 4 m^2/m^3. With the old drip point density, the value of the specific effective area was 160 ± 7 m^2/m^3. This shows that after changing the drip point density the difference in the values of the effective area was unimportant.

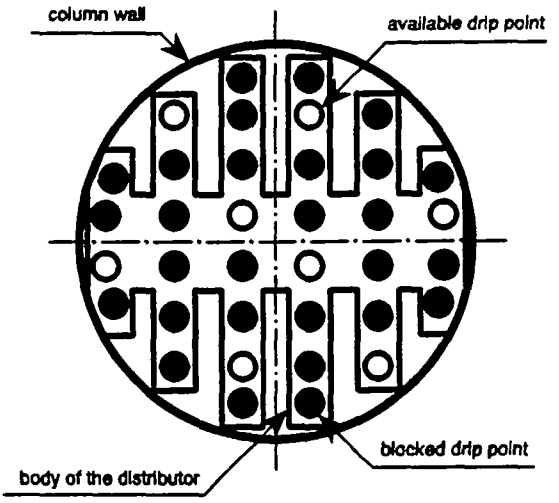

Figure 4.11 Reduction of available drip point density of the distributor, from 527 points/m² (Runs 1 to 46) to 117 points/m² (Runs 47 to 50).

For MELLAPAK 125.Y, the ratio of the specific effective area to geometric area was the highest of all the MELLAPAK types. This packing was therefore chosen to study whether a higher packing height would reduce the specific effective area values by a constant factor, which would reveal if "dead area" would have been measured.

The table in the appendix K presents the results for runs 47 to 48. Table 4.6 compares data from three packing elements with two packings for an F-Factor of 2.65. This represents a height increase of 50% (from 420 to 630 mm). The values of all other experimental variables were maintained as before.

Table 4.6 Influence of the packing height (MELLAPAK 125.Y).

B [m³/m²h]	Effective mass transfer area with a F-Factor = 2.65 [m²/m³] 3 packings h = 630 mm	2 packings h = 420 mm	Reduction [%]
19.8	160 ± 7	207 ± 18	23
40.1	185 ± 6	222 ± 42	17
57.7	220 ± 11	235 ± 13	6
71.5	250 ± 0	265 ± 45	6

Remark: The errors shown come directly from the calculations of the standard deviation of a set.

There is indeed a reduction of the effective area values of MELLAPAK 125.Y when the packing height is higher. The reduction of effective area values of MELLAPAK 125.Y is also dependent on the specific liquid load. The reduction is smaller, the higher the specific liquid loads. It is reasonable to suppose that increasing the specific liquid loads, decreases the influence of channelling effects, thus reducing the difference. The relative error in the mass transfer area estimation reduces with more packing elements. This was mentioned at the end of section 3.4, chapter IV.

If a "dead area" was measured, it would be due to the sampling circuit (section 4.3, chapter II). Thus, this "dead area" would be independent of the packing height and of the specific liquid load in the column. The measured total area would be equal to the "real" effective area added to a "dead" extra area:

$$A_{T\ 2p} = A_{r\ 2p} + A_d \qquad (4.18.a)$$

and

$$A_{T\ 3p} = A_{r\ 3p} + A_d \qquad (4.18.b)$$

If specific mass transfer area were to stay constant, the absolute effective area for three packings is related to the effective area for two packings by:

$$A_{r\ 3p} = 1.5 \cdot A_{r\ 2p} \qquad (4.19)$$

The ratio between the "dead" extra area and the real effective area with two packing elements is:

$$\frac{A_d}{A_{r\ 2p}} = \frac{(1.5*C-1)}{(1-C)} \qquad (4.20)$$

The constant C is obtained by dividing the measured values for 2 packing elements by three packing elements.

$$C = \frac{A_{T\ 2p}}{A_{T\ 3p}} \qquad (4.21)$$

The ratio of (4.20) has the values of -3.2, -4.0, -9.8 and -9.8 for the specific liquid loads of 19.8, 40.1, 57.7 and 71.5 m^3/m^2h respectively. These values, which are not constant and have a negative sign, suggest that no extra area could have been measured.

Bravo and Fair (1982) predicted in their correlation (equation (1.33)) for irregular packings that the effective area would be proportional to the packing height to the power of -0.4. An increase of 50 % of the packing height would thus reduce the effective area by about 15 %. Considering that irregular packings can be denser than MELLAPAK 125.Y and that denser packings may be less sensitive to an increase of the packing height, the reduction of effective area values presented by MELLAPAK is thus not high. The results in table 4.6 show that the reduction was less than 17 %, except for the smallest liquid load.

The influence of the F-Factor on effective area values with increasing packing height can be studied, since it was observed that the drip point density did not influence the results. Consequently, it is possible to make a comparison with data obtained with two and three packing elements of MELLAPAK 125.Y, with a specific liquid load of 19.8 m^3/m^2h.

Figure 4.13 plots the efective area as a function of the F-Factor. For three packing elements, a distributor of drip-point density 117 points/m^2 was employed and the error of ± 20 % in evaluating the effective area (table 4.2, section 2, chapter II) was used in plotting the error bars. For two packing elements, a drip-point density 527 points/m^2 was employed and the value of ± 26 % (table 4.2, section 2, chapter II) was used in plotting the error bars.

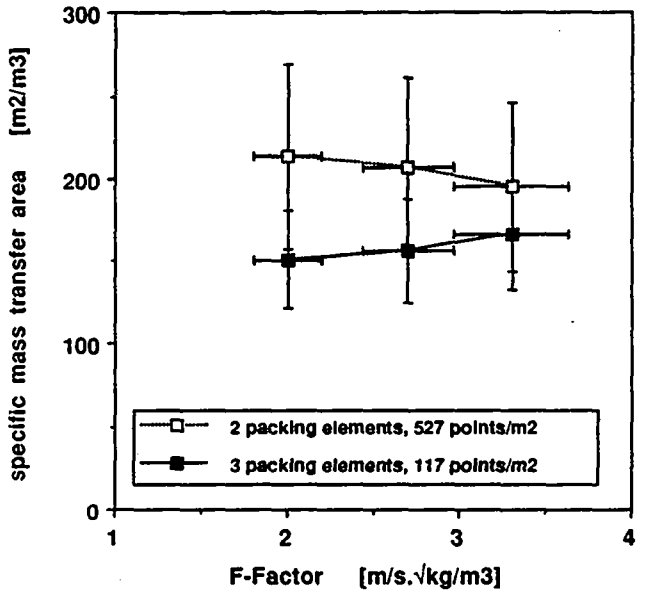

Figure 4.12 The influence of the packing height with a specific liquid load of 19.8 m^3/m^2h (MELLAPAK 125.Y).

It is interesting to note that increasing the F-Factor reduces the difference between the values of effective areas obtained with different heights.

Therefore, channeling effects are reduced with increasing specific liquid loads and F-Factors. The detected channeling is actually small and is also partly due to the wall of the glass column, which was wavy.

4 Conclusions

Effective mass transfer areas of the SULZER structured packing MELLAPAK 250.Y, 125.Y and 500.Y were measured in a pilot column with 295 mm internal diameter and a packing height of 420 mm. The fast pseudo-first order reaction of CO_2 with NaOH was used. All parameters which influence the absorption rate were determined simultaneously with a wetted wall column (chapter III), rather than using correlations from other sources for their estimation.

All three types of MELLAPAK studied can provide an effective mass transfer area higher than the geometric area defined by the packing surface up to a factor of 2, depending on the liquid and gas flows and on the geometric area of the packing. Increasing the geometric area of the packing increases the effective mass transfer area, although the ratio of the specific mass transfer area to the specific geometric area is reduced.

When the specific geometric area of the packing increases by reducing the corrugation height of a MELLAPAK sheet, the available space between the sheets reduces. The possibility of formation of liquid drops and waves at the liquid interface is smaller, thus reducing the creation of an extra area in packings with high specific geometric area. The effective mass transfer area thus tends to be limited to the film over the packing and the corresponding wetted area.

The influence of the specific liquid load on the effective area values is the same for all packings. A general correlation for the ratio of the effective area to the geometric area is proposed in terms of a liquid Reynolds number with all measured MELLAPAK types. This general correlation (equation (4.17)) was able to cover all results as shown in the figure 4.7, in section 3.4. For MELLAPAK 500.Y at low F-Factors, far from full capacity, the equation (4.15) from section 3.2 is possibly more accurate. The F-Factor has generally little influence on effective area values, except for 500.Y.

Experiments with 25 mm ceramic rings showed that the obtained results in this work tend to be higher, but not significantly, than those given by the literature. For this packing, this work has shown that the effective area is not only influenced by the specific liquid load, but also by the F-Factor. The data in the literature could actually have been influenced by very low F-Factors, low liquid loads and a high ratio of packing height to column diameter. These variables consistently reduce the measured values of effective area.

Higher packing height produces lower mass transfer area values. The lower the liquid load and the F-Factor, the more important is the influence of the packing height. The experiments confirmed the unlikelihood of having measured dead areas.

Therefore, both sets of experiments add credibility to the fact that for MELLAPAK the ratio of the effective area to the geometric area under certain conditions can be as high as 2.

The reduction of 78 % of the drip point density had no effect on the effective area of MELLAPAK 125.Y. Nevertheless, the drip point density of 117 points/m^2 is in the upper limit of commercial liquid distributor.

This work was presented at the ACHEMA 1991 (International Meeting on Chemical Engineering and Biotechnology) in Frankfurt, Germany.

ACKNOWLEDGEMENT FOR CHAPTER IV

The measurements presented in this chapter had the important contribution of Alberto Menendez Bangerter. Together with Alberto, it was possible to accomplish an ambitious and extensive experimental plan. The data presented in sections 3.1 to 3.3 was used by Alberto to write the diploma work for obtaining his degree in chemical engineering (MENENDEZ BANGERTER (1990)). His report won a prize for the best diploma work in chemical engineering at the EPFL in 1991. I thank Alberto for his important contribution and friendship.

NOMENCLATURE FOR CHAPTER IV

a	[m^2/m^3]	specific area
A	[m^2]	area
B	[m^3/m^2h]	specific liquid load (equation (1.3))
c	[mol/m^3]	carbonate or CO_2 concentration in the solution
C	[-]	constant defined in the equation (4.21)
d	[m]	diameter
D	[m^2/s]	diffusivity
F-Factor	[$m/s.\sqrt{kg/m^3}$]	equation (1.1)
G	[mol/s]	gas flowrate
h	[m]	packing height
k_G	[m/s]	gas phase mass transfer coefficient
K_{OH}	[1/s]	pseudo-first order reaction constant rate
L	[m^3/s]	liquid flowrate
M	[g/mol]	molecular weight
n	[$mol/m^2.s$]	specific absorption rate
N	[mol/s]	absorption rate
p	[mmHg] [atm]	pressure
T	[K]	temperature
w	[m/s]	superficial velocity
$\bar{x}$		average of a set (section 6.1, chapter II)
y	[mol/mol]	gas-phase mol fraction
z	[m]	coordinate
μ	[kg/ms]	viscosity
ρ	[kg/m^3]	density
σ	[-]	standard deviation of a set (equation (2.11), section 6.1, chapter II)
Ψ	[$mol/m^3.atm$]	as defined by equation (3.1)
ϕ	[mol/m^2s]	as defined by equation (3.11)

Dimensionless Numbers

Re	[-]	Reynolds
Sc	[-]	Schmidt
Sh	[-]	Sherwood

Subscripts

b	bulk
c	column
CO_2	carbon dioxide
d	dead area
e	effective
G	gas
h	hydraulic
i	interface
L	liquid
m	logarithmic average
OH	ion hydroxide
p	packing
r	real
α	begin - in
ω	end - out

Superscript

*	equilibrium

REFERENCES FOR CHAPTER IV

BORNHUTTER, K. and A. MERSMANN (1991). "Stoffübertragung mit modernen Füllkörpern grosser Abmessungen". Chem.Ing.Tech. 63(2), 132-133.

BRAVO, J.L. and J.R. FAIR (1982). "Generalized correlation for mass transfer in packed distillation columns". Ind.Eng.Chem.Process Des.Dev. 21, 162-170.

DANCKWERTS, P.V. and M.M. SHARMA (1966). "The absorption of carbon dioxide into solutions of alkalis and amines (with some notes on hydrogen sulphide and carbonyl sulphide)". The Chemical Engineer 44, CE244-CE280.

DHARWADKAR, S.W. and S.B. SAWANT (1985). "Mass transfer and hydrodynamic characteristics of tower packings larger than 0.025 m nominal size". The Chemical Engineering J. 31, 15-21.

ECKERT, J.S.; FOOTE, E.H. and R.L. HUNTINGTON (1958). "Pall rings - new type of tower packing". Chem.Eng. Progress 54(1), 70-75.

FAIR, J.R. and J.L. BRAVO (1990). "Distillation columns containing structured packing". Chem.Eng.Progress 86, 19-29.

FAIR, J.R. and J.L. BRAVO (1987). "Prediction of mass transfer efficiencies and pressure drop for structured tower packings in vapor/liquid service". I.Chem.E.Symp.Ser. 104, A183-A201.

HüTTINGER, K.J. and F. BAUER (1982). "Benetzung und Stoffaustausch in Filmkolonnen". Chem.Ing.Tech. 54(5), 449-460.

KOLEV, N. (1973). "Wirksame Austauschfläche von Füllkörperschüttungen". Verfahrenstechnik 7(3), 71-75.

LINEK, V.; PETRICEK, P.; BENES, P. and R. BRAUN (1984). "Effective interfacial area and liquid side mass transfer coefficients in absorption columns packed with hydrophilised and untreated plastic packings". Chem.Eng.Res.Des. 62(1), 13-21.

MEIER, W., STOECKER, W.D. and B. WEINSTEIN (1977). "Performance of a new, high efficiency packing". Chem.Eng.Progress 73(11), 71-77.

MENENDEZ BANGERTER, A. (1990). "Mesure de l'aire de transfert de masse du garnissage Mellapak-Sulzer". Lausanne: Travail de diplôme EPFL.

MOHUNTA, D.M.; VAIDYANATHAN, A.S. and G.S. LADDHA (1969). "Effective interfacial areas in packed columns". Indian Chemical Engineer April, 39-42.

NORMAN, W.S. (1974). "Effective interfacial area and liquid side mass transfer coefficients in a packed column". Chem.Eng.Sci. 29(8), 1844.

ONDA, K.; TAKEUCHI, H. and Y. OKUMOTO (1967). "Effect of packing materials on the wetted surface area" (in japanese). J.Chem.Eng.Japan 31, 126-134.

PERRY, D.; NUTTER, D.E. and A. HALE (1990). "Liquid distribution for optimum packing performance". Chem.Eng.Progress January, 30-35.

PURANIK, S.S. and A. VOGELPOHL (1974). "Effective interfacial area in irrigated packed columns". Chem.Eng.Sci. 29, 501-507.

SAHAY, B.N. and M.M. SHARMA (1973). "Effective interfacial area and liquid and gas side mass transfer coefficients in a packed column". Chem.Eng.Sci. 28, 41-47.

SCHULTES, M. (1990). "Einfluss der Phasengrenzfläche auf die Stoffübertragung in Füllkörperkolonnen". Düsseldorf: VDI-Verlag.

SHARMA, M.M. and P.V. DANCKWERTS (1970). "Chemical methods of measuring interfacial area and mass transfer coefficients in two-fluid systems". British Chemical Engineering 15(4), 522-528.

SHI, M.G. and A. MERSMANN (1985). "Effective interfacial area in packed columns". Ger.Chem.Eng. 8, 87-9-.

SPIEGEL, L. and W. MEIER (1987). "Correlations of the performance characteristics of the various Mellapak types". I.Chem.E.Symposium Series 104, A203-A215.

STIKKELMAN, R.; de GRAAUW, J.; OLUJIC, Z.; TEEUW, H. and H. WESSELINGH (1989). "A study of gas and liquid distributions in structured packings". Chem.Eng.Technol. 12, 445-449.

TEMPLEMAN, J.J. and K.E.PORTER (1965). "Experimental determination of wall flow in packed columns". Chem.Eng.Sci. 20, 1139-1140.

VAZQUEZ, G.; ANTORRENA, G.; CHENLO, F. and F. PALEO (1989). "Effect of viscosity on interfacial area in the absorption of CO_2 by carbonate/bicarbonate systems". Chem.Biochem.Eng.Q. 3(1-2), 7-12.

VFF-FABRIKEN GmbH (1986).
Catalog: "Berechnungen". Catalog number: 0-T-2.1 and 0-T-2.2.

VIDWANS, A.D. and M.M. SHARMA (1967). "Gas-side mass transfer coefficient in packed columns" Chem.Eng.Sci. 22, 673-684.

YOSHIDA, F. and T. KOYANAGI (1958). "Liquid phase mass transfer rates and effective interfacial area in packed absorption columns". Ind.Eng.Chemistry 50, 365-374.

YOSHIDA, F. and Y. MIURA (1963). "Effective interfacial area in packed columns for absorption with chemical reaction". AIChE J. 9(3), 331-337.

1 Problem analysis

The volumetric mass transfer coefficient $k_L a$ is used for determination of the packed column height using the HTU-NTU method (section 1.3, chapter I). Knowledge of the value of $k_L a$ is particularly useful for selective absorption, when the mass transfer of different compounds is controlled either by the gas phase or by the liquid phase resistance. An industrial example is the absorption of H_2S (gas side controlled) and CO_2 (liquid side controlled) into MDEA, discussed by Bomio et al. (1988). Design for selective absorption is complex since an insufficient packing height may result in insufficient absorption of the gas side controlled components, whereas too great a packing height may result in a poor selectivity.

A literature review is available in section 2.2, chapter I. For structured packings, execpt for the measurements of Bereiter (1975), no other measurements seem to be reported. In the literature, the product $k_L a$ is generally termed as the liquid phase mass transfer coefficient. In this work, the volumetric mass transfer coefficient $k_L a$ of three different types of the SULZER structured packing MELLAPAK (250.Y, 500.Y and 125.Y) were measured. The liquid phase mass transfer coefficient itself, k_L, will be the subject of chapter VI.

1.1 The system O_2-water-air for measuring $k_L a$

Since it is difficult with the current technology to measure concentrations at the gas-liquid phase interface, bulk concentrations, which lead to values of $k_{OL} a$, are measured. Consequently, it is not possible, in principle, to evaluate directly either the liquid phase height of a transfer unit HTUL (section 1.3, chapter I) or the actual product $k_L a$.

A relationship between k_{OL} and k_L was given in equation (1.6), section 1.2.1, chapter I. Hence:

$$\frac{1}{k_{OL} a} = \frac{1}{k_L a} + \frac{1}{k_G \cdot a \cdot H} \qquad (5.1)$$

When the gas is not very soluble in the liquid, ie. for a large value of the Henry constant - H -, the influence of $k_G a$ becomes negligible. Here, a judicious choice of sparingly soluble gases in water overcomes the difficulty of determining $k_L a$, since $k_{OL} a$ approaches the value of $k_L a$. Table 5.1, overleaf, gives values for the Henry constant for dissolved carbon dioxide, oxygen, nitrogen and hydrogen in water.

Carbon dioxide is frequently used for $k_L a$ experiments (section 2.2.1, chapter I). The determination of concentrations of dissolved CO_2 in water is relatively straightforward. However, Sherwood and Holloway (1940), one of the first to carry out $k_L a$ experiments, point out that "experimental studies of the liquid-film resistance should cover the entire economical ranges of L and G for all industrially important gases, which range in solubility from HCl to CO_2, and at the same time to subordinate the gas-film resistance. These facts make it necessary to employ solute gases of even less solubility than CO_2". However, in the literature, this system is used frequently for measuring $k_L a$ in packed columns (table 1.5, chapter I).

Table 5.1 The Henry constant for selected gases.

Gases	$H * 10^{-4}$ [atm] Temperature [°C] 10	20	30	Reference
CO_2	0.106	0.143	0.186	Incropera et al.(1981)
O_2	3.27	4.01	4.75	Perry (1984)
H_2	6.36	6.83	7.29	Perry (1984)
N_2	6.68	8.04	9.24	Perry (1984)

For the determination of dissolved oxygen in water, the use of dissolved oxygen electrodes, also known as pO_2 probes, is efficient for rapid on-line measurements (section 5.3, chapter II). The solubility of CO_2 in water is about 25 to 30 that of O_2 (table 5.1). Thus, the system O_2-water-air is adequate for obtaining accurate experimental data for k_La determination.

If straightforward techniques for measuring levels of dissolved H_2 or N_2 in water existed, then these gases would be used, since they are even less soluble in water.

1.2 Calculation methodology

HTU_{OL} and $k_{OL}a$ may be obtained from equations (1.22) and (1.23) (section 1.3, chapter I), since for sparingly soluble gases, k_La and $k_{OL}a$, as HTU_L and HTU_{OL}, have almost the same value. Hence:

$$k_La = \frac{B}{h} \cdot NTU_{OL} \cdot \frac{1}{3600} \qquad (5.2)$$

The number of overall liquid phase transfer units, NTU_{OL}, can be evaluated using equation (1.24), section 1.3, chapter I. As the concentrations are so small (dilute systems), this equation may be simplified to:

$$NTU_{OL} = \int_{x_\alpha}^{x_\omega} \frac{dx}{(x^* - x)} \qquad (5.3)$$

The equilibrium line is straight, assuming that temperature and pressure stay constant throughout the column with no change in the oxygen solubility. In the course of this work, no change in the liquid temperature was detected and the experiments were carried out with a packed column height of 420 mm, over which a negligible pressure drop would be expected. Hence:

$$y = m \cdot x^* \qquad (5.4)$$

A straight operating line obtained with a mass balance around the bottom of the column is given by:

$$y = y_\alpha + \frac{L}{G} \cdot (x - x_\omega) \qquad (5.5)$$

The notation has the following meaning: at the top of the column (z=0) are x_α and y_ω and at the bottom (z=h) are x_ω and y_α.

Substituting both equations (5.4) and (5.5) for x^* in equation (5.3), and integrating, yields:

$$NTU_{oL} = \frac{1}{\left[1 - \frac{L}{mG}\right]} \cdot \ln \left(\left[1 - \frac{L}{mG}\right] \cdot \frac{(x_\alpha - x^*_\omega)}{(x_\omega - x^*_\omega)} + \frac{L}{mG} \right) \qquad (5.6)$$

Due to a very low solubility: $\frac{L}{mG} \rightarrow 0$ and: $x^*_\alpha \cong x^*_\omega$.

The error in the above assumption, that the equilibrium concentrations at the column inlet and outlet are equal, is negligible. For O_2 dissolved in water at 20°C and 1 atm, $m = H$ (at 1 atm) $= 4.01 \times 10^4$ (Table 5.1). For the extreme case with a high liquid load of 75 m^3/m^2h ($\cong$ 285 kmol/h) and a small gas flow of 100 m^3/h ($\cong$ 4.08 kmol/h), then:

$$\frac{L}{mG} = 1.74\ 10^{-3} \qquad \text{and} \qquad \left[1 - \frac{L}{mG}\right] = 0.998$$

There are important consequences. The establishment of a mass balance becomes very difficult, since it is difficult to detect variations of the O_2 concentration in the gas phase. The O_2 mole fraction in the gas flow is constant along the column and equals the concentration of O_2 in the inlet air stream, which is saturated with water vapor. Consequently, the influence of axial dispersion in the gas phase is negligible.

Equation (5.6) may thus be simplified to:

$$NTU_{oL} = \ln \left(\frac{(x_\alpha - x^*)}{(x_\omega - x^*)} \right) \qquad (5.7)$$

and equation (5.2) becomes:

$$k_La = \frac{B}{h} \cdot \ln \left(\frac{(x_\alpha - x^*)}{(x_\omega - x^*)} \right) \cdot \frac{1}{3600} \qquad (5.8)$$

Equation (5.8) is of great practical value since with it there is no need to measure absolute concentration values. It is only necessary to determine the ratio, at the column inlet to the column outlet, of the difference between the value measured under operating conditions and the value under equilibrium conditions. Moreover, this difference may be expressed in any units. The experiments may be carried out easily and accurately, and conveniently with pO_2-probes (section 5.3, chapter II).

The error in the determination of $k_L a$ from an error propagation study with equation (5.2) is given by:

$$\frac{\Delta k_L a}{k_L a} = \frac{\Delta B}{B} + \frac{\Delta NTU_{oL}}{NTU_{oL}} + \frac{\Delta h}{h} \qquad (5.9)$$

Hence,

$$\frac{\Delta k_L a}{k_L a} = \left|\frac{\Delta B}{B}\right| + \left| \frac{1}{\ln\left[\frac{(x - x^*)_\omega}{(x - x^*)_\alpha}\right]} \cdot \left[\frac{\Delta(\Delta x_\omega)}{\Delta x_\omega} + \frac{\Delta(\Delta x_\alpha)}{\Delta x_\alpha}\right] \right| + \left|\frac{\Delta h}{h}\right| \qquad (5.10)$$

The following conclusions may be drawn from equation (5.10):
- the liquid flow rate must be kept constant and be measured precisely.
- keeping the inlet concentration high reduces the error.
- the error increases with higher $k_L a$, as Δx_α becomes smaller.

The liquid phase does not necessarily have a plug flow in the packing. The undesirable effect of axial dispersion of the liquid phase is specially important for irregular packings. Delaloye (1986) uses a model proposed by von Stockar and Cevey (1984) for the Peclet number to correct their $k_L a$ data. Both of these works carried out experiments with 25 mm Raschig rings. The reduction of the $k_L a$ values of Delaloye (1986) was of the order of 10 %. Linek et al. (1984) also correct their data, and claim that there can be a reduction of up to 30 % of the $k_L a$ values with 50 mm plastic Pall rings at low specific liquid loads. However, the authors do admit that the "literature gives rather discrepant data on the liquid phase Peclet number" for irregular packings. Other than these cases, no importance seems to have been accorded in the literature to the effect of axial dispersion on the $k_L a$ data of irregular packings (section 2.2.1, chapter I).

For structured packings, however, the effect of axial dispersion would be expected to be much less important, since the clearly defined channels avoid this undesirable effect. Furthermore published data for the liquid phase Peclet number for MELLAPAK are not available. Consequently, in the present work the $k_L a$ data have not been corrected for axial dispersion.

Linek et al. (1984), using irregular packings, find almost identical $k_L a$ values, regardless of whether they were determined from absorption or desorption experiments. This should also be the case for structured packings, particularly due to their defined flow channels and consequently lack of stagnation zones. Therefore, since desorption experiments are simpler and cheaper, due to the reduced loss of the transfered solute, this method has been used in this work.

2 Materials and methods

Experiments were carried out in the pilot plant presented in chapter II, and whose main column had an internal diameter of 295 mm. The packing height was of two elements (420 mm) for all MELLAPAK types. The broad range of F-Factors (equation (1.1)) and specific liquid loads (equation (1.3)) for the experiments and also the need for a column close to industrial size justified the need of such a complex apparatus (as discussed in chapter I). The procedure to pack the column with the structured and irregular packings is given in the appendix B. Chapter II gives the background for conducting the experiments. Capacity is defined in section 1.3, chapter I. The definitions of "run", "point", "set" and "data point" are to be found at the end of section 6.1, chapter II.

In order to evaluate $k_L a$, the following values had to be measured: the liquid flow rate and the bulk concentrations of dissolved O_2 at the inlet and outlet of the column during equilibrium conditions and desorption experiments. To determine the F-Factor, the gas flow rate, atmospheric pressure, gas pressure and temperature at column inlet were measured. In appendices L to N, the gas and liquid flow rates for each point are given together with the results. The inlet gas and liquid temperature were maintained at 22°C, as for the mass transfer area experiments.

The procedure for the experiments is outlined in figure 5.1, and the steps are described in detail in appendix D. The steps which have the word "Execute" were executed with the computer program KLA4.PGM (section 5.3.3, chapter II). Required material and manpower is given at the end of appendix D. Risk analysis is given in appendix E. The procedure has 4 main parts: calibration of the pO_2 probes, data acquisition with the system in equilibrium, data acquisition during desorption experiments and measurement of the liquid flow.

The pO_2 probes were calibrated before each run (section 5.3.2, chapter II) and then were installed in the pilot plant. The liquid sampling uptake was controlled so that the pO_2-probe response was not sensitive to the sample flow (section 5.3.1, chapter II).

With the small circuit of the solution, water was continuously circulated in the main column COL1, until equilibrium conditions with the air flowing in the main column were established. After a minimum period of 15 minutes to ensure steady state, at least 15 data points at minute intervals were taken. The average of these data points gave the equilibrium concentration value for probes C11 and C12.

During the desorption experiments, water previously saturated with O_2 in reactor R11 came into contact with air from the laboratory in the main column COL1. After a minimum period of 5 minutes to ensure steady state conditions of the flow in the column, the concentrations of dissolved O_2 at the column inlet and outlet were measured. Data points were stored at minute intervals. At least 15 data points were taken. Each of these values, together with the average value for equilibrium concentration, gave a $k_L a$ value (equation (5.8)). The average of these values gave the $k_L a$ of a point. Bubbling O_2 into reactor R11 during the experiments had the important advantage of keeping the O_2 inlet concentration in the column high, which reduced experimental errors (equation (5.10)), as well as cost and saturation time.

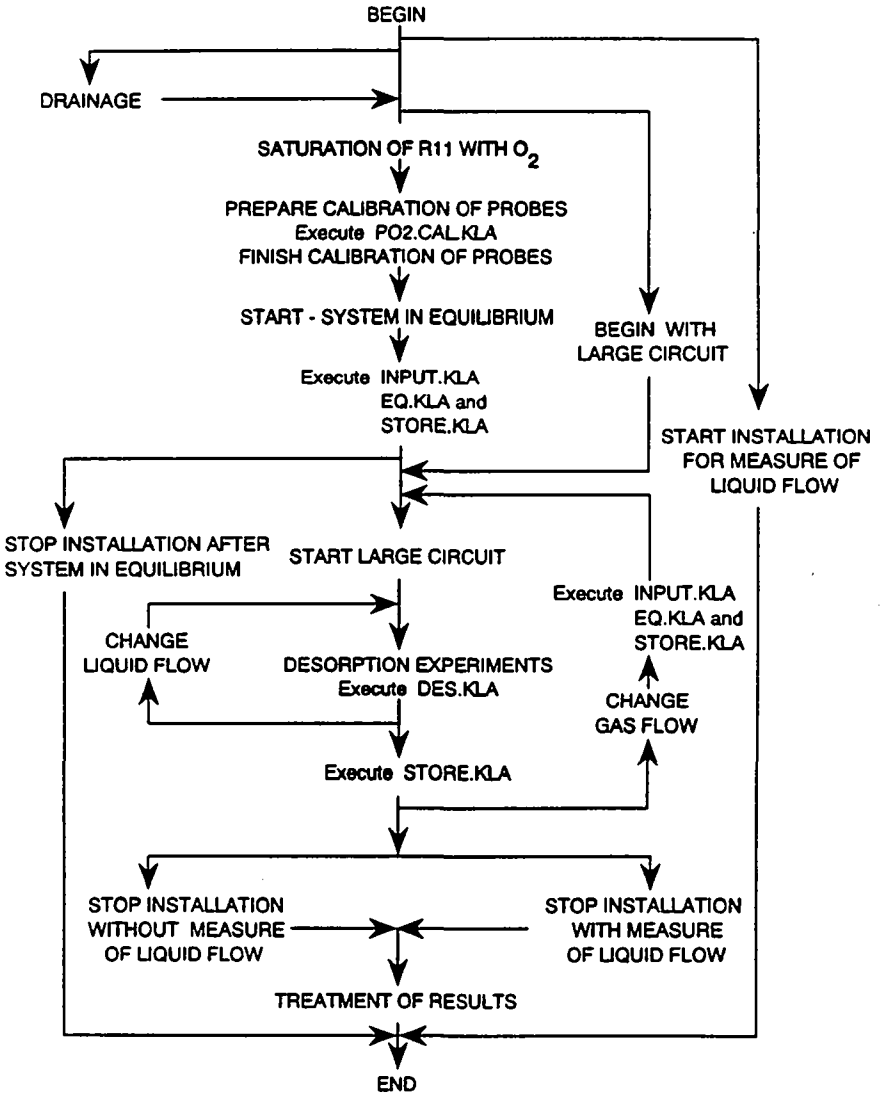

Figure 5.1 Flowchart of the procedure for the $k_L a$ experiments.

Measurements of the liquid flow were executed as described in section 5.1.1, chapter II. These measurements were carried out when the concentration of O_2 in the reactor R11 was close to equilibrium conditions.

Initial runs were executed in order to develop the procedure for fine tuning of the experiments. The reported experiments began with MELLAPAK 250.Y (runs 10 to 19), followed by 500.Y (runs 20 to 28) and 125.Y (runs 29 to 35).

Section 5, chapter II, described all the necessary instrumentation used during the k_La experiments. Variations in the measured O_2 concentration with the column operating under equilibrium conditions were less than 5 %. A negligible pressure drop for engineering purposes, small differences between the air and liquid temperature, together with fluctuations of these values, may account for such discrepancies. An estimate of the precision of experimental variables is presented in table 5.2.

Table 5.2 Estimation of experimental precision.

Parameter	Error	Remarks
B	$< \pm$ 1 %	see section 5.1.1, chapter II
F-Factor	$< \pm$ 10 %	see section 5.1.2, chapter II
$\frac{\Delta x}{x}$	$\pm$ 5 %	
h	$< \pm$ 1 %	

Despite the fact that a precise calculation of the error of the k_La value is not possible, an estimate using equation (5.10) can be made. Assuming that:

$x_\alpha = 0.7$; $x_\omega = 0.3$; $x^*_\alpha = x^*_\omega = 0.2$; and considering $\Delta(\Delta x) = 0.005$

Then: $\frac{\Delta k_La}{k_La} = 5.7$ %

Therefore, the k_La values are considered to have been measured within a precision of less than 6 %, which is acceptable for engineering design.

Other sources of experimental errors were due to the response time of the probes, the fact that the concentration of dissolved O_2 inside the distributor may not have been uniform and that, in practice, the runs were in a "pseudo steady-state" (section 1, chapter II). All these errors are considered to have been negligible.

Confidence in the results for all MELLAPAK types stems from the reproducibility of the measured values of points with the same liquid and gas flowrates, and the net difference between values from different gas and liquid flowrates. Last but not least, during a run, if a specific liquid load were repeated, the k_La values would be equal or very close to the values one would expect. The table 5.3 gives the experimental error defined as the average ratio of the standard deviation of a set divided by its mean (equation (2.11) in section 6.1, chapter II).

Table 5.3 Estimate in evaluating the k_La.

MELLAPAK	Error	Remarks
125.Y	2.7 %	
250.Y	1.6 %	
500.Y	11.3 %	for all sets
	3.0 %	sets 2.3, 2.6, 2.9 and 2.11 were not included

The points in the sets 2.3, 2.6, 2.9 and 2.11 (all for MELLAPAK 500.Y) were measured close to 100 % capacity according to the program SULPAK from SULZER BROTHERS LIMITED (section 1.4, chapter I). Local flooding at the sleeves was observed during the measurements of the points of sets 2.9 and 2.11, although the column was not flooded and the pressure drop stayed constant during the runs. Table 5.4 shows for MELLAPAK 500.Y that closer to 100 % capacity, the ratio of the standard deviation of a set divided by its mean increases.

Table 5.4 The influence of capacity on the experimental uncertainty.

Set	% capacity	Error [%]	B [m^3/m^2h]	F-Factor
2.3	88	16.2	13.41	1.9
2.6	92	19.0	17.36	1.9
2.11	95	37.5	21.29	1.9
2.09	97	39.3	42.6	1.4

This instability may be related to large scale liquid maldistribution caused by sleeves. In the work of Stikkelman et al. (1989), partial flooding, starting at the bottom sleeves of the elements, was observed. The liquid is prevented from flowing through the sleeves. To prove this effect of sleeves in maldistribution, they removed the standard sleeves and wrapped the packing with tape to prevent any horizontal migration along the wall. An improved liquid distribution was obtained.

In the glass column used in this work, the internal walls were uneven (section 4, chapter II). This column might therefore also give a certain contribution to maldistribution. Mangers and Ponter (1980.b) improved performance of a glass column wall with horizontal circumferential polymer stripes, which increased wettability. However, the increase was considered not great enough to be of industrial relevance.

The order in which the specific liquid load was varied did not have an influence on the k_La data for either MELLAPAK 500.Y or 125.Y. Although not verified, such effects would not be expected to be present with MELLAPAK 250.Y. However, Mangers and Ponter (1980.a) observed hysteresis effects with glass Raschig rings when the liquid flowrate was decreased and increased incrementally. Their explanation for this phenomenon is that a decreasing flowrate sequence induces a larger wetted area.

3 Results and discussions

In this section, measurements of k_La are presented and their significance discussed. Capacity is defined in section 1.3, chapter I. Definitions of run, point and set are to be found at the end of section 6.1, chapter II. Error bars are not shown in the figures for clarity. The k_La values are determined with an error of less than ± 6 % (section 2), the specific liquid loads with an error of less than ± 1 % and the F-Factor with an error of less than ± 10 % (table 5.2, section 2).

3.1 The k_La for MELLAPAK 250.Y

The table in appendix L presents the results for runs 10 to 19. Figure 5.2 plots all k_La sets as a function of the specific liquid load.

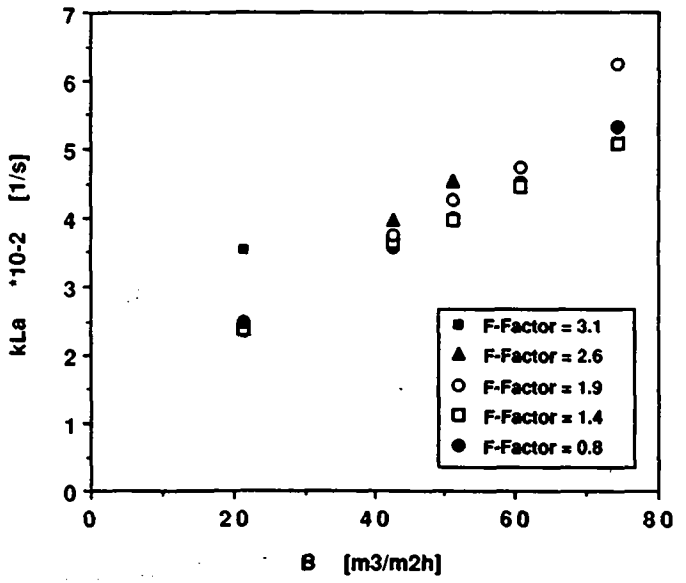

Figure 5.2 k_La versus specific liquid load for MELLAPAK 250.Y.

For MELLAPAK 250.Y, k_La increases with the specific liquid load. Figure 5.3 illustrates k_La as a function of the F-Factor.

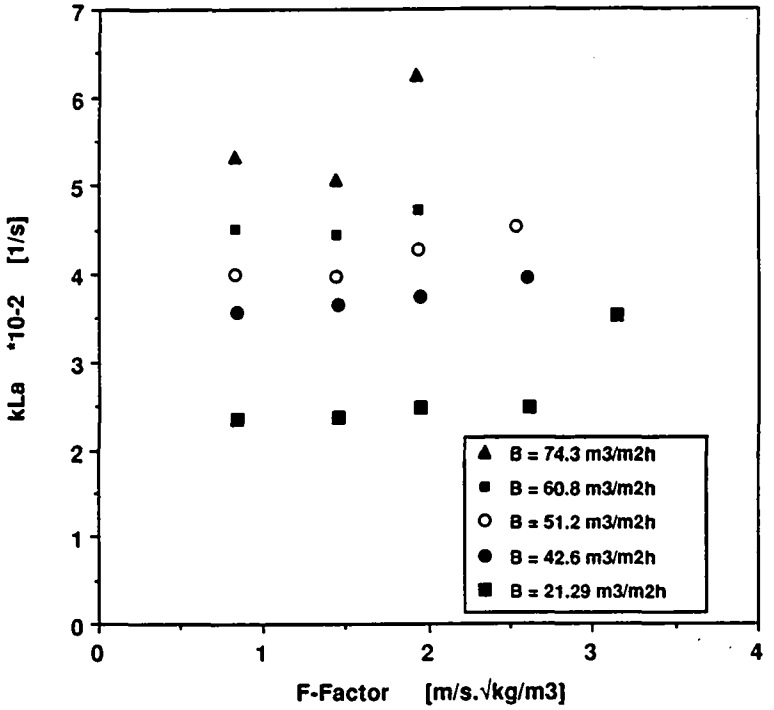

Figure 5.3 $k_L a$ versus F-Factor for MELLAPAK 250.Y.

The $k_L a$ values change little with respect to the F-Factor, presenting higher values only near and above 100 % capacity. Consequently, an empirical correlation for $k_L a$ as a function of the specific liquid load far from 100 % capacity may be proposed. The correlation was obtained by least squares regression, using mean $k_L a$ values from sets with the lowest F-Factor of 0.8 with a specific liquid load up to 60.8 m^3/m^2h. Hence:

$$k_L a = 3.58 \cdot 10^{-3} \cdot B^{0.615} \qquad (5.11)$$

For design purposes, the important parameter is HTUL. Substituting equation (5.11) into equation (1.19) (section 1.3, chapter I):

$$HTU_L = 77.7 \cdot 10^{-3} \cdot B^{0.385} \qquad (5.12)$$

Figure 5.4 compares measured values with those predicted by the correlation (5.12). The agreement is particularly good for F-Factor of 1.4. The correlation predicts slightly conservative values for F-Factor of 1.9 and those above 100 % capacity. Therefore, near 100 % capacity, the design of the packing height is on the safe side with correlations (5.11) and (5.12).

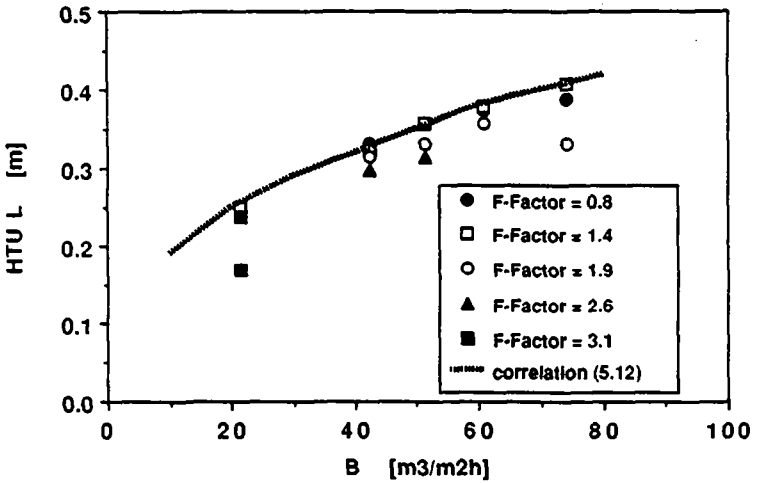

Figure 5.4 HTU_L for MELLAPAK 250.Y with a proposed correlation.

3.2 The $k_L a$ for MELLAPAK 500.Y

The table in appendix M presents the results for runs 20 to 28. Figure 5.5 plots all $k_L a$ sets as a function of the specific liquid load.

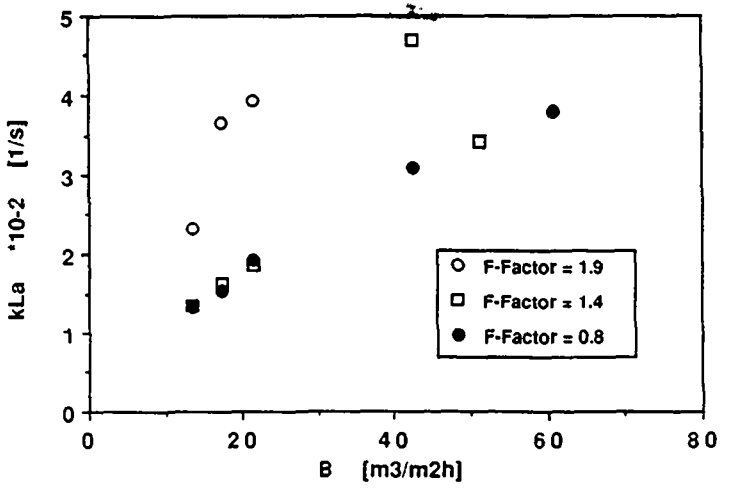

Figure 5.5 $k_L a$ versus specific liquid load for MELLAPAK 500.Y.

The $k_L a$ for MELLAPAK 500.Y increases with the specific liquid load. Figure 5.6 illustrates $k_L a$ as a function of the F-Factor.

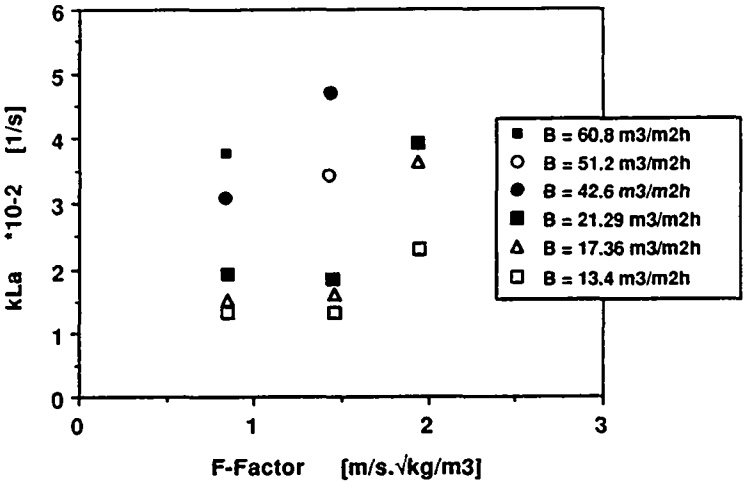

Figure 5.6 $k_L a$ versus F-Factor for MELLAPAK 500.Y.

Far from 100 % capacity, $k_L a$ varies little with the F-Factor. It was observed during the runs that under such conditions, several packing sheets near the wall were actually dry. The surface of the packing was not being totally used by the liquid. The small channels of 500.Y could have actually separated the liquid from the gas.

However, when the F-Factor influences the $k_L a$, the latter increases very rapidly. The experimental values for the $k_L a$ also fluctuate significantly (table 5.4, section 2). It may be that for a given specific liquid load, a higher gas flow not only will increase the turbulence at the phase interface, increasing the liquid renewal rate at the interface, but will also spread the liquid over the packing, increasing the specific area for mass transfer (figure 4.3, section 3.2, chapter IV) and the liquid phase mass transfer coefficient k_L.

An empirical correlation for $k_L a$ as a function of the specific liquid load far from 100 % capacity is proposed. This correlation was obtained by least squares regression, using mean $k_L a$ values from sets with the lowest F-Factor of 0.8. Hence:

$$k_L a = 2.13 \cdot 10^{-3} \cdot B^{0.706} \qquad (5.13)$$

For design purposes, the important parameter is HTUL. Substituting equation (5.13) into the equation (1.19) (section 1.3, chapter I):

$$HTU_L = 13.0 \cdot 10^{-2} \cdot B^{0.294} \qquad (5.14)$$

Figure 5.7 compares the measured values with those predicted by the correlation (5.14). The agreement is particularly good for F-Factors of 0.8 and 1.4. The sets in table 5.4 (section 2) and the point 21.3 (B=51.2 m^3/m^2h and F-Factor=1.4), which could only be measured once, are not plotted in figure 5.7. Since close to 100 % capacity, $k_L a$ increases steeply with the F-Factor, the $k_L a$ values given by equation (5.13) (or HTUL values given by equation (5.14)) may be useful for a conservative design in this region.

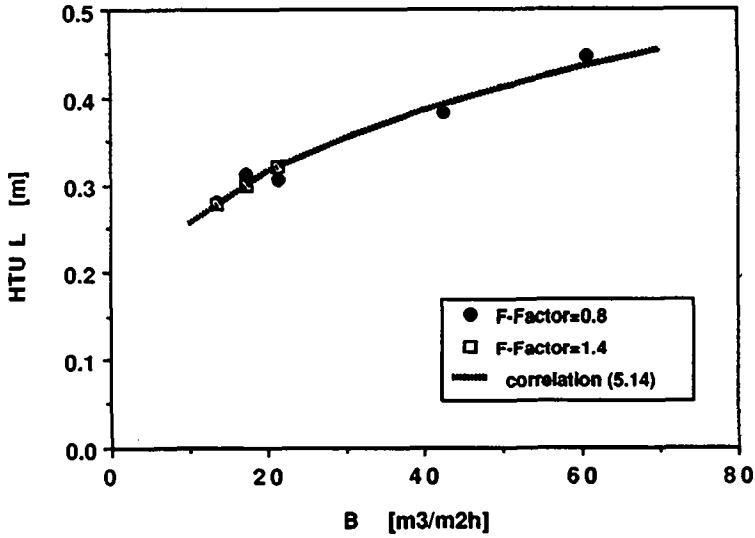

Figure 5.7 HTU_L for MELLAPAK 500.Y with a proposed correlation.

3.3 The $k_L a$ for MELLAPAK 125.Y

The table in appendix N presents the results for runs 29 to 35. Figure 5.8 plots all $k_L a$ sets as a function of the specific liquid load.

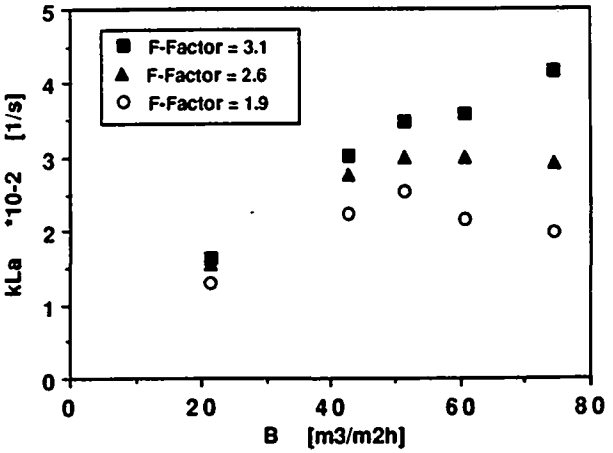

Figure 5.8 k_La versus specific liquid load for MELLAPAK 125.Y.

The k_La does not necessarily increase with the specific liquid load. If the F-Factor is low, k_La may decrease with the specific liquid load, even if the percentage capacity is increasing. The influence of the gas flow on the k_La is depicted in figure 5.9.

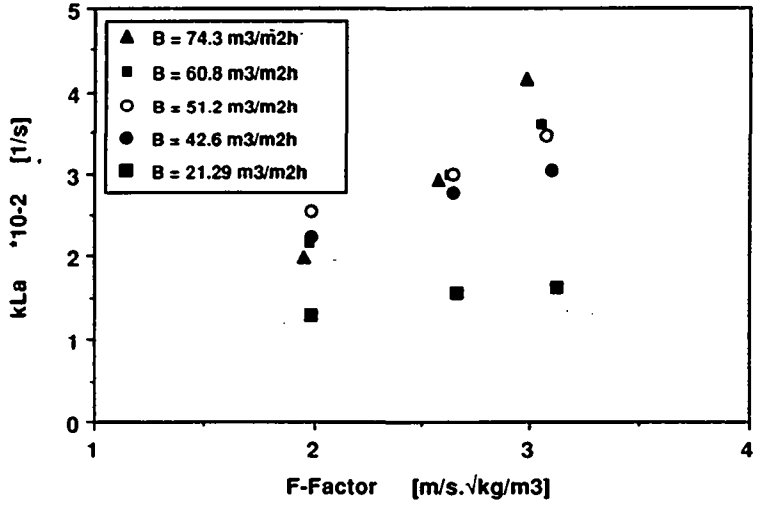

Figure 5.9 k_La versus F-Factor for MELLAPAK 125.Y.

The $k_L a$ values of MELLAPAK 125.Y increase with the F-Factor. Such an increase is small with the specific liquid load of 21.29 m^3/m^2h, when the program SULPAK indicated low values of capacity. Near and above 100 % capacity, the influence of the F-Factor on $k_L a$ is pronounced and may enhance the $k_L a$ values significantly. The program SULPAK indicated that for F-Factor of 2.6 and specific liquid loads above 60.8 m^3/m^2h and for F-Factor of 3.1 and specific liquid loads above 42.6 m^3/m^2h the column was operating at over 100 % capacity, although signs of existence of flooding was not detected and the results were reproducible.

It remains to be verified if the $k_L a$ values for MELLAPAK 125.Y would be different with a higher packed height, since this packing is a low density packing and the experiments were carried out with two packing elements. In section 3.7, chapter IV, it was shown that a higher packing height of MELLAPAK 125.Y reduces the effective area values especially at low specific liquid loads. However, with high specific liquid loads (60.8 m^3/m^2h and 74.3 m^3/m^2h) and an F-Factor of 2.65, the 6 % reduction of the effective area with the packing height was within experimental error. Thus, measured $k_L a$ values at high specific liquid loads may be correct. However, the influence of a higher packing height on the $k_L a$ values at low specific liquid loads may have to be checked. Consequently, more information may be available for interpreting the maximum in figure 5.8, if it is confirmed.

The important design parameter is HTUL, which is plotted in figure 5.10 as a function of the specific liquid load.

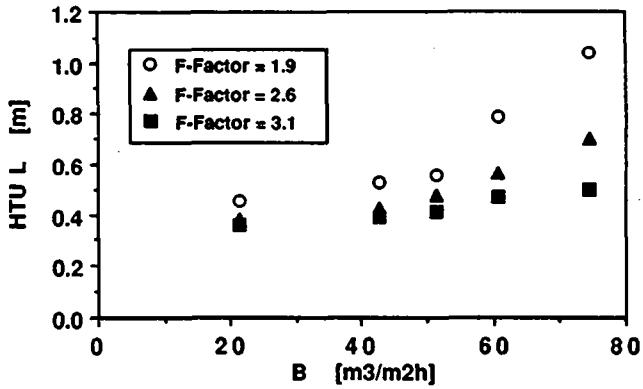

Figure 5.10 HTUL versus specific liquid load for MELLAPAK 125.Y.

For a given F-Factor, in the range which was studied, HTUL values of 125.Y increase with the specific liquid load, which would be expected. At the specific liquid load of 21.29 m^3/m^2h, HTUL is almost independent of the F-Factor. However, HTUL increases slightly with the specific liquid load, if the F-Factor is high, or significantly, if the F-Factor is low.

3.4 Comparison and discussion of k_La of MELLAPAK

Figure 5.11 compares k_La data for MELLAPAK 250.Y, 500.Y and 125.Y at similar specific liquid loads and F-Factors. Data over 100 % capacity are not plotted. For a given specific liquid load, k_La with the highest F-Factor was measured at flow condition above 90 % capacity.

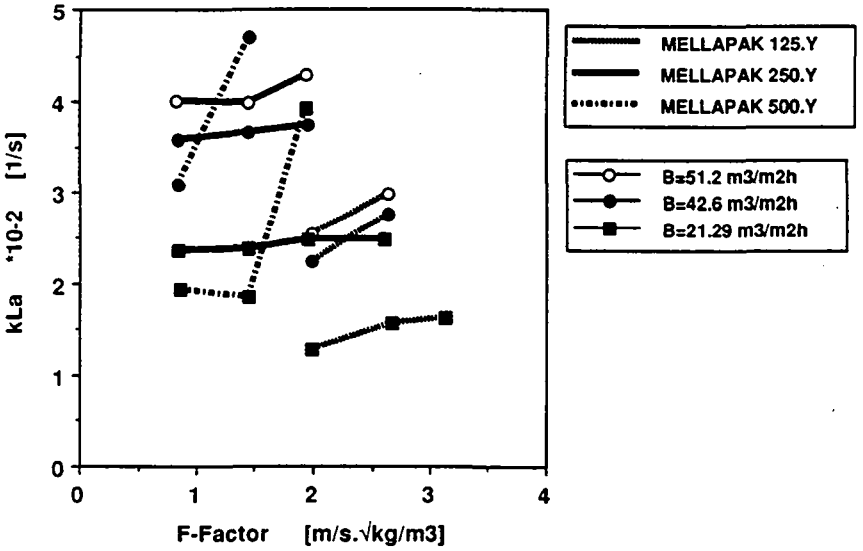

Figure 5.11 k_La values versus F-Factor for all MELLAPAK types.

The k_La values depends primarily on the specific liquid load. The influence of the F-Factor is especially pronounced near 100 % capacity and depends on the packing. The k_La may not necessarily increase with the geometric area of the packing. The influence of each parameter is discussed below.

For the MELLAPAK types studied, in the range of gas and liquid flowrates depicted in figure 5.11, increasing the specific liquid load, there is an increase of k_La values. However, as pointed out in section 3.3, with the F-Factor of 1.9, k_La values of MELLAPAK 125.Y may decrease with the specific liquid load. This may demand further study.

At low capacity, the gas flow may be small to promote turbulence and liquid renewal. Therefore, k_La increase little with the F-Factor. For the same gas and liquid flows, the k_La values of 125.Y are the lowest. MELLAPAK 250.Y present the highest k_La values, even when compared to 500.Y.

An explanation may be that separate courses with minimal pressure drop for the gas and liquid flows may occur in the 500.Y packing. In chapter IV, at low capacity, effective area values of MELLAPAK 500.Y was shown to be lower than the geometric area, indicating that the whole surface area offered by the packing was not used. This was not the case for 250.Y, which presents effective areas higher than the geometric. Although MELLAPAK 250.Y has less specific geometric area, gas and liquid may be better mixed at low capacity. Consequently, a liquid may remain less time attached to the channel walls of the 250.Y packing, through which it flows. This may result in an enhancement of the liquid renewal and, thus, in high k_La values.

The influence of the F-Factor seems to be important the closer to 100 % capacity, especially for 500.Y. The k_La values of 500.Y may increase significantly, due to the greater surface area. Actually, the 500.Y packing presents effective areas which may be less than the geometric area (figure 4.3, chapter IV). It was additionally shown in chapter IV that not only the effective area associated with the 500.Y packing is greater than that associated with the 250.Y and 125.Y packings, but the difference increases with the specific liquid load and F-Factor. Therefore, the effect of high gas flowrates in spreading the liquid over the packing and in creating turbulence at the gas-liquid interface, which enhances liquid renewal and increases k_La, is more pronounced for 500.Y, than for 250.Y and for 125.Y.

The design parameter of the column height is HTUL, which is plotted in figure 5.12. Data over 100 % capacity are not plotted. For a given specific liquid load, HTUL with the highest F-Factor is at flow condition above 90 % capacity.

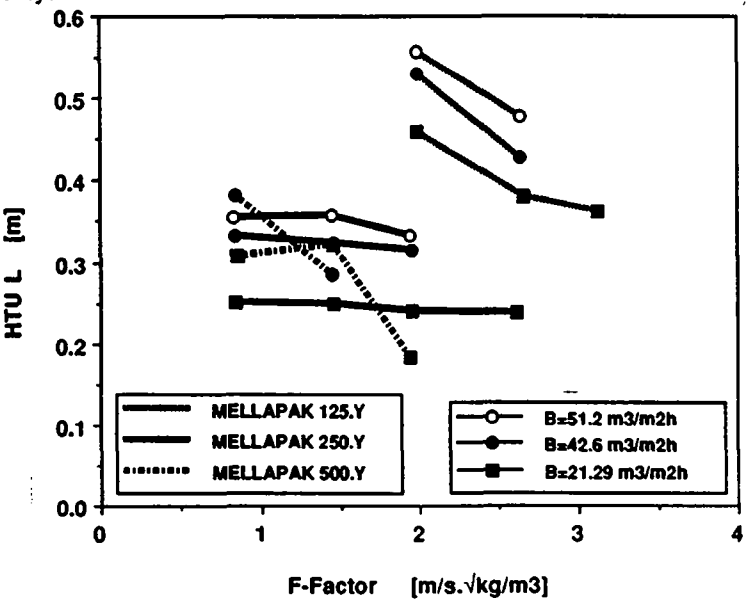

Figure 5.12 HTU_L values versus F-Factor for all MELLAPAK types.

For an absorption separation process that is liquid-side controlled and far from 100 % capacity, MELLAPAK 250.Y offers the lowest HTUL values than the other two types for a given specific liquid load. With a F-Factor of 0.8, MELLAPAK 250.Y has HTUL values about 18 and 13 % lower than 500.Y for specific liquid loads of 21.29 and 42.6 m^3/m^2h respectively. If the column is operating near to 100 % capacity, HTUL values of MELLAPAK 500.Y reduce significantly and may be the smallest. MELLAPAK 125.Y has the highest HTUL values in the range of flows shown in figure 5.12.

The HTUL values for both MELLAPAK 250.Y and 500.Y as a function of the specific liquid load for a F-Factor of 0.8 may be evaluated with the correlations (5.12) and (5.14) respectively. The correlations for evaluating k_La are (5.11) and (5.13) for 250.Y and 500.Y respectively. Since the F-Factor has almost no influence on the HTUL (and k_La) values far from 100 % capacity, these correlations may be used with a negligible error over this range. With MELLAPAK 250.Y operated near 100 % capacity, the design of the packing height using HTUL values given by (5.12) is on the safe side. The equation (5.14) for predicting HTUL values for 500.Y near 100 % capacity result in conservative values. The safety factor implicit therein is, however, even higher than in the correlation for 250.Y, though unquantifiable. No correlation for HTUL of MELLAPAK 125.Y is proposed.

3.5 Comparison with information from the literature

Except for the experimental work of Bereiter (1975) with the SULZER wire gauze packing BX and the HTU correlation proposed by Bonio (1977) with the data from Bereiter, no other experimental or theoretical work with structured packings was found in the literature.

The gas-liquid system used by Bereiter (table 1.5, chapter I) is different from the one used in this work. However, the system is supposed to be liquid-side controlled. Bereiter gives his data in the form of k_L values. The equation used for obtaining his k_L values is identical to equation (5.8) divided by the geometric area. In order to compare his data with the data of the present work, the k_L values from Bereiter were multiplied by the packing geometric area of 486 m^2/m^3 and are plotted in figure 5.13 with k_La values for MELLAPAK 250.Y and 500.Y as given by equations (5.11) and (5.13).

The k_La data from Bereiter is a monotonically increasing function of the specific liquid load and is independent of the gas velocity far from flooding conditions. This corresponds to trends observed in the course of this work for MELLAPAK 250.Y and 500.Y. Bonio (1977), with an equation for the HTUL (equation (1.45)) obtained with the data from Bereiter, proposes a value of 0.22 for the exponent of the liquid flow. This value is similar to the value of 0.294 in equation (5.14) for MELLAPAK 500.Y, which has a similar structure and geometric area.

The k_La values of the BX packing are higher than MELLAPAK 250.Y and 500.Y. For a specific liquid load of 20 m^3/m^2h, the k_La of BX is twice the k_La of 250.Y and 2.6 times higher than the k_La of 500.Y. The difference increases slightly with lower specific liquid loads. Higher k_La values of BX is probably due to the high specific geometric area (486 m^2/m^3) and the wire gauze surface and structure of the BX packing. Furthermore, the column used by Bereiter may have unduly increased the k_La values.

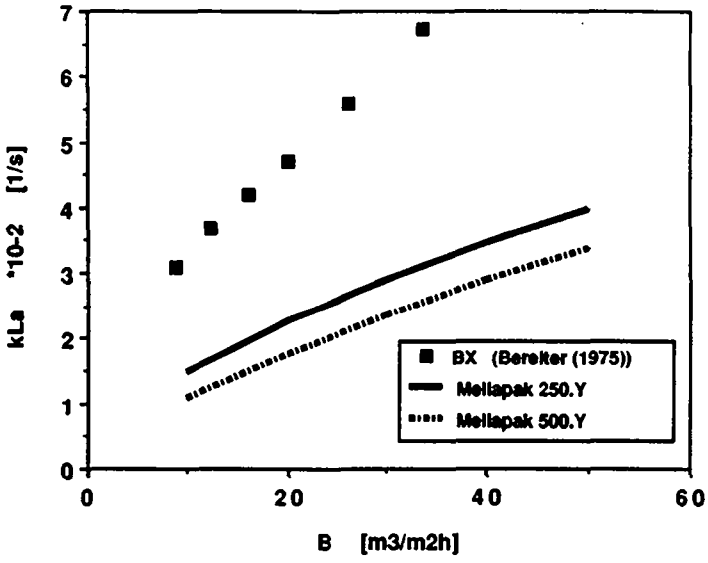

Figure 5.13 Comparison of $k_L a$ values for MELLAPAK and the SULZER wire gauze packing BX.

The capillary effect of the wire gauze surface of the SULZER BX packing causes an increase of the wetted area. The wetted area may be equal to the geometric area, which was not be the case of metal sheet packings, as MELLAPAK 500.Y (chapter IV). Thus, the resulting effective area of wire gauze packings may be higher compared to the effective area of metal sheet surfaces, since droplet formation and interface turbulence would be expected to occur in both packings. The surface structure of the BX packing correspond to a MELLAPAK type X, with the slope angle of the corrugation equal to 30° (figure 1.3, chapter I). The channels are in a more vertical position. This may be positive for liquid side controlled processes, since the liquid renewal may be enhanced, due turbulence and shear stresses at the interface.

The catalog of SULZER BROTHERS LIMITED (1991) presents data from distillation experiments for the number of theoretical stages per meter for the packings BX, 250.Y and 500.Y as a function of the F-Factor. The number of theoretical stages per meter for the BX packing increases considerably with a decrease of the F-Factor, which is not the case for MELLAPAK 250.Y and 500.Y. With MELLAPAK, the number of theoretical stages per meter increases little with a decrease of the F-Factor. For an F-Factor of 1, the BX packing presents a number of theoretical stages per meter about two times higher compared to MELLAPAK 250.Y and 1.5 times higher compared to MELLAPAK 500.Y. The data come from distillation experiments, in which mass transfer is usually gas-phase controlled. Thus, the data is more related to $k_G a$ than to $k_L a$. Nevertheless, the BX packing is also known to be more efficient than MELLAPAK in absorption processes.

However, k_La values of Bereiter from absorption experiments with the BX packing may be higher not only because the BX packing is more efficient, but also because of the use of artificially dimensioned packing element, which was not truly representative. Bereiter used a column of 185 mm diameter packed to a height of 171 mm, which correspond to the height of an element of the SULZER wire gauze packing BX. His column could not be higher. Therefore, in order to be able to create a change of flow direction, when large scale mixing occurs, a BX element was artificially cut into two. The two parts were installed in the column, rotated by 90 degrees. The influence of a change of flow direction on mass transfer efficiency is expected to be more pronounced with a small column height of 170 mm than with a height of 340 mm. This would be the height resulting of two actual BX packing elements. Therefore, the data proposed by Bereiter may not be representative of a typical column packed with the SULZER wire gauze packing BX.

At this point, a short discussion of the packing height in the present work is required. The information in the work of Stikkelmann et al. (1989) support that the packing height for MELLAPAK 250.Y and 500.Y in this work (420 mm - 2 elements) was not low. The authors state that "the natural flow of the liquid, with a gas flow rate below the loading point is practically established after the second element" with MELLAPAK 250.Y. The liquid distributor with high drip point density contributes for an uniform distribution from the top of the column. The values measured in the present work are expected to be representative of typical MELLAPAK 250.Y and 500.Y elements. Possibly, for MELLAPAK 125.Y, which is a low density packing, an influence of the height could have been detected, especially at low specific liquid loads (section 3.3, chapter V).

The variation of the k_La for MELLAPAK 250.Y and 500.Y with specific liquid load and F-Factor is similar to the variation of the k_La for irregular packings. As discussed in section 2.2.2.1, chapter I, various sources state that k_La is in principle almost independent of the gas flow, only increasing with the gas flow near flooding. This behavior is detected with MELLAPAK 250.Y and 500.Y. The gas flow has, however, an important influence on the k_La values for MELLAPAK 125.Y.

The k_La for MELLAPAK 250.Y and 500.Y is proportional to the liquid load to a power of 0.615 and 0.706 respectively. These values are in the range given in table 1.7, section 2.2.2.1, chapter I for irregular packings. The average exponent from different correlations for the liquid flow is 0.61 with a standard deviation of 0.18. The average exponent from different experimental works is 0.76 with a standard deviation 0.17. This information may be used to confirm the trend of the results in this work, although it must be kept in mind that the flow in a structured packing is different to that in irregular packings. This difference influences both the effective area and the liquid phase mass transfer coefficient k_L, via hold-up and contact length, which is the length when liquid renewal occurs (chapter VI).

The absolute values of k_La for MELLAPAK 250.Y far from 100 % capacity, when the k_La data would not be expected to be significantly influenced by the gas flow, are compared to the values given by the equation of Norman (1961) and Mohunta et al. (1969) in figure 5.14 overleaf. The correlation from Mohunta (equation (1.44)) was considered by the review paper of Laurent and Charpentier (1974) to be the best for a great number of different packings (pall rings, intalox saddles and raschig rings) made of different materials (ceramic, plastic and steel) with a deviation of ± 20 %. The correlation from Norman (equation (1.43)) was proposed as a single equation for different types of dumped packings (raschig rings and berl saddles) with a maximum deviation of ± 20 % and was considered by Au Yeung and Ponter (1983) to be convenient to use.

In order to plot k_La versus the specific liquid load, the correlations from the literature must be in a simpler form, such as:

$$k_La = \text{coefficient} \cdot B^{\text{exponent}}$$

The coefficient and exponent of the liquid load are given in table 5.5. The values used for the density, viscosity and diffusivity of oxygen in water are given below table 5.5. For the equation of Mohunta, which employs the specific geometric area, this value was taken as 250 m^2/m^3, as for MELLAPAK 250.Y.

Table 5.5 Values for the k_La correlations from the literature.

Reference	coefficient 10^{-3}	exponent
Mohunta et al. (1969)	1.487	0.75
Norman (1961)	1.766	0.75

Values:

$$\rho_L = 998 \text{ kg/m}^3;\ \mu_L = 1000\ 10^{-6} \text{ kg/m.s};\ D_{O_2} = 0.24\ 10^{-8} \text{ m}^2/\text{s}$$

Figure 5.14 shows the comparison between the values from table 5.5 and those determined from this study. The k_La values for MELLAPAK 250.Y are higher than the k_La predicted by the other two correlations. All indicate approximately the same dependence on the specific liquid load.

The k_La values for MELLAPAK 250.Y are 40 to 70 % higher than from Mohunta's prediction with decreasing specific liquid loads from 90 to 20 m^3/m^2h. As a consequence, the HTU values for MELLAPAK 250.Y are 58 to 71 % smaller than the HTU values for an irregular packing with the same specific geometric area. Norman proposes k_La values 19 % higher than Mohunta. The equation from Norman neither results from theoretical considerations nor takes into account the specific area of the packing. Nevertheless, the k_La values for MELLAPAK 250.Y far from 100 % capacity are 10 to 35 % higher than k_La calculated with Norman's equation.

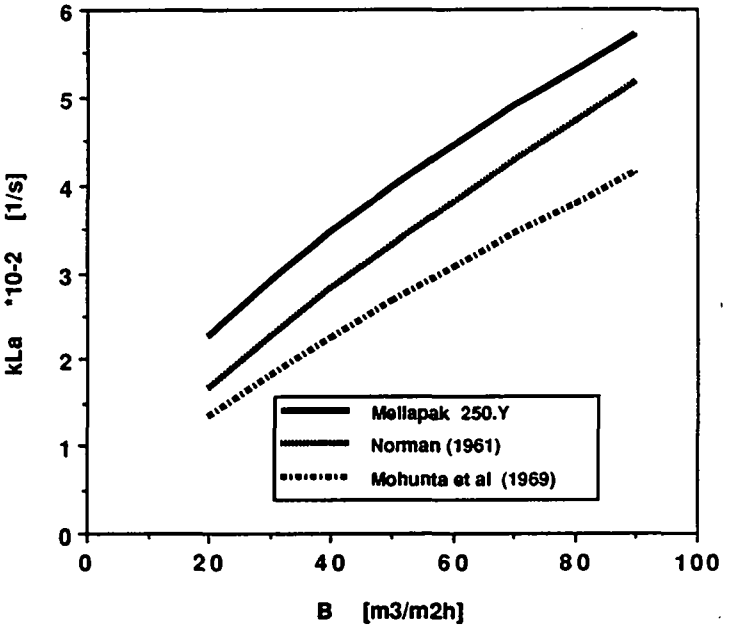

Figure 5.14 Comparison of $k_L a$ of MELLAPAK 250.Y with $k_L a$ predicted by two correlations in the literature.

The $k_L a$ data for MELLAPAK 500.Y far from 100 % capacity was not plotted in figure 5.14, since in the correlation of Mohunta, the specific area was taken as 250 m^2/m^3. According to Mohunta, when the geometric area is doubled, the $k_L a$ value of irregular packings decreases of 5.6 % (equation (1.44)). With the fact above and table 5.5, the coefficient of the $k_L a$ correlation (5.13) for 500.Y is 52 % and 20 % higher than the values given by Mohunta and Norman respectively.

This indicates that the SULZER structured packings MELLAPAK 250.Y and 500.Y offer higher $k_L a$ values than irregular packings with the same geometric area and therefore a shorter column may be used. Additionally, for a given specific liquid load, different MELLAPAK types allow column operation with higher values of F-Factors than several irregular packings, without causing the column to flood. In addition, the pressure drop associated to structured packings is also smaller.

One of the important application of MELLAPAK is for selective absorption. Selectivity characteristics is obtained by the high mass transfer area values (chapter IV) with not necessarily high $k_L a$ values. Consequently, substances, the transfer of which is essentially gas-side controlled, are absorbed readily, whereas those whose transfer is liquid-side controlled, are absorbed sparingly.

4 Conclusions

The $k_L a$ values of the SULZER structured packing MELLAPAK 250.Y, 500.Y and 125.Y were measured in a pilot column with 295 mm internal diameter and a packing height of 420 mm. The $k_L a$ data were obtained with the desorption of oxygen from demineralized water into air.

MELLAPAK 250.Y and 500.Y exhibit higher $k_L a$ values than irregular packings with the same specific geometric area. MELLAPAK 500.Y, which has a specific geometric area close to the SULZER packing BX, without the capillary effect of the wire gauze, exhibit lower $k_L a$ values than the published values of the latter, as it would be expected. However, the published $k_L a$ values of the BX packing may not be representative of a typical BX element.

The $k_L a$ values for MELLAPAK 250.Y and 500.Y, for the SULZER wire gauze packing BX and for irregular packings, have similar dependencies on the specific liquid load, ie. the exponent affecting the specific liquid load is similar. The $k_L a$ values are also practically independent of the gas flow, increasing with the F-Factor near 100 % capacity.

Far from 100 % capacity, in studied range of gas and liquid flows, $k_L a$ values for MELLAPAK 250.Y are the highest, even compared to those of 500.Y. Empirical correlations for $k_L a$ and HTUL values as a function of the specific liquid load are proposed for MELLAPAK 250.Y and 500.Y.

Close to 100 % capacity, especially for 500.Y, $k_L a$ increases with the F-Factor. The empirical correlations give conservative values.

MELLAPAK 125.Y presents $k_L a$ values, which may increase or decrease with the specific liquid load, depending on the F-Factor. This could be examined using a higher packed column. For a given gas and liquid flowrate, measured $k_L a$ values for MELLAPAK 125.Y were lower than those for 250.Y and 500.Y.

ACKNOWLEDGEMENT FOR CHAPTER V

I would like to thank Julie Friend for the very hard and enthusiastic work during the two months when the experiments were carried out. Julie Friend was a third year chemical enginnering student from Iowa State University on an exchange program with the EPFL.

NOMENCLATURE FOR CHAPTER V

a	$[m^2/m^3]$	specific area
B	$[m^3/m^2h]$	specific liquid load (equation (1.3))
D	$[m^2/s]$	diffusivity
F-Factor	$[m/s.\sqrt{kg/m^3}]$	equation (1.1)
G	[kg/h] [mol/h]	gas flowrate
h	[m]	packing height
H	$[Pa.m^3/mol]$ [atm]	Henry constant
HTU	[m]	height of a transfer unit
k_G	$[mol/m^2.s.Pa]$	gas phase mass transfer coefficient
k_L	[m/s]	liquid phase mass transfer coefficient
L	[kg/h] [mol/h]	liquid flowrate
m	[-]	slope of the equilibrium line
M	[g/mol]	molecular weight
NTU	[-]	number of transfer units
p	[mmHg]	pressure
x	[mol/mol]	liquid-phase mol fraction
μ	[kg/ms]	viscosity
ρ	$[kg/m^3]$	density

Subscripts

G	gas
L	liquid
o	overall
O_2	oxygen
p	packing
α	begin - in
ω	end - out

Superscript

*	equilibrium

REFERENCES FOR CHAPTER V

AU-YEUNG, P. and A.B. PONTER (1983). "Estimation of liquid film mass transfer coefficients for randomly packed absorption columns". The Can.J.of Chem.Eng. 61(4), 481-493.

BEREITER, R. (1975). "Druckverlust und Flüssigkeitsseitiger Stoffaustausch in Sulzer Gewebepackungen". Zürich: PhD Thesis ETH-Zürich 5618.

BOMIO, P. (1977). "Stoffaustauschmessungen an der Sulzer-Packungen aus Kunststoff". Chem.Ing.Tech. 49(11), 895-897.

BOMIO, P.; LASO, M.; BREU, K. and N. WYNN (1988). "Improving selectivity, capacity and efficiency of hydrogen sulphide/carbon dioxide removal columns with SULZER structured packing". Vienna: presented at SULPHUR 88.

DELALOYE, M. (1986). "Influence de la viscosité du liquide sur le transfert de matière dans une colonne à garnissage à l'échelle pilote". Lausanne: PhD Thesis EPFL 657.

INCROPERA, F.P. and D.P. DeWITT (1981). "Fundamentals of Heat Transfer". New York: John Wiley & Sons, page 786.

LAURENT, A. and J.C. CHARPENTIER (1974). "Aires interfaciales et coefficients de transfert de matière dans les divers types d'absorbeurs et de réacteurs gaz-liquide". The Chem. Engineering J. 8, 85-101.

LINEK, V.; PETRICEK, P.; BENES, P. and R. BRAUN (1984). "Effective interfacial area and liquid side mass transfer coefficients in absorption columns packed with hydrophilised and untreated plastic packings". Chem.Eng.Res.Des. 62(1), 13-21.

MANGERS, R. and A. PONTER (1980.a). "Liquid phase resistance to mass transfer in a laboratory absorption column packed with glass and polytetrafluoroethylene rings - Part I: The effects of flowrate sequence, repacking, packing depth and initial liquid distribution". The Chem. Engineering J. 19, 139-146.

MANGERS, R. and A. PONTER (1980.b). "Liquid phase resistance to mass transfer in a laboratory absorption column packed with glass and polytetrafluoroethylene rings - Part II: The effects of column wall and ring wettabilities". The Chem. Engineering J. 19, 147-151.

MOHUNTA, D.M.; VAIDYANATHAN, A.S. and G.S. LADDHA (1969). "Prediction of liquid phase mass transfer coefficients in columns packed with raschig rings". Indian Chemical Engineer july, 73-79.

NORMAN, W.S. (1961). "Absorption, distillation and cooling towers". New York: John Wiley & Sons, chapter 6.

PERRY, R. (1984). " Perry's chemical engineers' handbook". 6th Edition. Singapore: McGraw-Hill Book Co., pages 3.97-3.98 and 18.23.

SHERWOOD, T.K. and F.A.L. HOLLOWAY. (1940). "Performance of packed towers - Liquid film data for several packings". Trans.Am.Inst.Chem.Eng. 36, 39-70.

STIKKELMAN, R.; de GRAAUW, J.; OLUJIC, Z.; TEEUW, H. and H. WESSELINGH (1989). "A study of gas and liquid distributions in structured packings". Chem.Eng.Technol. 12, 445-449.

SULZER BROTHERS LIMITED (1991). "Separation columns for distillation and absorption". Winterthur: Publication number 221306.

von STOCKAR, U. and P.F. CEVEY (1984). "Influence of the physical properties of the liquid on axial dispersion in packed columns". Ind.Eng.Chem.Process Des.Dev. 23, 717-724.

1 Problem analysis

The liquid phase mass transfer coefficient expresses the resistance to mass transfer by diffusion in the liquid boundary layer at the gas-liquid interface. The liquid phase mass transfer coefficient k_L of packed columns cannot be directly determined experimentally. A literature review with correlations for irregular packings is available in section 2.2.2.2, chapter I. Estimates of k_L may vary widely. In this chapter, k_L is determined for three different MELLAPAK types (250.Y, 500 and 125.Y) using the equations developed below.

The k_L may only be accurately obtained from experimental measurements of the mass transfer area and of k_La. Thus:

$$k_L = \frac{k_La}{a} \tag{6.1}$$

Using empirical correlations developed in previous chapters for k_La and effective mass transfer area as a function of the specific liquid load yields:

$$k_L = C_1 \cdot B^{C_2} \tag{6.2}$$

Although different gas-liquid systems were used to measure values of k_La and effective mass transfer area, it is assumed in this work that the system did not influence the data in any way. The effective area during desorption and chemical absorption experiments would be expected to be all equal, since with structured packings, the defined channels avoid the existence of stagnation zones of mass transfer.

A model for k_L with a sound theoretical basis is however desirable. The penetration theory proposed by Higbie (section 1.2.1, chapter I) could be applied for predicting k_L. According to this theory,

$$k_L = 2 \cdot \sqrt{\frac{D}{\pi \cdot \bar{t}}} \tag{1.10}$$

For the contact time, $\bar{t}$, Billet (1983) proposed a model, which, adapted for the structured packing MELLAPAK, yields:

$$\bar{t} = \frac{h_L \cdot L}{\frac{B}{\cos 45^\circ} \cdot \frac{1}{3600}} \cdot \frac{1}{100} \tag{6.3}$$

The contact time has an adjustable parameter which is the contact length, L. The liquid holdup far from 100 % capacity is principally a function of the specific liquid load, with F-Factor being of negligible importance. Hence, the data can be correlated in the form of:

$$h_L = C_3 \cdot B^{C_4} \tag{6.4}$$

From equations (1.10), (6.3) and (6.4), an expression for k_L is obtained:

$$k_L = 2 \cdot \sqrt{\frac{D}{\pi \cdot L \cdot C_3 \cdot 36 \cdot \cos 45^\circ}} \cdot B^{(1-C_4)/2} \tag{6.5}$$

2 Results and discussions

2.1 The k_L for MELLAPAK 250.Y and 500.Y

Chapter V proposed k_La correlations for low F-Factors, at conditions far from 100 % capacity. The correlations (5.11) and (5.13), for MELLAPAK 250.Y and 500.Y respectively, give the k_La as a function of the specific liquid load raised to a certain exponent. The effective mass transfer areas were correlated in a general expression (equation (4.17)). For low F-Factors, the correlation (4.15) is more accurate for determining the effective area of MELLAPAK 500.Y. Table 6.1 presents the values of the coefficients and of the exponents of the above mentioned correlations.

Table 6.1 Values for the empirical correlations for the effective mass transfer area and k_La far from 100 % capacity.

	k_La [1/s]		mass transfer area [m^2/m^3]	
	coefficient *10^{-3}	exponent on B	coefficient	exponent on B
MELLAPAK 250.Y	3.58	0.615	99	0.34
MELLAPAK 500.Y	2.13	0.706	150	0.312

Thus, for each MELLAPAK type, dividing the k_La correlation by the effective area correlation yields for k_L an expression given by (6.2). Table 6.2 below gives the values for the exponents and coefficients of the resulting correlation.

Table 6.2 Values for the k_L correlation (6.2) with measured values.

	C_1 *10^{-5}	C_2
MELLAPAK 250.Y	3.62	0.28
MELLAPAK 500.Y	1.42	0.39

The semi-empirical model for predicting k_L for MELLAPAK 250.Y and 500.Y (equation (6.5)), using the penetration theory, requires knowledge of the liquid holdup and of the contact time.

The liquid holdup was measured by SULZER BROTHERS LIMITED (1990) and it is almost independent of the F-Factor, increasing rapidly as 100 % capacity is neared. Table 6.3 presents the average values of the liquid holdup for certain specific liquid loads.

Table 6.3 Experimental measurements of holdup in MELLAPAK. (courtesy of SULZER BROTHERS LIMITED (1990)).

MELLAPAK 250.Y		MELLAPAK 500.Y	
B $[m^3/m^2h]$	Holdup [%]	B $[m^3/m^2h]$	Holdup [%]
1.4	2.0	25.0	11.0
5.4	3.5	50.0	14.0
15.9	5.5	75.0	17.0
31.8	6.5	87.5	18.0
63.7	9.0		
79.6	10.5		

These values were correlated by least squares regression to obtain expression (6.4). Table 6.4 below gives the values for the coefficients and exponents of correlation (6.4). The exponents of the specific liquid load for the holdup correlation and for the mass transfer area correlation (table 6.1) are similar, indicating the same trend of both holdup and effective area with the specific liquid load. This trend was predicted by Bravo and Fair (1982).

Table 6.4 Values for the holdup correlation (6.4).

	C_3	C_4
MELLAPAK 250.Y	1.76	0.397
MELLAPAK 500.Y	3.04	0.397

The contact length was determined by comparing k_L values from equation (6.2) with the predicted k_L given by equation (6.5). As both values should be the same, the evaluation of the adjustable parameter (contact length) is possible. The diffusivity of O_2 in water is 2.4×10^{-9} m^2/s (Incropera and DeWitt (1981)). Table 6.5 shows the contact length for different specific liquid loads. The average contact lengths are 61 and 102 mm for MELLAPAK 250.Y and 500.Y respectively. The standard deviation is 1 and 8 mm for MELLAPAK 250.Y and 500.Y respectively.

Table 6.5 The contact length.

B	$L * 10^{+3}$ [m]	
$[m^3/m^2h]$	MELLAPAK 250.Y	MELLAPAK 500.Y
21.29	59.6	114.2
42.6	61.4	101.1
51.2	61.9	97.8
60.8	62.4	94.9

A simple experiment checked whether the values were reasonable. Water was injected at the top of the packing and the length of the liquid film was observed. Figure 6.1 shows the results. The measured values for the contact length of approximately 62 mm and 102 mm for MELLAPAK 250.Y and 500.Y respectively, compare well with the values in table 6.5. Packing 500.Y, with a smaller corrugation angle (figure 1.3, chapter I), retain the liquid film longer than 250.Y. The larger corrugation angle of 250.Y is associated with a greater wetted area and consequently greater viscous losses of momentum and earlier detachment due to gravity. The corrugation angle of MELLAPAK 250.Y and 500.Y was measured and was approximately 82° and 63° respectively.

a) b)

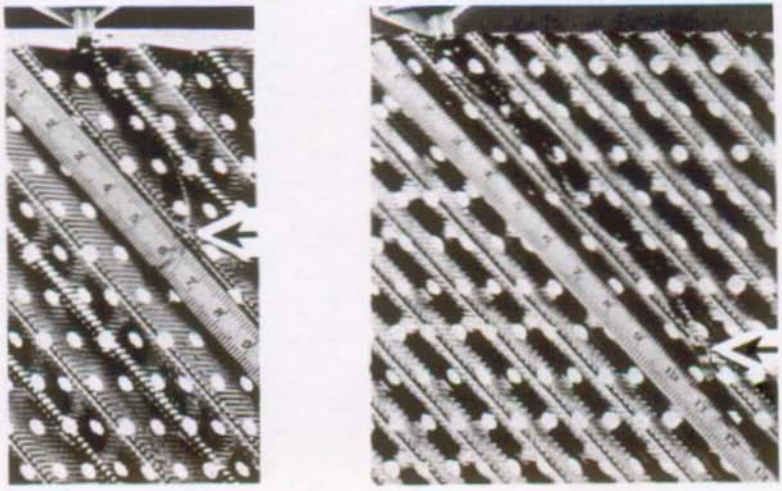

Figure 6.1 Liquid film over the packing.
a) MELLAPAK 250.Y b) MELLAPAK 500.Y.

From equation (6.5), using for the contact length the values of 61 mm and 102 mm for MELLAPAK 250.Y and 500.Y respectively, the following expressions are obtained:

for MELLAPAK 250.Y: $k_L = 3.34 \cdot 10^{-5} \cdot B^{0.302}$ (6.6)

for MELLAPAK 500.Y: $k_L = 1.97 \cdot 10^{-5} \cdot B^{0.302}$ (6.7)

Figure 6.2 shows the comparison between data from equation (6.2) evaluated with experimental correlations (table 6.1) and values from correlations (6.6) and (6.7).

The error in the evaluation of k_La is less than 6 % (section 2, chapter 5) and in the evaluation of mass transfer area is 9 and 8 % (table 4.2, chapter 4) for MELLAPAK 250.Y and 500.Y respectively. Therefore, in the evaluation of k_L of 250.Y and 500.Y, the errors are less than 15 % and 14 % respectively. These errors are conservative estimation. The results are discussed in section 2.3.

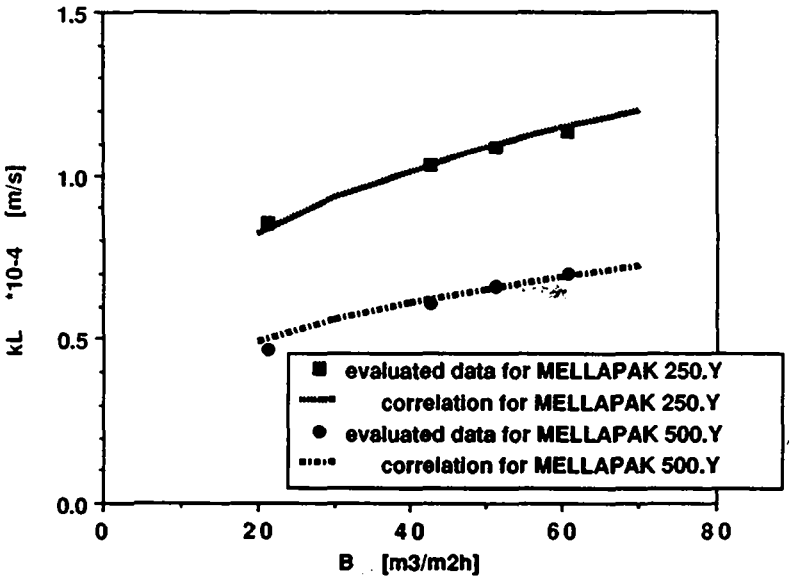

Figure 6.2 Model for predicting k_L compared with experimental data.

2.2 The k_L for MELLAPAK 125.Y

For MELLAPAK 125.Y, it was not developed an empirical or a semi-empirical model, as in the last section. Figure 6.3 shows the result of the division of k_La data by the effective mass transfer area. The values of this area adopted for the division are from the general correlation (4.17) (figure 4.8, chapter IV) using the different specific liquid loads. In chapter IV, it was seen that the effective area values of MELLAPAK 125.Y do not vary significantly with the F-Factor.

The error in the evaluation of k_La is less than 6 % (section 2, chapter 5) and in the evaluation of mass transfer area is 15 % (table 4.2, chapter 4) for MELLAPAK 250.Y and 500.Y respectively. Therefore, the error in the evaluation of k_L of 125.Y is less than 21 %. This error is a conservative estimation. The results are discussed in section 2.3.

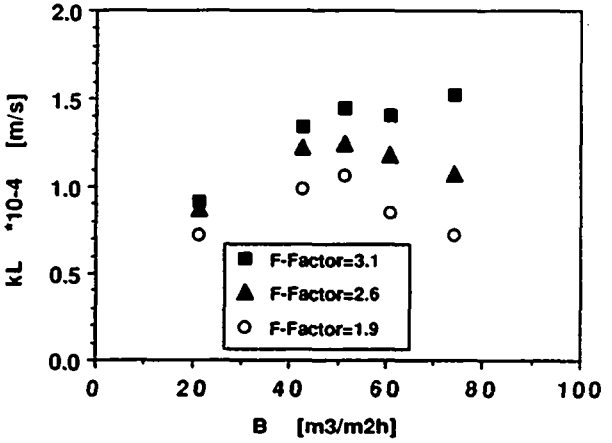

Figure 6.3 The k_L values for MELLAPAK 125.Y.

2.3 Discussion

A semi-empirical model using the penetration theory gives the correlations (6.6) and (6.7) for predicting k_L with 250.Y and 500.Y. This is possible because the numerical value of the adjustable parameter of this model, the contact length, was confirmed experimentally with the measurement of the length of a film over the packing and it did not vary significantly with the specific liquid load (table 6.5). From equation (6.5) and tables 6.2 and 6.4, it can be verified that the contact length depends on the specific liquid load with the power of 0.043 and -0.177 for 250.Y and 500.Y. The contact length does however vary significantly with the packing size. The contact length would also be expected to be a function of F-Factor and physical properties.

For low F-Factors, far from 100 % capacity, the k_L for 250.Y is about 69 % higher than for 500.Y, as holdup and contact length of 500.Y are greater, the contact time is greater (equation (6.3)); and the value of k_L is then, according to the penetration theory, smaller (equation (1.10)).

Increased F-Factors would be expected to increase k_L by reducing the contact time, ie. by increasing the liquid renewal rate due to turbulence. The increase of k_L with F-Factor may be more pronounced with 500.Y, since the k_La and the effective mass transfer area for 500.Y are strongly dependent on the F-Factor, as seen in chapters IV and V. High F-Factors are responsible for spreading the liquid over the 500.Y packing and for creating turbulence at the gas-liquid interface. As a result, near 100 % capacity, the k_L of 500.Y would be expected to be higher than for 250.Y.

MELLAPAK 125.Y is a packing with low geometric area and density. Figure 6.3 shows the strong dependence of the F-Factor on the k_L with a similar trend as presented by the k_La. For the smallest F-Factor of 1.9, MELLAPAK 125.Y has k_L values between 500.Y and 250.Y. With higher F-Factors, the k_L values for 125.Y are higher than for 250.Y and 500.Y. The 125.Y packing has

the smallest holdup. Although the contact length was not determined, it would also be expected to be small. This packing is the one in which liquid droplet formation more occurs (section 3.4, chapter IV). All these facts are in the same direction of increasing k_L values. Unfortunately, it is not possible to explain with the available data the maximum in figure 6.3 for the smallest F-Factor. Further measurements with a higher packing height for MELLAPAK 125.Y should confirm the results (section 3.3, chapter V).

No reports have been found in the literature involving measurements of k_La and effective areas of structured packings from which k_L has been calculated. Thus, comparisons with the present work are not possible. On the other hand, an inspection of tables 1.1 and 1.5 in chapter I shows that measurements of k_La and effective areas of irregular packings are sometimes reported together, however, without evaluation of k_L. This may be linked to the fact that k_L alone is not a design parameter.

In section 2.2.2.2, chapter I, it was concluded that k_L values may be more accurate determined by simply dividing k_La values by effective area values. Effective areas and k_La of irregular packings were measured by Mohunta et al (1969.a) and Mohunta et al (1969.b) respectively. For both parameters, correlations are proposed, which seem accurate not alone for their own data, but also for different packings and systems in the literature (section 2.1.2 and 2.2.2.1, chapter I). Using their equations for k_La (1.44) and effective area (1.28) and considering the liquid density, viscosity and diffusivity of oxygen in water to be respectively 998 kg/m^3, 1 x 10^{-3} kg/m.s and 0.24 x 10^{-8} m^2/s, yields:

$$k_La = 2.356 \cdot 10^{-3} \cdot a_p^{-1/12} \cdot B^{0.75} \qquad (6.8)$$

and

$$a_e = 1.414 \cdot a_p^{2/3} \cdot B^{1/3} \qquad (6.9)$$

With equations (6.1), (6.8) and (6.9), it is found that

$$k_L = 2.065 \cdot 10^{-3} \cdot a_p^{-3/4} \cdot B^{0.417} \qquad (6.10)$$

Equation (6.10) with values of geometric area of 250 m^2/m^3 and 500 m^2/m^3 is compared to equation (6.6) and (6.7), for MELLAPAK 250.Y and 500.Y respectively, in figure 6.4. Considering that equations (6.8) and (6.9) have each a potential error of ± 20 % associated with them, the relative error in the evaluation of the k_L with equation (6.10) is ± 40 %.

Equation (6.10) predicts k_L values from 28 to 51 % higher for irregular packings of specific geometric area equivalent to MELLAPAK. It is possible that the k_L of irregular packings is higher, since the contact length may be smaller and the contact time may be therefore reduced. If irregular packings present higher k_L values, the ratio of effective area to the geometric area is, however, smaller than for MELLAPAK, with the result that the value of k_La is lower compared to that of structured packings.

The exponent on the liquid load in equation (6.10) is 0.417. The work of Dharwadkar and Sawant (1985), in which k_La and mass transfer area were measured, without evaluation of k_L, suggests that k_L varies with the specific liquid load in the power range of 0.177-0.373 for the packings which were studied. The k_L correlations (1.53), (1.54) and (1.57) listed in section 2.2.2.2, chapter I, suggest exponents of 0.45, 0.59 and 0.5.

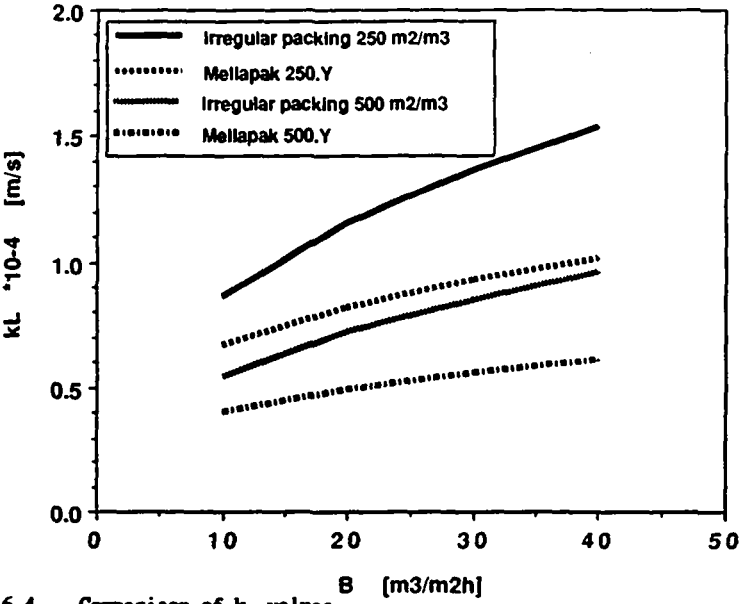

Figure 6.4 Comparison of k_L values.

The dependence of k_L with the liquid flow may be theoretically estimated. The velocity profile of a completely developed laminar film flowing down an inclined plate with constant wetted area is given by equation (6.11). For obtaining this expression, the Navier-Stokes equation was used and the shear stress at the gas-liquid interface was considered to be negligible.

$$w(y) = \frac{\rho.g.\sin\alpha}{\mu} \cdot \left[\delta.y - \frac{y^2}{2}\right] \qquad (6.11)$$

The average film velocity is:

$$\bar{w} = \frac{1}{\delta} \cdot \int_0^{\delta} w(y) \cdot dy = \frac{\rho.g.\sin\alpha.\delta^2}{3.\mu} \qquad (6.12)$$

The volumetric liquid flowrate is:

$$V = \bar{w} \cdot \delta \cdot b \qquad (6.13)$$

A theoretical estimate of the liquid holdup is:

$$h_L = b.\delta \qquad (6.14)$$

From equations (6.12), (6.13) and (6.14):

$$h_L = \left[\frac{3.\mu}{\rho.g.\sin\alpha}\right]^{1/3} \cdot b^{2/3} \cdot V^{1/3} \qquad (6.15)$$

The exponent of 1/3 on the liquid flow in equation (6.15) is similar to the exponent of 0.397 of the holdup equation (6.4) (table 6.4). This indicates that far from flooding conditions, the wetted area of the packing may not vary significantly with the gas flow.

From equations (6.12) and (6.13),

$$\bar{w} = \frac{\rho.g.\sin\alpha.V^{2/3}}{3.\mu.b^2} \qquad (6.16)$$

Therefore, the average velocity is a function of the liquid flow to the power of 2/3. Assuming the contact time to be the ratio of the contact length to the average velocity, with equation (1.10), k_L is given by:

$$k_L = 2 . \sqrt{\frac{D}{\pi.L} . \bar{w}} \qquad (6.17)$$

Thus, from equations (6.16) and (6.17), k_L is proportional to the liquid flow to the power of 1/3. Correlations (6.6) and (6.7) propose an exponent of 0.302, which is in accordance to the theoretical estimate and is within the range suggested by Dharwadkar and Sawant (1985).

These authors state additionally that "the value of the k_L decreases with increase in the packing size for the same type of packing". However, this statement is in disagreement with their own data for Pall rings, since 50 mm metal and polypropylene Pall rings have higher k_L values than the corresponding packings of 38 mm at a superficial liquid flow of 6.10^{-3} m/s. What may happen is that k_L decreases with an increase in the specific geometric area, as suggested by equation (6.10). The specific geometric area of irregular packings reduces with an increase of the packing size.

From equation (6.17), k_L is inversely proportional to the square root of the contact length, which defines when a liquid renewal occurs. The contact length would be expected to increase with increased size of an irregular packing, thus reducing k_L. However, the liquid holdup may well decrease, thereby creating conditions which favor liquid renewal, which would increase k_L. Depending upon the packing and the system, one or the other effect may be predominant.

For Bolles and Fair (1982) "the individual mass transfer coefficient should be more heavily dependent on the system itself than on the geometric characteristics of the packing". Indeed, systems with different physical properties have an influence on both the contact length and holdup, and thus on the k_L. Nevertheless, the geometry of the packing is also an extremely important parameter in the determination of the flow over the packing and of the liquid holdup. It is therefore unsound to assume a negligible influence of the packing geometry on k_L.

The k_L values of MELLAPAK decrease with an increase of the specific geometric area, since the contact length becomes bigger. The k_L values of 250.Y are 69 % higher than for 500.Y. Equation (6.10) predicts a 68 % increase of k_L when the geometric area reduces by a factor 2. However, the k_L values for 125.Y compared to 250.Y do not follow the above trend.

3 Conclusions

The use of the penetration theory in predicting values for k_L with MELLAPAK 250.Y and 500.Y, apart from furnishing a model with a theoretical basis, validates the effective area and k_La data obtained in previous chapters. The k_L values for MELLAPAK 125.Y are described graphically and its variation with the specific liquid load and F-Factor is similar to that presented by the k_La.

The contact length was found to vary little with the specific liquid load. Therefore, the contact length is a characteristic flow dimension of the packing. This fact enabled the use of the penetration theory for building a model for k_L. The contact length of 500.Y is greater than for 250.Y. The contact length would be expected to depend also on the F-Factor and physical properties.

The k_L semi-empirical model for MELLAPAK 250.Y and 500.Y (equations (6.6) and (6.7)) predicts a relationship between k_L and specific liquid load which is in accordance with theoretical considerations and literature data for other packing types. An increase of the specific geometric area of a MELLAPAK type causes a decrease of k_L. For low F-Factors, far from 100 % capacity, the k_L for 250.Y is about 69 % higher than for 500.Y. Depending on the F-Factor, the k_L values of 125.Y are of the same order of magnitude or even higher than the values of 250.Y.

Irregular packings, with the same specific geometric area as MELLAPAK, may present higher k_L values. This is possibly due to the fact that the contact length is smaller, and the liquid renewal rate of irregular packings therefore higher. A possible higher liquid holdup of irregular packings may reduce the effect of a higher liquid renewal rate.

This work has been accepted for presentation at the conference DISTILLATION AND ABSORPTION of the Institution of Chemical Engineers, at Birmingham, England, September 7-9th, 1992.

NOMENCLATURE FOR CHAPTER VI

a	[m^2/m^3]	specific mass transfer area
b	[m]	film width
B	[m^3/m^2h]	specific liquid load (equation (1.3))
C		coefficient of empirical model
D	[m^2/s]	diffusivity
F-Factor	[$m/s.\sqrt{kg/m^3}$]	equation (1.1)
g	[m/s^2]	gravity
h_L	[%]	liquid holdup
HTU	[m]	height of a transfer unit
k_L	[m/s]	liquid phase mass transfer coefficient
k_La	[1/s]	volumetric mass transfer coefficient
L	[m]	contact length
t	[s]	time

V	[m^3/s]	volumetric liquid flowrate
w	[m/s]	velocity
y	[m]	coordinate perpendicular to the direction of the liquid flow
α		inclination angle of an inclined plate
δ	[m]	film thickness
ρ	[kg/m^3]	density
μ	[kg/ms]	dynamic viscosity

Subscript

e	effective
L	liquid
p	packing
1, 2, ...	indexes

Superscript

-	mean

REFERENCES FOR CHAPTER VI

BILLET, R. (1983). "Fluiddynamisches Verhalten und Wirksamkeit von Gegenstromapparaten für Gas-Flüssig-Systeme bei flüssigkeitsseitigem Stoffübergangswiderstand". Festschrift der Fakultät für Maschinenbau, Ruhr-Universität Bochum, pages 24-31.

BRAVO, J.L. and J.R. FAIR (1982). "Generalized correlation for mass transfer in packed distillation columns". Ind.Eng.Chem.Process Des.Dev. 21, 162-170.

DHARWADKAR, S.W. and S.B. SAWANT (1985). "Mass transfer and hydrodynamic characteristics of tower packings larger than 0.025 m nominal size". The Chemical Engineering J. 31, 15-21.

INCROPERA, F.P. and D.P. DeWITT (1981). "Fundamentals of Heat Transfer". New York: John Willey & Sons, page 785.

MOHUNTA, D.M.; VAIDYANATHAN, A.S. AND G.S. LADDHA (1969.a). "Effective interfacial areas in packed columns". Indian Chemical Engineer april, 39-42.

MOHUNTA, D.M.; VAIDYANATHAN, A.S. AND G.S. LADDHA (1969.b). "Prediction of liquid-phase mass transfer coefficients in columns packed with raschig rings". Indian Chemical Engineer july, 73-79.

SULZER BROTHERS LIMITED (1990). Winterthur: Private Communication (unpublished data).

SUMMARY OF FINDINGS

The present work involving structured packings contributes for the investigation of mass transfer problems in packed columns. Measurements with structured packings are almost non existing in the literature. The data and correlations proposed in the literature for effective areas and k_La of irregular packings may only be valid for the systems, flow conditions and equipment of the original investigation.

The purpose of this investigation was to measure mass transfer parameters of three types of SULZER structured packings, namely MELLAPAK 250.Y, 500.Y and 125.Y. The specific mass transfer areas and the volumetric liquid phase mass transfer coefficient k_La were measured in a pilot plant column, using ranges of specific liquid loads and F-Factors employed in the industry. The methods used to obtain these values have been used in the literature; this work verified their adequacy.

With the k_La and effective mass transfer area data, the liquid phase mass transfer coefficient k_L was evaluated. This was possible, since the measurements of effective areas and k_La were carried out with similar gas and liquid flow conditions and at same temperature and pressure.

In chapter I, it was pointed out that under certain conditions, it has been accepted that irregular packings may present effective areas higher than the geometric, enhancing mass transfer. Indeed, the SULZER structured packings MELLAPAK are efficient in particular due to the fact that the area effective for mass transfer assumes high values. For a given volume of MELLAPAK, depending on the gas and liquid flowrates and on the geometric area of the packing, effective areas can be even higher than the geometric area up to a factor of 2. This occurs because the liquid does not flow smoothly over the packing sheets without detachment. Effective area results also from turbulence at the gas-liquid interface and from liquid droplets. Therefore, the effective area may become higher than that which would correspond to a wetted packing.

An increase of the geometric area, reduces the available space between the sheets. The possibility of formation of liquid drops and turbulence at the phase interface depends on the available space between packing sheets. If this space is smaller, the formation of more effective area reduces. The specific effective area increases less than linearly with the geometric area for identical gas and liquid flow rates.

With the present data from absorption experiments, the ratio of the effective area to the geometric area was correlated as a function of a Reynolds number (equation (4.17), section 3.4, chapter IV). This correlation overestimates effective area values for MELLAPAK 500.Y with low F-Factors. In this case, the equation (4.15), in section 3.2, chapter IV gives more realistic values for effective areas of MELLAPAK 500.Y. This packing present effective areas strongly dependent on the F-Factor. For MELLAPAK 250.Y and 125.Y, the F-Factor has little influence on effective area values, especially far from 100 % capacity. The applicability of the data and correlations with systems having different viscosities and densities has not been experimentally determined.

The effective areas were measured in this work using absorption followed by a chemical reaction of CO_2 with NaOH, since from physical mass transfer

experiments, it does not seem possible to evaluate directly effective areas. The difference between effective areas of absorption with and without chemical reaction may not be significant in structured packings, since these force a defined flow, reducing or making negligible the influence of stagnation zones, where the concentration driving force tends to zero.

The reaction of CO_2 with NaOH has been widely accepted as being a suitable method for measuring effective areas. However, the measured values of the reaction rate constant appearing in the literature are not in agreement. Therefore, a kinetic parameter, which is the proportionality factor between the absorption rate and the effective area, was measured in this work. This parameter is composed of different terms, including the reaction rate constant. It was determined with a wetted wall column, which provided a known mass transfer area, which was easily changed.

If the wetted wall column were not useful for such measurements, the whole method would not be valid for packed columns. The liquid flow over the packing is like a series of short wetted wall columns. The wetted wall column in this work had a height of 80 and 52 mm, thus having the same order of magnitude of the contact length. As seen in chapter VI, the contact length is the distance over which a surface renewal occurs. MELLAPAK 250.Y and 500.Y have a contact length of 61 mm and of 102 mm respectively. This fact confirms that the used height of the wetted wall column was adequate.

Although the values of effective area of 25 mm ceramic rings from the present work tend to be slightly higher than those reported in the literature (5 to 20 %), they fell well in the range of experimental uncertainty. The data in the literature are usually obtained with low specific liquid loads, low F-Factors and high ratio of column height to diameter. These conditions all tend to reduce the measured values of the effective mass transfer area. Therefore, the comparison of the results with literature data indicated that the experimental methodology employed in this work is correct.

Despite of the high drip point density of the liquid distributor (527 points/m^2), the influence of liquid distribution on the effective area of 125.Y was not detected when the drip point density was reduced of 78 %. However, with an increase of 50 % of the packing height of 125.Y, there was a reduction of effective area values. This reduction was actually more pronounced with lower F-Factor and specific liquid load, which is to be expected, since channeling effects are more significant. The unlikelihood of having measured "extra areas" is confirmed by the fact that the measured values with MELLAPAK 125.Y did not reduce by a constant factor.

With the information from the three paragraphs above, it is concluded that the reaction and experimental procedure used in this work is correct and adequate for measuring effective areas of packed columns.

The measured areas were obtained from absorption experiments. For distillation, it may be that the effective areas are higher. The coupling between the heat and mass transfer processes in distillation may play a role in determining effective area. Furthermore, surface tension distribution at the liquid phase interface, which may break the liquid film into rivulets and droplets, is more likely to occur with distillation. Both facts above tend to increase effective areas.

The k_La values were measured using physical desorption of O_2 from demineralized water into air. From this data, it was found that, the k_La values for the SULZER packing MELLAPAK 250.Y are higher than the values reported for irregular packings. This positive characteristic reduces the necessary packing height for a given separation task. The k_La values of the packings 250.Y and 500.Y are lower than the k_La values for the SULZER metal gauze packing BX, since the latter present a large specific geometric area and an important capillary effect.

Increasing the surface area of the MELLAPAK packing does not necessarily increase k_La, as the film renewal and interface turbulence have an important influence. The shape of the packing is important because it can facilitate this renewal and avoid that the gas and liquid flow independently. Generally, k_La values of different packings increase with the liquid flow. The gas flow has an influence on k_La values only near 100 % capacity.

The k_La for MELLAPAK 250.Y is slightly higher than for MELLAPAK 500.Y, at flow conditions far from 100 % capacity. However, MELLAPAK 500.Y presents a steep increase of k_La with the F-Factor near 100 % capacity and, thus, k_La for 500.Y may be the highest. High gas flows have an important influence on k_La values via both effective area (chapter IV) and renewal rate (k_L). The k_La values for MELLAPAK 125.Y increase or decrease with the specific liquid load, depending on the F-Factor. This could be examined with a higher column, since MELLAPAK 125.Y is the packing with lower density.

It did not prove possible, with the present data, to develop a simple correlation applicable for all MELLAPAK types. Empirical correlations for k_La and HTUL of MELLAPAK 250.Y and 500.Y as a function of the specific liquid load were proposed respectively in sections 3.1 and 3.2, chapter V. These correlations are valid far from 100 % capacity, when the F-Factor has no influence on the k_La values. Operation near to 100 % capacity tends to increase the k_La values. Thus, the correlations proposed yield conservative values for design and the safety factor implicit in the correlation for MELLAPAK 500.Y is even higher than in the correlation for MELLAPAK 250.Y.

The HTUL values of all three types of MELLAPAK, in the range of the gas and specific liquid loads studied, increase with the specific liquid load and decrease with the F-Factor. Values of HTUL of MELLAPAK 250.Y are less sensitive to a variation of the F-Factor. MELLAPAK 125.Y presents the highest HTUL values. MELLAPAK 500.Y may present the lowest HTUL values, when near 100 % capacity.

The liquid phase mass transfer coefficient, k_L, for 250.Y and 500.Y was evaluated with a correlation based on the penetration theory, which is valid far from 100 % capacity. It was possible to develop this correlation, since the contact length, which is therein does not change significantly with the specific liquid load, far from 100 % capacity. The values of the contact length for MELLAPAK 250.Y and MELLAPAK 500.Y was estimated to be respectively 61 and 102 mm. This may imply that measurements in columns with small diameter may not be valid, because such apparatus could disturb the development of the full contact length. This fact may reinforce the use of pilot columns for measurements of mass transfer parameters.

The k_L decreases with an increase of the geometric area for the same type of packing, because holdup and contact length increases. Higher values of k_L are associated with irregular packings than with MELLAPAK 250.Y and

500.Y, possibly due to the smaller contact length presented by irregular packings, which increases the liquid renewal rate.

MELLAPAK offers good selectivity characteristics, because the values for mass transfer area are high and k_L values may be low. Thus, substances, the transfer of which is essentially gas-side controlled, are absorbed readily, whereas those which are liquid-side controlled, are absorbed sparingly.

The exponents on the liquid load for k_L and effective areas, apart from being substantially independent of the MELLAPAK type (250.Y and 500.Y), exhibit similar values. This may imply that for an increase of the specific liquid load both the mass transfer area and the k_L may have an equal influence in enhancing the mass transfer process via $k_L a$.

RECOMMENDATIONS FOR MODIFIED MELLAPAK SURFACE STRUCTURE

As a guideline for the design of high efficient packings, the liquid film over the packing should be systematically broken into droplets. The packing's surface should enable the formation of a new film until a new break. This mechanism forces an increase of the renewal rate, which increases k_L and the creation of additional area. An enhancement of the packing efficiency may be obtained. Holdup values should be small.

Liquid droplets are particularly formed in sharp edges and corners. Moreover, every change of the flow direction causes an enhancement in mass transfer. In this sense, it is recommended that the plane surface of the MELLAPAK types 250.Y and 125.Y should be broken from time to time, by suspending a part of the sheets, as illustrated in figure 7.1. The gas-liquid interaction and liquid droplet formation should increase, without a reduction of the geometric area. This would not be possible for MELLAPAK 500.Y, since the width of the surface is small. The small holes, which exist in the surface of MELLAPAK, may already be responsible for performing a similar role to the suggested structure.

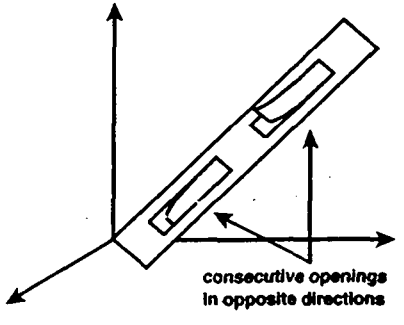

Figure 7.1 Suggestion of a new surface structure of MELLAPAK for mass transfer enhancement.

RECOMMENDATIONS FOR FUTURE WORK

More reliable data and understanding is necessary for accurate design of industrial separation columns with structured packings. Consequently, the use of high factors of safety, which increase the cost of such columns unnecessarily, would be avoided.

The evaluation of the volumetric gas phase mass transfer coefficient $k_G a$ could be a natural sequel to this research. These experiments would bring a complete picture of mass transfer with the structured packing MELLAPAK.

Future work could also study the influence of operational conditions on the mass transfer parameters $k_L a$, $k_G a$ and effective areas with different F-Factors and specific liquid loads, as employed in the present work. The influence of temperature and pressure should be studied too. Additionally, experiments with a change of the packing height could be carried out, especially with MELLAPAK 125.Y.

Mass transfer measurements with different physical properties is important. For such, new experimental methodologies may have to be developed. In this sense, measurements of effective areas with different viscosities may be a very hard task. A change of the viscosity may be associated with changes in other physical properties, such as diffusivity and surface tension. For the reaction of CO_2 with NaOH, if diffusion processes become more difficult, the danger of depletion might be even more serious. Depletion is the lack of hydroxide ions at the interface, which, disturbing the pseudo-first-order character of the reaction of CO_2 with NaOH, causes the method to be unsuitable for measuring effective areas.

The effect of various surface treatments and packing shapes on $k_L a$ and on the effective area is an interesting field of study, which would help in the design of more efficient packings. These experiments could begin by measurements of the effective area of the SULZER metal gauze packing, which exhibits an excellent wettability. Due to this fact, until now, it has been stated that the effective area equals the geometric area, which may not hold if there is liquid droplet formation: then the effective area is higher.

Measurement of axial dispersion in MELLAPAK could result in corrections to $k_L a$ data. However, the channel structure of MELLAPAK should prevent this undesired effect, especially when the rate of liquid renewal is significant. Thus, with a thin film over the packing and a small contact length, the influence of axial dispersion due to laminar flow is reduced to negligible values. This could be checked for 500.Y far from 100 % capacity. Axial dispersion due to backflow is improbable due to the mist eliminator effect of MELLAPAK. However, backflow should be more important with decrease in the packing geometric area. The point at which the liquid is sampled at the bottom of the column could be changed to obtain a profile of the effective area and of mass transfer coefficients in a cross section of the column.

Filming the flow inside the packing may increase the knowledge of mass transfer and hydrodynamics of structured packings. Such film could verify the presence of liquid droplets. A video may be most readily made with MELLAPAK 125.Y, in which the sheets are most widely spaced, and which exhibits the higher ratio of effective to geometric area. However, the act of filming the flow must not interfere with the flow itself.

CODE	DESCRIPTION FUNCTION
COL1	Main column in glass (QUICKFIT). Internal diameter: 295 mm. Column where measurements are made.
COL2	Secondary column in glass (QUICKFIT). Internal diameter: 295 mm. For gas temperature-and-humidity regulation.
B11	Side channel pump SIHI AOLK 4101 2 kW with "EX" protection. Pumps solution in the large circuit.
B12	Peristaltic pump Takes sample from bottom of COL1.
B13	Peristaltic pump Takes sample from top of COL1.
B14	Peristaltic pump Takes liquid sample from reactor R11.
B21	Peristaltic pump Takes gas sample from COL1.
B31	Side channel pump SIHI AOLK 3101 1.35 kW. Pumps water in the gas temperature-and-humidity regulating circuit.
B41	Centrifugal pump DIETZMOTOREN-KG DR 80b/2q 1.1 kW. Pumps solution in the small circuit.
C11	pO_2 Probe INGOLD. (only for k_La experiments) Measures concentration of O_2 in the solution entering COL1.
C12	pO_2 Probe INGOLD. (only for k_La experiments) Measures concentration of O_2 in the solution exiting COL1.
C13	pO_2 Probe INGOLD. (only for k_La experiments) Measures concentration of O_2 in R11.
D21	SULZER packing - Mellapak 250.Y. Mist eliminator at the exit of COL1.
E11	Degasser Degasses the solution exiting COL1.
FL11	Filter DN 32 PVC Filters the solution before the distributor of COL1.
FL12	Filter DN 25 PVC Filters the solution after HE11.
F11	Rotameter KROHNE G51.14 DN 50 stainless steel float (large flow).
F12	G41.12 DN 50 stainless steel float (small flow). Flow of solution entering COL1.
F13	Rotameter KROHNE G51.14 DN 50 stainless steel float. Flow of industrial water entering COL1.
F14	Rotameter KROHNE G19.12/ DN 15 stainless steel float.
F15	Rotameter KROHNE G19.25 DN 15 stainless steel float. Flow of cooling water for HE11.
F21	Instrument to measure volumetric flow of BARCOL-AIR AG Type HQMFC DN 160 and DN 100 (interchangeable) linked to a pressure sensor PI of ROLF MURI AG with a range of 0-350 Pa. Flow of gas entering COL1.
F22	Mass flow controller BROOKS 5851 E/A1 - A 1 B 2 A 1.
F23	Measures and regulates flow of CO_2

CODE	DESCRIPTION	FUNCTION
F24	Rotameter KROHNE 235903-1/1	Measures flow in the gas sampling circuit.
F31	Rotameter KROHNE G41.18 DN 25 stainless steel float.	Flow of water entering COL2.
F51	Rotameter KROHNE G19.08 DN 15 stainless steel float.	Flow of O_2 and N_2 to R11.
G21	Ventilator MEIDINGER FVR 4001.	Aspiration of gas. In parallel with G22.
G22	Ventilator MEIDINGER FVR 4000.	Aspiration of gas. In parallel with G21.
H11	Electric heating coil 1 kW.	Heating of solution in R41. Control with T12.
HE11	Heat exchanger	Final temperature control before COL1.
P11	U tube (WATER)	Measure of pressure (exit gas - COL1).
P12	U tube (WATER)	Measure of pressure (entering gas - COL1).
P13	U tube (WATER)	with angle of 40°. Measure of pressure drop in COL1.
P31	Manometer	Pressure in R31.
P32	U tube (WATER)	Pressure of exit gas from COL2.
P33	U tube (WATER)	Pressure of entrance gas into COL2.
P34	U tube (WATER)	Pressure drop in COL2.
pH11	pH-electrode	Measurement of the pH in reactor R14.
R11	Reactor 2500 l	Stocking of solution of large circuit.
R12	Reactor 120 l	For measuring flow and hold-up.
R13	Basin	For loading R11 with solid NaOH.
R14	Reactor 300 l	For neutralizing the solution from R11.
R31	Reactor 800 l	Stocking of water of the gas temperature-and-humidity regulating circuit.
R41	Reactor 300 l	Stocking of solution of the small circuit.
R42	Reactor 200 l	Stocking of solution of the small circuit.
R43	Basin	Collects liquid sample drawn off from COL1.
RCH	Evaporator CARBAGAS Type TF2.	Provides a constant flow of CO_2.
SM21	Static mixer SULZER SMV (4 elements)	For a homogeneous mixture CO_2-air.
T11	Thermometer	Temperature of solution in R11.
T12	Pt100	Temperature of solution entering COL1. Heating control of H11.
T13	Pt100	Temperature in COL1.
T21	Pt100	Temperature of gas entering COL1.
T31	Thermometer	Temperature of water in R31.
V111	Globe valve for F11.	
V112	Globe valve for F12.	Regulates flow of solution entering COL1.
V113	Globe valve	Regulates by-pass flow.
V121	Globe valve	Regulates air flow at the beginning of gas circuit.
V122	Globe valve	Regulates gas flow entering COL1.
V123	Globe valve	Regulates flow of gas aspirated by G21.
V124	Globe valve	Regulates flow of gas aspirated by G22.

CODE	DESCRIPTION	FUNCTION
V131	Globe valve	Regulates water flow in COL2.
V151	Globe valve	Entrance of cooling water for R11.
V152	Globe valve	Entrance of vapor for R11.
V153	Globe valve	Entrance of N_2 for R11.
V154	Globe valve	Entrance of O_2 for R11.
V161	Globe valve	Entrance of cooling water for R31.
V162	Globe valve	Entrance of vapor for R31.
V171	Globe valve	Feeds water to COL1.
V172	Globe valve for F14.	
V173	Globe valve for F15.	Cold industrial water for HE11.
V174	Globe valve	To cool R41.
V210	Gate valve	Choice of large circuit with small siphon.
V211	Gate valve	Choice of large circuit with large siphon.
V212	Pneumatic valve piloted by an electromagnetic valve LUCIFER RUEP 2.	Exit of R11.
V213	Gate valve	Drainage of R11.
V214	Gate valve	Drainage of large circuit.
V215	Gate valve	By-pass of pump B11.
V216	Gate valve	For the choice of large circuit.
V217	Gate valve	For liquid flow and hold-up measurements.
V218	Gate valve	To drain R12.
V219	Gate valve	To isolate R11 from the by-pass circuit.
V2110	Gate valve	Drains the tubing between E11 and R11.
V2111	Gate valve	Valve at the exit of R11 with manual manipulation.
V2112	Gate valve	Sample from bottom of COL1.
V2113	Gate valve	Sample from top of COL1.
V2114	Gate valve	Sample from R11.
V2115	Gate valve	Entrance of solid NaOH into R11.
V2116	Gate valve	By-pass of the filter FL12.
V2117	Gate valve	Entrance in reactor R14.
V2118	Gate valve	Drainage of reactor R14.
V221	Gate valve	To eventually draw off condensate.
V222	Gate valve	To eventually draw off condensate.
V231	Pneumatic valve piloted by an electromagnetic valve LUCIFER RUEP 2.	Drainage of R31.
V232	Gate valve	Drainage of the gas temperature-and-humidity regulating circuit.
V233	Gate valve	By-pass of pump B31.
V234	Gate valve	Drains siphon between R31 and COL2.
V235	Gate valve	Drainage of R31 before B31.
V240	Gate valve	Drains siphon of small circuit.
V241	Gate valve	For entrance into reactor R41.
V242	Gate valve	Exit of small circuit.
V243	Gate valve	Drains small circuit.
V244	Gate valve	For entrance into reactor R42.
V245	Gate valve	For exit from reactor R41.
V246	Gate valve	For exit from reactor R42.
V247	Gate valve	Drains reactor R42.
V248	Gate valve	To connect R43 to R41.

CODE	DESCRIPTION	FUNCTION
V249	Gate valve	To connect R43 to R42.
V2410	Gate valve	To connect R43 to R11.
V251	Gate valve	Exit of cooling water from R11.
V252	Gate valve	Exit of condensate from R11.
V253	Gate valve	Drains coil of R11.
V261	Gate valve	Exit of cooling water from R31.
V262	Gate valve	Exit of condensate from R31.
V263	Gate valve	Drains coil of R31.
V271	Gate valve	Industrial cold water for HE11 and stirrer of R11.
V272	Gate valve	To cool motor for the stirrer of R11.
V273	Gate valve	Valve near stirrer of R11.
V274	Gate valve	To cool HE11.
V275	Gate valve	To cool R14.
V311	3-way pneumatic gate valve SCHUBERT-SALZER 3620 piloted by an electromagnetic gate valve LUCIFER 131 K 06 with anti-explosive box.	For liquid flow and hold-up measurements.
V312	3-way gate valve	Choice between closing the large circuit or filling the plant with industrial water.
V321	glass 3-way gate valve	Gas sampling at top/bottom of the column COL1.
V322	3-way gate valve	Entrance of air to dry gas sampling circuit.
V323	3-way gate valve	Entrance of calibration gas for the gas analyser.
W11	Balance BUSCH Type 2.306.1-11 Ex. max 300 kg.	Weight measurements at the time of liquid flow and hold-up measurements.

Explanation of the code for the instrumentation and equipment in the table

Xabc

X: installation component
a: (only for valves)
- 1- globe valve
- 2- gate valve
- 3- 3-way valve

b:
- 1- large circuit of solution
- 2- gas circuit
- 3- gas temperature-and-humidity-regulating circuit
- 4- small circuit of solution
- 5- utilities for R11
- 6- utilities for R31
- 7- cold industrial or drinking water.

c: component number

All the steps given below should be folowed with the sketch of the main column, given by figure 2.3, section 4, in chapter II.

1 Procedure to change the MELLAPAK packing in the main column.

To change the MELLAPAK type, two people are necessary. The work lasts one and a half hours if done slowly. A top bar of the column frame should be removed to facilitate the work.

1.a Removal of the previous MELLAPAK type

1) Remove bolts between flange 1 and flange in the gas circuit.
2) Remove ground cable linked to flange 1, flange 2 and column frame.
3) Install two bolts in flange 2, opposite to gas outlet. These bolts will be necessary afterwards to suspend part 1.
4) Check that the three bars between flanges 3 and 4 prevent flange 3 from falling over port 1, when flange 3 is loosened.
5) Bring down the hoist, putting the rope around the gas exit from part 1 and the bolts of step 3.
6) Person 2 carefully holds part 1, while person 1 removes all bolts between flanges 2 and 3.
7) Person 1 operates the hoist, lifting part 1. Person 2 guides part 1 until it lies safely on the platform.
8) Remove the gasket.
9) Unscrew the tubing of the liquid inlet.
10) Take away the tube that guides the liquid into the distributor.
11) Put four bolts in flange 3 in opposing positions to be able to suspend together parts 2 and 3 of the column.
12) Bring down the hoist, putting the rope around the bolts of step 11.
13) Person 2 carefully holds parts 2 and 3, while person 1 removes all bolts between flanges 6 and 7.
14) Person 1 operates the hoist, lifting together parts 2 and 3. Person 2 guides parts 2 and 3 until they lie safely on the platform. Do pay attention that flange 3 in no case hits port 1.
15) Remove the gasket and tubes of the gas and liquid sampling.
16) Person 1, operating the hoist, slowly suspends the distributor. Person 2 guides the distributor to the platform.
17) Slowly take out the distributor's locating grid. It comes out with some difficulty, since the internal walls of the column are wavy.
18) Person 1 lifts the MELLAPAK elements with the hoist. Person 2, wearing gloves, guides the packing out of the column.

1.b Installation of the new MELLAPAK type

1) Person 1, operating the hoist, will help to introduce the packing elements into the column. Person 2, still wearing gloves, unfolds the collar around each element. Person 2 guides the new MELLAPAK type into the column, verifing that the sheets of two consecutive packing elements are at an angle of 90° to each other.
2) Gently put back by hand the distributor's locating grid. Check with a level that it is in a horizontal position.
3) Person 1, operating the hoist, lifts the distributor. Person 2 guides the distributor into the column. Be sure that the distributor lies perfectly on its grid.
4) Introduce the tube that guides the liquid into the distributor. Install the tubes of the gas and liquid sampling.
5) Reinstall the gasket.
6) Person 1 lifts parts 2 and 3 with the hoist. Person 2 guides parts 2 and 3 to the top of the column.
7) Person 1 positions five bolts between flange 6 and flange 7, leaving a space of one hole between each.
8) Persons 1 and 2 together screw opposing bolts between flange 6 and flange 7.
9) Reinstall the tube that guides the liquid into the distributor. Fix the tube of liquid inlet.
10) Reinstall the gasket.
11) Person 1 operates the hoist, lifting part 1. Person 2 guides part 1 to lie it over part 2. Person 2 keeps holding carefully part 1, while person 1 positions four bolts between flanges 2 and 3, leaving one space between each bolt. Person 1 positions two bolts between flange 1 and gas outlet. These must be removed again for step 13. Safety reasons, however, demand their installation here.
12) Persons 1 and 2 together screw opposing bolts between flange 2 and flange 3.
13) Remove the rope of the hoist.
14) Screw four bolts between flange 1 and gas tube, leaving a space between each bolt.
15) Connect the ground cable between part 1, part 2 and the column frame.

2 Procedure to pack the main column with irregular packing.

To remove or install irregular packing in the main column, two people are necessary. The work lasts at least 4 hours and it must be done slowly. It is more difficult than with the structured packings.

2.a Removal of the irregular packing

1) Same procedure as for topic 1.a until step 17.
2) Remove the packing pieces first by hand and then with a bucket, when it is very deep. Be carefull not to break the pieces.

2.b Installation of the irregular packing

1) Same procedure as for topic 1.a until step 17. Remove the packing inside part 4 of the column, as well as all intrumentation connected to COL1.
2) Put four bolts in flange 7 in opposite directions to be able to suspend part 4 of the column. Remove the fixation to the column frame.
3) Person 2 carefully holds part 4, while person 1 removes all bolts between flanges 8 and 9.
4) Person 1 operates the hoist, lifting part 4. Person 2 guides parts 4 until it lies safely on the platform.
5) Part 4 of the column will be mounted on the platform on a special blind flange. Install the red ring which was between parts 4 and 5 of the column over the special blind flange. Part 4 of the column is to be mounted on the red ring and to be fixed tightly to the blind flange. Install valves in the red ring.
6) Part 4 of the column should be fixed to the column frame. Take the hoist away. Be careful that flange 7 does not fall over ports 2 and 3.
7) Install wire grid over the supporting grid. Fill part 4 completely with water. Attention to leakages.
8) Let the pieces fall slowly and randomly inside part 4. Do not stir the water. The number of pieces put inside must be known to determine the specific geometric area. Instead of counting all pieces (which takes too long), weigh a known large quantity of pieces before puting them inside. Determine the weight of all extra packing pieces which will be put inside the column. A simple calculation gives the number of pieces inside part 4. The specific geometric area results from the multiplication of the number of pieces by the geometric area of one piece divided by the packed volume in the column.
9) Drain off all the water using the valves installed in step 5.
10) Bring down the hoist, putting the rope around the bolts of step 4.
11) Dismount part 4 from the blind flange.
12) Person 1 operates the hoist, lifting part 4. Install the red ring back in the column over part 2. Person 2 guides parts 4 until it lies safely over the red ring on the main column.
13) Person 2 carefully holds part 4, while person 1 positions all bolts between flanges 8 and 9.
14) Persons 1 and 2 together screw opposing bolts between flanges 8 and flange 9.
15) Check with a level that part 4 is in a vertical position.
16) Fix part 4 of the column to the column frame. Connect all instrumentation to the column.
17) Same procedure as for topic 1.b after step 2.

Procedure for the experiments

The flowchart of the procedure for these experiments is given in figure 4.1, section 2, chapter IV. The different steps with their tasks are detailed below.

DRAINAGE
Completely open the following valves:
1 Large circuit (only if reactor R11 has neutral pH)
  1st floor: V2117, V2118; 2nd floor: V214; 3rd floor: V218, V2110;
  Office H4 595: V212
2 Drawing off the condensate
  4th floor: V222; 5th floor: V221
3 Gas temperature-and-humidity-regulating circuit
  2nd floor: V232; 3rd floor: V234; Office H4 595: V231
4 Small circuit (only if reactors R11, R41 and R42 have neutral pH)
  3rd floor: V240, V243, V245, V246, V247

If the reactor R42 does not have neutral pH, fill R11 with the solution from R42 for later neutralisation:
Close on 3rd floor: V216, V245 Close on 4th floor: V111, V112
Open on 3rd floor: V246, V242, V219 Open on 4th floor: V113
Turn on pump B41. 3rd floor

START LARGE CIRCUIT FOR MEASURE OF LIQUID FLOW
1 Open the following valves:
  4th floor: V111, V112, V113, V271, V272, V274, V172, V173
  3rd floor: V211, V216, V217, V219
  1st floor: V2117
2 Close V241, V242, and V244. 3rd floor
3.1 Turn on electricity at control board.
3.2 Start stirrer of reactor R11.
3.3 Open V212.
3.4 Turn on pump B11. H4 595
4.1 Turn on the series of thermometers.
4.2 Close V2112. 4th floor
5.1 Close V218.
5.2 Verify that balance W11 with R12 is in place.
5.3 Tare balance W11. 3rd floor
6.1 For each chosen flow:
  Adjust V111, V112 and V113. 4th floor
  Put V311 at position EXTERIEUR. Measure the time.
  Put V311 at position CIRCUIT. H4 595
  Open V113 and close V111 and V112. 4th floor
  Read the weight indicated by W11.
  Open V218 to drain R12 into R14.
  Neutralisation of R14 (see below) 1st floor
  Close V218. Tare W11. 3rd floor

Neutralisation of R14:
a) Cool R14 with industrial water.
b) Turn on stirrer of R14.
c) Put a calibrated pH electrode into R14.
d) Introduce acid into R14 until the pH value is between 6.5-9.0.
e) Stop stirrer of R14.
f) Take the pH elctrode out of R14.
g) Open V2118 to drain off R14.
h) Stop cooling in R14.
i) Close V2118 1st floor

7.1 Stop the stirring in reactor R11.
7.2 Turn off pump B11.
7.3 Close V212.
7.4 Turn off electricity at control board. H4 595
8 Close V211 and V219. 3rd floor
9.1 Turn off series of thermometers.
9.2 Close V113, V271, V272, and V274.
9.3 Leave partially open: V111, V112, V2112, V172, and V173. 4th floor

PREPARATION OF 2M NaOH SOLUTION
1 Turn on electricity at control board. H4 595
2.1 Open V271, V272 and V113
2.2 Close V111 and V112 4th floor
3.1 Fill reactor R11 (2500 l) with demineralized water.
Max. flow: 20 l/min.
3.2 Open V2115
3.3 Turn on stirrer of R11. Position: 5.0 3rd floor
4 Introduce slowly and carefully 200 kg of solid grains of NaOH by R13.
(Control the temperature in R11. To cool R11 - open V251 and V151)
At the end, rince R13 with water. 4th floor
5.1 Take a sample from R11 to verify the concentration.
5.2 Stop stirrer of R11.
5.3 Close V219 and V2115 3rd floor
6.1 Close V271 and V272 4th floor

CHANGE CO_2 BOTTLES
1.1 Close corresponding CO_2 manifold valve.
1.2 Close bottle valve.
1.3 Open screw of bottle 1/4 of a turn to reduce pressure.
1.4 Change bottles. 5th floor

PREPARE CO_2 SYSTEM
1.1 Fill RCH with demineralised water.
1.2 Plug in potentiometer and adjust it.
1.3 Open valves on the bottles.
1.4 Open valves of the CO_2 manifold.
1.5 Open valve before RCH.
1.6 Open valve after RCH.
1.7 Adjust high pressure reducer.
1.8 Open the needle valve.
1.9 Adjust low pressure regulator (at least 5 bars). 5th floor

START LARGE CIRCUIT
1 Turn on electricity at control board. H4 595
2 Fill reactor R31 with demineralized water.
Max. flow: 20 l/min. 3rd floor
3.1 Completely close the following valves:
3rd floor: V241, V242, V244 4th floor: V113
3.2 Partially open the following valves:
4th floor: V111, V112, V121, V122, V172, V173 5th floor: V131
3.3 Completely open the following valves:
3rd floor: V211, V216, V219, V2410 4th floor: V271, V272, V274
5th floor: V123, V124
4 Determine the temperature of R31.
To heat R31 with vapor, open V262 and V162.
To cool R31 with industrial water, open V261 and V161.
Start the stirrer of reactor R31: position 2.0. 3rd floor
5 Turn on the series of thermometers.
Turn on the gas analyser and perform calibration.
Let air flow through the gas sampling circuit. 4th floor
6.1 Open V231.
6.2 Turn on B31.
6.3 Turn on G21 or G22.
6.4 Turn on stirrer of R11.
6.5 Open V212 and turn on B11. H4 595
7.1 Adjust V111, V112, V113, V172, and V173.
7.2 Stop air flow in the gas sampling circuit.
7.3 Prepare gas sampling circuit for probe taking.
7.4 Turn on B21, checking the flow that passes in the gas analyser.
7.5 Open and regulate the mass flow controllers F22 and F23.
7.6 Open V2112 and V2113.
7.7 Turn on pumps B12 and B13. 4th floor

MEASUREMENTS OF "a"
Person 1
For each liquid load:
During the first two minutes, control of the rotameters F11 or F12.
Every 4 minutes (2-6-10):
Put flasks for probe taking (IN/OUT) in R43.
Control and write down the flowrates F11/F12, F14 and F15.
Take away flasks from R43.
Read pressures P12 and P13.
Control and write down the flowrates F11/F12, F14 and F15.
Person 2
For each liquid load:
During the first minute, start the program.
Every 2 minutes (1-3-5-7-9):
data acquisition with the computer of a gas flow.
acquisition of a flow from a channel of the mass flow controller.
change the channel.
acquisition of CO_2 concentration.
acquisition and manual control of T21, T12 and T13.
acquisition and manual control of F14 and F15.
acquisition of CO_2 concentration.
The position of the gas probe taking must be changed after 2-4 readings.
When the liquid load changes, give information to the computer.
At the end of the experiment, store and list of the results.

CHANGE LIQUID FLOW
1.1 Adjust the new liquid flow with V111, V112, and V113.
1.2 Turn off pumps B12 and B21.
1.3 Let air flow through the gas sampling circuit.
1.4 Empty the collector to take a sample at the bottom of the column.
1.5 After 30s, put the collector in the desired position.
1.6 Prepare gas sampling circuit for sampling.
1.7 Turn on pumps B12 and B21. 4th floor

CHANGE GAS FLOW
1 Close supply of CO_2 (F22 and F23). 4th floor
2 Turn off B11. Close V212. Turn off G21 or G22 (if necessary) to change F21. H4 595
3.1 Partially close V131 (if gas flow becomes stronger).
3.2 Adjust V123 and V124. 5th floor
4.1 Turn off pumps B12, B13 and B21.
4.2 Partially close V111 and V112. Completely close V113.
4.3 Change F21 if necessary.
4.4 Adjust V121 and V122 for desired flow.
4.5 Empty collector to take a sample from bottom of column.
4.6 Let air flow through the gas sampling circuit.
4.7 Prepare gas sampling circuit for sampling. 4th floor
5 Open V212 and turn on B11. H4 595
6.1 Adjust V111, V112.
6.2 Turn on B12, B13 and B21. 4th floor
7 Turn on G21 or G22. H4 595
8 Adjust V131. 5th floor
9 Adjust F22 and F23. 4th floor

STOP THE PLANT
1.1 Close mass flow controllerers.
1.2 Close the gas analyser and stop the pump B21. 4th floor
2.1 Turn off G21 or G22.
2.2 Stop stirring in reactors R11 and R31.
2.3 Turn off pumps B11 and B31.
2.4 Close V212 and V231.
2.5 Turn off electricity at control board. H4 595
3.1 Turn off series of thermometers.
3.2 Turn off B12 and B13.
3.3 Close V113, V271, and V274.
3.4 Leave V111, V112, V172, and V173 partially open.
3.5 Leave V2112 and V2113 open. 4th floor
4 Close V211, V219, V2410. Close V162 and V262 or V161 and V261. 3rd floor

CLEAN THE COLUMN WITH H_2O OR ACID

1 Fill reactor R41 with demineralized water.
2 Fill reactor R42 with diluted acid.
3 For cleaning with acid:
Close the valves: 3rd floor: V216, V241, V245 4th floor: V113
Open the valves: 3rd floor: V242, V244, V246 4th floor: V111, V112
Turn the pump B41 on (3rd floor).
Stop the pump B41.
4 For cleaning with water:
Close the valves: 3rd floor: V216, V244, V246 4th floor: V113
Open the valves: 3rd floor: V241, V242, V245 4th floor: V111, V112
Turn the pump B41 on (3rd floor).
Stop the pump B41.

STOP CO_2 SYSTEM

1.1 Close valve after RCH.
1.2 Turn off potentiometer and unplug it.
1.3 Close valve before RCH (when it is cool).
1.4 Close the valves on the bottles.
1.5 Close all valves of the manifold.
1.5 Open an unused CO_2 manifold to reduce the pressure. 5th floor

TITRATION

1. Prepare the sample to titrate:
Mix togther equal volumes (15 ml) of the solution and 1 M HCl.
2. Bring the sample to the DOSIMAT. Put a clean pH-electrode into the solution. Install the exchange unit with 1 M HCl on the DOSIMAT. Switch on the DOSIMAT and the pH-METER.
Set with the DOSIMAT's keyboard:
a) using the key RATE:
the adding rate of 15 ml/min and the filling rate of 20 ml/min.
b) the operation mode DIS C using the key MODE.
c) using the key ΔVOLUME:
V-DIS - the maximum estimated volume of 1 M HCl to be consumed.
V-LIM - a volume above which the feeding of HCl must stop.
Set the pH-METER - press buttons: "meas" and "pH".
3. Run the program DOSPH7.PGM, inputing the necessary data.
When required, press the GO key on the keyboard to add 1 M HCl.
4. When the BEEP tone sounds, immediately press the button FILL.
5. Install the exchange unit with 0.1 M HCl. Using the key RATE on the DOSIMAT's keyboard, define the feeding rate of 1 ml/min and the filling rate of 20 ml/min. Set with the key ΔVOLUME:
a) V-DIS - the maximum estimated volume of 0.1 M HCl to be consumed.
b) V-LIM - a volume above which the feeding of HCl must stop.
6. When required, press the GO key on the keyboard to add 0.1 M HCl.
7. When the BEEP tone sounds, press the button FILL.
8. Follow the instructions given by the program until its end.
Press the pH-METER's button "stand-by".
Clean the pH-electrode with water.

LIST OF VALVES THAT REMAIN IN PRINIPLE IN A DETERMINED POSITION:

-ALWAYS COMPLETELY OPEN:
4th floor: V2112, V2113
3rd floor: V217, V273
2nd floor: V2111
-ALWAYS CLOSED WHEN INSTALLATION STOPS:
5th floor: V221, F22, F23
4th floor: V113, V222, V171, V271, V274
Office H4 595: V212, V231
3rd floor: V210, V218, V219, V2110, V2114, V2115, V2116, V234, V240, V243, V243, V247, V151, V152, V153, V154, V251, V252, V253, V161, V162, V261, V262, V263, V174
2nd floor: V213, V214, V215, V232, V233
1st floor: V2117, V2118
-ALWAYS POSITION CIRCUIT for the 3-way valves:
Office H4 595: V311
4th floor: V312, V322, V323

Liquid flowrates used for the experiments

CODE	ROTAMETER POSITION	B [m^3/m^2h]	Number of points
F12	60	12.3 ± 0.1	7
F12	100	19.8 ± 0.1	8
F11	70	40.1 ± 0.3	5
F11	85	48.9 ± 0.1	6
F11	100	57.7 ± 0.3	5
F11	120	71.5 ± 0.6	5

Gas flowrates used for the experiments

VALVES V122	V123	CO_2 Flow F22 and F23	F21 [Volt]	approx F-Factor	
2	1	25 %	2.0	0.8	***
C	0	40 %	0.7	1.4	
0.75	0	50 %	1.5	1.9	
1.5	0	80 %	2.7	2.5	
2.5	0	90 %	3.9	3.1	

The values are approximate, considering G21 working.
Code: C - closed 0 - opened
Remark: *** - use small tube from BARCOL-AIR AG.

Required material and manpower

Required material for all runs:

CO_2:

20 bottles 40 l with dip tube from CARBAGAS AG. During a run, 3 bottles are connected and one bottle stays ready for replacement. Do not ever empty a bottle completely.

Calibration gases:

20 l of a certificated gas mixture 1% CO_2 in synthetic air.
1 N_2 bottle

demineralized water:

2500 l for each solution in reactor R11.
800 l to fill the reactor R31.
300 l to fill the reactor R41/R42.

NaOH:

1000 kg of solid NaOH for 5 different 2 M NaOH solutions of 2500 l.

HCl solutions for titration:

36 l of a HCl 1M solution.
24 l of a HCl 0.1 M solution

Required manpower:

To run the experiments two people are required. For safety reasons, two people should be present together in the laboratory during an experiment.

Procedure for the experiments

The flowchart of the procedure for these experiments is given in figure 4.1, section 2, chapter IV. The different steps with their tasks are detailed below.

DRAINAGE

Completely open the following valves:

1 Large circuit
2nd floor: V214; 3rd floor: V218; Office H4 595: V212
2 Drawing off the condensate
4th floor: V222; 5th floor: V221
3 Gas temperature-and-humidity-regulating circuit
2nd floor: V232; 3rd floor: V234; Office H4 595: V231
4 Small circuit
3rd floor: V240, V243, V245, V246, V247

SATURATION OF R11 WITH O_2

1 Turn on electricity at control board. H4 595
2 Cool motor for stirrer of R11 - Open V271 and V272 (1 turn). 4th floor
3.1 Fill reactor R11 (2500 l) with demineralized water.
Max. flow: 20 l/min.
3.2 Start stirrer of R11 and adjust it: pos. 4.5.
3.3 Heat R11 with vapor (weak flow). Open V252 and V152.
3.4 Stop heating at ~ 80°C - Close V152 and V252.
3.5 Close R11 tightly (V210, V211, V219, and V212).
3.6 Cool R11 slowly (weak flow). Open V251 and V151.
3.7 Introduce O_2 when T11 ~ 60°C.
3.8 Stop cooling at ~ 20°C - Close V151 and V251.
Stop stirring in R11. 3rd floor
4 Control saturation with C13. Close V272 and V271. 4th floor

If there is already a considerable concentration of O_2 in R11,
(if necessary) fill R11 with demineralized water from R42:
Close on 3rd floor: V216, V245 Close on 4th floor: V111, V112
Open on 3rd floor: V246, V242, V219 Open on 4th floor: V113
Turn on pump B41 and introduce O_2 into R11.

PREPARE CALIBRATION OF PROBES

1.1 Completely fill the two cylinders with demineralized water.
1.2 Slowly bubble O_2 and N_2 through each cylinder for 1 hour.
1.3 Control the stationary state with the pO_2 probes. 4th floor

FINISH CALIBRATION OF PROBES

1.1 Put probes back in their respective tubes in the plant.
1.2 Stop bubbling.
1.3 Close cylinders with rubber stoppers. 4th floor

START - SYSTEM IN EQUILIBRIUM

1. Turn on electricity at control board. H4 595
2 Fill reactors R31 and R41 with demineralized water.
Max. flow: 20 l/min. 3rd floor
3.1 Completely close the following valves:
3rd floor: V211, V216, V244, V246, V249, V161, V162, V261, V262
4th floor: V113
Office H4 595: V212, V231
3.2 Partially open the following valves:
4th floor: V111, V112, V121, V122, V172, V173
5th floor: V131
3.3 Completely open the following valves:
3rd floor: V241, V242, V245, V248
4th floor: V271, V272, V274
5th floor: V123, V124
4.1 Determine the temperature of R31.
To heat R31 with vapor, open V262 and V162.
To cool R31 with industrial water, open V261 and V161
(Very weak flows are usually sufficient).
Turn on stirrer of R31: position 2.0.
4.2 Turn on pump B41.
4.3 Turn on stirrer of R41.
4.4 Turn on heater H11/Adjust V174 (~ 1/12 of a turn). 3rd floor
5.1 Turn on series of thermometers.
5.2 Adjust V111, V112.
5.3 Open V2112 and V2113. Turn on pumps B12 and B13. 4th floor
6.1 Open V231.
6.2 Turn on B31.
6.3 Turn on G21 or G22. H4 595
7.1 Adjust V121 and V122. 4th floor
8 Adjust V131. 5th floor

START LARGE CIRCUIT

1 Turn off pumps B12 and B13.
Partially close V111 and V112. 4th floor
2.1 Turn off pump B41.
2.2 Stop stirring in R41.
2.3 Stop H11/V174.
2.2 Close V242, V241, and V248.
2.3 Open V211, V216, V219, and V249. 3rd floor
3.1 Turn on stirrer of R11.
3.2 Open V212 and turn on B11. H4 595
4.1 Adjust V111, V112, V113, V274, V172, and V173.
4.2 Turn on B12 and B13. 4th floor

CHANGE LIQUID FLOW

1 Introduce O_2 in R11 to increase C13 (open V154). 3rd floor
2.1 Adjust the new liquid flow with V111, V112, and V113.
2.2 Turn off pump B12.
2.3 Empty the collector that takes sample at the bottom of the column.
2.4 After 30s, put the collector in the desired position.
2.5 Turn on pump B12. 4th floor
3 Stop O_2 for R11 (close V154). 3rd floor

CHANGE GAS FLOW

1	Turn off B11. Close V212. Turn off G21 or G22 if it is necessary to change F21.	H4 595
2.1	Partially close V131 (if gas flow becomes stronger).	
2.2	Adjust V123 and V124.	5th floor
3.1	Turn off pumps B12 and B13.	
3.2	Partially close V111 and V112. Completely close V113.	
3.3	Change F21 if necessary.	
3.4	Adjust V121 and V122 for desired flow.	
3.5	Empty collector to take a sample from bottom of column.	4th floor
4.1	Close V211, V216, V219, V244, and V249.	
4.2	Open V241, V242, V245, and V248.	
4.3	Turn on pump B41.	
4.4	Turn on stirrer of R41.	
4.5	Turn on heater H11/Adjust V174 (~ 1/12 of a turn).	3rd floor
5.1	Adjust V111, V112.	
5.2	Turn on B12 and B13.	4th floor
6	Turn on G21 or G22.	H4 595
7	Adjust V131.	5th floor

STOP INSTALLATION WITHOUT MEASURE OF LIQUID FLOW

1.1	Turn off G21 or G22.	
1.2	Stop stirrer of R11 and R31.	
1.3	Turn off pumps B11 and B31.	
1.4	Close V212 and V231.	
1.5	Turn off electricity at control board.	H4 595
2.1	Turn off series of thermometers.	
2.2	Turn off B12 and B13. Take pO_2 probes from the installation.	
2.3	Close V113, V271, and V274.	
2.4	Leave V111, V112, V172, and V173 partially open.	
2.5	Leave V2112 and V2113 open.	4th floor
3	Close V211, V219, V162 and V262 or V161 and V261.	3rd floor

STOP INSTALLATION WITH MEASURE OF LIQUID FLOW

1.1	Turn off G21 or G22.	
1.2	Stop stirring in reactor R31.	
1.3	Turn off pump B31.	
1.4	Close V231.	H4 595
2.1	Turn off B12 and B13. Take pO_2 probes from the installation.	
2.2	Close V2112.	4th floor
3.1	Close V218, V162 and V262 or V161 and V261.	
3.2	Verify that balance W11 with R12 is in place.	
3.3	Tare balance W11.	3rd floor
4.1	For each chosen flow:	
	Adjust V111, V112 and V113.	4th floor
	Put V311 at position EXTERIEUR. Measure the time.	
	Put V311 at position CIRCUIT.	H4 595
	Open V113 and close V111 and V112.	4th floor
	Read the weight indicated by W11.	
	Open V218 to drain R12.	
	Close V218. Tare W11.	3rd floor

5.1 Stop the stirrer of R11.
5.2 Turn off pump B11.
5.3 Close V212.
5.4 Turn off electricity at control board. H4 595
6 Close V211 and V219. 3rd floor
7.1 Turn off series of thermometers.
7.2 Close V113, V271, V272, and V274.
7.3 Leave partially open: V111, V112, V2112, V172, and V173. 4th floor

START INSTALLATION FOR MEASURE OF LIQUID FLOW
1 Open the following valves:
4th floor: V111, V112, V113, V271, V272, V274, V172, V173
3rd floor: V211, V216, V219
2 Close V241, V242, and V244. 3rd floor
3.1 Turn on electricity at control board.
3.2 Start stirring in reactor R11.
3.3 Open V212.
3.4 Turn on pump B11. H4 595
4.1 Turn on the series of thermometers.
4.2 Close V2112. 4th floor
5 Follow the procedure STOP INSTALLATION WITH MEASURE OF LIQUID FLOW from point 3.1 to the end.

STOP INSTALLATION AFTER SYSTEM IN EQUILIBRIUM
1.1 Turn off pump B41.
1.2 Stop stirring in R41.
1.3 Stop H11/V174.
1.4 Close V242, V241, and V248.
1.5 Close V261 and V161 or V262 and V162. 3rd floor
2.1 Turn off G21 or G22.
2.2 Turn off B31.
2.3 Close V231.
2.4 Stop stirring in R31.
2.5 Turn off electricity at control board. H4 595
3.1 Turn off B12 and B13. Take pO_2 probes from the installation.
3.2 Close V113, V271, V272, and V274.
3.3 Leave open: V111, V112, V2112, V172, and V173. 4th floor

BEGIN WITH LARGE CIRCUIT
1 Turn on electricity at control board. H4 595
2 Fill reactor R31 with demineralized water.
Max. flow: 20 l/min. 3rd floor
3.1 Completely close the following valves:
3rd floor: V241, V242, V244, V246, V248, V161, V162, V261, V262
4th floor: V113
Office H4 595: V212, V231
3.2 Partially open the following valves:
4th floor: V111, V112, V121, V122, V172, V173
5th floor: V131
3.3 Completely open the following valves:
3rd floor: V211, V216, V219, V249
4th floor: V271, V272, V274
5th floor: V123, V124

4 Determine the temperature of R31.
To heat R31 with vapor, open V262 and V162.
To cool R31 with industrial water, open V261 and V161.
Start the stirrer of reactor R31: position 2.0. 3rd floor
5 Turn on the series of thermometers. 4th floor
6.1 Open V231.
6.2 Turn on B31.
6.3 Turn on G21 or G22. H4 595
7 Follow the procedure START LARGE CIRCUIT from point 3.1 to the end.

OBSERVATIONS:

1) DO NOT TURN OFF THE AMPLIFIERS OF THE pO_2 PROBES.
(The probes must be polarized at least 6 hours before the runs).

2) LIST OF VALVES THAT REMAIN IN PRINIPLE IN A DETERMINED POSITION:

-ALWAYS COMPLETELY OPEN:
4th floor: V2112, V2113
3rd floor: V217, V273
2nd floor: V2111
-ALWAYS CLOSED WHEN INSTALLATION STOPS:
5th floor: V221
4th floor: V113, V222, V171, V271, V274
Office H4 595: V212, V231
3rd floor: V210, V218, V219, V2110, V2114, V2115, V2116, V234, V240, V243, V247, V2410, V151, V152, V153, V154, V251, V252, V253, V161, V162, V261, V262, V263, V174
2nd floor: V213, V214, V215, V232, V233, V235
1st floor: V2117, V2118
-ALWAYS POSITION CIRCUIT for the 3-way valves:
Office H4 595: V311
4th floor: V312, V322, V323

Liquid flowrates used for the experiments

CODE	ROTAMETER POSITION	B [m^3/m^2h]	Number of points
F12	60	13.41 ± 0.02	5
F12	80	17.36 ± 0.03	5
F12	100	21.29 ± 0.07	7
F11	70	42.6 ± 0.3	5
F11	85	51.2 ± 0.2	5
F11	100	60.8 ± 0.3	5
F11	120	74.3 ± 0.3	10

Gas flowrates used for the experiments

VALVES V122	VALVES V123	F21 [Volt]	approx F-Factor	
2	1	2.0	0.8	***
C	0	0.7	1.4	
0.75	0	1.5	1.9	
1.5	0	2.6	2.5	
2.5	0	3.9	3.1	

The values are approximate for G21 working.
Code: C - closed 0 - opened
Remark: *** - use small tube from BARCOL-AIR AG.

Required material and manpower

Required material:

oxygen:

about 90 l O_2 saturates 2500 l water at 25°C. Heating the reactor to 80°C and introducing O_2 during cooling reduces consumption. About 600 Nl/h is used to keep the main reactor saturated. An estimated consumption of 50 Nl/h of O_2 is used for probe calibration (secton 5.3.2, chapter II).

nitrogen

an estimated consumption of 50 Nl/h for probe calibration.

demineralized water:

2500 l to fill the main reactor R11.
800 l to fill the reactor R31.
300 l to fill the reactor R41.
Once the all reactors are full, there is no need to empty them. To fill the reactors, do not use flowrates higher than 20 l/min. The school facilities can not supply higher flows.
Flowrate measurements need about 120 l/point.

Required manpower:

To run k_La experiments efficiently and with precision, two people are necessary:

Person 1:

mantain constant and proper working conditions. Acts to correct eventual changes, especially of liquid flow and temperature.

Person 2:

runs computer, inputs data points, takes notes.

The best way to prevent any accident is to follow with attention all steps of the procedure. The situation of all equipments and valves in the table "Etat de l'installation" must be always valid. The pilot plant may be stopped completely at any moment:

EMERGENCY STOP:
Control board in office H4 595.
2nd floor.

In principle, k_La experiments offer no risk whatsoever. All runs were conducted with air and water with dissolved oxygen at 22°C and at atmospheric pressure. The noise from the fans might dammage the audition. Despite the fact that noise absorbers (the noise was about 100 dB) were installed at the fans' exit, earphones were always used.

The experiments for measuring the mass transfer area uses 2500 l of a NaOH solution initially 2M, which may damage eyes and skin severely. Therefore, accidents had to be prevented by means of a carefull planification, using the experience acquired during the k_La measurements and previous experiments with air and water, when eventual leakages in the pilot plant were controlled. The use of protection glasses during the experiments is OBLIGATORY. Gloves should be used during probe taking.

A system to fill the reactor R11 with NaOH solid grains was conceived, so that there would not be any possible contact with NaOH solution. The solid grains are fed on the forth floor and flow by gravity in a tube into the reactor R11, which is closed and has demineralised water inside being stirred. The temperature of the reactor R11 must be controlled. Special care has to be taken during the discharge of solid grains of NaOH into the container R13 on the forth floor. The use of glasses, gloves and even of a gas mask is very important.

A perfect comprehension of the pilot plant is absolutely required before the experiments. The table below summurises sytematically what action to take if a not attend stituation occurs.

Table E.1 Troubleshooting.

	CAUSE		ACTION
1	Leakage of NaOH solutions		
	1.1 No experiment is running	1.1	Follow procedure DRAINAGE.
	1.2 During an experiment	1.2	Stop de plant immediately.
2	Flooding of the column	2	Reduce the liquid flow rate, by oppening V113 and V219 (eventually stop the pump B11).
3	Lack of compressed air	3	The valves V212 and V231 close and the pumps B11 and B31 stop automatically.
4	Power cut	4	The valves V212 and V231 close and the pumps B11 and B31 stop automatically.
5	An equipment in the control board switches off (yellow light on).	5	Open the control board and reset the fuse.

H=80 mm

Carbonate IN		Carbonate OUT		Flowrate		Density	Absorption rate		Gas composition	
mean *10-3 [mol/l]	std *10-3 [mol/l]	mean *10-3 [mol/l]	std *10-3 [mol/l]	mean *10-2 [kg/min]	std *10-2 [kg/min]	[kg/l]	mean *10-4 [mol/s]	std *10-4 [mol/s]	mean *10-2 [-]	std *10-2 [-]
163	1	214	1	42	1	1.062	3.4	0.2	70	3
54	1	107	1	48	1	1.078	3.9	0.2	80.1	0.6
93	1	142	5	47	2	1.078	3.6	0.6	78	1
153	2	169	2	55	2	1.080	1.4	0.3	31.0	0.1
168	1	233	5	46.8	0.5	1.080	4.7	0.5	95	5
15	1	32	0	51.9	0.5	1.080	1.4	0.1	31	2
23	0	52	0	57.7	0.3	1.080	2.58	0.01	55.6	0.6
79	1	135	1	53.4	0.4	1.083	4.6	0.2	94	6

H=52 mm

Carbonate IN		Carbonate OUT		Flowrate		Density	Absorption rate		Gas composition	
mean *10-3 [mol/l]	std *10-3 [mol/l]	mean *10-3 [mol/l]	std *10-3 [mol/l]	mean *10-2 [kg/min]	std *10-2 [kg/min]	[kg/l]	mean *10-4 [mol/s]	std *10-4 [mol/s]	mean *10-2 [-]	std *10-2 [-]
34	0	60	1	66.5	0.2	1.081	2.7	0.1	76	2
49	0	72	5	66.7	0.9	1.080	2.4	0.5	67	1
69	0	84	1	67.2	0.1	1.081	1.6	0.1	50.6	0.3
81	2	109	3	68.2	0.0	1.081	2.9	0.5	94	5

Notes:

mean: mean value of an average from at least four measurements

std: standard deviation of the average

Point	B [m3/m2h]	F-Factor	aG/aL [-]	aL [m2/m3]	mean aL [m2/m3]	std aL [m2/m3]	aL std/mean [%]	cap [%]	Set
35.1	12.3	3.25	0.63	337	373	51	14	90	1.1
35.3	12.3	3.20	0.92	408					
1.1	19.8	1.45	0.94	292					
10.4	19.8	1.46	0.68	347	314	29	9	55	1.2
38.2	19.8	1.48	1.25	302					
2.1	19.8	1.99	1.00	318					
9.4	19.8	1.93	0.79	315	310	12	4	70	1.3
36.1	19.8	1.99	1.21	296					
3.1	19.8	2.67	-	317	310	10	3	89	1.4
8.2	19.8	2.66	0.55	302					
4.1	19.8	3.22	0.74	309					
7.1	19.8	3.21	0.99	240	299	55	18	***	1.5
35.2	19.8	3.21	1.16	348					
5.1	40.1	0.85	0.97	360	360	0	0	46	1.6
6.1	40.1	0.83	0.71	359					
1.3	40.1	1.44	0.87	316					
10.2	40.1	1.47	0.71	399	336	55	16	67	1.7
38.1	40.1	1.49	1.54	294					
2.3	40.1	1.95	0.70	327					
9.2	40.1	1.94	0.68	413	359	47	13	82	1.8
11.1	40.1	1.97	0.79	338					
36.2	40.1	1.97	1.27	324					
3.3	40.1	2.63	0.35	373	353	28	8	***	1.9
8.1	40.1	2.67	0.60	333					
37.1	48.9	2.48	0.95	415					
37.2	48.9	2.52	1.43	351	383	35	9	***	1.10
37.3	48.9	2.47	1.10	403					
5.3	57.7	0.83	0.83	370	386	23	6	52	1.11
6.3	57.7	0.83	0.69	402					
1.2	57.7	1.44	0.92	407	407	0	0	74	1.12
10.3	57.7	1.46	0.69	407					
2.2	57.7	1.96	0.82	381	369	17	5	90	1.13
9.3	57.7	1.93	0.72	356					
3.2	57.7	2.54	0.46	447					
8.3	57.7	2.46	-	484	477	28	6	***	1.14
12.1	57.7	2.48	0.96	501					

Point	B [m3/m2h]	F-Factor	aG/aL [-]	aL [m2/m3]	mean aL [m2/m3]	std aL [m2/m3]	aL std/mean [%]	cap [%]	Set
5.2	71.5	0.83	0.86	397					
6.2	71.5	0.82	0.72	364	366	30	8	57	1.15
14.1	71.5	0.85	0.84	337					
1.4	71.5	1.44	1.04	324					
10.1	71.5	1.45	0.65	447	409	74	18	80	1.16
13.1	71.5	1.48	0.71	457					
2.4	71.5	1.94	0.75	413	438	35	8	96	1.17
9.1	71.5	1.93	0.64	463					

Notes:

Definitions of point and set are to be found in section 6.1, chapter II.

aL: specific effective area calculated using equation (4.11).

aG: specific effective area calculated using equation (4.12).

mean: mean value of a set

std: standard deviation for the mean value of a set (equation (2.11)).

cap: "% capacity" (section 1.3, chapter I).

* * * The program SULPAK indicated more than 100 % capacity.

Point	B [m3/m2h]	F-Factor	aG/aL [-]	aL [m2/m3]	mean aL [m2/m3]	std aL [m2/m3]	aL std/mean [%]	cap [%]	Set
15.1	12.3	0.87	0.95	280	323	59	18	44	2.1
18.2	12.3	0.85	0.74	365					
16.1	12.3	1.47	0.67	392	409	24	6	66	2.2
17.2	12.3	1.44	0.84	426					
19.1	12.3	1.73	0.67	432	432	0	0	76	2.3
20.1	12.3	1.73	0.72	431					
15.3	19.8	0.87	0.87	344	390	65	17	51	2.4
18.1	19.8	0.86	0.63	435					
16.2	19.8	1.47	0.56	503					
17.1	19.8	1.43	0.67	529	514	13	3	74	2.5
21.1	19.8	1.45	0.71	510					
15.2	40.1	0.87	0.67	495	470	35	7	64	2.6
18.3	40.1	0.84	0.46	444					
33.1	48.9	0.83	0.74	529	543	20	4	68	2.7
34.2	48.9	0.82	0.72	556					
15.4	57.7	0.82	0.83	437	485	68	14	72	2.8
18.4	57.7	0.80	0.37	533					
33.2	71.5	0.78	0.74	561	584	33	6	78	2.9
34.1	71.5	0.78	0.67	606					

Notes:

Definitions of point and set are to be found in section 6.1, chapter II.

aL: specific effective area calculated using equation (4.11).

aG: specific effective area calculated using equation (4.12).

mean: mean value of a set

std: standard deviation for the mean value of a set (equation (2.11)).

cap: "% capacity" (section 1.3, chapter I).

* * * The program SULPAK indicated more than 100 % capacity.

Point	B [m3/m2h]	F-Factor	aG/aL [-]	aL [m2/m3]	mean aL [m2/m3]	std aL [m2/m3]	aL std/mean [%]	cap [%]	Set
22.1	19.8	1.99	0.55	251	213	54	25	61	3.1
27.3	19.8	1.98	1.03	174					
23.1	19.8	2.73	0.27	220	207	18	10	79	3.2
26.3	19.8	2.71	0.95	193					
24.1	19.8	3.25	0.63	160	195	49	25	91	3.3
25.3	19.8	3.21	0.70	230					
22.3	40.1	1.96	0.83	220	204	23	12	72	3.4
27.1	40.1	2.01	1.29	187					
23.3	40.1	2.70	2.61	252	222	42	18	91	3.5
26.1	40.1	2.74	0.87	191					
24.3	40.1	3.20	1.03	188	209	30	13	* * *	3.6
25.1	40.1	3.21	0.59	229					
29.2	48.9	1.98	1.13	269	278	13	4	76	3.7
31.1	48.9	1.96	0.87	286					
28.2	48.9	3.21	1.57	242	252	14	6	* * *	3.8
30.1	48.9	3.18	0.56	261					
22.2	57.7	1.98	0.55	220	214	8	5	80	3.9
27.4	57.7	1.99	0.88	207					
23.2	57.7	2.71	0.61	244	235	13	6	99	3.10
26.4	57.7	2.69	1.55	225					
24.2	57.7	3.16	1.18	285					
25.4	57.7	3.14	1.41	283	287	5	2	* * *	3.11
30.2	57.7	3.15	1.67	293					
22.4	71.5	1.95	0.46	405					
27.2	71.5	1.98	1.24	128	235	119	51	80	3.12
29.1	71.5	1.97	0.59	194					
31.2	71.5	1.96	1.07	211					
23.4	71.5	2.65	-	297	265	45	17	* * *	3.13
26.2	71.5	2.67	2.05	233					
24.4	71.5	3.12	1.69	294					
25.2	71.5	3.13	1.69	240	259	31	12	* * *	3.14
28.1	71.5	3.17	2.17	242					

Notes:

Definitions of point and set are to be found in section 6.1, chapter II.

aL: specific effective area calculated using equation (4.11).

aG: specific effective area calculated using equation (4.12).

mean: mean value of a set

std: standard deviation for the mean value of a set (equation (2.11)).

cap: "% capacity" (section 1.3, chapter I).

* * * The program SULPAK indicated more than 100 % capacity.

Point	B [m3/m2h]	F-Factor	aG/aL [-]	aL [m2/m3]	mean aL [m2/m3]	std aL [m2/m3]	aL std/mean [%]	Set
45.2	12.3	0.32	1.61	110	108	3	2.8	4.1
46.2	12.3	0.32	1.63	105				
40.1	12.3	0.47	1.09	137	137	0	0	4.2
43.2	12.3	0.48	1.09	137				
41.1	12.3	0.87	0.90	139	140	1	0.7	4.3
42.2	12.3	0.89	0.76	141				
39.1	12.3	1.31	0.93	155	159	6	3.8	4.4
44.2	12.3	1.31	0.91	163				
45.4	19.8	0.32	1.32	161	145	23	15.9	4.5
46.4	19.8	0.32	1.56	129				
40.3	19.8	0.47	1.06	159	154	7	4.5	4.6
43.4	19.8	0.47	1.20	149				
41.3	19.8	0.88	0.88	165	173	11	6.4	4.7
42.1	19.8	0.86	0.77	181				
39.2	19.8	1.30	0.95	199	198	1	0.5	4.8
44.1	19.8	1.31	1.03	197				
45.1	40.1	0.32	1.75	154	147	10	6.8	4.9
46.3	40.1	0.31	1.73	140				
40.4	40.1	0.46	1.23	159	161	3	1.9	4.10
43.1	40.1	0.47	1.32	163				
41.2	40.1	0.83	1.00	191	195	6	3.1	4.11
42.3	40.1	0.85	0.97	199				
45.3	57.7	0.31	1.52	183	182	1	0.5	4.12
46.1	57.7	0.31	1.39	181				
40.2	57.7	0.45	1.34	159	162	4	2.5	4.13
43.3	57.7	0.44	1.26	164				

Notes:

Definitions of point and set are to be found in section 6.1, chapter II.

aL: specific effective area calculated using equation (4.11).

aG: specific effective area calculated using equation (4.12).

mean: mean value of a set

std: standard deviation for the mean value of a set (equation (2.11)).

Point	B [m3/m2h]	F-Factor	aG/aL [-]	aL [m2/m3]	mean aL [m2/m3]	std aL [m2/m3]	aL std/mean [%]	Set
47.1	19.8	2.70	1.76	165	160	7	4.4	5.1
48.3	19.8	2.67	0.87	154				
47.3	40.1	2.65	0.76	188	184	6	3.3	5.2
48.1	40.1	2.68	0.77	179				
47.2	57.7	2.66	0.07	223				
47.5	57.7	2.64	0.75	229	220	11	5.0	5.3
48.4	57.7	2.65	0.85	207				
47.4	71.5	2.62	0.81	250	250	0	0.0	5.4
48.2	71.5	2.63	0.76	250				
49.2	19.8	2.00	0.99	148	151	4	2.6	5.5
50.3	19.8	2.03	1.03	154				
49.1	19.8	2.70	0.87	159	156	4	2.6	5.6
50.2	19.8	2.71	1.04	152				
49.3	19.8	3.22	1.25	157	166	13	7.8	5.7
50.1	19.8	3.31	0.63	174				

Notes:

Definitions of point and set are to be found in section 6.1, chapter II.

aL: specific effective area calculated using equation (4.11).

aG: specific effective area calculated using equation (4.12).

mean: mean value of a set

std: standard deviation for the mean value of a set (equation (2.11)).

Point	B [m3/m2.h]	F-Factor	HTU L [m]	kLa *10+2 [1/s]	mean kLa *10+4 [1/s]	std kLa *10+4 [1/s]	kLa std/mean [%]	cap [%]	Set
17.01	21.29	0.83	0.247	2.39	236	5	2.1	38	1.01
16.01	21.29	0.85	0.255	2.32					
14.01	21.29	1.44	0.254	2.33	237	5	2.1	57	1.02
10.01	21.29	1.45	0.246	2.40					
12.01	21.29	1.94	0.234	2.53	248	7	2.9	72	1.03
11.01	21.29	1.96	0.243	2.43					
13.01	21.29	2.59	0.238	2.48	248	0	0.0	91	1.04
19.01	21.29	2.63	0.238	2.48					
15.01	21.29	3.11	0.169	3.49	353	5	1.4	* * *	1.05
18.01	21.29	3.17	0.166	3.56					
17.02	42.6	0.83	0.329	3.60	357	5	1.4	48	1.06
16.02	42.6	0.84	0.335	3.53					
14.02	42.6	1.45	0.324	3.65	366	1	0.4	69	1.07
10.02	42.6	1.45	0.322	3.67					
12.02	42.6	1.94	0.315	3.75	375	0	0.0	85	1.08
11.02	42.6	1.96	0.315	3.75					
13.02	42.6	2.58	0.295	4.01	397	6	1.4	* * *	1.09
19.02	42.6	2.62	0.301	3.93					
17.03	51.2	0.82	0.356	4.00	400	0	0.0	51	1.10
16.03	51.2	0.84	0.356	4.00					
10.03	51.2	1.44	0.364	3.91	398	9	2.3	73	1.11
14.03	51.2	1.44	0.352	4.04					
12.03	51.2	1.93	0.332	4.28	428	0	0.0	90	1.12
11.03	51.2	1.95	0.332	4.28					
13.03	51.2	2.54	0.313	4.54	453	1	0.3	* * *	1.13
19.03	51.2	2.54	0.315	4.52					
17.04	60.8	0.82	0.375	4.50	452	3	0.6	55	1.14
16.04	60.8	0.84	0.372	4.54					
10.04	60.8	1.44	0.385	4.38	446	11	2.5	77	1.15
14.04	60.8	1.44	0.372	4.54					
12.04	60.8	1.93	0.351	4.81	473	11	2.4	95	1.16
11.04	60.8	1.95	0.363	4.65					
17.05	74.3	0.82	0.381	5.42	533	13	2.4	60	1.17
16.05	74.3	0.83	0.394	5.24					
10.05	74.3	1.44	0.428	4.82	507	35	6.9	83	1.18
14.05	74.3	1.44	0.389	5.31					
12.05	74.3	1.92	0.326	6.33	625	12	1.9	* * *	1.19
11.05	74.3	1.93	0.335	6.16					

Notes:

Definitions of point and set are to be found in section 6.1, chapter II.

mean: mean value of a set.

std: standard deviation for the mean value of a set (equation (2.11)).

cap: "% capacity" (section 1.3, chapter I).

* * * The program SULPAK indicated more than 100% capacity.

Point	B [m3/m2.h]	F-Factor	HTU L [m]	kLa *10+2 [1/s]	mean kLa *10+4 [1/s]	std kLa *10+4 [1/s]	kLa std/mean [%]	cap [%]	Set
26.01	13.41	0.85	0.287	1.30	133	4	3.2	46	2.01
27.01	13.41	0.85	0.274	1.36					
24.04	13.41	1.45	0.282	1.32	134	2	1.6	69	2.02
25.01	13.41	1.47	0.276	1.35					
28.03	13.41	1.94	0.144	2.58	232	38	16.2	88	2.03
23.02	13.41	1.96	0.182	2.05					
27.04	17.36	0.85	0.307	1.57	154	4	2.7	50	2.04
26.02	17.36	0.85	0.319	1.51					
24.01	17.36	1.45	0.294	1.64	162	4	2.2	74	2.05
25.02	17.36	1.46	0.303	1.59					
28.02	17.36	1.93	0.117	4.13	364	69	19.0	92	2.06
23.03	17.36	1.95	0.153	3.15					
26.05	21.29	0.85	0.302	1.96	193	5	2.5	53	2.07
27.02	21.29	0.85	0.313	1.89					
21.01	21.29	1.44	0.356	1.66	185	17	9.1	77	2.08
24.05	21.29	1.45	0.297	1.99					
24.02	21.29	1.46	0.313	1.89					
23.01	21.29	1.93	0.136	4.36	393	155	39.3	97	2.09
28.01	21.29	1.93	0.114	5.20					
22.01	21.29	1.94	0.132	4.48					
20.01	21.29	1.95	0.352	1.68					
26.04	42.6	0.84	0.387	3.06	309	4	1.4	67	2.10
27.05	42.6	0.84	0.379	3.12					
21.02	42.6	1.43	0.438	2.70	470	176	37.5	95	2.11
24.03	42.6	1.44	0.221	5.36					
25.03	42.6	1.44	0.196	6.03					
21.03	51.2	1.43	0.415	3.43	343	- - -	- - -	* * *	2.12
26.03	60.8	0.84	0.451	3.74	378	6	1.5	77	2.13
27.03	60.8	0.84	0.442	3.82					

Notes:

Definitions of point and set are to be found in section 6.1, chapter II.

mean: *mean value of a set.*

std: standard deviation for the mean value of a set (equation (2.11)).

cap: "% *capacity" (section 1.3, chapter I).*

* * * *The program SULPAK indicated more than 100% capacity.*

Point	B [m3/m2.h]	F-Factor	HTU L [m]	kLa *10+2 [1/s]	mean kLa *10+4 [1/s]	std kLa *10+4 [1/s]	kLa std/mean [%]	cap [%]	Set
29.01	21.29	1.99	0.473	1.25	129	6	4.4	64	3.01
30.01	21.29	1.99	0.445	1.33					
33.01	21.29	2.64	0.384	1.54	156	2	1.4	82	3.02
34.01	21.29	2.67	0.377	1.57					
32.01	21.29	3.12	0.352	1.68	163	7	4.4	91	3.03
31.01	21.29	3.12	0.374	1.58					
30.02	42.6	1.98	0.510	2.32	224	11	5.0	75	3.04
29.02	42.6	1.99	0.548	2.16					
33.03	42.6	2.63	0.433	2.73	276	4	1.3	95	3.05
34.03	42.6	2.65	0.425	2.78					
32.03	42.6	3.10	0.388	3.05	303	4	1.2	***	3.06
31.02	42.6	3.10	0.394	3.00					
29.03	51.2	1.98	0.574	2.48	255	8	3.2	79	3.07
30.03	51.2	1.99	0.539	2.64					
29.05	51.2	2.00	0.560	2.54					
33.05	51.2	2.63	0.473	3.01	299	4	1.2	99	3.08
34.02	51.2	2.64	0.481	2.96					
35.04	51.2	3.05	0.425	3.35	347	8	2.2	***	3.09
32.02	51.2	3.07	0.407	3.50					
35.01	51.2	3.08	0.405	3.51					
31.03	51.2	3.08	0.407	3.50					
29.04	60.8	1.97	0.747	2.26	216	15	6.9	83	3.10
30.04	60.8	1.98	0.823	2.05					
33.04	60.8	2.61	0.572	2.95	300	6	2.1	***	3.11
34.05	60.8	2.64	0.555	3.04					
35.06	60.8	3.04	0.468	3.61	359	4	1.0	***	3.12
35.02	60.8	3.05	0.474	3.56					
30.05	74.3	1.94	1.075	1.92	199	9	4.6	88	3.13
29.06	74.3	1.96	1.006	2.05					
33.02	74.3	2.58	0.714	2.89	293	6	1.9	***	3.14
34.04	74.3	2.58	0.695	2.97					
35.05	74.3	2.96	0.496	4.16	415	1	0.3	***	3.15
35.03	74.3	3.00	0.498	4.14					

Notes:

Definitions of point and set are to be found in section 6.1, chapter II.

mean: mean value of a set.

std: standard deviation for the mean value of the set (equation (2.11)).

cap: "% capacity" (section 1.3, chapter I).

*** The program SULPAK indicated more than 100% capacity.

```
\ PROGRAM KLA4.PGM
\
\ Author: Marcelo Henriques de Brito
\ 4th version of KLA.PGM
\
\ For data acquisition and calculation of the volumetric mass transfer
\ coefficient - kLa -.
\ Desorption of oxygen from water into saturated air.
\ The pilot plant has a column packed with the structured packing
\                                   MELLAPAK - SULZER.
\
\ Parts of the program:
\
\       PO2.CAL.KLA
\               calibration of the probes
\       INPUT.KLA
\               input of general information concerning the experiment
\       EQ.KLA
\               measurement of equilibria concentrations
\               column with pressure drop
\       DES.KLA
\               desorption experiments by desired operating conditions
\       STORE.KLA
\               storing and printing results of an experiment
\       PRTFILE.KLA
\               printing the contents of the file "kladt.dat"
\       DISK.KLA
\               transfers data to Lotus file "mastereq.wks" in a diskette
\               and "mastermes.wks" in drive a
\
\ Support subroutines:
\
\       INST.DATA.IN
\               acquisition of flow rates in the column COL1
\               (channels: AD0 to AD1)
\       INST.DATA
\               treatment of the data obtained with the procedure INST.DATA.IN
\       CONC.MEAS.IN
\               acquisition of O2 concentrations from INGOLD pO2 probes
\               (channels: AD2 to AD4)
\       CONC.MEAS
\               treatment of the data obtained with the procedure CONC.MEAS.IN
\       PO2.CAL.ZERO
\               procedure to calibrate the zero of pO2 probes
\       PO2.CAL.BALANCE
\               procedure to calibrate the balance of pO2 probes
\       PO2.CAL.VALUE
\               procedure to calculate the calibration values of pO2 probes
\
\ Program done with ASYST version 2.01
\
\ File dictionary
\
\ File to store all data of the experiments
\       file c:\asyst\kladt.dat
\       Description
\               begin
\                       register 1 - position 1 - number of experimental runs
\                                    position 2 - total number of stored registers
\                       For each experiment:
\                       begin
\                               register 1 - data from vector gen.inlo
\                               register 2 - data from matrix eq.data
\                               register 3 - data from matrix mes.data
\                       end
\               end
\
\ File to store calibration data from pO2 probes
\       file c:\asyst\po2cal.dat
\       Description
\               begin
\                       register 1 - last stored data from probe 1
\                       register 2 - last stored data from probe 2
\                       register 3 - last stored data from probe 3
\               end
\
\ Variables dictionary
\
\ General information concerning the experiment
  real dim[ 8 ] array gen.inlo
\ run, date, atmospheric pressure [mmHg], packing number.type,
\ number of packing elements, column section [m2], packing height [m],
\ quantity of points
\ code:
\       packing number.type: a.b
\       a - packing number: 125 ; 250 ; 500
\               b - packing type:       1 - Mellapak Y ; 2 - Mellapak X
\
\       quantity of points: a.b
\               a - number of measured points during procedure EQ.KLA
\               b - number of measured points during procedure DES.KLA
\
\ Data obtained during procedure EQ.KLA
\ Control of the maximum data points for matrix eq.data
integer scalar endloop.eqdata
250 endloop.eqdata :=
```

```
\ Defining matrix eq.data
  real dim[ endloop.eqdata , 8 ] array eq.data
\ run, counter, time [s], G [m3/h], L [m3/h], C11*, C12*, Validity
\ code:
\               validity: 0 - average , 1 - steady state , 2 - transient state
\ remark:
\               if validity = 0
\               then
\                               on the field counter it is stored C11*-C12*
\                               on the field time it is stored the point where steady state
\                                       conditions are achieved.
\
\ Data obtained during procedure DES.KLA
\ Control of the maximum data points for matrix mes.data
integer scalar endloop.mesdata
250 endloop.mesdata :=
\ Defining matrix mes.data
  real dim[ endloop.mesdata , 8 ] array mes.data
\ run, counter, time [s], G [m3/h], L [m3/h], C11, C12, Validity
\ code:
\               validity: 0 - change of the liquid flow, 1 - steady state
\ remark:
\ in the line where there is a change of the liquid flow it is stored:
\ run, Gas density [kg/m3], F-Factor [m/s*sqrt(kg/m3)],
\ average of Gas flowrate with aditional correction for actual pressure and
\ temperature [m3/h], number of points with the same liquid load,
\ P12 [mmHg], T21 [C], void
\
\ Vector for procedures STORE.KLA and PRTFILE.KLA
real dim[ 1 , 8 ] array store.values
\ for procedure STORE.KLA
\               number of experiments, number of stored registers, void, void, void,
\               void, void, void
\ for procedure PRTFILE.KLA:
\               to help to print
\
\ Data obtained during procedure CONC.MEAS.IN and treated by CONC.MEAS
real dim[ 3 ] array conc.values
\ C11, C12, C13
\
\ Data obtained during procedure INST.DATA.IN and treated by INST.DATA
real dim[ 2 ] array inst.values
\ F14, F21
\
\
\ Control variables
integer scalar check                    \ controls the end of the program
integer scalar choice                   \ to run a selected part of the program
integer scalar check.po2.cal  \ controls loop in the procedure PO2.CAL.KLA
integer scalar check.eq                 \ controls loops in the procedure EQ.KLA
integer scalar check.des                \ controls loops in the procedure DES.KLA
integer scalar check.store              \ controls loops in the procedure STORE.KLA
integer scalar check.prtfile1 \ controls end of procedure PRTFILE.KLA
integer scalar check.prtfile2 \ controls end of file
integer scalar check.prtfile3 \ controls end of block to be printed
integer scalar i                                \ counter and pointer
integer scalar ii                               \ another counter and pointer
integer scalar i.acq                    \ counter for data acquisition
\
\ Channels for data acquisition (analog input) using RTI-815-A-32:
RTI-800/815
\
\               0 - Liquid flow                 F14
0 0 a/d.template F14
\               1 - Gas flow Pt sensor          F21
1 1 a/d.template F21
\               2 - pO2 probe - liquid in       C11
2 2 a/d.template C11
\               3 - pO2 probe - liquid out      C12
3 3 a/d.template C12
\               4 - pO2 probe - reactor R11     C13
4 4 a/d.template C13
\
\ Buffers for data acquisition
integer dim[ 120 ] array indata
integer dim[ 16 ] array avg.data
\
\ Data acquisition control
dp.real scalar time.begin
\ time when data acquisition begins
\
\ Variables for probe calibration
real dim[ 2 , 2 , 3 ] array line.cal
\ ( zero , analog value , probe number ) ,
\ ( balance , analog value , probe number )
\
real dim[ 3 , 2 ] array ad.scale.value
\ a/d.scale values for pO2 Probes: C11 , C12, C13
\
integer scalar probe.#.cal
\ pO2 probe to be calibrated
\
integer scalar check.cal
\ controls loops in the procedure PO2.CAL.MAIN
\
\
```

```
            C11
                        1 a/d.gain !ndata cyclic template.buffer
                        a/d.init
            C12
                        1 a/d.gain !ndata cyclic template.buffer
                        a/d.init
            C13
                        1 a/d.gain !ndata cyclic template.buffer
                        a/d.init
            F14
                        1 a/d.gain !ndata cyclic template.buffer
                        a/d.init
            F21
                        0 a/d.gain !ndata cyclic template.buffer
                        a/d.init
\
integer scalar gasflow.type
\ specifies type of the instrument used for measuring the gas flow rate
\           1 - DN 160
\           2 - DN 100
\
\ F14 is a paddlewheel sensor GEORGES FISCHER type MK 515 DN 15.
\ It was installed for these experiments to give a rough estimate
\ of the liquid flow. It is not used for kLa calculations.
\
\ ------------------------------------------
\
: conc.meas.in
\
\ Variables
\
\           OUT:        conc.values
\           INTERNAL: avg.data, i.acq, !ndata
\
\ Performing data acquisition C11
  1 i.acq :=
  begin
            begin
                        C11         a/d.in>array
                        ?buffer.switch
            until
            !ndata mean avg.data [ i.acq ] :=
    i.acq 1 + i.acq :=
            i.acq 17 =
  until
  avg.data mean conc.values [ 1 ] :=
\
\ Performing data acquisition C12
  1 i.acq :=
  begin
            begin
                        C12         a/d.in>array
                        ?buffer.switch
            until
            !ndata mean avg.data [ i.acq ] :=
            i.acq 1 + i.acq :=
            i.acq 17 =
  until
  avg.data mean conc.values [ 2 ] :=
\
\ Performing data acquisition C13
  1 i.acq :=
  begin
            begin
                        C13         a/d.in>array
                        ?buffer.switch
            until
            !ndata mean avg.data [ i.acq ] :=
            i.acq 1 + i.acq :=
            i.acq 17 =
  until
  avg.data mean conc.values [ 3 ] :=
\
stack.clear
\
\ End of the procedure CONC.MEAS.IN
\
;
\
\ ------------------------------------------
\
: po2.cal.zero
\
\ Variables
\
\           IN:         conc.values, probe.#.cal
\           OUT:        line.cal
\           INTERNAL: check.cal
\
\ Call of procedure CONC.MEAS.IN
\
screen.clear
\
: check.cal :=
cr ." pO2 Probe calibration. " cr cr
\
```

```
cr ." pO2 Probe calibration for probe number " probe.#.cal . cr
cr ." Begin calibration to set the zero. "
cr ." Press any key to continue. " pckey cr cr
begin
        conc.meas.in
        conc.values [ probe.#.cal ] .
        cr ." Is the value stable ? (y/n) "
        pckey ?drop 121 =
        if
                cr ." Please input the amplifier displayed number: "
                #input line.cal [ 1 , 1 , probe.#.cal ] :=
                conc.values [ probe.#.cal ] line.cal [ 1 , 2 , probe.#.cal ] :=
                0 check.cal :=
        then
        check.cal 0 =
until
\
\ End of the procedure PO2.CAL.ZERO
\
;
\
\ ------------------------------------------
\
: po2.cal.balance
\
\ Variables
\
\       IN:     conc.values, probe.#.cal
\       OUT:    line.cal
\       INTERNAL: check.cal
\
\ Call of procedure CONC.MEAS.IN
\
screen.clear
\
1 check.cal :=
cr cr cr ." pO2 Probe calibration for probe number " probe.#.cal . cr
cr ." Continue calibration to set the balance. "
cr ." Press any key to continue. " pckey cr cr
begin
        conc.meas.in
        conc.values [ probe.#.cal ] .
        cr ." Is the value stable ? (y/n) "
        pckey ?drop 121 =
        if
                cr ." Please input the amplifier displayed number: "
                #input line.cal [ 2 , 1 , probe.#.cal ] :=
                conc.values [ probe.#.cal ] line.cal [ 2 , 2 , probe.#.cal ] :=
                0 check.cal :=
        then
        check.cal 0 =
until
\
\
\ End of the procedure PO2.CAL.BALANCE
\
;
\
\ ------------------------------------------
\
: po2.cal.value
\
\ Variables
\
\       IN:     line.cal, probe.#.cal
\       OUT:    ad.scale.value
\
\ Changes file PO2CAL.DAT
\
\ Determination of ad.scale.value
\
-2048 line.cal [ 1 , 2 , probe.#.cal ] - line.cal [ 2 , 2 , probe.#.cal ]
        line.cal [ 1 , 2 , probe.#.cal ] - /
        line.cal [ 2 , 1 , probe.#.cal ] line.cal [ 1 , 1 , probe.#.cal ] - *
        line.cal [ 1 , 1 , probe.#.cal ] +
        ad.scale.value [ probe.#.cal , 1 ] :=
\
 2047 line.cal [ 1 , 2 , probe.#.cal ] - line.cal [ 2 , 2 , probe.#.cal ]
        line.cal [ 1 , 2 , probe.#.cal ] - /
        line.cal [ 2 , 1 , probe.#.cal ] line.cal [ 1 , 1 , probe.#.cal ] - *
        line.cal [ 1 , 1 , probe.#.cal ] +
        ad.scale.value [ probe.#.cal , 2 ] :=
\
\ storing result
file.open po2cal.dat
probe.#.cal subfile ad.scale.value sub[ probe.#.cal , 1 ; 1 , 2 ] array>file
file.close
\
\ As C13 is used just as an indicative value, the calibration is done
\ only from time to time
ad.scale.value [ 3 , 1 ] 0 =
if
        file.open po2cal.dat
        3 subfile file>unnamed.array ad.scale.value sub[ 3 , 1 ; 1 , 2 ] :=
        file.close
then
```

```
\
stack.clear
\
\ End of the procedure PO2.CAL.VALUE
\
;
\
\ ------------------------------------------
\
: conc.meas
\
\ Variables
\
\           IN:         ad.scale.value, conc.values
\           OUT:        conc.values
\           INTERNAL: i.acq
\
\ Call of procedure CONC.MEAS.IN
\
            conc.meas.in
            1 i.acq :=
            begin
                        conc.values [ i.acq ] ad.scale.value dup
                                    [ i.acq , 1 ] swap [ i.acq , 2 ]
                                    a/d.scale conc.values [ i.acq ] :=
                        i.acq 1 + i.acq :=
                        i.acq 4 =
            until
\
stack.clear
\
\ End of the procedure CONC.MEAS
\
;
\
\ ------------------------------------------
\
: inst.data.in
\
\ Variables
\
\           OUT:                    inst.values
\           INTERNAL: avg.data, i.acq, indata
\
\
\ Performing data acquisition F14
 1 i.acq :=
 begin
            begin
                        F14         a/d.in>array
                        ?buffer.switch
            until
            indata mean avg.data [ i.acq ] :=
            i.acq 1 + i.acq :=
            i.acq 17 =
 until
 avg.data mean inst.values [ 1 ] :=
\
\ Performing data acquisition F21
 1 i.acq :=
 begin
            begin
                        F21         a/d.in>array
                        ?buffer.switch
            until
            indata mean avg.data [ i.acq ] :=
  i.acq 1 + i.acq :=
            i.acq 17 =
 until
 avg.data mean inst.values [ 2 ] :=
\
\ stack.clear
\
\ End of the procedure INST.DATA.IN
\
;
\
\ ------------------------------------------
\
: inst.data
\
\ Variables
\
\           IN:         inst.values, gasflow.type
\           OUT:        inst.values
\
\ Call of procedure INST.DATA.IN
\
\ Data acquisition from the pilot plant
inst.data.in
\
\ Evaluating the liquid flow rate
\
inst.values [ 1 ] 365 >
if
            inst.values [ 1 ] -228.4030 229.2509 a/d.scale inst.values [ 1 ] :=
```

```
            inst.values [ 1 ] 0.042575 * 0.061270 - inst.values [ 1 ] :=
else
            inst.values [ 1 ] -728.3180 712.5695 a/d.scale inst.values [ 1 ] :=
            inst.values [ 1 ] 0.013996 * 0.056888 + inst.values [ 1 ] :=
then
\
\ Evaluating the measured gas flow rate
\
inst.values [ 2 ] -10.3385 10.6661 a/d.scale inst.values [ 2 ] :=
350. inst.values [ 2 ] 10. / *
gasflow.type
case
            1 of .5 ** 4.066 exp * inst.values [ 2 ] := endof
            2 of .5 ** 3.093 exp * inst.values [ 2 ] := endof
               cr ." THE TYPE OF THE INSTRUMENT TO MEASURE GAS FLOW "
                     cr ."          WAS NOT SPECIFIED ! "
endcase
\
\
stack.clear
\
\ End of the procedure INST.DATA
\
;
\
\ ------------------------------------------
\
: input.kla
\
\ Variable
\
\           OUT:       gen.info
\
screen.clear
0 gen.info :=
cr ." Input of general information about the experience " cr
\
file.open kladt.dat
1 subfile file>unnamed.array [ 1 ] 1 + dup gen.info [ 1 ] :=
file.close
\
cr cr ." The run number is " .
cr ." Please enter today's date (dd.mm): "
#input gen.info [ 2 ] :=
cr ." Please enter the atmospheric pressure [mmHg]: "
#input gen.info [ 3 ] :=
cr ." Please enter the packing number: "
cr ."     1 - 125 "
cr ."     2 - 250 "
cr ."     3 - 500 "
cr ." Your choice: "
#input 1. 10. / + gen.info [ 4 ] :=
cr ." Please enter number of packing elements: "
#input dup gen.info [ 5 ] :=
.295 2 ** 3.14159 * 4. / gen.info [ 6 ] :=
gen.info [ 5 ] .210 * gen.info [ 7 ] :=
\
cr cr ." Are all data correct ? (Y/N) "
pckey ?dup 121 <> \ verification if key is different than "N"
if
            cr cr ." Please enter data again. " cr cr
            myself
then
cr
stack.clear
\
\ End of the procedure INPUT.KLA
\
;
\
\ ------------------------------------------
\
: po2.cal.kla
\
\ Variables
\
\           IN:     ad.scale.value, conc.values
\           OUT:  ad.scale.value, check.po2.cal, probe.#.cal
\
\ Call of procedures PO2.CAL.ZERO, PO2.CAL.BALANCE, PO2.CAL.VALUE
\ and CONC.MEAS
\
1 check.po2.cal :=
\
begin
            screen.clear
            cr ." Please choose one of the following operations: "
            cr ."          0- Calibration of probe C13. "
            cr ."          1- Calibration of probe C11. "
            cr ."          2- Calibration of probe C12. "
            cr ."          3- Simultaneous calibration of C11 and C12. "
            cr ."          4- Calibration control (control of the response). "
            cr ."          5- Display of the calibration values. "
            cr ."          6- Exit of this part of the program. "
            cr ." Your choice is " #input dup dup
            cr cr ." You would like to perform step " .
```

```
cr ." Are you sure? (y/n) "
pckey ?drop 121 =
if
 case
        0 of
                3 probe.ll.cal :=
                po2.cal.zero po2.cal.balance po2.cal.value endof
        1 of
                1 probe.ll.cal :=
                po2.cal.zero po2.cal.balance po2.cal.value endof
        2 of
                2 probe.ll.cal :=
                po2.cal.zero po2.cal.balance po2.cal.value endof
        3 of
                1 probe.ll.cal := po2.cal.zero
                2 probe.ll.cal := po2.cal.zero
                1 probe.ll.cal := po2.cal.balance
                2 probe.ll.cal := po2.cal.balance
                1 probe.ll.cal := po2.cal.value
                2 probe.ll.cal := po2.cal.value                 endof
        4 of
\ Control whether calibration was done
                ad.scale.value [ 1 , 1 ] 0 = ad.scale.value [ 2 , 1 ] 0 = or
\
                if
                        cr cr ." The Probes C11 and C12 are not calibrated. "
                else
                        conc.meas
                        cr cr ." Concentrations "
                        cr ."  C11  ,  C12  ,  C13 "
                        conc.values . cr
                then
                cr cr ." Press any key to continue. " pckey             endof
        5 of
                screen.clear cr cr ." pO2 Probes - Calibration values "
                ad.scale.value sub[ 1 , 1 ; 1 , 2 ] cr ." For C11  -  ".
                ad.scale.value sub[ 2 , 1 ; 1 , 2 ] cr ." For C12  -  ".
                ad.scale.value sub[ 3 , 1 ; 1 , 2 ] cr ." For C13  -  ".
                cr cr ." Press any key to continue. " pckey             endof
        6 of
\
\ Control whether calibration was done
                ad.scale.value [ 1 , 1 ] 0 = ad.scale.value [ 2 , 1 ] 0 = or
                if
                        cr cr ." The Probes C11 and C12 are not calibrated. "
                        cr cr ." Do you want to exit this part anyway? (y/n) "
                        pckey ?drop 121 =
                if
                        0 check.po2.cal :=
                else
                        myself
                then
                else
                        0 check.po2.cal :=
                then                                                    endof
                1 check.po2.cal :=
 endcase
then
check.po2.cal 0 =
until
\
\ End of the procedure PO2.CAL.KLA
\
;
\
\ ------------------------------------------
\
: eq.kla
\
\ Variables
\
\       IN:             conc.values, endloop.eqdata, gen.info,
\                       inst.values
\       OUT:            gen.info, eq.data
\       INTERNAL: check.eq, i, ii, time.begin
\
\ Call of procedures CONC.MEAS and INST.DATA
\
screen.clear
cr ." pO2 Probe calibration - column with pressure drop " cr
cr ." Please set gas and liquid flowrates. "
\
cr ." Press any key and program starts acquisition. "
pckey
1 i :=
0 ii :=
1 check.eq :=
0. eq.data :=
rel.time time.begin :=
begin
        i
        cr cr ." Data acquisition is being performed for point " .
        inst.data
        conc.meas
```

```
rel.time time.begin - 1000. / eq.data [ i , 3 ] :=
cr ." Concentrations "
cr ." C11 , C12 , C13 "
conc.values . cr
cr ." Flow rates in the column COL1 "
cr ." F14 , F21 "
inst.values . cr
gen.info [ 1 ] eq.data [ i , 1 ] :=
i eq.data [ i , 2 ] :=
inst.values [ 2 ] eq.data [ i , 4 ] :=
inst.values [ 1 ] eq.data [ i , 5 ] :=
conc.values [ 1 ] eq.data [ i , 6 ] :=
conc.values [ 2 ] eq.data [ i , 7 ] :=
cr ." Are steady state conditions achieved ? (y/n) "
pckey ?drop 121 =
if
        1 eq.data [ i , 8 ] :=
        ii 1 + ii :=
        ii cr cr ." Number of points since steady state was achieved = " .
        cr cr ." Do you consider that enough points were obtained ? (y/n) "
        pckey ?drop 121 =
        if
                cr cr ." Are you sure? (y/n) "
                pckey ?drop 121 =
                if
                        0 check.eq :=
                then
        else
                i 1 + i :=
                i endloop.eqdata =
                if
                        cr ." The storage capacity is over. "
                        cr ." You may redo this part of the program again. "
                        cr ." Nevertheless all stored data will be lost. "
                        i 1 - i :=
                        0 check.eq :=
                then
        then
else
        2 eq.data [ i , 8 ] :=
        i 1 + i :=
        0 ii :=
        i endloop.eqdata =
        if
                cr ." The storage capacity is over. "
                cr ." You may redo this part of the program again. "
                cr ." Nevertheless all stored data will be lost. "
                i 1 - i :=
                        0 check.eq :=
                then
        then
        check.eq 0 =
until
\
\ Number of points obtained with procedure eq.kla
gen.info [ 8 ] ii :=
gen.info [ 8 ] ii - i + 1 + gen.info [ 8 ] :=
\
\ Evaluating the average under steady state conditions
1 check.eq :=
begin
        eq.data [ i , 8 ] 1 =
        if
                i 1 - i :=
                i 0 =
                if
                        1 i :=
                        0 check.eq :=
                then
        else
                0 check.eq :=
                i 1 + i :=
        then
        check.eq 0 =
until
\
\ Filling in the matrix eq.data at the average position
gen.info [ 8 ] ii :=
i eq.data [ ii , 3 ] :=
gen.info [ 8 ] i - ii :=
eq.data sub[ i , ii ; 4 , 4 ] trans[ 1 , 2 ] mean
gen.info [ 8 ] ii :=
eq.data sub[ ii , 1 ; 4 , 4 ] :=
gen.info [ 1 ] eq.data [ ii , 1 ] :=
eq.data [ ii , 7 ] eq.data [ ii , 6 ] - eq.data [ ii , 2 ] :=
\
\ End of the procedure EQ.KLA
\
;
\
\ ------------------------------------------------
\
: des.kla
\
\ Variables
\
```

```
\           IN:     conc.values, endloop.mesdata, gen.info, inst.values
\           OUT:    gen.info, mes.data
\           INTERNAL: check.des, i, ii, time.begin
\
\ Call of procedures CONC.MEAS and INST.DATA
\
screen.clear
cr ." Desorption Experiments "
cr ." Measurement of O2 concentrations under operating conditions. " cr
cr ." Please set gas and liquid flow rates. "
\
cr ." Press any key and program starts acquisition. "
pckey
1 i :=
0 ii :=
1 check.des :=
0. mes.data :=
rel.time time.begin :=
begin
        \
        cr cr ." Data acquisition is being performed for point " .
        inst.data
        conc.meas
        rel.time time.begin - 1000. / mes.data [ i , 3 ] :=
        cr ." Concentrations "
        cr ."  C11  ,  C12  ,  C13 "
        conc.values . cr
        cr ." Flow rates in the column COL1 "
        cr ."  F14  ,  F21  "
        inst.values . cr
        inst.values [ 1 ] gen.info [ 6 ] /
        cr cr ." The liquid load is about " . ."  m3/m2h " cr
        cr ." Is this liquid load staying constant ? (y/n) "
        pckey ?drop 121 =
        if
                gen.info [ 1 ] mes.data [ i , 1 ] :=
                i mes.data [ i , 2 ] :=
                inst.values [ 2 ] mes.data [ i , 4 ] :=
                inst.values [ 1 ] mes.data [ i , 5 ] :=
                conc.values [ 1 ] mes.data [ i , 6 ] :=
                conc.values [ 2 ] mes.data [ i , 7 ] :=
                1 mes.data [ i , 8 ] :=
                ii 1 + ii :=
                ii cr cr ." Number of points with this liquid load - " .
                cr cr ." Have you finished the experiment ? (y/n) "
                pckey ?drop 121 =
                if
                        cr ." Are you sure? (y/n) "
                        pckey ?drop 121 =
                        if
                                0 check.des :=
                        then
                else
                        1 check.des :=
                        i 1 + i :=
                        i endloop.mesdata =
                        if
                                cr ." The storage capacity is over. "
                                cr ." You may redo this part of the program again. "
                                cr ." Nevertheless all stored data will be lost. "
                                i 1 - i :=
                                0 check.des :=
                        then
                then
        else
                1 i <
                if
                        mes.data [ i 1 - , 8 ] 0 <>
                        if
                                gen.info [ 1 ] mes.data [ i , 1 ] :=
                                1 check.des :=
                                begin
\
cr cr ." Please give the following data for the old liquid load: "
cr ." man. Pressure at the bottom of the column P12  [mmH2O] - "
#input mes.data [ i , 6 ] :=
gen.info [ 3 ] mes.data [ i , 6 ] 13.55 / - mes.data [ i , 6 ] :=
cr ." Gas temperature  [C] - "
#input mes.data [ i , 7 ] :=
cr ." Are all data correct ? (y/n) "
pckey ?drop 121 =
if
        0 check.des :=
then
\
                                        check.des 0 =
                                until
                                1 check.des :=
                                mes.data [ i , 6 ] 760. / 10 5 ** * 28.967 * 8314. /
                                        mes.data [ i , 7 ] 273.15 + / mes.data [ i , 2 ] :=
                                mes.data sub[ i ii - , ii ; 4 , 1 ] trans[ 1 , 2 ] mean
                                        760. mes.data [ i , 6 ] / *
                                        mes.data [ i , 7 ] 273.15 + 293.15 / *
                                        mes.data sub[ i , 1 ; 4 , 1 ] :=
                                mes.data [ i , 4 ] gen.info [ 6 ] / 3600. /
                                        mes.data [ i , 2 ] sqrt * mes.data [ i , 3 ] :=
```

```
                                    ii mes.data [ i , 5 ] :=
                                    0 mes.data [ i , 6 ] :=
                                    i 1 + i :=
                                    0 ii :=
                            then
                    then
                    i endloop.mesdata =
                    if
                            cr ." The storage capacity is over. "
                            cr ." You may redo this part of the program again. "
                            cr ." Nevertheless all stored data will be lost. "
                            i 1 - i :=
                            0 check.des :=
                    then
            then
            check.des 0 =
until
\
\ Filling in the matrix mes.data at the last position
i 1 + i :=
gen.info [ 1 ] mes.data [ i , 1 ] :=
1 check.des :=
begin
            cr cr ." Please give the following data for the last liquid load: "
            cr ." man. Pressure at the bottom of the column P12  [mmH2O]  - "
            #input mes.data [ i , 6 ] :=
            gen.info [ 3 ] mes.data [ i , 6 ] 13.55 / - mes.data [ i , 6 ] :=
            cr ." Gas temperature  (C) - "
            #input mes.data [ i , 7 ] :=
            cr ." Are all data correct ? (y/n) "
            pckey ?dup 121 =
            if
                    0 check.des :=
            then
            check.des 0 =
until
mes.data [ i , 6 ] 760. / 10 5 "" *
            28.967 * 8314. / mes.data [ i , 7 ] 273.15 + / mes.data [ i , 2 ] :=
mes.data sub[ i ii - , ii ; 4 , 1 ] trans[ 1 , 2 ] mean
            760. mes.data [ i , 6 ] / *
            mes.data [ i , 7 ] 273.15 + 293.15 / *
            mes.data sub[ i , 1 ; 4 , 1 ] :=
mes.data [ i , 4 ] gen.info [ 6 ] / 3600. / mes.data [ i , 2 ] sqrt *
            mes.data [ i , 3 ] :=
ii mes.data [ i , 5 ] :=
0 mes.data [ i , 6 ] :=
\
\
```

```
\ Number of points obtained with procedure des.kla
gen.info [ 6 ] ii :=
i 10000. / ii + gen.info [ 6 ] :=
\
\
cr ." The experiment is over. Please press any key to continue. "
pckey
\
\ End of the procedure DES.KLA
\
;
\
\ ------------------------------------------------
\
: store.kla
\
\ Variables
\
\           IN:                     eq.data, gen.info, mes.data
\           INTERNAL: check.store, i, ii, store.values
\
\ Changes file KLADT.DAT
\
screen.clear
0 store.values :=
\
\ Storing results
\
\
cr ." What would you like to execute? "
cr ."       1- Store general information about the experiment (INPUT.KLA) "
cr ."         and equilibria concentrations (EQ.KLA). "
cr ."       2- Store data from desorption experiments (DES.KLA). "
cr ."       3- End this part of the program. "
cr ." Your choice is " #input dup dup
cr cr ." You would like to perform step ". 
cr ." Are you sure? (y/n) "
pckey ?drop 121 =
if
        case
          i of
                    file.open kladt.dat
                    1 subfile file>unnamed.array store.values :=
\                   storing information from gen.info
                    store.values [ 1 , 1 ] 1 + store.values [ 1 , 1 ] :=
                    store.values [ 1 , 2 ] 1 + store.values [ 1 , 2 ] :=
                    gen.info append.array>file
\                   storing matrix eq.data
```

```
                gen.info [ 8 ] ll :=
                store.values [ 1 , 2 ] ll + store.values [ 1 , 2 ] :=
                0 check.store :=
                begin
                        check.store 1 + check.store :=
                        eq.data [ check.store , 1 ] 0 <>
                        if
                                eq.data sub[ check.store , 1 ; 1 , 8 ] append.array>file
                        else
                                ll check.store :=
                        then
                        check.store ll =
                until
\
                1 subfile store.values trans[ 2 , 1 ] xsect[ 1 ] array>file
                file.close                                              endof
\
        2 of
                file.open kladt.dat
                1 subfile file>unnamed.array store.values :=
\               storing matrix mee.data
                gen.info [ 8 ] ll :=
                gen.info [ 8 ] ll - 10000. * i :=
                store.values [ 1 , 2 ] i + store.values [ 1 , 2 ] :=
                0 check.store :=
                begin
                        check.store 1 + check.store :=
                        mee.data [ check.store , 1 ] 0 <>
                        if
                                mee.data sub[ check.store , 1 ; 1 , 8 ] append.array>file
                        else
                                i check.store :=
                        then
                        check.store i =
                until
\
                1 subfile store.values trans[ 2 , 1 ] xsect[ 1 ] array>file
                file.close                                              endof
        3 of
                cr ." Routine STORE.KLA is done. "
                cr ." Please press any key to continue. " pckey
                                                                        endof
        myself
        endcase
else
        myself
then
\
```

```
\               End of procedure STORE.KLA
\
;
\
\ ------------------------------------------
\
: prtfile.kla
\
\ Variables
\
\               INTERNAL: check.prtfile1, check.prtfile2, check.prtfile3,
\                                       store.values
\
\ Prints file KLADT.DAT
\
screen.clear
-1 4 fix.format
cr ." The file kladt.dat will be printed. " cr
cr ." Please do check that the printer is switched on. "
cr ." Press any key when ready. "
pckey
\
\ Printing file "kladt.dat"
out>printer console.off
cr cr ." File kladt.dat "
console
0. store.values :=
file.open kladt.dat
1 check.prtfile1 :=
cr ." The run number to print is = "
#input check.prtfile3 :=
2 check.prtfile2 :=
begin
        check.prtfile2 subfile file>unnamed.array store.values :=
        store.values [ 1 , 1 ] check.prtfile3 =
        if
                0 check.prtfile1 :=
        else
                check.prtfile2 1 + check.prtfile2 :=
        then
        1 subfile file>unnamed.array store.values :=
        store.values [ 1 , 2 ] check.prtfile2 =
        if
                0 check.prtfile1 :=
        then
        0 check.prtfile1 =
until
1 check.prtfile1 :=
```

```
begin
        check.prtfile2 subfile file>unnamed.array store.values :=
        store.values [ 1 , 1 ] check.prtfile3 =
        if
                check.prtfile2 subfile file>unnamed.array
                out>printer console.off . console
                check.prtfile2 1 + check.prtfile2 :=
        else
                0 check.prtfile1 :=
        then
        1 subfile file>unnamed.array store.values :=
        store.values [ 1 , 2 ] check.prtfile2 <
        if
                0 check.prtfile1 :=
        then
        0 check.prtfile1 =
until
file.close
-1 3 fix.format
\
cr cr ." Printing is over. Please press any key to continue. "
pckey
stack.clear
\
\ End of the procedure PRTFILE.KLA
\
;
\
\ ------------------------------------------
\
: disk.kla
\
\ Variables
\
\       IN: gen.info, eq.data, mes.data
\       INTERNAL: i,ii
\
\ Changes files a:\mastereq.wks and a:\mastermes.wks
\
screen.clear
cr ." To store results please insert diskette with the files "
cr ." a:\mastereq.wks and a:\mastermes.wks in drive A: "
cr cr ." Please press any key when ready. " pckey ?drop drop
load.overlay 123io.sov
123file.open a:\mastereq.wks
7 1 123write.across
gen.info [ 8 ] i :=
i 1 + i :=
eq.data sub[ 1 , i ; 1 , 8 ] array>123file
123file.close
123file.open a:\mastermes.wks
10 1 123write.across
gen.info [ 8 ] i :=
gen.info [ 8 ] i - 10000. * ii :=
ii 1 + ii :=
mes.data sub[ 1 , ii ; 1 , 7 ] array>123file
123file.close
cr cr cr cr ." The run is stored in the diskette. "
cr ." Thank you for your attention. "
cr cr cr ." Please press any key to continue. "
pckey
screen.clear
\
\ End of procedure DISK.KLA
\
;
\
\ ------------------------------------------
\ ------------------------------------------
\
: kla
\
\ MAIN PROGRAM
\
\ Variables
\
\       check, check.po2.cal, choice, gen.info, inst.values
\
\ Call of procedures    DES.KLA, EQ.KLA, INPUT.KLA,
\                                       INST.DATA, PO2.CAL.KLA, PRTFILE.KLA, STORE.KLA
\
\ Definitions
        -1 3 fix.format
        normal.display
        screen.clear
        stack.clear
\
\
        500 400 tune 500 200 tune 500 600 tune
        cr ." WELCOME TO THE PROGRAM KLA.PGM ! "
        cr ." ------------------------"
        cr
        cr ." Have a good time and a lot of luck ! " cr
        cr cr
        cr ." Please enter type of the instrument to measure the gas flow: "
        cr ."       1 - DN 160 "
```

```
        cr ."       2 - DN 100 "
        cr ." Your choice "
        #input gasflow.type :=
        cr cr cr ." Please press a key to begin. "
        pckey
\
\
\ Running the program
        1 check :=
        begin
                screen.clear
                choice 1 >
                if
                        gen.info [ 1 ]          cr ." This is experiment number " .
                        choice cr ." You have already executed step " . cr
                else
                then
                cr ." Please choose one of the following operations: "
                cr ."       0- Probe calibration and checking "                 (PO2.CAL.KLA) "
                cr ."
                cr ."       1- Displaying data from the pilot plant " cr
                cr ."       2- Input of general information about the experience "   (INPUT.KLA) "
                cr ."
                cr ."       3- Measurements of equilibrium concentrations "
                cr ."         column with pressure drop "                       (EQ.KLA) "
                cr ."
                cr ."       4- Desorption experiments "                         (DES.KLA) "
                cr ."
                cr ."       5- Storing data "                                   (STORE.KLA) "
                cr ."
                cr ."       6- Printing contents of the files with stored data "    (PRTFILE.KLA) "
                cr ."
                cr ."       7- Transfer data to a Lotus file "                  (DISK.KLA) "
                cr ."
                cr ."       8- End of the program "
                cr ." Your choice is " #input dup dup
                cr cr ." You would like to perform step " .
                cr ." Are you sure? (y/n) "
                pckey ?drop 121 =
                if
                        case
                                0 of        po2.cal.kla                                 endof
                                1 of inst.data
                                        screen.clear
                                        cr cr ." Flow rates in the column COL1 "
                                        cr ."  F14   ,  F21   "
                                        cr ." [m3/h] , [m3/h] " cr
                                        inst.values . cr
                                        gen.info [ 6 ] 0 <>
                                        if
                                                inst.values [ 1 ] gen.info [ 6 ] /
                                                cr ." B [m3/m2h] = " .
                                                inst.values [ 2 ] gen.info [ 6 ] / 3600. /
                                                        1.1 sqrt *
                                                cr ." F-Factor [m/s.sqrt(kg/m3)] = " . cr
                                        then
                                        cr ." Press any key to continue "
                                        pckey                                       endof
                                2 of input.kla                  2 choice :=  endof
                                3 of
                                        check.po2.cal 0 =
                                        if
                                                eq.kla
                                                3 choice :=
                                        else
                                                cr cr ." Probes must be calibrated before. "
                                                pckey
                                        then                                        endof
                                4 of
                                        check.po2.cal 0 =
                                        if
                                                des.kla
                                                4 choice :=
                                        else
                                                cr cr ." Probes must be calibrated before. "
                                                pckey
                                        then                                        endof
                                5 of store.kla                  5 choice :=  endof
                                6 of prtfile.kla        6 choice :=  endof
                                7 of disk.kla           7 choice :=  endof
                                8 of 0 check :=                                     endof
                                1 check :=
                        endcase
                then
                check 0 =
        until
        screen.clear
        cr ." Thank you for the attention ! "
        cr cr ." End of the program  KLA.PGM. "
\
\
\ END OF THE PROGRAM
;
\
```

```
\ PROGRAM DOSPH8.PGM
\
\ Author: Marcelo Henriques de Brito
\ 8th version of DOSPHACQ.PGM
\
\ For titrations of carbonate-NaOH solutions.
\ Use of HCl 1 M until chosen pH and HCL 0.1 M afterwoods.
\
\ Data acquisition from the Dosimat 665 and pH-Meter 632.
\ Channels:
\   A\D 0 - Analog input of the dosimat (green/black;yellow/red)
\   A\D 1 - Analog input of the pH-Meter
\
\ Probe at the begining of the programm:
\   15 ml Probe from the experiment + 15 ml HCl 1 M
\
\ Dosimat configuration:
\   Pistonvolume/V: 4 (special key: 4)
\   DIS C mode
\             during titration with 1 M HCl:
\                       max. Volume: to be estimated for each experiment
\                       rate up: 15 ml/min
\                       rate down: 20 ml/min
\             during titration with 0.1 M HCl:
\                       max. Volume: to be estimated for each experiment
\                       rate up: 1 ml/min
\                       rate down: 20 ml/min
\
\ Variables dictionary
\
  real dim[ 550 ] array dosimat.measure     \ measured values
  real dim[ 550 ] array phmeter.measure     \ measured values
  real dim[ 550 ] array phmeter.diff        \ derivative of pH
  real dim[ 5 ] array results
\ containe: run number, flask, probe,
\                       OH concentration and CO3 concentration
  real dim[ 5 ] array store
\ contents of the first register of file IATRES and used for printing IATRES.
\             position 1: number of stored registers
  integer dim[ 20 ] array average0.enter    \ average of input values from
\                       the dosimat
  integer dim[ 20 ] array average1.enter    \ average of input values from
\                       the pH-meter
  real scalar added.HCl1M
  real scalar equiv.point2
  real scalar equiv.point3
  real scalar olddose.value
  real scalar oldph.value
  real scalar ph.change
  integer scalar stop.loop \ ( true: 0 ; false: 1 )
  integer scalar ii \ loop index
  integer scalar jj \ last measured value
  integer scalar endloop    \ loop control
  integer scalar syncper    \ sync.period
  8 string filename
\
RTI-800/815
0 0 a/d.template ad0
1 1 a/d.template ad1
\
: definitions6
\ synchronization period
  200 syncper :=
\ end loop ( array dimension + 1 )
  551 endloop :=
\ Files
  file.template
    dosimat.measure []form.subfile
    2 times
  end
\
\ data entries
  -1 3 fix.format
  normal.display
  stack.clear
  screen.clear
  500 400 tune 500 200 tune 500 600 tune
  cr ." Welcome to the program DOSPH8 !"
;
: input2
  cr
  cr ." Please enter run number: "
  #input results [ 1 ] :=
  cr ." Please enter flask number: "
  #input results [ 2 ] :=
  cr ." Please enter probe size [ ml ]: "
  #input results [ 3 ] :=
  cr ." Please enter titration number: "
  #input results [ 4 ] :=
  results dup 2 *dup
  [ 1 ] 10000 * swap [ 2 ] 100 * + swap [ 3 ] + swap [ 4 ] +
  " FC" "." 7 "s# 6 "right "cat filename ":=
  cr ." Please enter desired pH to change Dosimat's exchange unit: "
  #input ph.change :=
  filename delet> file.sizes  0 >
  if
    cr
    cr ." Such data file (" inten.on filename "type inten.off ." ) exists! "
    cr ." Would you like to erase it? (Y/N) "
    pckey ?drop 121 <>  \ verification if key is different than "N"
    if
      myself
    then
  else
    cr cr ." Are all data correct? (Y/N) "
    pckey ?drop 121 <>  \ verification if key is different than "N"
    if
      myself
    then
  then
  cr
;
\ Initializations
: initial3
  cr cr ." Thank you for the input" cr
  cr ." The file " inten.on filename "type inten.off ."  will be created. "
  filename delet> file.create
  cr
  cr ." Please verify dosimat settings. Exchange unit with 1 M HCl."
  cr ." Program begins ... AS SOON AS YOU PRESS THE GO BUTTON!"
  cr cr cr
  ad0
    1 a/d.gain
    average0 enter template.buffer
    cyclic
    a/d.init
  ad1
    1 a/d.gain
    average1 enter template.buffer
    cyclic
    a/d.init
;
\
: datalake8
  syncper sync.period
  1 ii :=
  1 jj :=
  0 olddos.value :=
  0 oldph.value :=
  1 stop.loop :=
  without.frequencies  \ refers to the mean command
  stack.clear
\ First acquisition part: reducing pH with a 1 M HCl solution.
  begin
```

```
synchronize
begin
   ad0
   a/d.ln>array
   ad1
   a/d.ln>array
   ?buffer.switch
until
average0.enter  mean
-80.0000 80.0000 a/d.scale dup dup
added.HCl1M :=
olddos.value - 0.05 >
if
   olddos.value :=
   average1.enter  mean
   -2.9363 16.9820 a/d.scale dup
   oldph.value :=
   ph.change <
   if
      1500 600 tune 1000 400 tune
      cr cr cr ." Please press dosimat's FILL button."
      cr ." When ready, please type any key." pckey
            begin
                              ad0
                              a/d.ln>array
                              ?buffer.switch
                  until
                  average0.enter mean
                    -80.0000 80.0000 a/d.scale added.HCl1M :=
      0 stop.loop :=
   else
      oldph.value
      cr " Please wait, pH is still " type .
            olddos.value
      cr " The added HCl 1 M was " type . cr cr
      1 stop.loop :=
   then
then
stack.clear
 0 stop.loop =
until
1500 600 tune
screen.clear
cr cr added.HCl1M
." Do you confirm that the added HCl 1 M was " . ." ml (y/n)? "
pckey ?drop 121 <>
if
            cr cr ." Please give in the added quantity of HCl 1 M [ml] - "
            #input added.HCl1M :=
            added.HCl1M cr cr ." The added HCl 1 M was " . " ml. "
            cr ." Please type any key " key
else
             cr cr ." Thank you for confirming. Please type any key "
            key
then
cr cr cr ." Please change dosimat's exchange unit. Use now 0.1 M HCL."
cr ." When ready, please type any key."
pckey cr cr ." Thank you. Program will at last begin with data acquisition."
cr ." ... AS SOON AS YOU PRESS THE GO BUTTON !"
cr cr cr
\ Second acquisition part: titration with a 0.1 M HCl solution.
syncper sync.period
1 ii :=
1 jj :=
0 dosimat.measure :=
0 phmeter.measure :=
false
stack.clear
begin
 synchronize
 begin
   ad0
   a/d.ln>array
   ad1
   a/d.ln>array
   ?buffer.switch
until
average0.enter  mean
-80.0 80.0 a/d.scale dup
dosimat.measure [ jj ] - 0.05 >
if
   dosimat.measure [ ii ] :=
   average1.enter  mean
   -2.9363 16.9820 a/d.scale dup 2.7 >
   if
         phmeter.measure [ ii ] :=
         cr " data point: " dosimat.measure [ ii ] phmeter.measure [ ii ] ii
          "type . . . cr
         ii jj :=
         ii 1 + ii :=
   else
         phmeter.measure sub[ ii , endloop ] :=
         dosimat.measure dup [ ii ] swap sub[ ii , endloop ] :=
         endloop ii :=
   then
then
   stack.clear
   ii endloop =
until
jj endloop :=
\
\ storing results
\
filename defer> file.open
1 subfile dosimat.measure array>file
2 subfile phmeter.measure array>file
file.close
1500 600 tune  1500 600 tune 1500 600 tune
\
;
\
: datatreatment8
   0.2 set.cutoff.freq
   dosimat.measure  phmeter.measure
   smooth
   graphics.display
   xy.auto.plot
   cursor.off
   15 label.color
   0 label.dir
   0 char.dir
   normal.coords
   0.75 0.05 position " Volume HCl [ ml ] " centered.label
   90 label.dir
   90 char.dir
   normal.coords
   0.04 0.6 position " pH [ - ]" centered.label
   500 200 tune 500 200 tune 500 200 tune 800 400 tune
   cr ." Please type any key to continue"
   key
   screen.clear
   1 set.order
   3 set.degree
   dosimat.measure
   phmeter.measure smooth
   differentiate.data dup
   phmeter.diff :=
   xy.auto.plot
   cursor.off
   15 label.color
   0 label.dir
   0 char.dir
   normal.coords
   0.75 0.05 position " Volume HCl [ ml ] " centered.label
```

```
90 label.dir
90 char.dir
normal.coords
0.04 0.6 position " dpHdV [ 1/ml ]" centered.label
500 400 tune 500 400 tune 500 400 tune 800 200 tune
cr ." Please type any key to continue"
key
\ Calculating carbonate concentration
  screen.clear
  7 set.#.optima
  7 set.#.points
  1 ii :=
  begin
        phmeter.measure [ ii ] 7. <
        if
              phmeter.diff sub[ 1 , ii ]
              local minima
              ?array
              if
                    sort&index
                    [ 1 ] equiv.point2 :=
                    drop [ equiv.point2 ] equiv.point2 :=
              else
                    drop equiv.point2 :=
              then
              true
        else
              ii 1 + ii :=
              false
        then
  until
  begin
        phmeter.measure [ ii ] 6. <
        if
              endloop 1 - endloop :=
              phmeter.diff sub[ ii , endloop ]
              local minima
              ?array
              if
                    sort&index
                    [ 1 ] equiv.point3 :=
              drop [ equiv.point3 ] ii + 1 - equiv.point3 :=
              else
                    drop ii + 1 - equiv.point3 :=
              then
        true
        endloop 1 + endloop :=
        else
                    ii 1 + ii :=
                    false
              then
  until
  dosimat.measure dup [ equiv.point3 ] swap [ equiv.point2 ] -
  results [ 3 ] / 10 /
  results [ 5 ] :=
\ Calculating OH concentration
  results [ 3 ] added.HCl1M + dosimat.measure [ equiv.point2 ] 10 / +
              results [ 3 ] / results [ 5 ] - results [ 4 ] :=
\ Displaying calculated concentrations
  results dup [ 5 ] swap [ 4 ]
  " and [ CO3 ] [mol/l] = " " [ OH ] [ mol/l] = "
  cr "type . "type .
  ." . Please type a key. "
  key
\ Storing results
  cr ." Would you like to store the results? (Y/N) "
  pckey ?drop 121 <>
  if
    cr ." The results will not be stored. Please type any key. "
    key
  else
    cr ." The results will be stored. Please type any key. "
    key
    file.open IATRES
      results append.array>file
    file.close
\     number of stored registers
          file.open IATRES
          0 store :=
          1 subfile store file>array
          store [ 1 ] 1 + store [ 1 ] :=
          1 subfile store array>file
          file.close
  then
\ Printing
  cr ." Would you like to print the results of this titration? (Y/N) "
  pckey ?drop 121 <>
  if
    cr ." The results will not be printed. Please type any key. "
    key
  else
    cr ." The results will be printed. Please type any key. "
    key
          cr results . screen.print
  then
\ Printing IATRES
  cr ." Would you like to print the whole file IATRES? (Y/N) "
  pckey ?drop 121 <>
  if
    cr ." The results will not be printed. Please type any key. "
    key
  else
    cr ." The results will be printed. Please type any key. "
    key
          normal.display
          file.open IATRES
          1 subfile store file>array
          store [ 1 ] 1 + 1 do
                    i subfile store file>array
                    out>printer
                    store .
                    console
          loop
          file.close
  then
\ End from program.
  cr ." Thank you for your attention! "
  500 400 tune 500 200 tune 500 600 tune
;
\
\ main program
\
: dosph8
  definitions8
  input2
  initial3
  datatake8
  datatreatment8
;
\ end main program
```

MARCELO HENRIQUES DE BRITO
Brazilian, single, born on the 5th December, 1963 in Rio de Janeiro.

Permanent address:
Rua Conde de Afonso Celso 136,
CEP 22461 Jardim Botânico, Rio de Janeiro, RJ - BRAZIL.
Tel: 0055 / 21 / 2262751.

1. Formation

1969-1973	The British School, Rio de Janeiro.
1974-1980	Colégio de Aplicação UFRJ, Rio de Janeiro.
1981-1985	Diploma in mechanical engineering at the Federal University of Rio de Janeiro (UFRJ).
Nov.86-Oct.87	Candidate to PhD studies at the Swiss Federal Institute of Technology-Zürich and assistant to Prof. Dr. P. Suter for thermodynamics during summer semester 1987. Attendance of various lectures and laboratory classes. The exam was passed in summer 1987.
since Nov.87	PhD student and assistant to Prof. Dr. U. von Stockar at the Swiss Federal Institute of Technology-Lausanne, Institute of Chemical Engineering (IGC). Subject of the thesis: "Gas absorption experiments in a pilot plant column with the SULZER structured packing MELLAPAK". Supervisor: Prof. Dr. U. von Stockar.

2. Languages

Fluency in written and spoken English, French, German and Swiss German. Mother tongue is Portuguese. I was used to switch daily between different written and spoken languages in the past 4 years.

3. Work experience

Since November 1987:
In parallel with the thesis, assistant to the Prof. Dr. U. von Stockar in lectures and laboratory classes in the field of thermal unit operations at the Swiss Federal Institute of Technology-Lausanne. Additionally, I was responsible for a group of three students for the elaboration of a three-volume script (384 pages) for the Professor's lectures "Procédés de Séparation" (thermal unit operations).

Summer semester 1987:
Assistant for the course "Thermodynamics I" to Prof.Dr. P. Suter at the Swiss Federal Institute of Technology Zürich (ETH-Zürich).

March 1987 - April 1987:
Trainee at SULZER-ESCHER WYSS, Zurich; Department: Process engineering - crystallization plant with mechanical vapour compression. Introduction to the use of the CAD-Software AutoCAD 2.5.

August 1986 - October 1986:
Trainee at SULZER BROTHERS LIMITED, Winterthur; Departments: Mixing Process Equipment and Separation columns. Execution of experiments.

January 1986 - August 1986:
Engineer at SULZER DO BRASIL SA. Mechanical and thermohydraulic design of heat exchangers and falling film evaporator. Specification of components for a salt crystallization plant. Preparation of microcomputer programs for the mechanical design of vessels according to the ASME-Code.

March 1985 - December 1985:
Trainee at SULZER DO BRASIL SA, part-time, in the field of process engineering and equipment design. Design of machines for the fabrication of the SULZER structured packing MELLAPAK. Course in distillation. Design of cyclones and hydrocyclones.

January - December 1984:
"Development of a computer program for calculating an ideal refrigeration cycle" under the surpervision of Prof. Dr. A. Mac Dowell de Figueiredo. Scientific work with financial support from the Brazilian government (CNPq).

January - December 1983:
"Library of subroutines for the manipulation of graphs" under the surpervision of Dr. L. Markenzon. Scientific work with financial support from the Brazilian government (CNPq). This work won a prize from IBM and the University UFRJ.

4. Extra formation

Courses in administration and management at the Swiss Federal Institute of Technology - Lausanne:
"Accounting, Administration and Finances", "Communication, a professional and personal ability", "Technique for working efficiently", "Principles of company administration for engineers" and "Audio and visual aids, introduction and practice". Seminars and conferences of the "Chaire de Pédagogie et Didactique" about oral expression, communication styles, creativity, leadership, authority and management.

Computer courses at the Catholic University of Rio de Janeiro (PUC):
January - March 1986:
Computer languages (Pascal, Fortran, Cobol and Basic), Computer systems, Programming technique.
April - July 1986:
Operational systems, Data structures, Cobol and the Jackson technique.

Courses given by UFRJ and PETROBRAS:
October 1985 - March 1986:
Heat exchanger, Corrosion, Materials, Equipment inspection, Welding, Vibration in large machines and Lubrication.